

**REMOVAL OF
CARDIOVASCULAR OBSTRUCTIONS
BY SPARK EROSION**

Cover illustration: © TonyStone images

ISBN 90-9011073-9

Printed by ICG Printing Dordrecht

© Cornelis J. Slager

**REMOVAL OF
CARDIOVASCULAR OBSTRUCTIONS
BY SPARK EROSION**

**HET VERWIJDEREN VAN
CARDIOVASCULAIRE OBSTRUCTIES
MET VONKEROSIE**

PROEFSCHRIFT

ter verkrijging van de graad van doctor
aan de Erasmus Universiteit Rotterdam
op gezag van de rector magnificus
Prof. dr. P.W.C. Akkermans M.A.
en volgens besluit van het College voor Promoties

De openbare verdediging zal plaatsvinden op
woensdag 17 december 1997 om 15.45 uur

door

Cornelis Jacob Slager

geboren te Scherpenisse

PROMOTIECOMMISSIE

PROMOTOR: Prof. dr. ir. N. Bom
Prof. dr. J.R.T.C. Roelandt

OVERIGE LEDEN: Prof. dr. C. Borst
Prof. dr. P.W. Serruys
Prof. dr. P.D. Verdouw
Prof. dr. ir. J. Davidse
Prof. dr. G.T. Meester
dr. L.A. van Herwerden

This study was supported by grants from:
the Netherlands Heart Foundation: NHS 84.073, NHS 37.007 and NHS 91.100,
the Foundation for Technical Sciences (STW): RGN79-1257 and
the Interuniversity Cardiology Institute of the Netherlands, project 12.

Financial support by the Netherlands Heart Foundation for the publication of this thesis is gratefully acknowledged.

*De vreeze des HEREN
is het beginsel der wetenschap;
de dwazen verachten wijsheid en tucht.*

(Salomo: Spreuken 1 vs. 7)

In mijn naam leeft de herinnering voort aan mijn grootvaders:

Cornelis Slager en Jacob Boon.

"Verder leren" was in hun tijd geen optie.

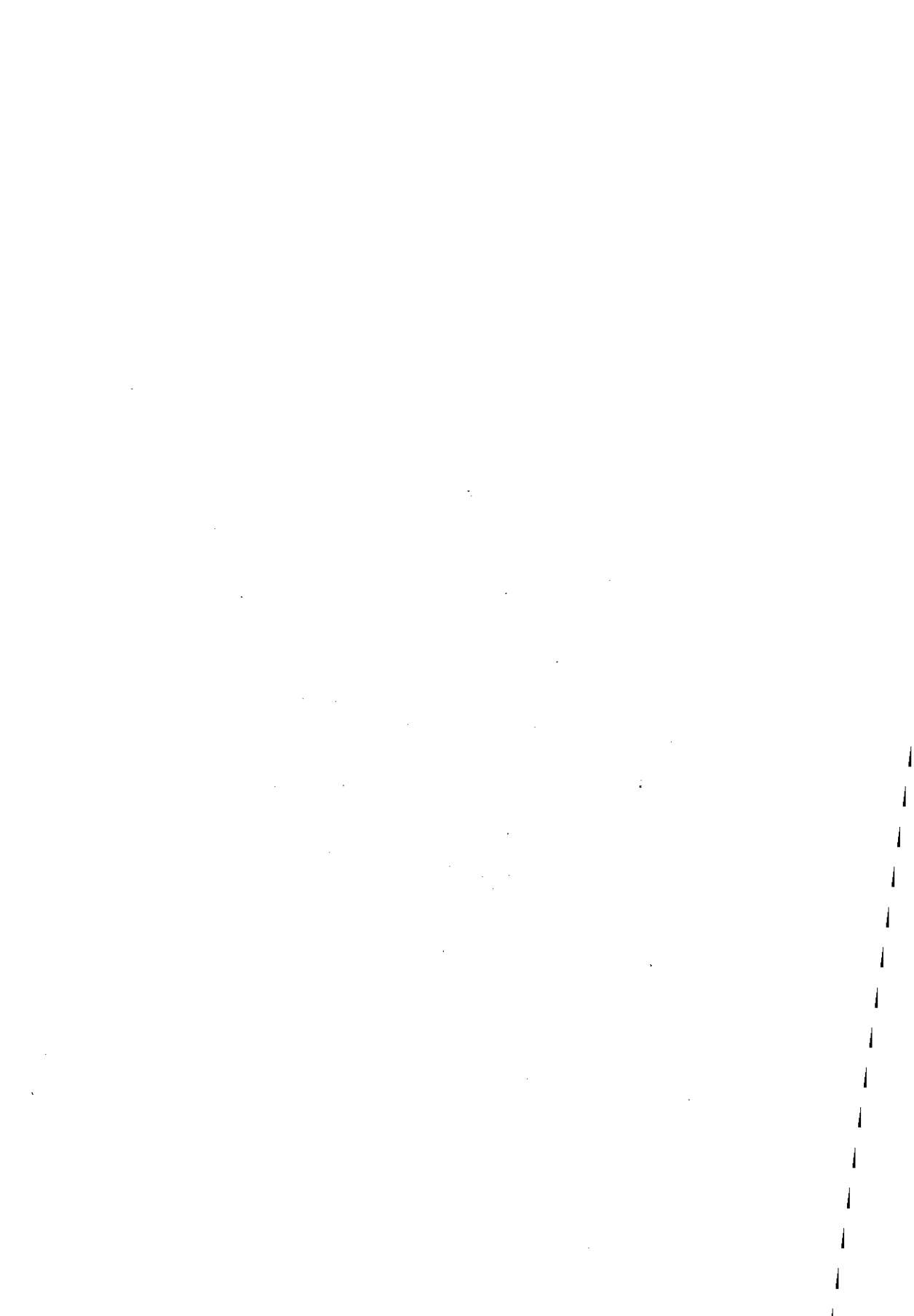
Ter dierbare nagedachtenis aan mijn vader Johannis Adriaan Slager

en tot eer van mijn moeder Helena Plona Boon.

Zij gaven mij de vrijheid en de middelen om te studeren.

CONTENTS

| | | |
|-----------|-------------------------------------------------------------------------------------------------------------------------------------------------------------------------------------|-----|
| Chapter 1 | Introduction and overview of thesis | 9 |
| Chapter 2 | Vaporization of atherosclerotic plaques by spark erosion <i>J Am Coll Card</i> 1985, 5(6), 1382-1386 | 19 |
| Chapter 3 | Electrical impedance of layered atherosclerotic plaques on human aortas <i>IEEE Trans Biomed Engng</i> 1992, 39(4), 411-419 | 27 |
| Chapter 4 | Intra-arterial ultrasonic imaging for recanalization by spark erosion <i>Ultrasound Med Biol</i> 1988, 14, 257-261 | 39 |
| Chapter 5 | Heart function after injection of small air bubbles in a coronary artery of pigs <i>J Appl Physiol</i> 1993, 75(3), 1201-1207 | 47 |
| Chapter 6 | Early and late arterial healing response to catheter-induced laser, thermal, and mechanical wall damage in the rabbit <i>Lasers in Surg and Med</i> , 1990, 10, 363-374 | 57 |
| Chapter 7 | Electrical nerve and muscle stimulation by radio frequency surgery: role of direct current loops around the active electrode <i>IEEE Trans Biomed Engng</i> 1993, 40(2), 182-187 | 71 |
| Chapter 8 | Directional plaque ablation by spark erosion under ultrasound guidance. First evaluation of a catheter incorporating both techniques | 79 |
| Chapter 9 | Spark erosion myectomy in hypertrophic obstructive cardiomyopathy <i>Ann Th Surg</i> 1994, 58(2), 536-540 | 91 |
| Appendix | Echo-vonkerosie rekanalisatie inrichting <i>Dutch Patent Application</i> 1987, nr. 87.00632 | 99 |
| | Summary, discussion and conclusions | 119 |
| | Samenvatting, discussie en conclusies | 127 |
| | Dankwoord | 137 |
| | Publications | 143 |
| | Curriculum vitae | 157 |



CHAPTER 1

INTRODUCTION AND OVERVIEW OF THESIS

INTRODUCTION

Coronary atherosclerosis, leading to coronary artery stenosis, is the main cause for ischemic heart disease in the Western countries. Stenoses manifest themselves by limiting blood supply to the myocardium thus causing complaints. A long history of degenerative atherosclerotic disease of the intimal wall of the coronary vessels has usually preceded these events. Probably because of this long term process the composition of the accumulated obstructive tissue is quite heterogeneous and consists of a variety of cells and extra cellular material like lipid containing macrophages, smooth muscle cells, monocytes, collagen, cholesterol crystals and calcium. In addition, fresh or organized thrombi may have been deposited on these plaques. Regression of these lesions may be obtained by lifestyle changes¹ or lipid lowering therapy². The acute invasive removal of such complex lesions, however, cannot be achieved by applying simple mechanical or chemical means.

Since the late sixties surgical treatment of patients with coronary obstructive disease is achieved by inserting bypasses over the diseased vessels with autologic transplanted veins or arteries which function as a shunt for the blood flow. The procedure involves opening of the thorax, arresting the heart and maintaining body blood supply by an extra corporeal pumping machine. Long term results of the bypass operation are good but the trauma and the high costs have motivated investigators to search for a less invasive surgical procedure. Recently first results of

bypass grafting on the beating heart, performed via a mini thoracotomy have been reported³.

Almost two decades ago Grüntzig⁴ introduced a much less invasive technique in which the obstruction is widened by balloon inflation. The balloon is introduced percutaneously, transluminally guided to the coronary obstruction after which a so called angioplasty (PTCA) is performed. The major problem after PTCA treatment has been vessel restenosis in 30 % - 40 % of the procedures within 6 months. This was the reason why a lot of new technical developments were started to combat this shortcoming. Recent animal studies on the process of restenosis after PTCA have shown that the damage to the adventitia stimulates its growth and remodeling which appears to be a major cause of lumen renarrowing^{5,6}.

In 1986 stents⁷ were introduced to avoid recoil of the dilated vessel and to fix flaps of dissected tissue against the wall. Recently it has been shown that implantation of stents in a dilated artery⁸ significantly reduces the problem of restenosis. This matched pair of techniques, balloon and stent, now rapidly gets a dominating position in the treatment of patients with coronary obstructions. The main reason of the success of the stent seems to be its capability to withstand adventitial shrinkage. Paradoxically, intima hyperplasia, originally thought to be the major determinant of restenosis, now even may appear to be more pronounced within stented vessels than in non stented vessels⁹.

A few years before the introduction of stents, development of a variety of new techniques had been started to remove vessel obstructions in a transluminal minimal invasive way. At that time it was already felt that the problem of restenosis occurring after PTCA might be related to the rather crude way of vessel widening by the balloon inflation and the inherently induced severe damage to media and adventitia. Furthermore, leaving the obstructive material in the vessel, rather than removing it, was not thought to be an optimal treatment. Such new techniques were for example atherectomy¹⁰, rotablation¹¹ and laser¹² which respectively applied cutting, grinding or pulverization and vaporization for the removal of the obstructive tissues.

Progress in this field has been rather slow and in the clinic only the most simple and straightforward operating mechanical techniques like rotablator and atherectomy have gained a position for treatment of a relatively small selected group of patients. However, an additional balloon dilatation is generally needed to open the vessel to an acceptable size. The much more advanced, but also more complicated technique of using laser light did not fulfill its promise to remove lesions in a selective way thereby leaving the normal wall unaffected. It turned out that treatment by laser with adjunctive balloon dilatation was associated with a higher rate of restenosis than using the balloon alone¹³. Currently use of the laser is limited to reopening totally occluded vessels with a small diameter (0.5 mm) laserwire after which a balloon dilatation can be applied¹⁴.

Besides plaque removal techniques other transluminal methods were developed and tested to modify atherosclerotic lesions by application of heat in the hope to reduce restenosis. Metal^{15,16} or sapphire tips¹⁷ and balloons^{18,19}, heated by electric current or laser light, have been used for this purpose. However, all these methods rather increased than reduced restenosis rate.

The search for a stand alone operating, minimally invasive technique, being able to remove obstructions and to widen the lumen up to normal dimensions without causing damage to the media and adventitia or leaving a foreign body in the vessel wall, is still a valuable goal, not at least from the point of view of cost effectiveness.

Spark erosion was introduced as a technique being competitive with the laser. The unique physical properties of laser light i.e. its monochromaticity and phase coherency were not thought to be essential for plaque removal. Both techniques have in common that they want to achieve controlled tissue removal by fragmentation induced by heat. Spark erosion applies heat on a microscopic scale to tissue by contacting it with a multitude of very tiny electric sparks. The effects of spark erosion on atherosclerotic lesions, its testing on safety and healing in animals, the study of side effects, its development in combination with guidance techniques and a first clinical application to hypertrophic obstructive cardiomyopathy are the subjects of this thesis.

From the historical point of view, the application of heat in medicine dates from very early times. Neolithic skulls seem to show clear evidence of thermal cauterization²⁰. According to Majno²¹ in the Smith Papyrus (approx. 1900 BC) the use of a cauterizing instrument, i.e. a "fire-drill", was recommended for treatment of ulcers and tumors in the breast:



Ancient prescription for cauterity by a "fire-drill"

The hieroglyph, literally depicting this instrument, is distinct from the other characters by the accompanying vertical line and reads as a modern pictograph.

Another ancient witness is found in the Ebers papyrus (approx. 1600 BC) which contains the world's first recorded hemostasis by applying heat²¹.

Widespread application of electricity in medicine dates from the first half of the 18th century. Physicists began to realize that electricity should not be regarded as "*an unimportant property of a few substances*" but that it had "*a connection with one of the greatest and most considerable phenomena in Nature, thunder and lightning*" (Klingenstierna 1755)²². Particularly the invention of the Leyden jar has stimulated a lot of new developments. This first capacitor holding a significant amount of electric charge was accidentally invented by Cunaeus, a lawyer visiting the laboratory of Musschenbroek at Leiden, in 1745²³. He amused himself with "*electrified*", i.e. electrostatically loaded, water in a glass vessel. However, rather than placing the vessel on an insulated stand as was generally thought to be necessary, he loaded and discharged the vessel holding it in one of his hands and thus painfully discovered the power of the Leyden jar. Musschenbroek after having repeated this experiment reported to the Paris Academy: "*I would like to tell you about a new, but terrible experiment, which I advise you never to try yourself, nor would I, who have experienced it and survived by the grace of God, do it again for all the kingdom of France. I was engaged in displaying the powers of electricity*"²⁵. So ample time before the dispute between Galvani and Volta, the relation between electric current and nerve and muscle stimulation was painfully perceived.

From 1745 to 1785 advancement in instrumentation allowed experimenters to produce sparks in their laboratories at lengths increasing from 2 cm (Franklin) to 70 cm (van Marum at the Teyler Foundation at Haarlem, the Netherlands) thereby transferring an increasing energy content from respectively 6 μ joule up to 2 kjoule, amply sufficient to electrocute small animals and to cause severe accidents²⁴.

Electric sparks, which were thought to be a special form of ordinary fire, became an exciting and entertaining subject for the public²⁵. Unfortunately those experiments did not contribute much to physical science. Neither did the therapeutic application of electric sparks to medicine. Many electrotherapists draw sparks from a Leyden jar to parts of the body to treat a great variety of diseases. For example, John Wesley, the founder of Methodism, left us a lot of case reports in his "The Desideratum" (1759) like: "*In 1757, while I was electrifying for a pain in my stomach (which was wholly removed by one shock) Silas Told, Schoolmaster, aged 48, came in and said, 'My heart is very bad, and I think I will try it too'. He did so, receiving a shock through the breast, and has been ever since perfectly well*"²⁶.

As soon as electric current could be generated at high intensity it was used to heat cauterization instruments. In this application heat transfer to tissue is by thermal conduction from the heated instrument. Physically this is quite different from heating tissue directly by passage of electric current. Therefore use of the name electrocautery should be restricted to those applications in which no current flows through tissue.

With the advent of alternating high frequency current generators, d'Arsonval demonstrated that high intensity electric current could pass the body without causing nerve and muscle stimulation²⁷. In 1897 Nagelschmidt demonstrated the value of local hyperthermia in the treatment of articular and circulatory diseases²⁸, and achieved this by applying high frequency current passing through the body. He called this method "diathermy" literally meaning "through heating". Commonly used frequencies were in the range of radio frequencies i.e. 500 kHz - 3 MHz. Unfortunately the term "surgical diathermy" has become erroneously in use to describe all surgical applications of high frequency current passage through body tissues, including cutting and coagulation. Currently it is well accepted to cover this wide field by the more general name "electrosurgery".

The effect of high frequency electric current passage through body tissue is dependent on the local current density, tissue impedance, tissue specific thermal characteristics and duration of application. Two electrodes are needed to pass the high frequency current through the body. For diathermic application, tissue damage by heat should not occur and both electrodes must be rather large to keep current density at a low level. When raising current density by reducing the dimension of the electrodes or raising current flow, so called white coagulation can be obtained. This was first demonstrated by Rivière in 1907²⁸. Continuing tissue heating at this relatively low current density level leads to tissue desiccation (dehydration). These applications are examples of so called bipolar operations in which both electrodes have similar dimensions.

In so called monopolar applications, the active electrode, has a much smaller area than its companion which is called the indifferent, dispersive, ground or return electrode. A high current density is achieved at the site of the active electrode which induces the desired thermal effect to the area to be treated. At the site of the return electrode current density remains low and no significant heating occurs. Dependent on factors like the shape of the active electrode, the applied voltage and the alternating current wave forms the effects which can be obtained may vary considerably. At a critical level of the voltage gradient, sparking will be provoked between the active electrode and the tissue. When generating sparks over a length of a few mm at a low repetition rate, fulguration (flashing as in lightning) is obtained²⁸. Those sparks destroy cells by raising them to high temperature and the tissue becomes carbonized. On the other hand sparks can also be used for cutting with minimal carbonization effect i.e. by using active electrodes like a needle point or the edge of a knife blade and pure sine wave current wave forms. This was discovered by de Forest²⁹. One of the first articles describing simultaneous cutting and coagulation of living tissue were published by Clark in 1911³². Knowledge of the quite varying effects of electrosur-

gery has mainly been obtained in an empirical way³³ and even nowadays the complex temporal and spatially varying electric, thermal and mechanical mechanisms involved have not been grasped in an exact model.

Since the 1920s manufacturers have been offering a variety of electrosurgical equipment with names like Portatherm, Cauterodyne, Super Diatherm etc. The design which became the most successful until the 1960s was from W.T. Bovie³⁰. This resulted in associating his name so closely with the electrosurgical cutting procedure that this became also known as the "Bovie knife". Particularly with the advent of solid state circuitry in the 1970s designs were completely changed, new safety features and hand activated controls were added³¹.

During the course of the century the field of surgical application widened to include less invasive procedures. The minimal invasive procedure of transurethral resection of the prostate was already described in 1932³⁴. More recently introduced procedures are for example laparoscopic cholecystectomy³⁵ and meniscectomy³⁶. Also in gynecology and dermatology electrosurgery is widely used³⁷. In cardiology, a minimal invasive application of radiofrequency energy is applied for treatment of cardiac arrhythmias³⁸. Near accessory pathways, tissue is heated and coagulated by radiofrequency current passage locally applied by a catheter tip electrode. This method is called radiofrequency ablation, which is kind of a misnomer as no tissue is removed.

Spark erosion, involving application of a new battery operated solid state radiofrequency generator design, new types of electrodes and uncommon electrical parameters, was introduced as a modified electrosurgical technique to be used for the vaporization of atherosclerotic plaques³⁹. This was accomplished by heating tissue by multiple sparks at such small spots and so fast that the applied heat is almost instantaneously used for conversion of the tissue contents into steam and gas. The provoked micro explosions fragment the tissue and blow the debris away from the target zone.

OVERVIEW OF THESIS

In chapter 2 the technique of spark erosion is described as well as a first series of *in vitro* and *in vivo* tests. Technical developments and the type of electrodes are described and we discuss how and why these deviate from common electrosurgical techniques. Tests of the technique on atherosclerotic segments of human aortic autopsy specimens gave an indication about its effectiveness in vaporizing plaques. *In vivo* tests are described to determine its electrical safety. Based on the first experiences, studies were defined which should be performed before *in vivo* application could be considered. These studies included areas of healing response, gas bubbles and coronary embolism, catheter guidance and steering techniques to prevent arterial perforation.

In chapter 3 a study on electrical impedance of atherosclerotic plaques, being an attractive parameter to guide the process of spark erosion, is described. Despite the finding that atherosclerotic material generally has a higher electric resistivity than normal arterial wall tissue, the conclusion had to be that *in vivo* applicable impedance measuring techniques would become too complicated and impractical to be used as a guidance technique for spark erosion.

In chapter 4 is described how the search for a guidance technique resulted in the idea to develop (see also Appendix) intravascular ultrasound as a new imaging modality. Particularly the idea of just using a single rotating piezo electric element as a transducer, enabled the design and fabrication of catheter prototypes sufficiently small to be combined with spark erosion. Feasibility tests of those early devices are presented and it was concluded that ultrasound, compared to other imaging modalities, like for example angiography, has a decisive advantage because of its capability to visualize the arterial cross section including the structure of the wall.

In chapter 5 is described how in pigs embolization of coronary arteries by air bubbles transiently affects heart function. Gas bubbles inevitably result from plaque vaporization and may

embolize the distal area of a treated vessel. Air bubbles were selectively injected in a coronary artery of pigs and global and regional myocardial functional parameters were studied. This study provided a first indication about the amount and size of bubbles which may be tolerated during application of gas producing plaque vaporization techniques.

In chapter 6 a study is presented on the healing response of the iliac artery in rabbits after spark erosion application and a comparison was made to other thermal plaque modification techniques being the metal laser probe and the Nd-YAG laser sapphire contact probe. Also some indications are given on the applicability of those techniques as well as on the arterial wall damage and complications. Because of the particular settings of this experiment neuromuscular stimulation during spark erosion application was observed.

Chapter 7 focuses on the problem of neuromuscular stimulation during radiofrequency surgery application. This issue intrigued many investigators because of the contradiction with the early observation of d'Arsonval²⁷. Experiments are described how to reveal previously unattended direct currents which probably explain most of the observed stimulation.

In chapter 8 the design, construction and first feasibility tests of a spark erosion catheter for plaque removal with integrated intravascular ultrasound guidance is described (see also the Appendix). Interaction between the spark erosion application and the echo imaging is discussed. Specific design considerations with respect to guidance, stimulation, bubble production and ablation efficiency are discussed.

In chapter 9 another unexpected spin-off application of spark erosion in the field of cardiac surgery is described. It is discussed how specific electrical characteristics and a special electrode design highly facilitate the myectomy procedure in hypertrophic obstructive cardiomyopathy. Operation results and long term outcome on a first series of 18 patients are presented.

REFERENCES:

1. Ornish D, Brown SE, Scherwitz LW, Billings JH, Armstrong WT, Ports TA, McLanahan SM, Kirkeide RL, Brand RJ, Gould KL. "Can lifestyle changes reverse coronary heart disease? The Lifestyle Heart Trial" *Lancet* 1990, 336, 624-626.
2. Watts GF, Lewis B, Brunt JN, Lewis ES, Coltart DJ, Smith LD, Mann JI, Swan AV. "Effects on coronary artery disease of lipid-lowering diet, or diet plus cholestyramine, in the St Thomas' Atherosclerosis Regression Study (STARS)" *Lancet*, 1992, 339, 563-569.
3. Subramanian VA, Sani G, Benetti FJ, Calafiore AM. "Minimally invasive coronary bypass surgery: a multi-center report of preliminary clinical experience" *Circulation* 1995, 92(8), 3093 (abstr.).
4. Grüntzig A, Hopff H. "Perkutane Rekanalisation chronischer arterieller Verschlüsse mit einem neuen Dilatationskatheter. Modifikation der Dotter-technik" *Dtsch Med Wochenschr* 1974, 99, 2502-2511.
5. Post MJ, Borst C, Kuntz RE. "The relative importance of arterial remodeling compared with intimal hyperplasia in lumen renarrowing after balloon angioplasty." *Circulation* 1994, 89, 2816-2821.
6. Kakuta T, Currier JW, Haudenschild CC, Ryan TJ, Faxon DP. "Differences in compensatory vessel enlargement, not intimal formation, account for restenosis after angioplasty in the hypercholesterolemic rabbit model" *Circulation* 1994, 89, 2809-2815.
7. Sigwart U, Puel J, Mirkovitch V, Joffre F, Kappenberger L. "Intravascular stents to prevent occlusion and restenosis after transluminal angioplasty". *N Engl J Med* 1987, 316, 701-706.
8. Serruys PW, de Jaegere P, Kiemeneij F et al. "A comparison of balloon-expandable stent implantation with balloon angioplasty in patients with coronary artery disease" *N Engl J Med* 1994, 331, 489-495.
9. Mintz GS, Pichard AD, Kent KM, Satler LF, Popma JJ, Wong SC, Painter JA, DeForty D, Leon MB. "Endovascular stents reduce restenosis by eliminating geometric arterial remodeling: a serial intravascular ultrasound study" *JACC*, 1995, 34A, 701-5 (abstr).
10. Simpson JB, Johnson DE, Thapliyal HV, Marks DS, Braden LJ. "Transluminal atherectomy: a new approach to the treatment of atherosclerotic vascular disease" *Circ* 1985, 72, III, 146(abstr).
11. Hansen DD, Auth DC, Vracko R, Ritchie JL. "Mechanical thrombectomy: a comparison of two rotational devices and balloon angioplasty in subacute canine femoral thrombosis" *Am Heart J* 1987, 165, 387-389.
12. Macruz R, Martins JRM, Tupinamba(s) AS, Lopes EA, Vargas H, Pena OF, Cravalho VB, Decourt LV. Possibilidades terapeuticas do raio laser em ateromas. *Arq Bras Cardiol* 1980, 34, 9-12.
13. Strikwerda S, Montauban van Swijndregt E, Foley DP, Boersma E, Umans VA, Melkert R, Serruys PW. "Immediate and late outcome of excimer laser and balloon coronary angioplasty: a quantitative angiographic comparison based on matched lesions" *JACC* 1995, 26, 4, 939-946.
14. Henson KD, Leon MB, Popma JJ, Pichard AD, Satler LF, Eigler N, Litvack F, Rothbaum D, Goldenberg T, Kent KM. "Treatment of refractory coronary occlusions with a new excimer laser catheter: Preliminary clinical observations" *Coron Artery Dis.* 1993, 4, 1001-6.
15. Litvack F, Grundfest W, Mohr FW, Jakubowski AT, Goldenberg T, Struhl B, Forrester JS. "Hot-tip' angioplasty by a

- novel radiofrequency catheter" *Circulation* 1987,76, 4, 47 (abstr).
16. Hussein H. "A novel fiberoptic laserprobe for treatment of occlusive vessel disease" *SPIE (Optical and Laser Technology in Medicine)*, 1986, 605, 59-66.
 17. Daikuzono N, Joffe SN. "Artificial sapphire probe for contact photocoagulation and tissue vaporization with the Nd:YAG laser" *Med Instr* 1985, 19, 173-178.
 18. Spears JR. "Percutaneous transluminal coronary angioplasty restenosis: potential prevention with laser balloon angioplasty" *Am J Cardiol* 1987, 60, 61B-64B.
 19. Becker GJ, Lee BI, Waller BF, Barry KJ, Kaplan J, Connolly R, Dreesen RG, Nardella P. "Radiofrequency balloon angioplasty. Rationale and proof of principle" *Invest Radiol* 1988, 23(11), 810-817.
 20. Major R.H. "A history of medicine" Oxford: Blackwell Scientific Publications, 1954.
 21. Majno G, "The Healing Hand. Man and Wound in the Ancient World" Harvard University Press, 1991, 96-97.
 22. Heilbron JL, "Electricity in the 17th and 18th centuries. A study of early modern physics" University of California Press, Berkeley, Los Angeles, London, 1979, 6.
 23. *Ibid.* 312-313.
 24. *Ibid.* 83, 441
 25. Roth, N. "Charles Rabiqueau and the Fire Show: Making the Forces of Nature Visible" *Medtronic News* 1994, 21, 2, 60-62.
 26. Dennis Stilling. *Artifact* "John Wesley: Electrotherapist" *Med Instr* 1974, 8(1), 66.
 27. d'Arsonval A. "Action physiologique des courants alternatifs a grand frequence". *Archives Physiol Norm Path* 1893, 5, 401-408, 788-790.
 28. Pearce JA. *Electrosurgery*. Chapman and Hall, London, 1986, 4.
 29. *Ibid.* 6-7.
 30. *Ibid.* 7-12.
 31. *Ibid.* 13.
 32. Clark W. "Oscillatory desiccation in the treatment of accessible malignant growths and minor surgical conditions" *J Adv Therap* 1911, 29, 169-183.
 33. Geddes LA, Silva LF, DeWitt DP, Pearce JA. "What's new in electrosurgical instrumentation?" *Med Instr.* 1977, 11, 6, 355-359.
 34. Kelly HA and Ward GE. *Electrosurgery*, WB Saunders, Philadelphia, 1932.
 35. Hunter JG, "Exposure, dissection, and laser versus electrosurgery in laparoscopic cholecystectomy" (Rev) *Am J Surg.* 1993, 165(4): 492-496.
 36. Bert JM. "Use of an electrocautery loop probe for arthroscopic meniscectomy: a five year experience with results, indications, and complications" *Arthroscopy* 1992, 8(2), 148-156.
 37. Ferris DC, Hainer BL, Serale JR, Powell JJ, Gay JN. "Gynecologic and dermatologic electrosurgical units: a comparative review" *J Fam Pract.* 1994, 39(2), 160-169.
 38. Borggreffe M, Budde T, Podczek A, Breithardt G. "High frequency alternating current ablation of an accessory pathway in humans" *JACC* 1987, 10(3), 576-582.
 39. Slager CJ, Essed CE, Schuurbiens JCH, Bom N, Serruys PW, Meester GT. "Vaporization of atherosclerotic plaques by spark erosion" *JACC* 1985, 5(6), 1382-1386.

CHAPTER 2

**VAPORIZATION OF
ATHEROSCLEROTIC PLAQUES
BY SPARK EROSION**

Cornelis J. Slager, Catharina E. Essed, Johan C.H. Schuurbiers, Nicolaas Bom,
Patrick W. Serruys, Geert T. Meester

Journal of the American College of Cardiology 1985, 5(6), 1382-1386

Vaporization of Atherosclerotic Plaques by Spark Erosion

CORNELIS J. SLAGER, MSc, CATHARINA E. ESSED, MD, JOHAN C. H. SCHUURBIERS, BSc,
NICOLAAS BOM, PhD, PATRICK W. SERRUYS, MD, GEERT T. MEESTER, MD, FACC

Rotterdam, The Netherlands

An alternative to the laser irradiation of atherosclerotic lesions has been developed. A pulsed electrocardiogram R wave-triggered electrical spark erosion technique is described. Controlled vaporization of fibrous and lipid plaques with minimal thermal side effects was achieved and documented histologically in vitro from 30 atherosclerotic segments of six human aortic autopsy specimens. Craters with a constant area and a depth that

varied according to the duration of application were produced. The method was confirmed to be electrically safe during preliminary in vivo trials in the coronary arteries of seven anesthetized pigs. The main advantages of this technique are that it is simpler to execute than laser irradiation and potentially more controllable.

(*J Am Coll Cardiol* 1985;5:1382-6)

In recent years, the use of lasers has been proposed for the improvement of perfusion through obstructed arteries (1-3). At present, several approaches can be distinguished depending on the type of obstruction. For example, argon laser-emitted wavelengths in the green part of the spectrum can be selectively absorbed by hemoglobin in fresh thrombi. This can be used to advantage as the vessel wall will be less affected by these wavelengths. When atherosclerotic material has to be removed, the selection of a particular type of laser is not so straightforward. Selective absorption at a particular wavelength by degenerated tissue has not been demonstrated. When atherosclerotic lesions can be stained selectively, a more refined application of the laser is feasible. Until now, the specific characteristics of the laser radiation, namely, its coherency and monochromaticity, have not been of decisive importance for the vaporization of atherosclerotic tissue. The only relevant variable for a successful application of the proposed laser types (4) is the energy density that can be obtained at the target area combined with maximal local absorption. Because carbon dioxide laser-emitted radiation (wavelength 10.6 μm) is strongly absorbed by water and biological tissue, this type of laser will produce the best results for tissue vaporization. Recently, appropriate optical fibers were developed for transluminal intravascular application (5). However, an in-

tense and localized delivery of energy can also be reached with other (less expensive) techniques.

In this report, we describe the application of a spark erosion technique to vaporize atherosclerotic plaques in specimens of human aortas obtained at autopsy. Spark erosion is commonly used in the electrical discharge machining technique and is specially suitable for the fabrication of small metal parts. The removal of material is performed by local melting and vaporization of the metal caused by controlled electrical sparks between a stamp electrode and the material to be processed. In medicine the well known radiofrequency electrosurgical cutting technique partly uses the same fundamental erosion process but also incorporates desired side effects such as dehydration and coagulation of the treated tissue to achieve hemostasis.

For the application of the spark erosion technique the electrosurgical cutting technique was modified to minimize dehydration and coagulation and to accentuate tissue vaporization. In addition, pulsed, rather than continuous application is used to enable triggered delivery restricted to the refractory period of the ventricular cycle. In this way potential influence on the heart's electrical activity can be avoided.

Methods

Autopsy material. Segments of atherosclerotic human aortas measuring approximately 4×7 cm were obtained at autopsy from six patients (age range 61 to 83 years). These segments were treated within 2 days of autopsy. Until then, they were covered by a gauze, wetted with saline solution and kept at a temperature of 4°C.

From the Thoraxcenter, Erasmus University and University Hospital Dijkzigt, Rotterdam, The Netherlands. Manuscript received August 6, 1984; revised manuscript received December 26, 1984, accepted January 9, 1985.

Address for reprints: Cornelis J. Slager, Jr, Thoraxcenter, Ee2322, Erasmus University Rotterdam, P.O. Box 1738, 3000 DR Rotterdam, The Netherlands.

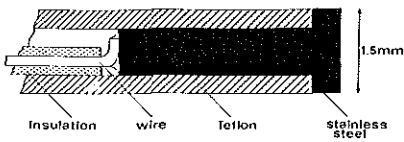


Figure 1. Schematic drawing of the spark erosion electrode used for the *in vitro* experiments.

Animal preparation. In a series of seven anesthetized closed chest pigs, tests were performed to study the effects of the spark erosion technique on the electrical aspects of the heart's activity. For this purpose, selective coronary catheterization was performed using a balloon angioplasty guiding catheter (8F). A flexible catheter (4F) with a wire electrode tip was passed through the lumen of this catheter and positioned 2 to 5 cm distal from the ostium in either the right, left circumflex or left anterior descending coronary artery. During the experiment, the electrocardiogram and aortic pressure (tipmanometry) were recorded continuously at a paper speed of 10 mm/s^{-1} .

Spark erosion. The electrical spark generator was designed and constructed in our workshop. For safety reasons, it is electrically isolated from the main voltage line. It has a balanced symmetric output stage coupled to the load by two series capacitors to prevent the primary delivery of any direct current. The output impedance equals 180Ω . The generated square-wave voltage has a peak to peak value of 1200 V at a frequency of 250 KHz.

Trigger unit. For *in vitro* use, a manual command immediately activates the generator during a period of 10 ms. For different atherosclerotic lesions, the applied number of successive exposures was varied from 1 to 10, with intervals of 2 to 4 seconds.

For *in vivo* application, an external synchronizing signal is used in addition to the manual command. This signal is derived from the electrocardiogram by an R wave peak-detecting circuit. An adjustable time delay can also be added to the synchronization procedure such that the generator pulse occurs with a delay of 100 to 1,000 ms after the signal of the peak detector, sensing the R wave of the electrocardiogram.

Electrodes. For the *in vitro* tests of the spark erosion technique, the aortic segment and a return electrode (area 4 cm^2) were immersed in saline solution (0.9%). The spark electrode (diameter 1.5 mm) has an active 4 mm^2 area ex-

posed to the tissue (Fig. 1). The distance between both electrodes varied from 2 to 10 cm. For the *in vivo* testing of electrical safety with respect to the heart's electrical activity, a subcutaneous needle (10 cm) functioned as the return electrode. Part of a flexible guidewire (diameter 0.4 mm) was used as the active electrode. To prevent perforation of the vessel wall, three small spherical epoxy resin droplets centered the electrode inside the lumen (Fig. 2). The resting length of the guidewire exposed to the blood is 2 mm.

Histologic study. After the *in vitro* tests with the spark erosion technique, the aortic segments were fixed in 10% buffered formalin. Samples of the treated lesions were dehydrated and embedded in paraffin. Sections perpendicular to the aortic wall were made at $5 \mu\text{m}$ and stained with hematoxylin-eosin.

Results

Aortic Segments

With the spark erosion technique, vaporized craters having a diameter slightly greater (1.6 to 1.7 mm) than that of the applied electrode could be easily created in human fibromuscular, collagenous and lipid-containing plaques. The depth of the craters varied with the total pulse time and was equal to $0.18 \pm 0.1 \text{ mm}$ times the number of applied 10 ms pulses. No difference in depth of the craters could be observed among the various types of lesions. During vaporization, small gas bubbles were produced in the target area.

Histology. Histologic examination of the treated fibromuscular or collagenous areas showed sharp edges of the vaporized craters and no necrotic debris within them. A small rim of coagulated tissue with a median thickness of $40 \mu\text{m}$ surrounded the craters (Fig. 3A).

In the plaques containing a significant amount of lipids, the edges of the craters were frayed and some residual coagulative material could be observed within. The coagulative zone was extended over a median distance of $200 \mu\text{m}$. Vaporization of superficial atheromatous layers was associated with more thermal damage (Fig. 3B) than vaporization of buried atheromatous layers (Fig. 3C).

In the plaques consisting of lipid and small scattered calcifications, the lipid was destroyed and the calcareous particles were found as debris in the crater lumen. No effect could be observed in mainly calcified areas and these areas have not been analyzed.

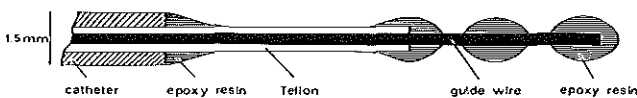


Figure 2. Flexible guidewire spark erosion electrode for the *in vivo* generation of sparks in the coronary arteries of pigs to test electrical safety of the technique. Epoxy resin droplets centered the electrode in the lumen to prevent vessel wall perforation.

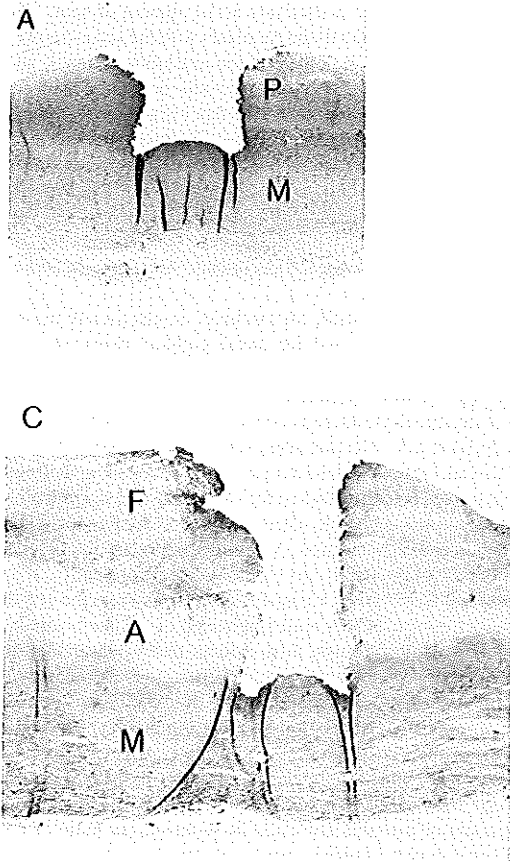


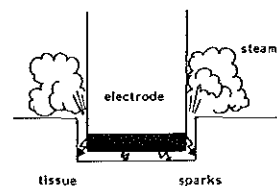
Figure 3. Histologic sections. A, Section through the aortic wall with a mainly fibrous plaque (P). Application of the spark erosion method in a direction perpendicular to the area of the plaque produced a punched-out crater extending to the superficial layers of the media (M). Two 10 ms pulses, each delivering approximately 1.7 J, produced this result. Note the very small dark rim that represents the coagulation zone. B, Section through the aortic wall with an atheromatous plaque with extensive lipid deposits (A). The crater created by the spark erosion technique was achieved with three 10 ms pulses, each delivering approximately 1.7 J. Note the frayed aspect of the border of the lesion and the broad dark coagulation zone. C, Section through the aortic wall with an atheromatous plaque (A) covered by a fibrous cap (F). The crater which extends to the superficial layers of the media (M) was achieved with four 10 ms pulses. Along the border of the crater, only a very small dark coagulation zone can be observed. (Hematoxylin-eosin stain; magnification 28× in A, 23× in B and 27× in C.)

Delivered energy. During spark erosion, the delivered peak to peak voltage to the load was measured on an oscilloscope. Because the output impedance of the generator and its open output voltage are 180 Ω and 1,200 V peak to peak, respectively, the load impedance can be derived from these data. In this way, it was shown that during the first 1 or 2 ms while the pulse was applied, the load resistance increased from an initial value of 200 to 800 Ω to a final value of 2 to 3 kΩ. Only at the higher final resistance values did sparking occur because the electrode became isolated from the tissue by the self-produced steam layer at that stage (Fig. 4). From these data, the power ratings delivered to the tissue can be derived. In the primary heating phase, the delivered power starts at a level of 300 to 500 watts and decreases to a level of 100 to 150 watts in the sparking phase. Therefore, the total energy delivered in a single shot pulse of 10 ms is in the range of 1.2 to 2.2 J.

Animal Studies

In seven pigs, intracoronary sparking was carried out in eight instances: five times in the proximal part of the left anterior descending coronary artery, two times in the left

Figure 4. Schematic drawing of the spark erosion process. The self-produced steam layer isolates the electrode from the tissue. Sparks jumping between the electrode and the tissue produce very high local energy densities that lead to tissue vaporization.



circumflex coronary artery and one time in the right coronary artery. At every location, ten 10 ms pulses, each immediately after the peak of the R wave on the electrocardiogram, were generated. In all eight cases, no effects on cardiac rhythm or aortic blood pressure could be observed.

In a following test, 10 pulses were given subsequently, each at a different time delay after the R wave, ranging from 100 to 1,000 ms by 100 ms increments. Pulses given at a delay of 300 ms or more after the R wave generally induced ectopic beats. Ventricular fibrillation did not occur.

Discussion

Laser techniques. In recent years, different types of lasers have been suggested and tried for potential curative application in the vascular field (1-3,5). The vaporization of vascular obstructions by radiation with intense laser light is tested on a considerable scale. This radiation is guided transluminally through flexible fiber optics to the end of the catheter. However, specific laser beam characteristics, such as coherency and monochromaticity, are not essential requirements to vaporize obstructions with the proposed types of lasers (4). In fact, the only property essential for successful application has been the controlled effective production of heat of a sufficiently high level at the target area. New types of lasers with nonthermic cutting capabilities (for example, those operating in the ultraviolet region [6] and those generating short high intensity pulses [7]) were announced recently. Experimental application of these laser techniques on diseased vascular tissue is probably under investigation now. In this study, we demonstrated the potential use of electrical spark erosion, which is a less complicated, less expensive and more easily controllable technique.

Electrical spark erosion. This technique is commonly used in industry for the accurate production of intricate holes in metals, but it is also used on a wide scale in the medical field for the cutting of biological tissue. The powerful erosion effects associated with the electrical sparks are a result of the extremely high current density that can be reached at the target point. At this point, the very small and well conducting ionization channel (the spark) makes contact with the tissue. In addition, the heat accumulated during the generation of the ionization channel also contributes to the eroding effect of the spark. We suppose that in biological tissue, both heating factors lead to such a rapid conversion of water into steam that cells "explode" and nonwater-containing tissue parts are fractioned into many small particles (Fig. 4). A similar explanation has been construed for cutting mechanisms of the carbon dioxide laser (8) and for electrosurgery (9). However, in the latter, more theoretical explanation of the mechanism of cutting by electrosurgery, the essential role of spark generation has not been mentioned.

The tissue border zone next to the vaporized area will

be exposed only to a relatively small amount of heat. The current density in the tissue decreases with the second power of the distance to the center of the ionization channel, and the power density (expressed in watts per cm^2) even decreases with the fourth power of this distance (9). The explosion effect further reduces the secondary transport of heat from the target area to the border zone as contact between both areas occurs only for a very short time. The heat accumulated in the steam will be easily absorbed by the vast tissue area over which it is distributed. These factors explain the minor importance of secondary heat-induced tissue damage.

Electrocautery with, for example, an electrically heated wire can also be used for tissue cutting. However, this technique must be clearly distinguished from electrosurgical cutting, in which sparking from a cold electrode and the subsequent electrothermal conversion process in tissue play a decisive role. Electrocautery relies on the heating of tissue from an external source through thermal conduction. It has not proved equally effective for vaporizing tissue while minimizing unwanted side effects such as dehydration, coagulation and carbonization. A recently proposed cautery technique (10,11), also based on the transport of heat from an external source, uses a copper shield mounted at the end of a fiber optics catheter which is heated by a laser beam.

Histologic findings. It is evident that when applied to electrically conducting tissue, the spark erosion process will produce results equivalent to those described after thermic laser utilization. Indeed, histologic examination of the zone around the craters produced by vaporization of fibromuscular and collagenous plaques shows a remarkably sharp edge with only a very small rim of coagulated tissue. The amount of material that could be removed per joule of delivered energy compares well with that described after the application of the carbon dioxide laser (12).

The diameter of the craters is mainly determined by the dimensions of the spark erosion electrode and only to a small extent by the spark erosion procedure itself. Sparks only jump over a short distance which is not influenced by the total duration of application. The characteristic of the process that allows for precise control of transversal destruction depth may become valuable for constructing devices for transluminal *in vivo* application with a reduced risk of vessel wall perforation.

The variability observed in the coagulative effect is caused by different local electrical and thermal conducting properties and by the varying water content of the treated tissue. In this respect, the influence of the distance between the reference electrode and the active electrode can be neglected as can be derived from the calculated power density function near the active tip (9).

Methodologic problems. The construction of special spark erosion catheters is rather easy because the flexibility required for intracoronary application can be acquired with

conventional techniques. Also, the use of thin flexible guide-wires as currently applied for the guidance of the balloon angioplasty catheters will be possible. However, these measures in themselves will not prevent wall perforation in all circumstances. New guiding principles for local transversal position control of spark erosion as well as for the laser procedure will have to be invented, especially for the treatment of asymmetric lesions.

Concerning the potential *in vivo* application of the pulsed spark erosion technique, the preliminary tests in pigs have shown that from the electrical point of view, the method can be safely applied. Further investigations must elucidate whether electrical safety is preserved in the presence of myocardial ischemia.

One of the areas deserving further attention is the local production of gas bubbles. Because of the relatively powerful short pulses used, more gas is produced at once, thus creating larger bubbles with a relatively long lifetime. Modification of the pulsing method and the electrode configuration combined, when necessary, with a suction technique may be used to treat this problem.

Clinical implications. The healing response after carbon dioxide laser application in diseased blood vessels has been reported to be quite good (12). Although further investigations will be necessary, we do not expect problems with respect to the vascular healing response after the application of spark erosion because the vaporization and coagulative effects of this technique are comparable with those produced by the carbon dioxide laser. It has also been demonstrated that adequate and rapid healing responses can be obtained after the application of other optimized electrical radiofrequency cutting techniques in dental surgery (13, 14). Apparently the passage of electrical current has no additional significant effect on the tissue healing response.

In conclusion, a low cost and controllable electrical spark erosion technique with great potential for the transluminal vaporization of atherosclerotic lesions has been developed. Before successful *in vivo* application, further studies have to be carried out regarding arterial healing response, controlled production or removal, or both, of gas bubbles and

debris and improvement of catheter guidance to prevent vessel wall perforation.

The assistance of R. H. van Bremen in performing the animal experiments is gratefully acknowledged. We also thank Dr. A. Saltups, Melbourne, Australia for his suggestions and help in improving the manuscript.

References

1. Choy DSJ, Stertzer S, Rotterdam HZ, Bruno MS. Laser coronary angioplasty: experience with 9 cadaver hearts. *Am J Cardiol* 1982;50:1209-11.
2. Abela GS, Normann S, Cohen D, Feldman RL, Geiser EA, Conti CR. Effects of carbon dioxide, Nd-YAG, and argon laser radiation on coronary atheromatous plaques. *Am J Cardiol* 1982;50:1199-205.
3. Lee G, Ikeda R, Herman J, et al. The qualitative effects of laser irradiation on human arteriosclerotic disease. *Am Heart J* 1983; 105:885-9.
4. Goldman L. *Applications of the Laser*. Cleveland, OH: CRC Press, 1973:156.
5. Eldar M, Battler A, Neufeld HN, et al. Transluminal carbon dioxide-laser catheter angioplasty for dissolution of atherosclerotic plaques. *J Am Coll Cardiol* 1984;3:135-7.
6. Lane RJ, Wynne JJ. Medical applications of excimer lasers. *Lasers and Applications* 1984;3:59-62.
7. Kaplan R. YAG lasers in breakdown mode surgery. *Lasers and Applications* 1984;3:53-7.
8. Hall RR, Beach AD, Baker E, Morison PCA. Incision of tissue by carbon dioxide laser. *Nature* 1971;232:131-2.
9. Honig WM. The mechanism of cutting in electrosurgery. *IEEE Trans Biomed* 1975;22:58-62.
10. Sanborn TA, Faxon DP, Haudenschild CC, Ryan TJ. Laser radiation of atherosclerotic lesions: decreased incidence of vessel perforation with a fiberoptic laser heated metallic tip (abstr). *J Am Coll Cardiol* 1984;3:490.
11. Lee G, Ikeda RM, Chan MC, et al. Dissolution of human atherosclerotic disease by fiberoptic laser heated metal cautery cap. *Am Heart J* 1984;107:777-8.
12. Gerrity RG, Loop FD, Golding LAR, Ehrhart LA, Argenyi ZB. Arterial response to laser operation for removal of atherosclerotic plaques. *J Thorac Cardiovasc Surg* 1983;85:409-21.
13. Oringer MJ. *Electrosurgery in Dentistry*. Philadelphia: WB Saunders, 1975:1090.
14. Eisenmann D, Malone WF, Kusck JK. Electron microscopic evaluation of electrosurgery. *Oral Surg* 1970;29:660-5.

CHAPTER 3

ELECTRICAL IMPEDANCE OF LAYERED ATHEROSCLEROTIC PLAQUES ON HUMAN AORTAS

Cornelis J. Slager, Anton C. Phaff, Catharina E. Essed, Nicolaas Bom,
Johan C.H. Schuurbiers, Patrick W. Serruys

Electrical Impedance of Layered Atherosclerotic Plaques on Human Aortas

Cornelis J. Slager, Anton C. Phaff, Catharina E. Essed, Nicolaas Bom, Johan Ch. H. Schuurbiens, and Patrick W. Serruys

Abstract—Electrical impedance measurements were performed on 13 atherosclerotic human aortic segments at 67 measuring spots in order to determine whether or not on the basis of these data a distinction can be made between atherosclerotic lesions and normal tissue. Stenosis localization and guidance of interventional techniques could be among the applications of an impedance measuring technique implemented on a catheter system.

The experimental results, obtained with a two-electrode measuring technique, show that the apparent resistivity of an atherosclerotic spot does not necessarily deviate much from the resistivity of normal tissue. This is clarified by histology which shows that the majority of lesions has a surface layer of connective, fibrous tissue having almost similar conducting properties as the normal arterial wall. For gaining a deeper understanding of the way in which the measured data come about, a physical model of an atherosclerotic lesion is presented and confronted with the data. Both experimental data and theoretical considerations lead to the conclusion that only when the superficial fibrous layer is absent or very thin in relation to the size of the measuring electrode, the measured resistivity at a lesion is much higher than at normal spots. This occurs as a consequence of the high ohmic properties of the calcified or lipid deposits in the atherosclerotic lesion.

INTRODUCTION

IN recent years much effort has been put in laser recanalization of obstructed atherosclerotic arteries [1]–[3]. Lately, we proposed an alternative technique for vaporizing atherosclerotic plaque: spark erosion [4]. Both techniques, laser vaporization as well as spark erosion, hardly discriminate between atherosclerotic plaque and normal vessel wall, thus carrying the risk of vessel wall perforation [5], [6]. Therefore, sensing techniques must be developed in order to control that only atherosclerotic tissue is attacked. The most obvious way to tackle the problem is to look for physical properties that distinguish atherosclerotic tissue from normal tissue. In the case of spark erosion it seems natural to look for differences in electrical properties in much the same way as it is natural to look for differences in optical properties in the case of

the laser [7]–[11]. This is one of the reasons why we decided to perform a study on the electrical impedance of atherosclerotic human aortic segments. Data on this subject are also needed for a better understanding of spark erosion and other new radiofrequency recanalization [12] and remodeling [13] techniques as well as for developing new intra-arterial impedance measuring methods [14].

METHODS AND MATERIALS

One of the main problems in impedance studies is the choice of electrodes. For our purposes we need an electrode that measures impedance at small spots and that is easily applicable on rather irregular surfaces. As the deposition of atherosclerotic plaque along the endothelial surface does not show a regular characteristic pattern it is not expected that anisotropy of its electrical conductance, if present at all, will be predictive for the type of tissue. For these reasons we considered the use of a four electrode impedance measuring method [15] not mandatory. Thus, for the present study we confined ourselves to the much easier to handle two electrode system. The locality of measurement is achieved by using a small spot electrode (area $\approx 0.1 \text{ mm}^2$) in conjunction with a large plate electrode (area $\approx 4 \text{ cm}^2$). The spot electrode consists of a small cavity in connection to a syringe filled with saline. This cavity contains a wrapped up piece of stainless steel foil ($\approx 2 \text{ cm}^2$), which is connected to an electrical lead. The connection with the spot of measurement is established by means of a capillary salt-bridge (Fig. 1). The complete electrode is fixed onto a vertical translation system by means of which it can be positioned against the measuring spot. The main advantages of this construction are firstly, a well-defined, stable metal–electrolyte interface of negligible impedance and secondly, a good and reproducible electrical contact with the measurement spot. The stainless steel plate electrode was glued onto the bottom of a Petri dish and connected to the second electrical lead.

Segments of human aorta (area $\approx 25 \text{ cm}^2$) were obtained at 13 autopsy procedures, stored at 4°C under a saline (0.9%) wetted gaze, and used within 24 h. For measurements, the samples were placed upon the saline wetted plate electrode, thus ensuring a good electrical contact between electrode and sample. Next, applying a slight pressure, the spot-electrode was brought in contact

Manuscript received April 30, 1990; revised July 12, 1991. This work was supported in part by the Netherlands Heart Foundation Grant 84.073 and the Inter University Cardiology Institute of the Netherlands.

C. J. Slager, C. E. Essed, and J. Ch. H. Schuurbiens are with Thoraxcenter, University Hospital Rotterdam-Dijkzigt, 3000 DR, Rotterdam, The Netherlands.

A. C. Phaff, N. Bom, and P. W. Serruys are with Thoraxcenter, Erasmus University Rotterdam, 3000 DR, Rotterdam, The Netherlands.

IEEE Log Number 9106410.

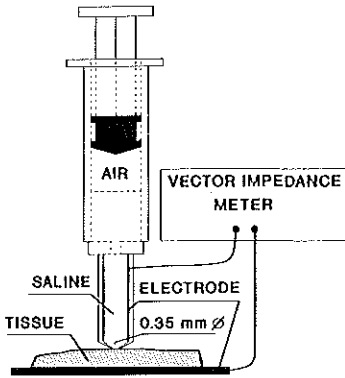


Fig. 1. Outline of the experimental setup.

with a well-chosen spot on the top-surface of the sample. Care was taken not to moisten the top-surface of the sample. Saline leakage from the cavity could be prevented by applying an air buffer above the fluid. The impedance between the electrodes was measured by means of an HP 4800A vector impedance meter at frequencies ranging from 5 to 500 kHz and at room temperature (21–23°C). Immediately after the measurement a slight circular impression surrounding the measuring spot could be observed, caused by the electrode's rim. Concentric with this mark a wider circle was drawn by a marking pencil and a map of the aortic segment was sketched to identify and label each measuring spot. For histologic examination strips of tissue were excised from the aortic segments, each containing one measuring spot in the midst. Subsequently, two transverse superficial incisions were made on the strip at equal distance of a few mm from the spot. Thus, the histologic section to be taken through the midst of the strip will show the cross section of the measuring spot just between the two easy identifiable transverse cuts. Staining was performed with hematoxylin-eosin and elastic-van Gieson. The histologic examination was meant to quantify the tissue composition in terms of tissue types and tissue thickness. Part of the measured impedance is caused by the saline path inside the spot-electrode itself. The impedance of the spot-electrode was measured separately by bringing the tip of the electrode in direct contact with the return electrode. At sufficiently high measuring frequencies, the impedance of the metal-electrolyte interface at the plate electrode vanishes [16] and we are left with the ohmic resistance of the salt bridge. Most measurements were carried out with an electrode having a salt bridge resistance of 2.38 kOhm at an electrode aperture of 0.35 mm.

In order to gather an idea about accuracy and reliability of the measuring methods, measurements were done on a saline gel (thickness 5 mm) with known ohmic resistance. For a gel of infinite thickness, the relation between the measured resistance (R), the aperture (d) and the resistiv-

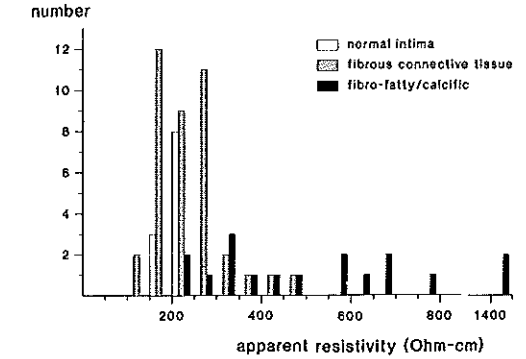


Fig. 2. Distribution of the apparent resistivity at 67 measuring spots subdivided on basis of the type of tissue contacting the measuring electrode.

ity (ρ) is [17]:

$$\rho = 2d \cdot R. \tag{1}$$

Repeated measurements of the gel resistance by means of the spot-electrode on the same day showed a mean variation of about 2%. As has been observed by microscopy, the aperture of the spot electrode could be deformed slightly over the course of the study. Thus, day-to-day variations could deviate by almost 10%. In order to account for most sources of error in the estimation of the electrode's aperture we performed a calibration procedure on the gel preceding each series of measurements and calculated an apparent aperture d_{app} for each series of tissue impedance measurements, according to:

$$d_{app} = \rho/2R \tag{2}$$

where ρ is the known resistivity and R the measured resistance of the gel.

EXPERIMENTAL RESULTS

Impedance was measured at 67 different spots on 13 aortic segments. Each spot was measured a number of times in succession with repeated positioning of the spot electrode. The mean spread in the outcome of the measurements on the same spot did not exceed 5%. As a function of frequency the impedance varied less than 3% and was practically resistive as indicated by the phase angle that never exceeded 4°. After correcting for the salt bridge resistance, the measured resistances ranged from 2 to 30 kOhm.

In practice, it will be convenient to work with an apparent resistivity rather than with the measured resistance. This apparent resistivity ρ_{app} is defined by

$$\rho_{app} = 2d_{app} \cdot R. \tag{3}$$

For a homogeneous medium of large thickness (i.e., $\gg d_{app}$), ρ_{app} will equal the resistivity of the medium.

TABLE I
EXAMPLE OF DATA OBTAINED FROM ONE AORTIC SEGMENT SHOWING DIFFERENT TYPES OF TISSUE

| Spot | Tissue Type and Thickness (mm) | | | Resistance (Ohm) | Apparent Resistivity (Ohm · cm) | Resistivity of layer 1 (Ohm · cm) |
|------|--------------------------------|---------|---------|------------------|---------------------------------|-----------------------------------|
| | Layer 1 | Layer 2 | Layer 3 | | | |
| A | n 0.21 | 0 | m 1.14 | 2520 | 171 | 169 |
| B | ct 0.67 | f 0.84 | m 0.80 | 3450 | 235 | 217 |
| C | ct 0.61 | f 0.52 | m 0.85 | 3820 | 260 | 246 |
| D | ff 0.12 | ct 0.16 | m 1.27 | 4850 | 330 | 415 |
| E | ff 0.24 | ct 0.15 | m 1.14 | 9650 | 656 | 820 |
| F | ct 1.33 | 0 | m 0.98 | 3420 | 233 | 240 |
| G | ct 0.82 | f 1.17 | m 0.97 | 4190 | 285 | 269 |
| H | n 0.20 | 0 | m 1.19 | 3590 | 244 | 265 |
| I | f 0.54 | ct 0.23 | m 1.14 | 21120 | 1436 | 1626 |

Abbreviations: *ct*: fibrous connective tissue, *f*: fat, *ff*: fibro-fatty, *m*: media, *n*: normal intima.

The group of 67 measuring spots may be divided into three classes consisting of 11 normal spots, 39 atherosclerotic spots characterized by a top layer of fibrous connective tissue, and 17 atherosclerotic spots without such a fibrous cap, showing fatty and calcific components in its superficial layer. The distribution of the apparent resistivity in these classes is shown in Fig. 2. The apparent resistivity of the normal spots is localized between 150 and 250 $\Omega \cdot \text{cm}$, whereas the apparent resistivity of the atherosclerotic spots covers a much wider range from 100 $\Omega \cdot \text{cm}$ up to 1450 $\Omega \cdot \text{cm}$. From the histograms it follows that most of the atherosclerotic lesions belonging to the group with a fibrous top layer have an almost normal apparent resistivity.

To gain insight into the results and their interpretation we will discuss a representative example out of the series of 13 aortic segments. On this sample nine well chosen spots were measured. Histologic examination revealed that in most cases the intima was thickened and displayed a layered structure. The histologic findings and the measured values of ρ_{app} are presented in Table I and Fig. 3. For the photograph, hematoxylin-eosin stained sections were selected, which provide the best discrimination between fatty and fibrous tissue components. Only a part (length 2 mm) of the sections covering the measuring spot, has been displayed.

From Table I it is clear that the apparent resistivity of a true atherosclerotic lesion (e.g., B, C) does not necessarily deviate much from the apparent resistivity of a comparatively normal aortic wall (A and H). However, there are also atherosclerotic spots (e.g., D, E) with negligible intima thickening, which have an apparent resistivity that is far greater than the apparent resistivity of a normal spot. The high-resistivity lesions always show fat or calcified deposits being incorporated in the superficial layers, whereas the superficial layer of the low resistivity lesions always consists of pure fibrous connective tissue. This indicates that the apparent resistivity is determined to a high degree by the resistivity of the superficial layer, which is high in case of fat and low in case of connective tissue.

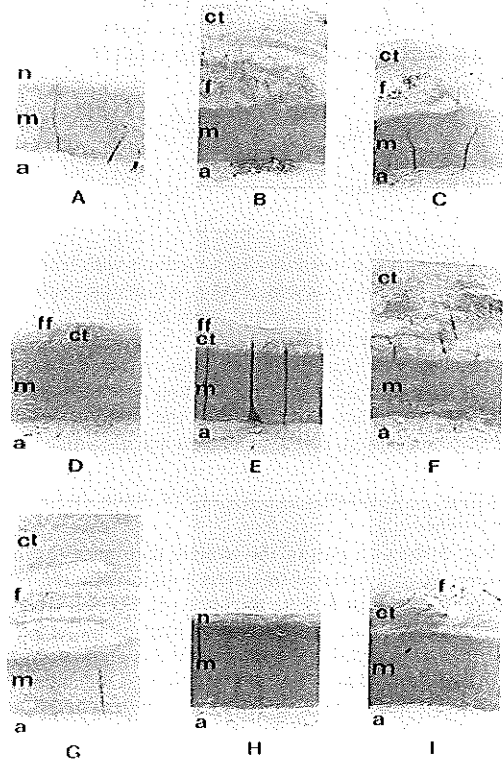


Fig. 3. Histologic sections (displayed length 2 mm) through the aortic wall at nine measuring spots (hematoxylin-eosin stain). Labeling corresponds with Table I. *a*: adventitia, *ct*: fibrous connective tissue, *f*: fat, *ff*: fibro-fatty, *m*: media, *n*: normal intima.

THEORETICAL MODEL

For the purpose of gaining a deeper understanding of the way in which the measured results come about, we will describe a physical model of an atherosclerotic lesion contacted by a two electrode measuring system.

Consider a medium consisting of N layers material of different composition and therefore of different resistivity. The superficial layer is brought into contact with a spot-electrode of aperture d , whereas the remaining surface of this layer is bordered by some medium of infinite resistivity. The bottom layer contacts a medium of finite resistivity, which, for our calculations, supposedly extends to infinity. This medium may be considered as the return electrode (Fig. 4). By definition the zero electrical potential is at infinity. Applying a voltage V to the spot-electrode will impress a current I into the compound medium. Our aim is to compute the electrical resistance (i.e., the ratio V/I) of this configuration.

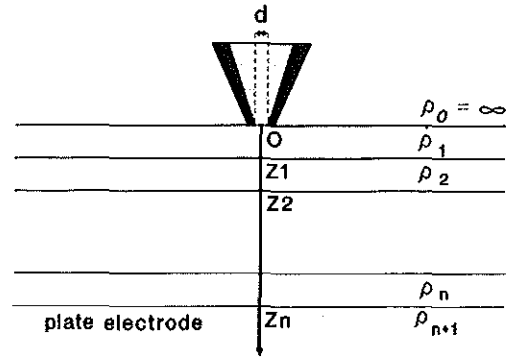


Fig. 4. Physical model of an atherosclerotic lesion between spot-electrode and plate-electrode.

For the most accurate solution of this problem one probably has to resort to the method of finite elements. However, we followed an analytical approach which closely approximates the exact solution. The derivation of this approximate solution is further clarified in the Appendix. Here, we only state the final result for the resistance R :

$$R = R_{\text{inf}} \frac{4}{\pi} \int_0^{\infty} F(x) \frac{\sin x}{x^2} J_1(x) dx \quad (4)$$

where by definition:

$$R_{\text{inf}} = \rho_1/2d. \quad (5)$$

R_{inf} represents the resistance of a medium with resistivity ρ_1 and of infinite thickness. $F(x)$ is a function containing information about the layered medium and $J_1(x)$ is the first order Bessel function.

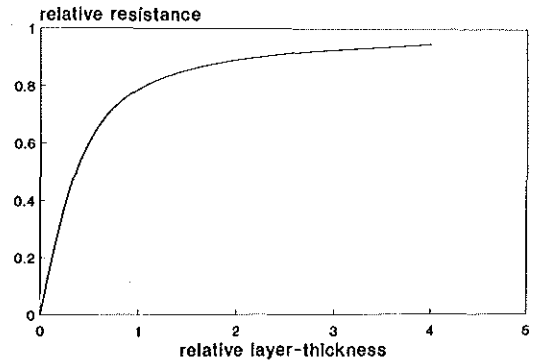


Fig. 5. The relative resistance of a homogeneous medium in dependence on the layer thickness/aperture ratio.

Next we describe the application of this theoretical model for a medium consisting of three layers, to present two examples that will elucidate the relation between plaque morphology and composition and electrode size.

Example 1: Resistance in Dependence on the Layer Thickness

Fig. 5 shows a plot of the relative resistance (i.e., resistance R of a layer of thickness t divided by the resistance of a layer of infinite thickness R_{∞}) versus the relative thickness (i.e., thickness t divided by the electrode aperture d). A relative resistance of 0.8 is already reached at a relative thickness of 1, indicating that the major part of the resistance is built up in the near vicinity of the spot-electrode. Here we note that the thickness of the samples was at least twice the electrode aperture and that the thickness (5 mm) of the gel, used for the calibration of the electrode's aperture, amply suffices.

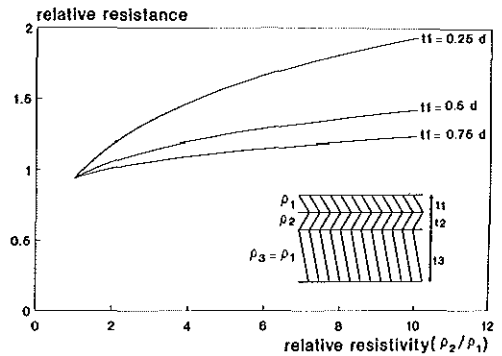


Fig. 6. The relative resistance of a layered medium in dependence on the resistivity of the middle layer for three thicknesses (t_1) of the superficial layer related to the electrode aperture d .

Example 2: Resistance in Dependence on the Resistivity of the Middle Layer

Fig. 6 shows a plot of the relative resistance R/R_{∞} (with $R_{\infty} = \rho_1/2d$) of a medium consisting of three layers, with thicknesses t_1 , t_2 , and t_3 , as a function of the resistivity of the second (middle) layer, assuming that $\rho_1 = \rho_3$. The three curves correspond with different thicknesses of the superficial layer t_1 being $0.25d$, $0.50d$, and

$0.75d$ with d being the electrode's aperture. In order to let these curves originate from the same position, the total thickness $t_1 + t_2 + t_3$ is kept at $3.75d$ and $t_2 = 0.75d$. From this figure it is clear that at increasing superficial layer thickness the sensitivity of the resistance to changes

in ρ_2 tends to decrease. It may be stated that for $t_1 \geq 0.75d$ the upper layer quite effectively shields the underlying layers from the spot-electrode.

These two numerical examples evidently show that the measured tissue resistance will be most sensitive to the resistivity of the superficial layer, which is clearly in support of the findings of our measurements.

APPLICATION OF THE MODEL

We analyzed our resistance data in terms of the above described three-layer model in order to see whether the spread in the apparent resistivity can be explained from the way in which the atherosclerotic plaques are composed as layered structures of different tissue types. As no separate impedance data of each type of tissue are available, our way to perform this analysis, is to make a reasonable estimate as to the resistivity of the underlying layers (connective tissue, media) and then to adjust the resistivity of the superficial substance of each measuring spot until the measured and the computed resistances match. For the tissue sample described in Table I the following estimated resistivities of the underlying layer have been applied:

$$\rho_{\text{connective tissue}} = \rho_{\text{media}} = 235 \Omega \cdot \text{cm}. \quad (6)$$

Throughout the calculations the impedance of a fourth layer, the adventitia, which contacted the saline wetted return plate electrode (4 cm^2), has been neglected. The estimated contribution of this layer (thickness $< 0.5 \text{ mm}$), to the measured resistance is less than 1%. Assuming (6), it necessarily follows from the resistance at spot I that $\rho_{\text{fat}} = 1626 \Omega \cdot \text{cm}$. This value for ρ has been used for the enclosed fatty layers in spots B , C and G . In the last column of Table I, the resistivity values of the superficial tissue layer are tabulated as obtained by the above described method. Apparently the resistivity values of the superficial fibro-fatty layers (D , E) change most while the mean resistivity value for connective tissue (A , B , C , F , G , H) equals $234 \Omega \cdot \text{cm}$ which affirms our first estimation. The presence of fat under the intimal connective tissue layer has only a minor influence on the apparent resistivity as can be derived from the data at spots B , C , and G . As suggested by Fig. 2 the apparent resistivity of fibrous tissue covering plaques is somewhat higher than the apparent resistivity of the normal intima. However, when comparing the true resistivities of both types of tissue the outcome may be different. To allow such a comparison to be made in a quantitative way we applied the model on the data of those sites depicted in Fig. 2 which are characterized by either a normal intima or a superficial layer of fibrous connective tissue. The following assumptions were used: the resistivity of fat is $1600 \Omega \cdot \text{cm}$ and the resistivity of the media is equal to the resistivity of the top layer. The results of this approach are depicted in Fig. 7. The similarity of the resistivities of both groups of tissue has increased as a result of this operation. However, as already suggested by the curves shown in Figs. 5 and 6, the effect of this operation is small.

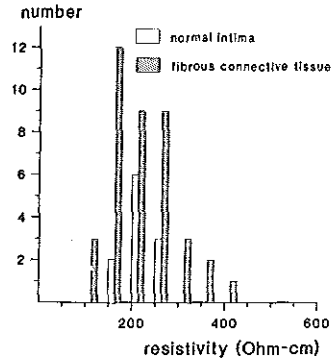


Fig. 7. Distribution of the resistivity of the superficial tissue layer at eleven normal spots and at 39 spots showing fibrous connective tissue, after application of our model (see text and Fig. 2).

DISCUSSION

The present study was undertaken as a first step in the evaluation and modeling of electrical impedance as a potential diagnostic parameter to characterize the differences between the normal and atherosclerotic parts of the arterial wall. A simple two-electrode measuring system was selected as this would reduce positioning problems of the electrode on the rather inhomogeneous and wavy surface of the diseased endothelium. Under these circumstances a four-electrode technique [15] seemed to us more difficult to handle. The major advantage of a four-electrode technique would be the inherent elimination of the impedance of the metal-electrolyte interface. However, a similar function could also be obtained with the two-electrode system, by the addition of a salt bridge.

From the measurement results it can be learned that the data obtained with the two-electrode measuring technique, before correcting for the layered nature of the lesions, provide directly a reasonable estimate of the resistivity of the contacted tissue. This local sensitivity feature, to be predicted on theoretical grounds for a nonsymmetrical two electrode set up, is highly appreciated. Thus, directly decisive impedance data may be obtained of the contacted tissue layer being considered for removal by an ablation technique. Whether impedance measuring techniques will be applicable for vascular tissue characterization *in vivo* depends on the ability to achieve a proper contact with the surface to be investigated. The potential shunting of current by blood will lower the detectability of differences in tissue impedance. Substitution of blood by low-conducting fluid would reduce this problem but has practical drawbacks. Obviously, the measurement of blood resistivity itself will be the easiest to perform, while the presented model and data of the vascular resistivities will be useful to give an indication of the expected accuracy of this application under varying circumstances [14]. The overlap in impedance of diseased and normal arterial wall must be minimal to provide a useful basis for guidance of intravascular tissue removal techniques. For practical reasons the current investigation was restricted to

aortic segments. Relatively few lesions showed a clear deviation in resistance from normal. The majority of obstructive lesions, having a superficial cap of fibrous connective tissue, show impedance values in the normal range. Unfortunately, the resistivity of fibrous connective tissue turns out to be almost equal to the resistivity of the normal arterial wall. Whether the detectability of impedance differences improves when studying muscular arteries like the coronary arteries is yet unknown. The normal media of such arteries contains less extracellular connective tissue components like elastin and collagen and a substantial layer of smooth muscle cells. This could theoretically lead to lower normal resistance values. However, the common thickening of the intima at higher age, by fibrous connective tissue addition, may well be sufficient to neutralize this potential advantage. Notable differences between morphology and composition of aortic and coronary plaque are unknown to us. Only the impression exists that ulcerating plaques, missing a fibrous cap, are more frequently seen in the larger elastic arteries than in the smaller muscular type of arteries.

Application of the presented model appeared to be very useful to get a quantitative insight in the parameters determining the sensitivity of the measurement in dependence on the resistivity of the different tissue layers. It also allowed to make a reasonable estimation of the specific resistivity of the contacted tissue layers. Since to our knowledge no data have been published before on the resistivity of atherosclerotic plaques we could not compare most of our findings with data obtained by others. Fat tissue is reported [18] to have a resistivity in the range of 1100–5000 $\Omega \cdot \text{cm}$. Except for one superficial true fatty lesion with a resistivity over 1600 $\Omega \cdot \text{cm}$ falling within this range (Table I) and one calcified lesion with an apparent resistivity over 1400 $\Omega \cdot \text{cm}$ the remaining 15 lesions without a fibrous cap (Fig. 2) had lower apparent resistivities ranging from 200 to 800 $\Omega \cdot \text{cm}$. The tissue composition of the latter group showed a mixture of fibrous and fatty parts which explains its resistivity varying between the value of fibrous connective tissue and that of the true fatty lesion. A tissue type coming close to fibrous connective tissue may be human skin tissue. The resistivity of human skin tissue measured at room temperature and at a frequency of 1 MHz is reported to be 289 $\Omega \cdot \text{cm}$ [18]. An estimate of the specific resistance of vein, pulmonary artery and bronchus is reported to vary from 250 to 700 $\Omega \cdot \text{cm}$ [19]. These data compare well with our findings depicted in Fig. 7.

We conclude that our model is very helpful in understanding the characteristics of impedance measurements on layered tissue structures. Generally, the impedance of the layer contacting the measuring electrode will dominate the measured impedance. Constituting atherosclerotic plaque components like fatty and calcified tissues appear to have a much higher resistivity than normal arterial wall. However, in most cases these components are covered by fibrous tissue with a resistivity not much deviating from normal. Therefore it appears to us that only

a limited number of lesions may be recognized by *in vivo* applicable impedance measuring methods.

APPENDIX

Derivation of equations describing the resistance of layered atherosclerotic plaques measured by a two-electrode technique using an analytical approach.

As suggested by the symmetry of our problem, we use cylindrical coordinates (r, φ, z) to describe our problem (see Fig. 4). The potential distribution $\varphi_i(r, z)$ in each layer has to obey Laplace's equation:

$$\varphi_i(r, z) = 0 \quad \text{for } i = 1, 2, \dots, N + 1. \quad (\text{A1})$$

At the interfaces the potential must be continuous and so must be the normal component of the current-density

$$\varphi_i(r, z) = \varphi_{i+1}(r, z) \quad \text{for } z = z_1, \dots, z_N \quad (\text{A2})$$

$$\sigma_i \frac{\delta \varphi_i(r, z)}{\delta z} = \sigma_{i+1} \frac{\delta \varphi_{i+1}(r, z)}{\delta z}$$

$$\text{for } z = z_i, i = 1, \dots, N$$

$$\text{where } \sigma_i = 1/\rho_i. \quad (\text{A3})$$

Through the surface of the top-layer no current can pass except at the electrode which is maintained at the potential V

$$\varphi_1(r, z) = V \quad \text{for } 0 \leq r < a \text{ and } z = 0 \quad (\text{A4})$$

$$\frac{\delta \varphi_1(r, z)}{\delta z} = 0 \quad \text{for } a \leq r < \infty \text{ and } z = 0 \quad (\text{A5})$$

where a = the radius of the electrode, $2a = d$. Furthermore, the potentials φ_i must vanish at infinity. Thus, everywhere on a closed surface, partly at infinity, either the potential or its normal derivative is specified and therefore a unique, stable solution exists inside this surface.

The solution of (A1) yields [20]–[22].

$$\varphi_i(r, z) = \int_0^\infty \{A_i(k)e^{-kz} + B_i(k)e^{kz}\} J_0(kr) dk \quad (\text{A6})$$

where J_0 is the Bessel function of zero order and where the coefficients $A_i(k)$ and $B_i(k)$ have to be determined from the boundary conditions.

The mixed boundary conditions lead to a pair of dual integral equations, for which, to our knowledge, no analytical solution is available. Therefore, in order to proceed with our analysis, we have to resort to some method of approximation. This can be done by replacing the boundary condition (A4), which prescribes the potential at the electrode by a boundary condition which prescribes the current density at the electrode according to

$$\sigma_1 \left. \frac{\delta \varphi_1(r, z)}{\delta z} \right|_{z=0} = \frac{I}{2\pi a} \frac{1}{\sqrt{a^2 - r^2}} \quad \text{for } 0 \leq r < a. \quad (\text{A7})$$

This is the current density that would exist in case of a homogeneous medium extending to infinity. The validation of the replacement of boundary condition (A4) by boundary condition (A7) will be discussed later on. Again the new boundary equations result in a pair of dual integral equations:

$$\int_0^{\infty} \{A_1(k) - B_1(k)\} J_0(kr) k dk = 0 \quad (A8)$$

for $a \leq r < \infty$

$$\sigma_1 \int_0^{\infty} \{A_1(k) - B_1(k)\} J_0(kr) k dk = \frac{I}{2\pi a} \frac{1}{\sqrt{a^2 - r^2}} \quad (A9)$$

for $0 \leq r < a$.

The solution to these equations is well known [20]–[22] and reads

$$A_1(k) - B_1(k) = \frac{I}{2\pi\sigma_1} \frac{\sin ka}{ka}. \quad (A10)$$

In order to fulfil the boundary conditions at infinity it is necessary that $B_{N+1} = 0$. Now the interface conditions together with the boundary conditions provide us with $2N + 1$ inhomogeneous equations for the $2N + 1$ unknowns $A_1, B_1, A_2, \dots, A_N, B_2, \dots, B_N$ and A_{N+1} . These equations are solved by straightforward computation using Cramer's rule.

The potential at the surface $z = 0$ is given by

$$\varphi_1(r, 0) = \int_0^{\infty} \{A_1(k) + B_1(k)\} J_0(kr) dk. \quad (A11)$$

As a consequence of the replacement of boundary condition (A4) by boundary condition (A7), this potential does not have a constant value throughout the electrode.

In order to be able to define a unique resistance we must average this potential over the surface of the electrode

$$\langle V \rangle = \frac{1}{\pi a^2} \int_0^a 2\pi r \varphi_1(r, 0) dr. \quad (A12)$$

The resistance R is now obtained as $R = \langle V \rangle / I$, which may be written

$$R = \frac{1}{4a} \frac{4}{\pi} \int_0^{\infty} F(x) \frac{\sin x}{x^2} J_1(x) dx \quad (A13)$$

with $F(x)$ defined by

$$F(x) = \frac{A_1(x/a) + B_1(x/a)}{A_1(x/a) - B_1(x/a)}. \quad (A14)$$

All information about thickness and resistivity of the layers is contained in this function. We will write down $F(x)$ explicitly for $N = 3$

$$F(x) = \frac{\beta(\delta + h)(\epsilon + \beta nm) + \delta(\delta h + 1)(\epsilon m + \beta n)}{\beta(\delta - h)(\epsilon + \beta nm) + \delta(\delta h - 1)(\epsilon m + \beta n)} \quad (A15)$$

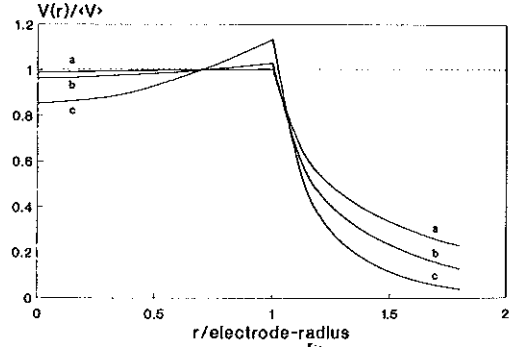


Fig. 8. Normalized potential profile over the electrode and over the surface of the top layer as obtained by our model. The curves *a*, *b*, and *c* correspond to different ratios of aperture/layer thickness being 1, 2, and 4, respectively.

where the following definitions hold

$$h = \frac{\sigma_1 - \sigma_2}{\sigma_1 + \sigma_2} \quad \delta = \exp(2xz_1/a)$$

$$m = \frac{\sigma_2 - \sigma_3}{\sigma_2 + \sigma_3} \quad \beta = \exp(2xz_2/a)$$

$$n = \frac{\sigma_3 - \sigma_4}{\sigma_3 + \sigma_4} \quad \epsilon = \exp(2xz_3/a)$$

If $\sigma_1 = \sigma_2 = \sigma_3 = \sigma_4$ then $h = m = n = 0$ and it follows that $F(x) = 1$. Inserting $F(x) = 1$ in formula (A13) one obtains for the resistance $R = \rho_1/2d$, that is Maxwell's classical result is restored.

Our ultimate aim is the evaluation of the right-hand side of expression (A13). This can be done numerically, making use of NAG-library routines for quadrature as well as the first order Bessel function.

Here it is worthwhile to note that, after our computations, we became aware of the fact that our problem carries much similarity with a problem from geophysics as reported already in 1930 by Stefanescu *et al.* [23]. They solved part of the present problem (i.e., the potential distribution over the top-surface) for an electrode with aperture $d = 0$, that is a point-electrode. The validation of the replacement of boundary condition (A4) by boundary condition (A7) will now be discussed. The most obvious way to do this, is to look how the potential at the electrode behaves under the impression of the current distribution as described by condition (A7). For several layer-thicknesses the potential profile; i.e., $V(r)$ as a function of r has been computed using formula A11. In order to obtain a normalized result, each potential profile was divided by the appropriate mean voltage $\langle V \rangle$. The results are depicted in Fig. 8 for three different layer-thicknesses, being $d, 0.5d$, and $0.25d$, with d being the electrode's aperture. The deviation of $V(r)$ from $\langle V \rangle$ may serve as a measure of the reliability of our method of computing resistances. Even at an aperture of four times the layer-thickness the potential does not deviate more from $\langle V \rangle$ than 15%. So

in this case we estimate the error in the resistance R to be less than 15%. Fortunately, in our measurements situations with aperture larger than medium-thickness rarely occurred and therefore the applied approximation adequately serves our purpose and will not introduce errors of importance.

REFERENCES

[1] G. S. Abela, S. J. Normann, D. Cohen, R. L. Feldman, E. A. Geiser, and C. R. Conti. "Effects of carbon dioxide, Nd-YAG, and argon laser radiation on coronary atheromatous plaques," *Amer. J. Cardiol.*, vol. 50, pp. 1199-1205, 1982.

[2] G. Lee, R. Ikeda, I. Herman, R. M. Dwyer, M. Bass, H. Hussein, J. Kozina, and D. T. Mason. "The qualitative effects of laser irradiation on human arterio-sclerotic disease," *Amer. Heart J.*, vol. 105, pp. 885-889, 1983.

[3] J. M. Isner, R. F. Donaldson, L. I. Deckelbaum, R. H. Clarke, S. M. Laliberte, A. A. Ucci, D. N. Salem, and M. A. Konstam. "The excimer laser: Gross, light, microscopic and ultrastructural analysis of potential advantages for use in laser therapy of cardiovascular disease," *J. Amer. Coll. Cardiol.*, vol. 6, pp. 1102-1109, 1985.

[4] C. J. Slager, C. E. Essed, J. C. H. Schuurbiens, N. Bom, P. W. Serruys, and G. T. Meester. "Vaporization of atherosclerotic plaques by spark erosion," *J. Amer. Coll. Cardiol.*, vol. 5, pp. 1382-1386, 1985.

[5] G. Lee, R. M. Ikeda, M. C. Chan, M. H. Lee, J. L. Rink, R. L. Reis, J. H. Theis, R. Low, W. J. Bommer, A. H. Kung, E. S. Hanna, and D. T. Mason. "Limitations, risks and complications of laser recanalization: A cautious approach warranted," *Amer. J. Cardiol.*, vol. 56, pp. 181-185, 1985.

[6] J. M. Isner and R. H. Clarke. "Laser angioplasty: Unravelling the Gordian knot," *J. Amer. Coll. Cardiol.*, vol. 7, pp. 705-708, 1986.

[7] M. R. Price, T. F. Deutsch, M. M. Matthews-Roth, R. Margolis, J. A. Parrish, and A. R. Oseroff. "Preferential light absorption in atheromas *in vitro*," *J. Clin. Invest.*, vol. 78, pp. 295-301, 1986.

[8] M. J. C. van Gemert, R. Verdaasdonk, E. G. Stassen, G. A. C. M. Schets, G. H. M. Gijssbers, and J. J. Bonnier. "Optical properties of human blood vessel wall and plaque," *Lasers Surg. Med.*, vol. 5, pp. 235-237, 1985.

[9] P. M. Selzer, D. Murphy-Chutorian, R. Ginsburg, and L. Wexler. "Optimizing strategies for laser angioplasty," *Invest. Radiol.*, vol. 20, pp. 860-866, 1985.

[10] C. Kittrell, R. L. Willet, C. de los Santos-Pacheco, N. B. Ratliff, J. R. Kramer, E. G. Malk, and M. S. Feld. "Diagnosis of fibrous arterial atherosclerosis using fluorescence," *Appl. Opt.*, vol. 24, pp. 2280-2281, 1985.

[11] G. S. Abela, J. M. Seeger, E. Barbieri, D. Franzini, A. Fenech, C. J. Pepine, and C. R. Conti. "Laser angioplasty with angioscopic guidance in humans," *J. Amer. Coll. Cardiol.*, vol. 8, pp. 184-192, 1986.

[12] V. Hombach, M. Höher, G. Arnold, P. Osypka, M. Kochs, T. Egeling, H. W. Höpp, H. Hirche, and H. H. Hilger. "Die Hochfrequenzangioplastie eine neue Methode zur Rekanalisation verschlossener arterieller Gefäße," *Corvas*, vol. 2, pp. 67-73, 1987.

[13] G. J. Becker, B. I. Lee, B. F. Waller, K. J. Barry, J. Kaplan, R. Connolly, R. G. Dreesen, and P. Nardella. "Radiofrequency balloon angioplasty. Rationale and proof of principle," *Invest. Rad.*, vol. 23, pp. 810-817, 1988.

[14] L. W. Martin, R. Zawodny, and R. A. Vogel. "Impedance measurement of absolute arterial diameter using a standard angioplasty catheter," *J. Amer. Coll. Cardiol.*, vol. 11, p. 130A, 1988.

[15] S. Rush, J. A. Abildskov, and R. McFee. "Resistivity of body tissues at low frequencies," *Circ. Res.*, vol. 12, pp. 40-50, 1963.

[16] B. Onaral, H. H. Sun, and H. P. Schwan. "Electrical properties of bioelectrodes," *IEEE Trans. Biomed. Eng.*, vol. 31, pp. 827-832, 1984.

[17] J. C. Maxwell, *A Treatise on Electricity and Magnetism*. 3rd ed. Dover, reprint 1954.

[18] L. A. Geddes and L. E. Baker. "The specific resistance of biological material: A compendium of data for the biomedical engineer and physiologist," *Med. Biol. Eng.*, vol. 5, pp. 271-293, 1967.

[19] H. P. Schwan and C. F. Kay. "Specific resistance of body tissues," *Circ. Res.*, vol. 4, pp. 664-670, 1956.

[20] J. D. Jackson, *Classical Electrodynamics*. New York, Wiley 1962, Ch. 3, p. 54.

[21] I. N. Sneddon, *Mixed Boundary Value Problems in Potential Theory*. Amsterdam: North-Holland, 1966, ch. 4, p. 80.

[22] W. R. Smythe, *Static and Dynamic Electricity*. New York: McGraw-Hill, 1968, ch. 5, p. 121.

[23] S. Stefanescu, C. Schlumberger, and M. Schlumberger. "Sur la distribution électrique potentielle autour d'une prise de terre ponctuelle dans un terrain à couches horizontales, homogènes et isotropes," *J. Physique*, vol. 1, pp. 132-140, 1930.



Cornelis J. Slager was born in Scherpenisse, Zeeland, The Netherlands, in 1945. He received the M.Sc. degree in electrical engineering from Delft University of Technology in 1971. During his graduate work he invented an automated border recognition system for ventriculograms.

After teaching electronics at the Delft University, he joined the Biomedical Technology Group of Delft University of Technology in 1971. During his research interests are in quantitative processing of cardiological images and in diagnostic and therapeutic instruments for interventional cardiology.

and in diagnostic and therapeutic instruments for interventional cardiology.



Anton C. Phaff was born in Amsterdam, The Netherlands, in 1952. He received the M.Sc. degree (summa cum laude) in solid state physics from the Free University of Amsterdam in 1979 and the Ph.D. degree in physics from the Eindhoven University of Technology. His thesis concerned a subject from the magnetism at low temperatures.

During 1986 and 1987 he joined the Biomedical Technology department of the Thoraxcenter, Erasmus University Rotterdam. Today he still

maintains ties with this group.



Catharina E. Essed was born in Amsterdam, The Netherlands, in 1953. She graduated in medicine from the Erasmus University, Rotterdam, in 1978 and specialized in pathology between 1978 and 1983.

During and after her specialization she worked mainly in cardiovascular pathology. Since 1989 she is assigned as a surgical pathologist to the Laboratory for Public Health in Friesland, the Netherlands.



Nicolaas Bom was born at Velsen, The Netherlands, in 1937. He received the M.Sc.-EE degree from the University of Technology, Delft, in 1961 and the Ph.D. from the Erasmus University, Rotterdam, in 1972.

In 1969 he joined the Thoraxcenter of the Erasmus University to set up a diagnostic ultrasound research and development program. Since 1974, he has been head of the Biomedical Engineering Group of the Thoraxcenter. He became Professor of Medical Ultrasound at the Interuniversity Cardiology Institute of the Netherlands (ICIN) and at the Erasmus University Rotterdam in 1979. In 1987 he received a honorary doctorate from the Technological faculty of the University of Lund, Sweden, for his work and inventions in the field of echocardiography.

Dr. Bom has been a member of the Scientific Board and the Board of Directors of ICIN since 1983.



Johan Ch. H. Schuurblers was born in Vlaardingen, The Netherlands, in 1950. He received a degree in electrical engineering from the College of Aeronautics and Electronics, Den Haag in 1972.

Until 1976, while studying electronic engineering, he was involved in industrial engineering. In 1976 he joined the Cardiology Department of the Dijkzigt Hospital as a research technician. His interests are in real-time image processing and analysis techniques, digital/analog hardware, software for biomedical signal processing and data acquisition and technical aspects of interventional cardiology.



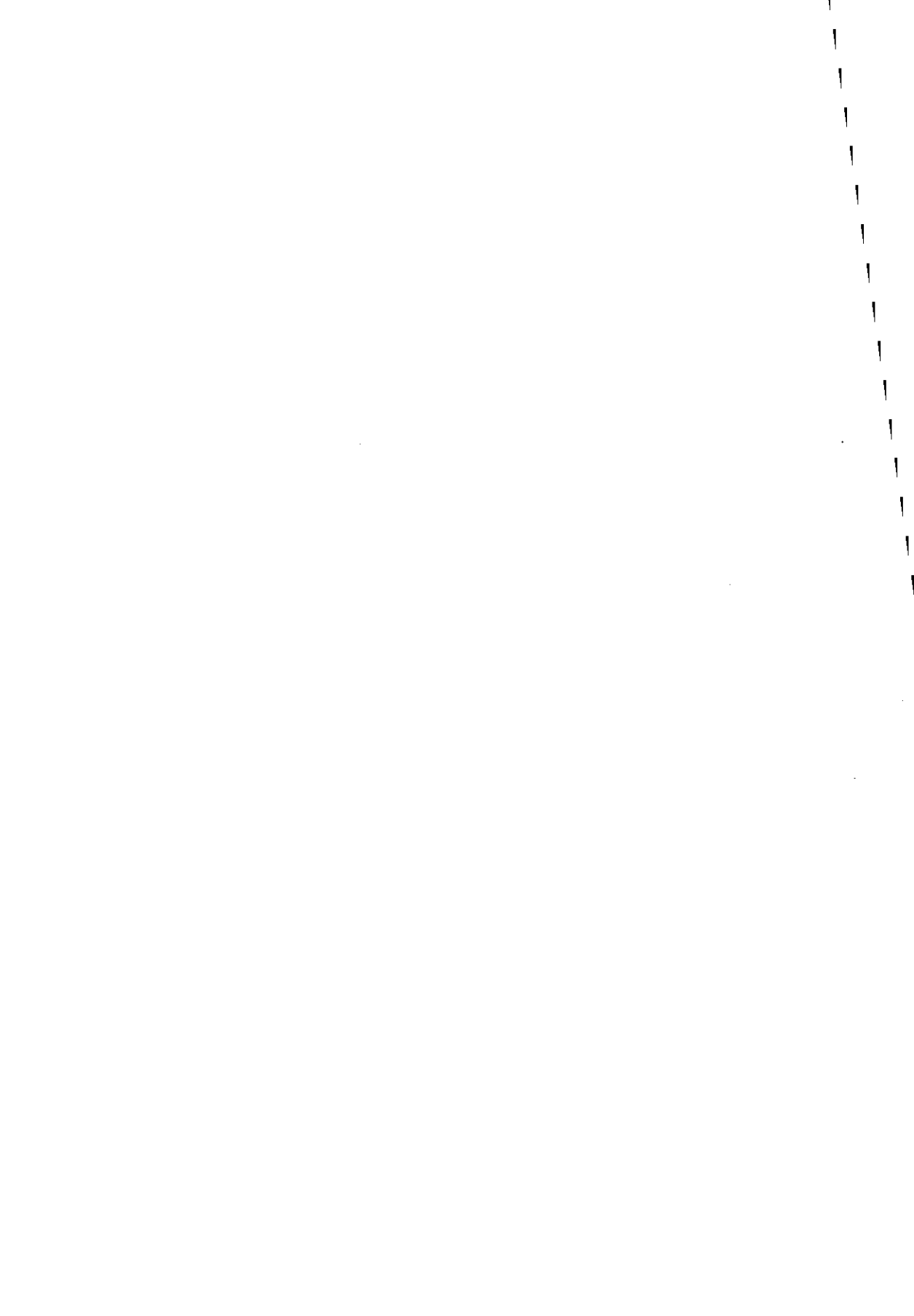
Patrick W. Serruys was born in Brussels, Belgium, in 1947. He received the M.D. degree from the University of Leuven (Belgium) in 1972 and passed the Board of Cardiology in Belgium and the Netherlands in 1976.

He has been the Director of the Clinical Research Program of the Catheterization Laboratory of the Thoraxcenter, Rotterdam, since 1980. He became Professor in Interventional Cardiology at the Erasmus University in 1988 as well as at the Inter University Cardiology Institute of the Netherlands (ICIN). His research interests include coronary artery disease, quantitative angiography, and interventional cardiology.

CHAPTER 4

**INTRA-ARTERIAL ULTRASONIC IMAGING FOR
RECANALIZATION BY SPARK EROSION**

Nicolaas Bom, Cornelis J. Slager, Frans C. van Egmond, Charles T. Lancée,
Patrick W. Serruys



Original Contribution

**INTRA-ARTERIAL ULTRASONIC IMAGING FOR RECANALIZATION
BY SPARK EROSION**

N. BOM, C. J. SLAGER, F. C. VAN EGMOND, C. T. LANCÉE and P. W. SERRUYS
Thoraxcenter, Erasmus University Rotterdam and University Hospital, Rotterdam-Dijkzigt; Interuniversity
Cardiology Institute of the Netherlands, Rotterdam, The Netherlands

(Received 8 July 1987; in final form 26 October 1987)

Abstract—Presently several new methods are being developed to recanalize obstructed arteries during catheterization. Intra-arterial high frequency ultrasonic imaging may be used as a guidance for these new techniques. Spark erosion is a new obstruction removal technology. Experiments have shown that this method can be applied in a selective way. An ultrasonic intra-arterial imaging system allows for the proper indication of the spark erosion catheter relative to the obstruction. The first *in vitro* results of this study illustrate that integration of catheter tip imaging and spark erosion is possible.

Key Words: Intra-arterial ultrasound, Recanalization, Miniature transducers.

INTRODUCTION

New ultrasonic imaging transducers are being developed for application inside the human body. For imaging at close range, high frequencies can be allowed and transducer size can be small. Little has been reported so far on very small transducers capable of imaging from within the human arteries. Nevertheless there exists a major clinical problem that might be solved if a high-quality intra-arterial ultrasonic imaging device were available.

Presently medical treatment for severe obstruction of the coronary arteries is the well known by-pass surgical procedure. A less traumatic recanalization method, introduced by Gruentzig *et al.* (1979) is the percutaneously applicable catheter balloon dilatation technique. With this method, the obstruction is stretched, not removed, by a small balloon that is gradually inflated. In approximately one third of the treated lesions restenosis occurs.

In the medical world many research efforts are directed towards the development of new techniques for complete removal of the obstruction during cardiac catheterization. Complete removal of the obstruction might reduce the occurrence of restenosis. Such techniques should in addition allow treatment of total or partial obstructions not accessible by the current balloon dilatation techniques. In 5–10% of

the treated cases the dilatation procedure is unsuccessful. Dilatation cannot be achieved if the balloon cannot pass the obstruction. In some other cases, notwithstanding the complete procedure being performed no dilatation results.

New methods currently being studied include a rotating abrasive tip as suggested by Hansen *et al.* (1986); an atherectomy catheter tip method by Simpson *et al.* (1986) and, for instance, a "hot tip" method as described by Sanborn *et al.* (1984). Also direct laser application is considered for desobstruction of arteries (Choy *et al.*, 1982; Cross *et al.*, 1986).

One of the main problems of such tissue removal techniques is to prevent arterial perforation. Arterial curvature and the eccentricity of the obstructions in relation to the arterial wall require proper steering of the catheter tip. When, for instance, a glass fiber catheter is guided through an eccentric remaining arterial lumen and laser energy being circumferentially applied to burn away the obstruction, the eccentricity introduces the risk of arterial wall perforation.

For optimal use, the new methods should be made either selective, *i.e.* normal wall tissue should not be affected by the removal technique, or guided by precise knowledge of the localization and geometry of the arterial obstruction. Intra-arterial echo imaging provides this information. This paper describes the technical aspects and first results of *in vitro* experiments with high frequency intra-arterial echo imaging integrated with a new recanalization method

—spark erosion—(Slager *et al.*, 1985) on the tip of a catheter. The described method is aimed in particular at application in cardiology.

Early transducers for use inside the human body

Already in 1960 Cieszynski (1960, 1961) obtained echoes from within the heart with a single catheter-mounted transducer introduced via the jugular vein in dogs. After their first initial report in 1963, Omoto *et al.* (1963) and Kimoto *et al.* (1964) published their experiences with an intravenous probe. The carrier of the probe consisted of a stainless steel tube with a 1.2 mm outside diameter and a wall thickness of .2 mm. Tomograms were obtained by rotation and withdrawal of the probe. Since transducer displacement was necessarily slow, tomograms were obtained using E.C.G. triggered echo acquisition.

In the meantime real-time imaging of two-dimensional cross-sections emerged. Carleton and Clark (1968) described a catheter-mounted omnidirectionally operating single element. Eggleton *et al.* (1970) described a rotating catheter system with four elements spaced 90° apart.

Our laboratory developed the first real-time intracardiac scanner (Bom *et al.*, 1972; Bom, 1973). A 32-element circular array with an outer diameter of 3.2 mm mounted at the tip of a No. 9 French catheter was constructed. Although the frame-rate (over 100 s⁻¹) no longer imposed any timing limitations, we experienced two major complications during *in vivo* experiments in pigs. Excessive motion in the left ventricular cavity and strong grating lobes. The net result was too ambiguous to be of much clinical value.

Spark erosion

As reported by Slager *et al.* (1985) spark erosion can be used to evaporate atherosclerotic plaques. The technique was studied in specimen of human aorta obtained at autopsy. It works well on fatty and fibrous tissue. The method is less suited for removal of purely calcified areas. It has been shown that optimization of the method is possible in order to obtain tissue evaporation combined with diminished side effects such as dehydration and coagulation. Histology showed very little thermal damage of the adjacent tissue zones. Similar to the nonselective laser fiber desobstruction method, spark erosion based on a single electrode may easily perforate the arterial wall because of the eccentric position of the remaining lumen. The eccentric composition of an occlusion in a coronary artery obtained at autopsy is shown in Fig. 1, panel A.

The results of spark erosion recanalization in the specimen shown in panel A, is demonstrated in panel

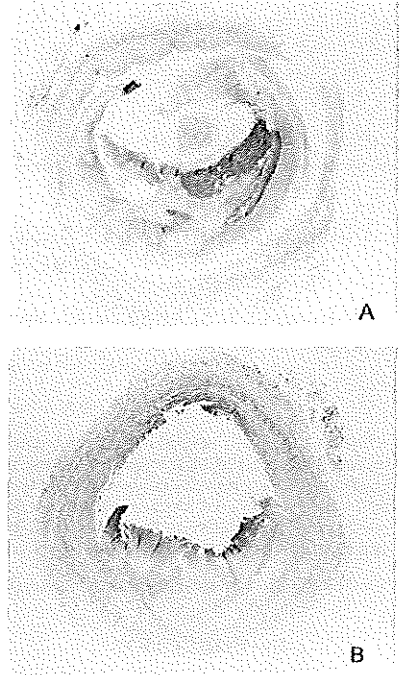


Fig. 1. Cross section (A) of a severely obstructed coronary artery showing eccentric geometry of the remaining lumen. After locally applied erosion, the lumen is eccentrically enlarged (B).

B of Fig. 1. In this example, the lumen was enlarged by use of a tubelike electrode. Spark erosion can be made steerable when more than one electrode is incorporated. Integration in a catheter tip of three electrodes together with the ultrasonic device for imaging of the obstruction was the basis for the first prototype as described hereafter (Slager, 1987).

DESIGN CONSIDERATIONS

In order to estimate a practical catheter diameter size, it is necessary to have knowledge of the internal coronary artery diameter in normal adults. McAlpin *et al.* (1973) indicate that the lumen diameter of the right coronary artery ranges from 3.2 ± 0.6 mm (proximal) to 2.7 ± 0.7 mm (distal). The main left coronary artery lumen diameter was measured to be 4.0 ± 0.7 mm. For the left anterior descending artery a range was measured of 3.4 ± 0.5 (proximal) to 1.9 ± 0.3 (distal) and for the circumflex of 3.0 ± 0.7 (proximal). From this material it was concluded that in a first approach a 2 mm outer diameter catheter would be sufficiently small.

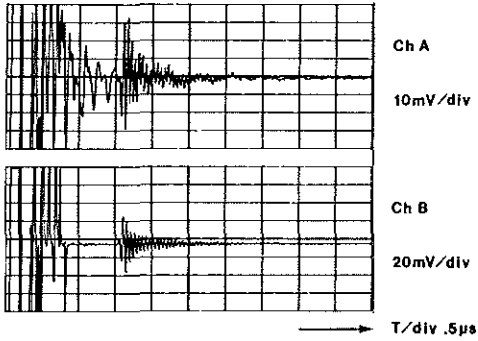


Fig. 2. The excitation pulse transient effect and reflected pulse from a wire target. Unprocessed signal (A) and averaged, background-corrected (B).

The previously described 32-element cylindrical catheter tip transducer as developed in our laboratory (Bom *et al.*, 1972) is too large with a 3.2 mm diameter. Diminishing its size to an outer diameter of 2 mm would be technologically difficult and would require an integrated circuit design for multiplexing transmit and receive signals. The main reason not to follow this course, was the expected transmission pulse transient effect masking the nearby structure echoes. We therefore opted for an approximately 20 MHz single element construction in combination with an acoustic mirror. The diameter of the transducer element was selected to be 1 mm, using conventional technology. In a first set-up this element was provided with air backing and mounted onto a metal bar for study of sensitivity, working frequency, dead zone, echo pulse length and beam characteristics.

As shown in Fig. 2, channel A, the dead zone of

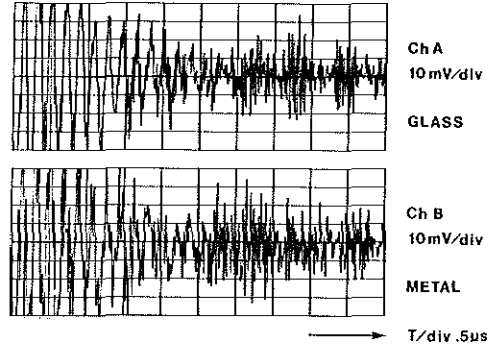


Fig. 4. Pulse transmission and echo reception via a glass mirror (A) and a metal mirror (B).

the unprocessed signal showing the reflection of a 100 μm wire, approximates 1.8 μs . Averaging ten pulse sequences and subtraction of background improves results drastically, as shown in channel B. For the strong reflecting wire no amplification was necessary in this case. The beam plot of the transducer is shown in Fig. 3.

As a next step the element was mounted in a 2.2 mm diameter rod and tested in combination with several mirrors. These mirrors were made of different, readily available materials. Reverberation was shown to be smaller with a glass than in a metal mirror. Comparison of the use of a metal and a glass mirror is shown with typical results in Fig. 4.

The beam plot of this assembly with a glass mirror is shown in Fig. 5.

A photograph of the test set is shown in Fig. 6. It represents the transducer assembly that can be step-

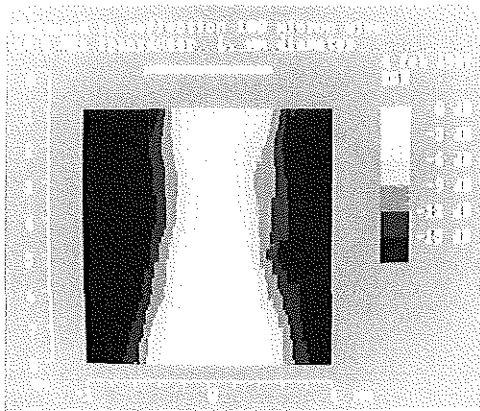


Fig. 3. Beam profile plotted as function of depth for the 1 mm diameter 18.3 MHz transducer.

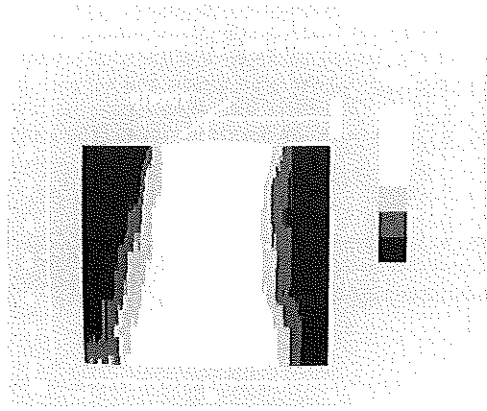


Fig. 5. Beam profile plotted as function of depth for the 1 mm diameter 19.3 MHz transducer with glass mirror.

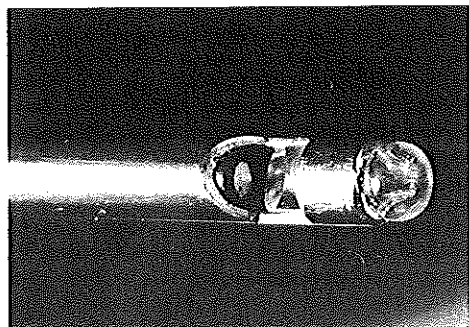


Fig. 6. Fixed transducer assembly driven by a stepping-motor as used for rotational cross-sectional imaging.

rotated and is equipped with angle coding for display purposes.

Experience gained with these preliminary trials led to our decision to design a mechanically rotating catheter tip device that would provide cross-sectional two-dimensional images. Single beam A-mode display resulting from only one or a few forward looking acoustic elements at the tip was regarded as too difficult to interpret.

Spark erosion electrodes must be positioned necessarily at the very tip of the catheter. The cross-sectional imaging plane and the spark erosion plane should preferably be as close together as possible.

RESULTS

In Fig. 7, a schematic drawing of the echo/recanalization catheter tip is shown. The outer diameter is 2 mm. The mirror (4) is mounted at the end of a flexible wire and can be rotated. The piezoelectric element (5) is positioned over an airbacking for optimal sensitivity. The tip consists of three mutually isolated electrodes. The three electrode wires (2) form an open cage for the echo signals and support the catheter tip. The three electrodes cause the cage echoes in some of the described results. The trans-

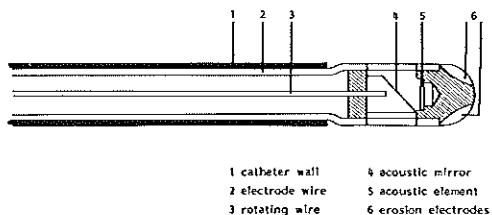


Fig. 7. Schematic drawing of the echo/recanalization catheter tip. Outer diameter is 2 mm.

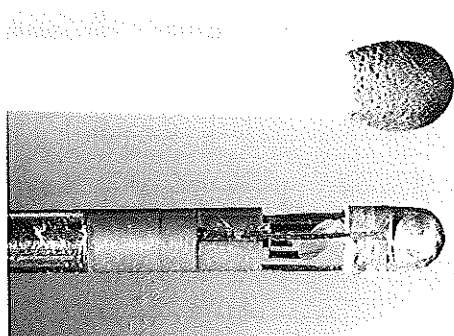


Fig. 8. First prototype for *in vitro* experiments. This prototype corresponds to the schematic drawing of Fig. 7.

ducer wires are glued onto two of the isolated spark erosion electrodes.

A photograph of a first prototype, with a rigid steel rod instead of a flexible catheter, designed for *in vitro* measurements, is shown in Fig. 8. An ultrasound intra-arterial image obtained from a specimen of the carotid artery is shown in Fig. 9. As a coupling liquid water was used. The diameter of the lumen of

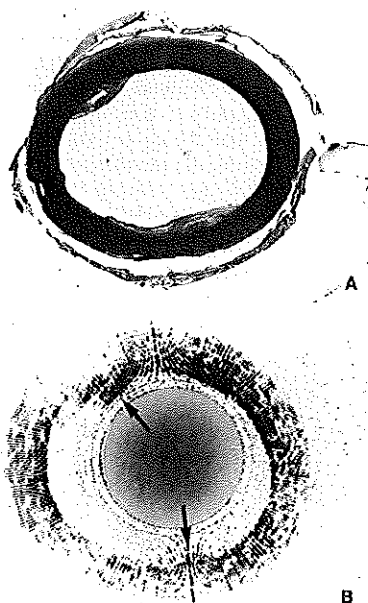


Fig. 9. First imaging results illustrated in an arterial specimen (A) and the corresponding intra-arterial echo image (B) as obtained with the transducer assembly shown in Fig. 6.

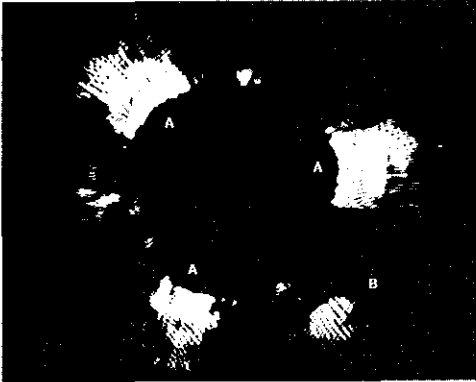


Fig. 10. First image obtained *in vitro* using the catheter shown in Fig. 8. On this image only the very strong echoes from the cage construction (A) and a plaque (B) are displayed.

this specimen approximates 5 mm. Inner and outer sides of the arterial wall are clearly visible. The two plaque areas are clearly visible on the anatomic cross section as well as on the echo image. This image has been obtained with the *in vitro* set-up with the device shown in Fig. 6. A first result from an *in vitro* image as obtained with the catheter is shown in Fig. 10. In this image the three cage echoes (A) and the echo of the calcified plaque (B) are clearly visible. These images show the possibilities of intra-arterial structure localization. Further studies must teach us the limitations caused by the cage echoes and the possible design modifications.

CONCLUSION

New recanalization methods such as spark erosion require steering in order to cope with the eccentricity of the occlusion. A possible method of guidance is ultrasonic imaging with a single miniature high frequency element. With a 20 MHz catheter tip prototype with a 1 mm diameter single element and rotating mirror technique first intra-arterial cross-sectional echo images were obtained *in vitro*. Our experiments show that it is technologically possible to integrate the imaging device and the spark erosion electrodes in a catheter tip with a diameter of only 2 mm. *In vitro* tests lead us to believe that this new method has great potential.

Acknowledgements—The construction of the catheter tip has been a cooperation of the Central Research Workshop of the Erasmus University Rotterdam, with the assistance of Messrs. R. Niesing, A. H. den Ouden, J. Bos and L. Bekkering, and the Productcenter of T.N.O.-Delft, where Messrs. Plukaard en Van Soest actually made the first prototype.

We furthermore acknowledge the contribution of the Audio Visual Center of the Erasmus University for the illustrations in this article.

REFERENCES

- Bom N., Lancée C. T. and Van Egmond F. C. (1972) An ultrasonic intracardiac scanner. *Ultrasonics* 10, 72–76.
- Bom N. (1973) Apparatus for ultrasonically examining a hollow organ. Patent specification 1,402,192, filed February 22.
- Carleton R. A. and Clark J. G. (1968) Measurement of left ventricular diameter in the dog by cardiac catheterization. Validation and physiologic meaningfulness of an ultrasonic technique. *Circ. Res.* 22, 545–548.
- Choy D. S. J., Sertzer S., Rotterdam H. Z. and Bruno M. S. (1982) Laser coronary angioplasty: experience with 9 cadaver hearts. *Am. J. Cardiol.* 50, 1209–1211.
- Cieszynski T. (1960) Intracardiac method for the investigation of structure of the heart with the aid of ultrasonics. *Arch. Immun. Ter. Dosw.* 8, 551–557.
- Cieszynski T. (1961) Intracardiac method of ultrasound heart-structure investigation. *Polsk. Przegląd. Chirurg.* 33, 1071.
- Cross F. W., Bowker T. J. and Bown S. G. (1986) Contact sapphire tip angioplasty with a pulsed Nd-YAG laser. *Lasers Med. Sci.* 1, 311.
- Eggleton R. C., Townsend C., Herrick J., Templeton G. and Mitchell J. H. (1970) Ultrasonic visualization of left ventricular dynamics. *Ultrasonics* 17, 143–153.
- Gruentzig A. R., Senning A. and Siegenthaler W. F. (1979) Nonoperative dilatation of coronary artery stenosis: percutaneous transluminal angioplasty. *N. Engl. J. Med.* 301, 61–68.
- Hansen D. D., Hall M., Intlekofer M. J., Auth D. and Ritchie J. L. (1986) *In vivo* rotational angioplasty in atherosclerotic rabbits; comparison of angiography and angiography. *Circulation* 74, Suppl. II: 362 (abstract).
- Kimoto S., Omoto R., Tsunemoto M., Muroi T., Atsumi K. and Uchida R. (1964) Ultrasonic tomography of the liver and detection of heart atrial septal defect with the aid of ultrasonic intravenous probes. *Ultrasonics* 2, 82–86.
- McAlpin R. N., Abbasi A. S., Grallman J. A. and Eber L. (1973) Human coronary artery size during life. *Radiology* 108, 567–573.
- Omoto R., Atsumi K., Suma K., Toyoda T., Sakurai Y., Muroi T., Fujimori Y., Idezuki Y., Tsunemoto M., Sugiura M. and Saegusa M. (1963) Ultrasonic intravenous sonde—2nd report. *Med. Ultrason. (Jpn)* 1, 11.
- Sanborn T. A., Faxon D. P., Haudenschild C. C. and Ryan T. J. (1984) Laser radiation of atherosclerotic lesions: decreased incidence of vessel perforation with a fiberoptic laser heated metallic tip (abstr). *J. Am. Coll. Cardiol.* 3, 490.
- Simpson J. B., Johnson D. E., Brader L. J., Gifford H. S., Thapliyal H. V. and Selmon M. R. (1986) Transluminal coronary atherectomy (TCA): results in 21 human cadaver vascular segments. *Circulation* 74, Suppl. II: 202 (abstract).
- Slager C. J., Essed C. E., Schuurbiers J. C. H., Bom N., Serruys P. W. and Meester G. T. (1985) Vaporization of atherosclerotic plaques by spark erosion. *J. Am. Coll. Cardiol.* 5, 1382–1386.
- Slager C. J. (1987) Echo/Vonkerosie Recanalisation Inrichting. Dutch Patent Application No. 8700632 of March 17.

CHAPTER 5

**HEART FUNCTION AFTER INJECTION OF SMALL AIR BUBBLES
IN A CORONARY ARTERY OF PIGS**

Jan Heim van Blankenstein, Cornelis J. Slager, Johan C.H. Schuurbiers,
Sipke Strikwerda, Pieter D. Verdouw

Heart function after injection of small air bubbles in coronary artery of pigs

J. H. VAN BLANKENSTEIN, C. J. SLAGER, J. C. H. SCHURBIERS,
S. STRIKWERDA, AND P. D. VERDOUW

*Thoraxcenter, Erasmus University Rotterdam and University Hospital Rotterdam-Dijkzigt,
3000 DR Rotterdam, The Netherlands*

VAN BLANKENSTEIN, J. H., C. J. SLAGER, J. C. H. SCHURBIERS, S. STRIKWERDA, AND P. D. VERDOUW. *Heart function after injection of small air bubbles in coronary artery of pigs.* *J. Appl. Physiol.* 75(3): 1201-1207, 1993.—By its nature, vaporization of atherosclerotic plaques by laser irradiation or spark erosion may produce a substantial amount of gas. To evaluate the effect of gas embolism possibly caused by vaporization techniques, air bubbles with diameters of 75, 150, or 300 μm , each in a volume of 2 $\mu\text{l}/\text{kg}$, were selectively injected subproximal in the left anterior descending coronary artery of seven anesthetized pigs (28 ± 3 kg). Systemic hemodynamics such as heart rate, left ventricular pressure and its peak positive first derivative, and mean arterial pressure did not change after air injection, whereas there was a minor change in peak negative first derivative of left ventricular pressure. After injection of air bubbles there was a maximal relative reduction of systolic segment shortening (SS) in the myocardium supplied by the left anterior descending coronary artery of 27, 45, and 58% for 75-, 150-, and 300- μm bubbles, respectively, and a relative increase of postsystolic SS (PSS) of 148, 200, and 257% for 75-, 150-, and 300- μm bubbles, respectively. Recovery of SS and PSS started after 2 min and was completed after 10 min. A difference in SS and PSS changes between different bubble size injections could be demonstrated. From this study it is clear that depression of regional myocardial function after injection of air bubbles could pass unnoticed on the basis of global hemodynamic measurements.

laser angioplasty; coronary air embolism; dissolving air embolism; myocardial wall motion

RECANALIZATION OF stenotic atherosclerotic coronaries can be accomplished by stretching, as well as removing, the obstruction. When the obstruction is removed by cutting or abrasive techniques, plaque components enter the blood stream as particles. In the case of application of vaporization techniques, like laser angioplasty (1, 6, 13) and spark erosion (23), gas bubbles are produced as well. Production of gas by spark erosion has prevented early intraluminal application; in addition, clinical application for laser angioplasty had to be adapted to avoid the so-called gas fill-up.

The effects of both venous (pulmonary) and arterial air embolisms in the human body have been well studied (4, 9, 11, 14). Studies on venous air embolism revealed that filtering by the pulmonary vessels protects the systemic and coronary circulation from air emboli from the originating venous circulation (3). Arterial air embolism

causes ischemia in the organs in which the air bubbles are trapped. Coronary air embolism has been studied by intracoronary injection of a bolus of air, and a serious depression of global heart function was shown (9, 21, 24). In one study (24) a mortality of 28% of the dogs was reported for a dose of 0.02 ml/kg, whereas surviving animals showed recovery of global heart function within 15 min. However, information on the recovery of regional myocardial function is lacking, which is mandatory, as global function may recover in the presence of a depressed regional function (15). Furthermore, the injection of a bolus of air is not representative for the production of gas during vaporization procedures.

In view of the observation of gas bubble formation in vitro with excimer laser ablation and spark erosion, more information is needed on the relationship between bubble size and the effects of coronary embolism on global and regional myocardial function. Therefore, in the present study we injected in a coronary artery of pigs air bubbles of a well-controlled size and in small amounts, as clinically expected, and followed the time course of depression and recovery of global and regional myocardial function.

METHODS

General. Experiments were performed in accordance with the National Institutes of Health "Guide for the Care and Use of Laboratory Animals," [DHEW Publication No. (NIH) 80-23, Revised 1980] and under the regulations of the Animal Care Committee of the Erasmus University Rotterdam.

After an overnight fast, cross-bred Landrace \times Yorkshire pigs (HVC, Hedel, The Netherlands) of either sex (25-32 kg, $n = 7$) were sedated with 20 mg/kg of ketamine im (AUV, Cuijk, The Netherlands), anesthetized with 5 mg/kg of metomidate iv (Janssen Pharmaceutica, Beerse, Belgium), intubated, and connected to a ventilator for intermittent positive pressure ventilation with a mixture of O_2 and N_2 (1:2, vol/vol). Respiratory rate and tidal volume were set to keep arterial blood gases within the normal range: $7.38 < \text{pH} < 7.50$; $35 \text{ Torr} < \text{PCO}_2 < 45 \text{ Torr}$, and $99 \text{ Torr} < \text{PO}_2 < 182 \text{ Torr}$. A multilumen 7-Fr catheter was placed in the superior caval vein for continuous infusion of 1) 5-23 $\text{mg} \cdot \text{kg}^{-1} \cdot \text{h}^{-1}$ of pentobarbital sodium (Sanofi, Paris, France); 2) 4 mg of the muscle relaxant pancuronium bromide (Organon Teknika, Box-

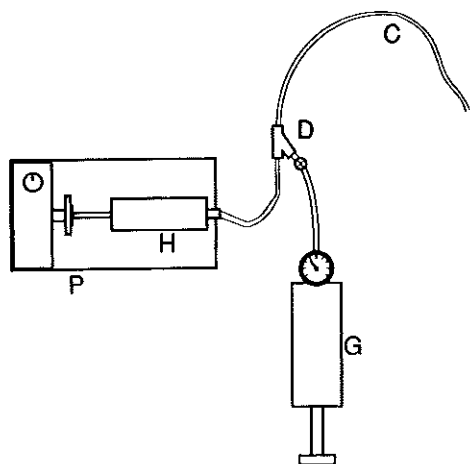


FIG. 1. Syringe, driven by infusion pump (P), injected Haemacel (H) through mixing device (D) in which also air from pressure source (G) was injected through micropipette. Catheter (C) positioned in coronary artery was connected to device (D).

tel, The Netherlands) before thoracotomy; 3) Haemacel, a gelatine-derived blood plasma substitute (Behringwerke, Marburg, Germany), to compensate for blood loss; or 4) a continuous infusion of norepinephrine (Pharmacy University Hospital, Rotterdam, The Netherlands) at 0.06–0.12 mg/h, if necessary, to keep mean arterial blood pressure (MAP) stabilized at >65 mmHg at baseline. Settings were not changed during the subsequent experimental runs.

Catheters were also positioned in the descending aorta for withdrawal of blood samples and measurement of central aortic blood pressure. A 7-Fr Sensodyn micrometer-tipped catheter (B. Braun Medical, Uden, The Netherlands) inserted via the left carotid artery was used to measure left ventricular pressure (LVP) and its first derivative (LVdP/dt). After thoracotomy an electromagnetic flow probe (Skalar, Delft; The Netherlands) was placed around the ascending aorta. The left anterior descending coronary artery (LADCA) was dissected free for placement of another electromagnetic flow probe (Skalar) around the vessel. Regional myocardial segment length was measured by sonomicrometry (Triton Technology, San Diego, CA) using two pairs of ultrasonic crystals (Sonotek Corporation, Del Mar, CA): one pair was placed in the mesocardial layers of the distribution of the distal LADCA, and the other pair for control purposes was placed in the mesocardial layers of the distribution of the left circumflex coronary artery (LCXCA). After 10,000 IU of heparin (Pharmacy University Hospital) were administered, followed by 5,000 IU every 2 h, a 3-Fr catheter for injection of air bubbles was inserted through a guiding catheter via the right carotid artery and positioned in the LADCA under fluoroscopy with its tip just distal from the first diagonal branch.

Production of air bubbles. A bubble generator was developed for the production of air bubbles (Fig. 1; Ref. 10). Haemacel was chosen as the carrying fluid because, unlike in physiological saline (0.9% NaCl), small bubbles

could be produced that did not coalesce as could be observed under *in vitro* tests at the exit of the catheter. Air was injected into Haemacel through a micropipette from a constant-pressure source, thereby producing uniformly sized bubbles. By using different dimensions of the tip of the micropipette, altering the velocity of Haemacel along the tip of the micropipette and/or the air pressure, the size of the generated bubbles could be varied. Calibration curves were determined to establish the relationship between the volume of air delivered per second and the various parameter settings. The velocity of Haemacel along the tip of the pipette was varied by changing the diameter of the bubble chamber from 1 to 0.75 mm while the volume flow remained at 3 ml/min. The volume flow of Haemacel was estimated to be globally one-tenth that of coronary blood flow (17). The apparatus was adjusted before each experimental run to produce bubbles with a diameter of either 75, 150, or 300 μ m (light microscopy revealed that tolerance was 10 μ m).

Experimental protocol. After surgical procedures were finished, a 30-min stabilization period was allowed before baseline recordings were made of aortic pressure, LVP, LVdP/dt, aortic blood flow, LADCA blood flow, and segmental length in the LADCA and LCXCA regions. All tracings were made at a paper speed of 50 mm/s. After baseline measurements, a control injection of bubble-free Haemacel was given for 1 min and global and regional cardiac functions were measured for 10 min.

Subsequently, air bubbles with diameters of 75, 150, or 300 μ m were injected after repeated baseline recordings at 15-min minimal intervals. The total amount of air delivered (2 μ l/kg) was equal for each bubble size and was related to body weight. On the basis of the previously obtained calibration curves the total time of air injection was used to control the delivered volume. A typical recording of the measured parameters during the 1st min after a 300- μ m bubble injection is shown in Fig. 2. Injections of air bubbles were always given in the same sequence. Duration of injection was 82 ± 22 (SD) s for the 75- μ m bubbles, 26 ± 11 s for the 150- μ m bubbles, and 11 ± 4 s for 300- μ m bubbles. This means that the ratio of gas flow to Haemacel flow varied from $\sim 1/75$ to $1/10$ for the 75- and 300- μ m bubbles, respectively.

Data analysis and presentation. From the sonomicrometric tracings, segment length was assessed at end diastole (EDL), end systole (ESL), and postsystole (PSL). End diastole was defined as the positive onset of LVdP/dt, end systole as the zero crossing of aortic blood flow, and postsystole as the zero crossing from negative LVdP/dt. Systolic segment shortening (SS) was calculated as

$$SS = \frac{EDL - ESL}{EDL} \times 100(\%)$$

and postsystolic segment length shortening (PSS) as

$$PSS = \frac{ESL - PSL}{ESL} \times 100(\%)$$

Statistics. Results are given as arithmetic means \pm SD. Changes in cardiovascular parameters after injection of the air bubbles were tested for significance ($P < 0.05$,

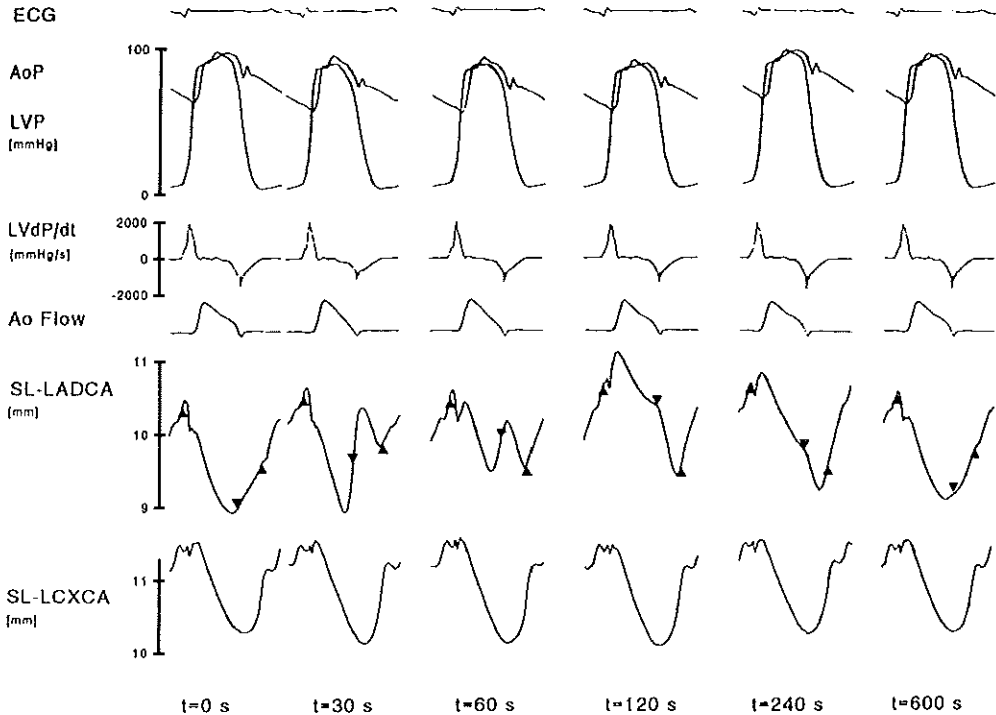


FIG. 2. Example of tracings after 300- μm bubble injection of electrocardiogram (ECG), aortic pressure (AoP), left ventricular pressure (LVP) and its first derivative (LVdP/dt), aortic flow (Ao Flow), and segmental length in left anterior descending coronary artery perfused region (SL-LADCA) and in left circumflex coronary artery perfused region (SL-LCXCA). Bubble injection started at $t = 0$ and lasted for 9 s. SL-LADCA signal clearly shows disturbed function and is normal again at $t = 600$ s. In this signal, end diastole, end systole, and postsystole are indicated by triangles.

one-sample analysis, Statgraphics 5.0) using a paired t test.

RESULTS

General. The number of measurements ($n = 7$) for each parameter equals the number of experiments. In one experiment the segmental length measurement in the LCXCA region was not obtained because of technical problems; for SS and PSS in this region, $n = 6$.

After animal preparation and positioning of the coronary catheter, two of the animals were rather hypotensive, and norepinephrine was used during the whole experiment to keep MAP > 65 mmHg. Although pressure did not change significantly during the 10-min experimental runs, a gradual drop of 10 mmHg to < 65 mmHg was observed over a 2-h period in another three animals that also received norepinephrine support during the last two experimental runs. Settings were never changed immediately before or during the measurement period.

Visual observations. Within 1 min after the injection of air bubbles, whitish colored regions could be observed on the apical part of the left ventricle and on the right ventricle at the interventricular groove, accompanied by paradoxical motion of the same regions. Within 5 min

the whitish colored regions became cyanotic while paradoxical motion disappeared. The cyanotic-colored regions slowly became pink, and after 10–15 min the heart looked normal again. In some cases the disappearance of cyanotic spots took > 0.5 h.

Systemic hemodynamics. After Haemaccel injection, peak positive LVdP/dt increased ($P < 0.05$) by 7% at $t = 30$ s and by 8% at $t = 60$ s (Table 1).

Injection of the bubbles had no effect on MAP, left ventricular peak systolic pressure, or heart rate (Table 1). Peak positive LVdP/dt increased ($P < 0.05$) maximally by 6–9% at $t = 30$ s for all bubble sizes. For 150- μm bubbles, the peak value of negative LVdP/dt decreased maximally by 11% ($P < 0.05$) during the interval from $t = 30$ s to 180 s, and a similar maximal reduction of 16% ($P < 0.05$) appeared at $t = 30$ and 60 s after injection of 300- μm bubbles (Fig. 3).

Segmental length shortening. After Haemaccel injection a short-lasting change, statistically not significant, for both SS and PSS in the LADCA perfused region was observed (Figs. 4 and 5).

Immediately after injection of air bubbles, SS in the LADCA area (SS-LADCA) significantly decreased for all bubble sizes compared with baseline values and showed maximal depression at $t = 90$ s. Simultaneously PSS in

TABLE 1. Systemic hemodynamics after injection of Haemacel and 75-, 150-, and 300- μ m bubbles

| | Time After Start of Injection at 0, s | | | | | | | | |
|-------------------------|---------------------------------------|------------------|------------------|-----------------|-----------------|-----------------|-----------------|-----------------|-----------------|
| | 0 | 30 | 60 | 90 | 120 | 180 | 240 | 360 | 600 |
| <i>HR, beats/min</i> | | | | | | | | | |
| Haemacel | 104 \pm 26 | 104 \pm 27 | 104 \pm 27 | 104 \pm 27 | 105 \pm 26 | 104 \pm 26 | 104 \pm 27 | 104 \pm 27 | 105 \pm 26 |
| 75 μ m | 105 \pm 24 | 104 \pm 23 | 104 \pm 23 | 104 \pm 23 | 104 \pm 23 | 104 \pm 23 | 104 \pm 23 | 104 \pm 24 | 104 \pm 24 |
| 150 μ m | 101 \pm 19 | 101 \pm 19 | 101 \pm 18 | 101 \pm 19 | 101 \pm 20 | 101 \pm 19 | 102 \pm 22 | 101 \pm 21 | 102 \pm 22 |
| 300 μ m | 102 \pm 22 | 101 \pm 21 | 102 \pm 23 | 103 \pm 23 | 102 \pm 23 | 103 \pm 24 | 104 \pm 23 | 103 \pm 23 | 103 \pm 23 |
| <i>MAP, mmHg</i> | | | | | | | | | |
| Haemacel | 74 \pm 7 | 75 \pm 7 | 75 \pm 7 | 76 \pm 7 | 75 \pm 8 | 74 \pm 7 | 75 \pm 9 | 73 \pm 8 | 73 \pm 10 |
| 75 μ m | 72 \pm 8 | 73 \pm 10 | 73 \pm 11 | 72 \pm 11 | 73 \pm 11 | 73 \pm 11 | 73 \pm 11 | 74 \pm 10 | 71 \pm 10 |
| 150 μ m | 70 \pm 9 | 70 \pm 9 | 70 \pm 9 | 70 \pm 9 | 69 \pm 8 | 68 \pm 9 | 73 \pm 10 | 74 \pm 10 | 70 \pm 8 |
| 300 μ m | 71 \pm 5 | 69 \pm 5 | 69 \pm 5 | 69 \pm 5 | 70 \pm 5 | 73 \pm 7 | 74 \pm 6 | 73 \pm 5 | 70 \pm 6 |
| <i>LVPSP, mmHg</i> | | | | | | | | | |
| Haemacel | 98 \pm 10 | 100 \pm 10 | 99 \pm 9 | 100 \pm 8 | 99 \pm 9 | 99 \pm 9 | 98 \pm 10 | 97 \pm 10 | 97 \pm 11 |
| 75 μ m | 94 \pm 8 | 96 \pm 10 | 96 \pm 11 | 95 \pm 10 | 95 \pm 11 | 96 \pm 11 | 96 \pm 10 | 96 \pm 10 | 94 \pm 10 |
| 150 μ m | 95 \pm 7 | 95 \pm 8 | 94 \pm 8 | 94 \pm 8 | 93 \pm 8* | 93 \pm 8 | 98 \pm 5 | 98 \pm 6 | 96 \pm 6 |
| 300 μ m | 97 \pm 3 | 95 \pm 6 | 95 \pm 6 | 95 \pm 5 | 97 \pm 5 | 99 \pm 5 | 99 \pm 3 | 98 \pm 2 | 95 \pm 5 |
| <i>+LVdP/dt, mmHg/s</i> | | | | | | | | | |
| Haemacel | 2,220 \pm 780 | 2,370 \pm 850* | 2,390 \pm 810* | 2,280 \pm 710 | 2,190 \pm 680 | 2,290 \pm 740 | 2,200 \pm 680 | 2,170 \pm 740 | 2,180 \pm 750 |
| 75 μ m | 1,940 \pm 560 | 2,110 \pm 560* | 2,040 \pm 500 | 1,980 \pm 470 | 1,960 \pm 490 | 1,920 \pm 550 | 1,920 \pm 550 | 1,940 \pm 540 | 1,930 \pm 600 |
| 150 μ m | 1,940 \pm 540 | 2,050 \pm 470* | 2,030 \pm 460 | 1,940 \pm 470 | 1,910 \pm 500 | 1,920 \pm 520 | 1,960 \pm 500 | 1,980 \pm 470 | 1,930 \pm 480 |
| 300 μ m | 2,060 \pm 520 | 2,190 \pm 560* | 2,070 \pm 510 | 2,000 \pm 480 | 2,040 \pm 460 | 2,090 \pm 490 | 2,110 \pm 420 | 2,050 \pm 480 | 2,010 \pm 500 |

Values are means \pm SD. HR, heart rate; MAP, mean arterial pressure; LVPSP, left ventricular peak systolic pressure; +LVdP/dt, peak positive left ventricular dP/dt. * $P < 0.05$ vs. time 0.

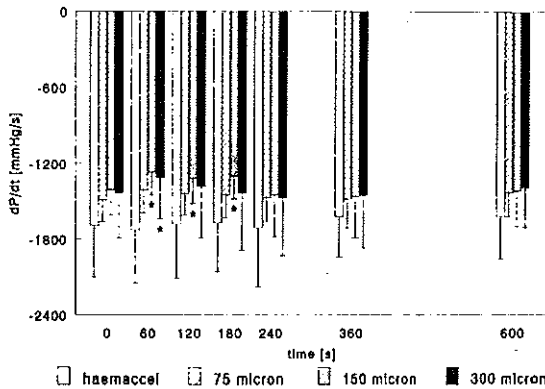


FIG. 3. Peak negative LVdP/dt for Haemacel and 75-, 150-, and 300- μ m bubbles. Data are means \pm SD. * Significantly different from baseline ($t = 0$ s) ($P < 0.05$).

the LADCA area (PSS-LADCA) increased ($P < 0.05$) and became positive. The relative peak reduction of SS-LADCA compared with baseline was 27% for 75- μ m, 45% for 150- μ m, and 58% for 300- μ m bubbles at $t = 90$ s. For PSS-LADCA the relative change was 148% for 75- μ m, 200% for 150- μ m, and 257% for 300- μ m bubbles at $t = 120$ s. When the relative changes between injections of three sizes of air bubbles were compared, there was a difference ($P < 0.05$) in SS between 75- and 150- μ m bubbles at $t = 60$ s, between 75- and 300- μ m bubbles at $t = 30$ s, and between 150- and 300- μ m bubbles at $t = 120$ s. A difference ($P < 0.05$) in PSS was observed between injections of 75- and 150- μ m bubbles at $t = 60$ s, between 75- and 300- μ m bubbles at $t = 90$ and 120 s, and between 150- and 300- μ m bubbles during the interval from $t = 90$ to 180 s.

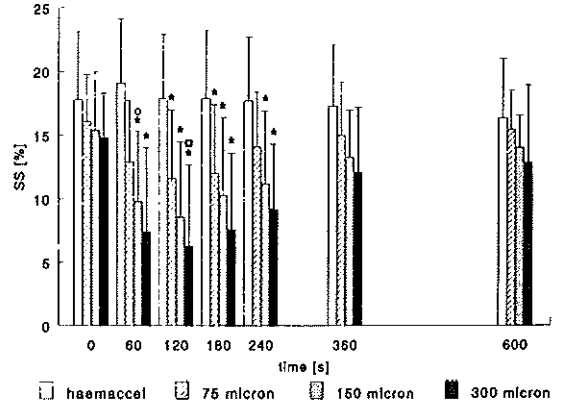


FIG. 4. Systolic segment length shortening (SS) in LADCA perfused region for Haemacel and 75-, 150-, and 300- μ m bubbles. Data are means \pm SD. * Significantly different from baseline ($t = 0$ s) ($P < 0.05$). Relative difference ($P < 0.05$): \square between 75- and 150- μ m bubbles; \square between 150- and 300- μ m bubbles.

In the control region of LCXCA a small increase ($P < 0.05$), $< 6\%$, of SS after injection of 75- and 150- μ m air bubbles could be observed at $t = 120$ s and for 300- μ m air bubbles at $t = 90$ s. PSS values in LCXCA area did not change significantly (Table 2).

DISCUSSION

Production of gas bubbles has been observed during studies in which tissue vaporization by CO₂; neodymium-yttrium, aluminum, garnet; argon; and excimer lasers was applied (1, 6, 13). That such gas production may be of clinical importance can be concluded from clinical protocols in which excimer lasers are used inter-

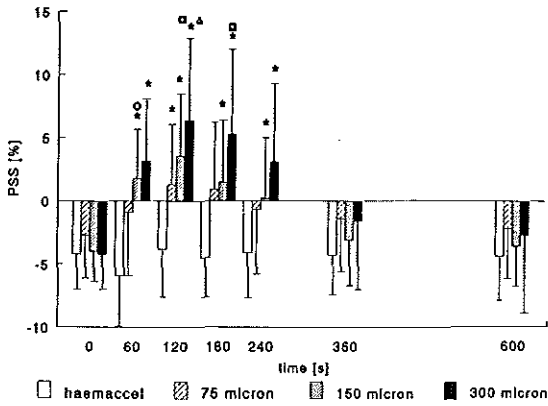


FIG. 5. Postsystolic segment length shortening (PSS) in LADCA perfused region for Haemacel and 75-, 150-, and 300- μ m bubbles. Data are means \pm SD. * Significantly different from baseline ($t = 0$ s) ($P < 0.05$). Relative difference ($P < 0.05$): ° between 75- and 150- μ m bubbles; □ between 75- and 300- μ m bubbles; □ between 150- and 300- μ m bubbles.

mittently to avoid gas fill-up in the treated artery. Whether gas bubbles produced by intravascular laser vaporization techniques also lead to embolism or induce additional chemical effects has not yet been studied.

In the present study we chose pigs as the experimental animal because they do not have arteriovenous anastomoses (22) and have a minimal coronary collateral circulation. For this reason air embolism in the native artery will depress the function of the myocardium maximally. Furthermore, the size of the pig heart allows us to study the regional effects of embolism without the major risk of losing the animal after a single injection of air bubbles. Pilot experiments have shown that with a dose of 2 μ l/kg several gas injections in the subproximal LADCA of pigs can be applied without serious long-term effects. This amount of injected air is at the high end of the range of what may be expected during current clinical coronary laser application. It has been determined that during excimer laser ablation of porcine aortic tissue under saline, production of gas reaches 0.3 μ l/pulse with a 1.6-mm-diameter catheter and an energy density of 50 $\text{mJ} \cdot \text{mm}^{-2} \cdot \text{pulse}^{-1}$ (8). The number of pulses used for one passage during a recanalization procedure, as measured for four patients treated in our hospital, varied from 650 to 1,200.

In the present study we chose to use air bubbles as a model of gas embolism. Air dissolves slowly in arterial blood and will lead to some worst-case scenario of coronary gas embolism. Bubbles of a controlled size were used rather than a single bolus to mimic the situation of gas production by intravascular vaporization techniques. Because of technical limitations, the smallest bubble size was restricted to 75 μ m diameter. Although the diameter ratio of 75-, 150-, and 300- μ m air bubbles is not more than 1:2:4, their volume ratio is 1:8:64.

The results of this study show that after injection of air bubbles global hemodynamic parameters such as heart rate, MAP, left ventricular peak systolic pressure, and LVdP/dt change only a few percent. This may be explained by a compensatory effect of nonembolized myocardium, which shows improvement of regional function after injection of bubbles, as seen from SS measurements in the control region of the LCXCA.

Although we did not determine any biochemical parameters indicative for anaerobic metabolism, the decrease in SS and the increase in PSS are strong evidence that ischemia developed during injection of the air bubbles. That regional function can be depressed while global hemodynamics remain unchanged has been shown before (15).

In general there was a clear functional depression after injection of bubbles. However, individual animal data showed great variability. Whether anatomic variations in the position of the heart in the thorax and in the coronary branching pattern, combined with buoyancy of the bubbles (16), could be a reason for variations in bubble distribution and subsequent regional function variability must be the subject of further study.

The time course of myocardial depression and recovery shows great similarity with data obtained after a bolus injection of air in the LADCA of dogs, as reported by Stegmann et al. (24). From Figs. 4 and 5 it may be derived that within ~ 2 min, recovery starts. This will occur after air bubbles have disappeared and reperfusion has started.

Trapping of an air embolus in the coronary microcirculation may occur as depicted in Fig. 6 (5, 7). As is described by Laplace's law, the pressure difference existing over a blood-air interface depends on the surface tension and the radius of the blood-air interface (18). At an equilibrium position the pressure difference over each distal

TABLE 2. SS and PSS after injection of Haemacel and 75-, 150-, and 300- μ m bubbles

| | Time After Start of Injection at 0, s | | | | | | | | |
|-------------|---------------------------------------|----------------|----------------|-----------------|-----------------|----------------|----------------|----------------|----------------|
| | 0 | 30 | 60 | 90 | 120 | 180 | 240 | 360 | 600 |
| | SS-LCXCA, % | | | | | | | | |
| Haemacel | 14.4 \pm 3.7 | 14.2 \pm 4.8 | 14.2 \pm 4.3 | 14.4 \pm 4.0 | 14.4 \pm 4.2 | 14.1 \pm 4.5 | 14.1 \pm 4.4 | 14.1 \pm 4.5 | 14.4 \pm 4.7 |
| 75 μ m | 13.4 \pm 4.9 | 13.5 \pm 5.4 | 13.4 \pm 5.5 | 13.2 \pm 5.1 | 13.5 \pm 4.9* | 13.6 \pm 5.0 | 13.5 \pm 4.8 | 13.4 \pm 5.0 | 13.3 \pm 4.9 |
| 150 μ m | 14.2 \pm 5.6 | 14.4 \pm 5.9 | 14.8 \pm 5.9 | 14.9 \pm 5.7 | 14.8 \pm 5.7* | 14.7 \pm 5.8 | 15.1 \pm 5.5 | 14.2 \pm 5.7 | 14.9 \pm 4.9 |
| 300 μ m | 13.9 \pm 5.7 | 14.2 \pm 6.4 | 14.5 \pm 6.3 | 14.7 \pm 6.2* | 14.6 \pm 6.1 | 14.4 \pm 6.1 | 14.2 \pm 6.2 | 14.2 \pm 5.9 | 14.2 \pm 6.1 |
| | PSS-LCXCA, % | | | | | | | | |
| Haemacel | -3.5 \pm 2.8 | -3.3 \pm 2.7 | -3.5 \pm 3.2 | -3.6 \pm 3.7 | -4.3 \pm 3.5 | -3.9 \pm 3.5 | -3.9 \pm 3.0 | -3.8 \pm 3.8 | -4.2 \pm 3.3 |
| 75 μ m | -3.1 \pm 2.5 | -3.3 \pm 3.0 | -2.5 \pm 2.8 | -3.5 \pm 3.6 | -3.4 \pm 4.0 | -3.9 \pm 3.8 | -3.2 \pm 3.5 | -3.2 \pm 3.4 | -3.1 \pm 3.5 |
| 150 μ m | -3.5 \pm 2.8 | -2.6 \pm 2.7 | -3.1 \pm 2.6 | -3.9 \pm 2.8 | -4.6 \pm 3.9 | -4.7 \pm 3.5 | -4.3 \pm 3.0 | -4.1 \pm 3.2 | -3.4 \pm 2.5 |
| 300 μ m | -3.7 \pm 2.7 | -3.8 \pm 3.7 | -3.3 \pm 3.3 | -4.0 \pm 3.4 | -4.2 \pm 3.7 | -3.9 \pm 3.0 | -4.2 \pm 3.6 | -3.8 \pm 3.5 | -3.5 \pm 3.0 |

Values are means \pm SD. SS, systolic segment shortening; PSS, postsystolic segment shortening; LCXCA, left circumflex coronary artery. * $P < 0.05$ vs. time 0.

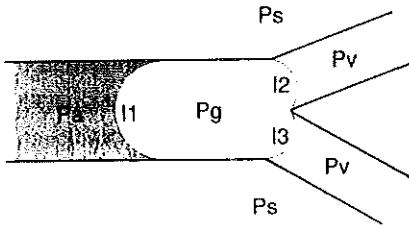


FIG. 6. At equilibrium, gas pressure (P_g) in bubble is equal to arterial blood pressure (P_a) plus Laplace pressure difference generated at interface I1 by blood surface tension. P_g minus venous pressure (P_v) equals Laplace pressure difference generated at interfaces I2 and I3 by blood surface tension. P_g in bubble is higher than P_a and P_v and also higher than surrounding tissue pressure (P_s).

interface (I2 and I3) minus the proximal (I1) value equals the driving blood pressure (b). If the proximal interface is much larger than the distal interfaces, i.e., has a low pressure difference, then it can be predicted that with an MAP of 73 ± 8 mmHg and a surface tension of 49 mN/m (19) for blood, an air bubble causes embolism in arterioles of $20 \mu\text{m}$ diameter. The blood pressure required to drive the embolus through capillary vessels of $6 \mu\text{m}$ diameter will be as high as 200 mmHg. The surface tension of the Haemaccel used as carrying fluid for air bubbles is of the same order of magnitude as that of blood and does not influence the trapping conditions.

The mechanism by which the air emboli disappear is not yet clear. Direct passage by arterial venous shunting is not likely because passage of microspheres of $9 \mu\text{m}$ diameter is negligible in pigs (22). Most likely the air bubbles shrink by diffusion of air into the blood and the surrounding tissue. This has been reported in other studies that showed that trapped air bubbles shrink by diffusion (7, 20). A diffusion gradient exists for gas from the trapped bubble into its surroundings (18, 20). When the air bubble's proximal interface reaches dimensions in the range slightly above capillary diameters, the bubble can pass the capillary vessel and reperfusion is started.

In the present study regional parameters in the LADCA region show greater functional depression with increasing bubble size. The chosen injection sequence of different bubble sizes is assumed to be of no influence, because all measurements returned to baseline values after each injection. A factor contributing to the observed differences might be the varying time needed for bubble injection. The relatively long-lasting infusion of $75\text{-}\mu\text{m}$ bubbles might cause a flattened response, as at the end of infusion primary embolized vessels could have opened again.

To estimate the sensitivity to injection time a simple two-compartment model has been applied, as depicted in Fig. 7. In this model the total charge Q delivered by the current source (CS) over a period of T seconds represents the total volume of air injected. Potential V_1 is related to the degree of embolization. Diffusion is represented by the discharge of capacitance C_1 over resistance R_1 . In the right-hand portion of the network, R_2 and C_2 represent a delay in functional response V_2 of the myocardium to the state of perfusion. By the time constants $R_1.C_1$

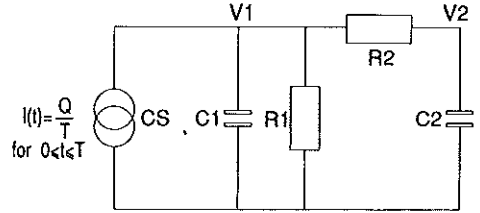


FIG. 7. Two-compartment model simulating effects of gas embolization on myocardial function. Current (I) source (CS) delivers charge (Q) to capacitor (C_1) in time T ; this simulates injection and storage of air bubbles in LADCA. Potential V_1 corresponds with degree of embolization, and V_2 is related to measured myocardial segment length in LADCA perfused region. Discharge of C_1 over resistance R_1 simulates diffusion of air from air bubbles. Delay in functional response due to embolization is simulated by network $R_2.C_2$.

and $R_2.C_2$ and a scale factor being varied, a curve fit (derivative-free nonlinear regression, BMDP PC-90) of V_2 on the data of SS-LADCA for $300\text{-}\mu\text{m}$ bubbles can be performed, with an excellent result ($r^2 = 0.97$) obtained with an injection time $t = 11$ s (Fig. 8). If the time constants found for the fit are kept constant and the injection time is varied from the actual average value of 11 s for the $300\text{-}\mu\text{m}$ bubbles to 82 s as the average value for the $75\text{-}\mu\text{m}$ bubbles, the main effect (Fig. 8) is a shift in the curve and only a minor effect on its amplitude. This simulation indicates that time of injection is not a major factor in explaining the difference in the magnitude of the depression in regional function between the observed different injections of air bubbles.

Hypothetically the relation between myocardial functional depression and bubble size might be explained by another aspect of the way by which bubbles distribute over the coronary tree. If the bubbles split at branches at equal ratio as volume flow of blood, their shape will be determined by the geometry of the vascular tree. The relationship between the diameters of branches stemming from a parent vessel can be given by (12)

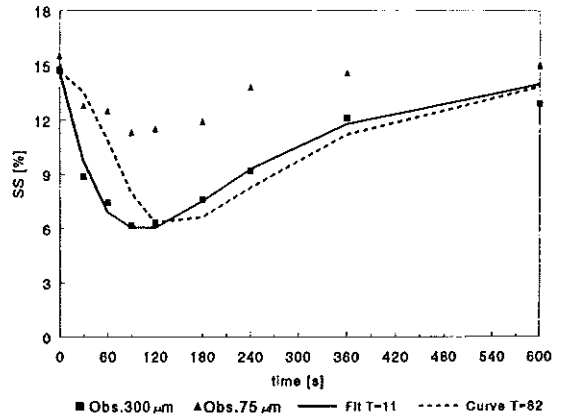


FIG. 8. Curve fit of V_2 from 2-compartment model to data of $300\text{-}\mu\text{m}$ bubbles (fit $T = 11$) with injection time $T = 11$ s ($r^2 = 0.97$). For obtained time constants, curve for injection time of $T = 82$ s is calculated (curve $T = 82$). Observed values for SS-LADCA, as in Fig. 4, for $300\text{-}\mu\text{m}$ (Obs $300 \mu\text{m}$) and $75\text{-}\mu\text{m}$ bubbles (Obs $75 \mu\text{m}$) are also given.

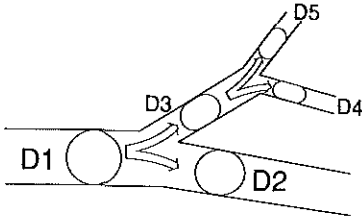


FIG. 9. Air bubble with diameter equal to that of vessel D1 splits into 2 so-called slugs in D2 and D3 if $n < 3$ for equation $R(\text{parent})^n = R(\text{branch1})^n + R(\text{branch2})^n$ (see text). If bubble in D3 passes bifurcation from D3 into D4 and D5 and $n < 3$, slugs will be further longitudinally stretched.

$$R(\text{parent})^n = R(\text{branch1})^n + R(\text{branch2})^n + R(\text{branch3})^n + \dots$$

In several studies the exponent n has been determined to vary between 2.4 and 3.2 (2, 12, 25) in normal vessels. For $n < 3$, an initially spherical air bubble will split into so-called slugs (Fig. 9). At each branching the slugs will become relatively longer, a phenomenon called tapering. In this scenario the ratio of length to diameter of a trapped slug increases with the number of branchings the slug has passed. As may be expected, long slugs need more time to dissolve than shorter ones. This suggested relationship between vascular geometry and the degree of embolization by bubbles points to a difficulty in extrapolating our observations to the clinical situation. The geometry of the vascular bed in patients with atherosclerotic disease may be quite different from that in the studied animals.

Implications. This study has shown that air bubbles of 75, 150, and 300 μm diameter injected selectively in the LADCA cause reversible wall motion abnormalities in healthy pigs. It also became clear that regional myocardial functional depression after injection of air bubbles could pass unnoticed on the basis of global hemodynamic measurements. Further clinical study of global and especially regional effects in myocardial function after applying new interventional gas-producing techniques is warranted.

The authors thank Rob van Bremen and Jan van Meegen for their assistance during the preparation of the animals.

This work was supported by The Netherlands Heart Foundation Grant 91.100.

Address for reprint requests: C. J. Slager, Laboratory for Haemodynamics, Thoraxcenter Ee2322, Erasmus Univ. Rotterdam, PO Box 1738, 3000 DR Rotterdam, The Netherlands.

Received 6 July 1992; accepted in final form 19 April 1993.

REFERENCES

- ABELA, G. S., S. NORMANN, D. COHEN, B. L. FELDMAN, E. A. GEISER, AND C. R. CONTI. Effects of carbon dioxide, Nd:YAG, and argon laser radiation on coronary atherosclerotic plaques. *Am. J. Cardiol.* 50: 1199–1205, 1982.
- ARTS, T. Propagation velocity and reflection of pressure waves in the canine coronary artery. *Am. J. Physiol.* 237 (Heart Circ. Physiol. 6): H469–H474, 1979.
- BUTLER, B. D., AND B. A. HILLS. The lung as a filter for microbubbles. *J. Appl. Physiol.* 47: 537–543, 1979.
- CHAN, K. S., AND WEN-JEI YANG. Survey of literature related to the problems of gas embolism in the human body. *J. Biomech.* 2: 299–312, 1969.
- CHANG, H. K., M. E. WEBER, J. THOMSON, AND R. R. MARTIN. Hydrodynamic features of pulmonary air embolism: a model study. *J. Appl. Physiol.* 51: 1002–1008, 1981.
- CLARKE, R. H., J. M. ISNER, R. F. DONALDSON, AND G. JONES. Gas chromatographic-light microscopic correlative analysis of excimer laser photoablation of cardiovascular tissues: evidence for a thermal mechanism. *Circ. Res.* 60: 429–437, 1987.
- CURTILLET, E. L'embolie gazeuse artérielle. *J. Chir.* 53: 461–482, 1939.
- GUSBERTS, G. *Tissue Ablation by CW Lasers, and a Pulsed XeCl Excimer Laser as Used in Excimer Laser Angioplasty* (PhD thesis). Amsterdam, The Netherlands: Univ. of Amsterdam, 1992, p. 108–112.
- GOLDFARB, D., AND H. T. BAHNSON. Early and late effects on the heart of small amounts of air in the coronary circulation. *J. Thorac. Cardiovasc. Surg.* 46: 368–378, 1963.
- GRULKE, D. C., N. A. MARCH, AND B. A. HILLS. Experimental air embolism: measurement of microbubbles using the Coulter counter. *Br. J. Exp. Pathol.* 54: 684–691, 1973.
- HEUPLER, F. A., JR., C. M. FERRARIO, D. B. AVERILL, AND C. BOTT-SILVERMAN. Initial coronary air embolus in the differential diagnosis of coronary artery spasm. *Am. J. Cardiol.* 55: 657–661, 1985.
- HUTCHINS, G. M., M. M. MINER, AND J. K. BOITNOTT. Vessel caliber and branch-angle of human coronary artery branch-points. *Circ. Res.* 38: 572–576, 1976.
- ISNER, J. M., R. H. CLARKE, R. F. DONALDSON, AND A. AHARON. Identification of photoproducts liberated by in vitro argon laser irradiation of atherosclerotic plaque, calcified cardiac valves and myocardium. *Am. J. Cardiol.* 55: 1192–1196, 1985.
- KAHN, J. K., AND G. O. HARTZLER. The spectrum of symptomatic coronary air embolism during balloon angioplasty: causes, consequences, and management. *Am. Heart J.* 119: 1374–1377, 1990.
- LAWRENCE, W. E., W. L. MAUGHAN, AND D. A. KASS. Mechanism of global functional recovery despite sustained posts ischemic regional stunning. *Circulation* 85: 816–826, 1992.
- LIEBERMANN, L. Air bubbles in water. *J. Appl. Physics* 28: 205–211, 1957.
- MCFALLS, E. O., D. J. DUNCKER, R. KRAMS, H. WARD, C. GORNICK, AND P. D. VERDOUW. Endothelium dependent vasodilatation following brief ischaemia and reperfusion in anaesthetised swine. *Cardiovasc. Res.* 25: 659–665, 1991.
- MOORE, W. J. *Physical Chemistry* (5th ed.). London: Longman, 1986, p. 239–240, 477–478.
- PERRY, J. C., E. S. MUNSON, M. H. MALAGODI, AND D. O. SHAH. Venous air embolism prophylaxis with a surface-active agent. *Anesth. Analg.* 54: 792–799, 1976.
- PRESSON, R. G., K. R. KIRK, K. A. HASELBY, J. H. LINEHAN, S. ZALESKI, AND W. W. WAGNER. Fate of air emboli in the pulmonary circulation. *J. Appl. Physiol.* 67: 1898–1902, 1989.
- RHODES, G. R., AND C. L. MCINTOSH. An experimental evaluation of coronary air embolism. *Surg. Forum* 27: 275–278, 1976.
- SCHAMHARDT, H. C. *Regional Myocardial Perfusion and Performance* (PhD thesis). Rotterdam, The Netherlands: Erasmus University Rotterdam, 1980, p. 67.
- SLAGER, C. J., C. E. ESSÉD, J. C. H. SCHURBIERS, N. BOM, P. W. SERRUYS, AND G. T. MEESTER. Vaporization of atherosclerotic plaques by spark erosion. *J. Am. Coll. Cardiol.* 5: 1382–1386, 1985.
- STEGMANN, T., W. DANIEL, L. BELLMANN, G. TRENKLER, H. OBLERT, AND H. G. BORST. Experimental coronary embolism. Assessment of time course of myocardial ischemia and the protective effect of cardiopulmonary bypass. *Thorac. Cardiovasc. Surg.* 28: 141–149, 1980.
- WIERINGA, P. A. *The Influence of the Coronary Capillary Network on the Distribution and Control of Local Blood Flow* (PhD thesis). Delft, The Netherlands: Technical University Delft, 1985, p. 61.

CHAPTER 6

EARLY AND LATE ARTERIAL HEALING RESPONSE TO CATHETER-INDUCED LASER, THERMAL, AND MECHANICAL WALL DAMAGE IN THE RABBIT

Antoon Oomen, Lieselotte van Erven, Walda V.A. Vandenbroucke,
Ruud M. Verdaasdonk, Cornelis J. Slager, Sharon L. Thomson, Cornelius Borst.

Early and Late Arterial Healing Response to Catheter-Induced Laser, Thermal, and Mechanical Wall Damage in the Rabbit

Antonius Oomen, MD, Lieselotte van Erven, MD,
Walda V.A. Vandenbroucke, MD, Rudolf M. Verdaasdonk, MSc,
Cornelius J. Slager, MSc, Sharon L. Thomsen, MD, and Cornelius Borst, MD

Interuniversity Cardiology Institute of the Netherlands (A.O., W.V.A.V.) and Experimental Cardiology Laboratory, Department of Cardiology, Heart-Lung Institute, University Hospital Utrecht, The Netherlands (L.v.E., R.M.V., C.B.); Thorax Center, Erasmus University Rotterdam, The Netherlands (C.J.S.); and Laser Biology Research Program, The University of Texas, M.D. Anderson Cancer Center, Houston, Texas 77030 (S.L.T.)

Pulsed lasers are being promoted for laser angioplasty because of their capacity to ablate obstructions without producing adjacent thermal tissue injury. The implicit assumption that thermal injury to the artery is to be avoided was tested. Thermal lesions were produced in the iliac arteries and aorta of normal rabbits by a) electrical spark erosion, b) the metal laser probe, and c) continuous wave neodymium-yttrium aluminum garnet (Nd-YAG) laser energy through the sapphire contact probe. High-energy doses were used to induce substantial damage without perforating the vessel wall. Thermal lesions (n=77) were compared with mechanical lesions (n=22) induced by oversized balloon dilation. Medial necrosis was induced by all four injury methods. Provided no extravascular contrast was observed after the injury, all damaged segments were patent after 1 to 56 days. The progression of healing with myointimal proliferation was remarkably similar for all injuries. At 56 days, the neointima measured up to 370 μm . In conclusion, provided no perforation with contrast extravasation occurred, the normal rabbit artery recovered well from transmural thermal injury. The wall healing response is largely nonspecific.

Key words: aneurysm, balloon angioplasty, laser angioplasty, myointimal proliferation, reocclusion, restenosis

INTRODUCTION

Pulsed laser irradiation is capable of precise and controlled tissue ablation without adjacent thermal tissue damage *in vitro* [1, 2]. In contrast, continuous wave (CW) laser irradiation produces extensive thermal injury to the tissue surrounding the ablation crater [3-5]. As a result, most experimental laser angioplasty studies with pulsed lasers postulate that these lasers are superior to CW lasers or thermal ablation devices because of the virtual absence of unwanted thermal arterial wall injury [1, 2, 6]. However, the assumption that thermal injury of the arterial wall is to be avoided needs further evaluation.

In this study, we therefore deliberately induced massive thermal injury, using high-energy doses. Our aim was to evaluate the healing response of the normal arterial wall after maximal thermal injury as compared with that after profound mechanical injury. Three methods were used: a) electrical spark erosion [7]; b) the metal laser probe heated with a CW neodymium-yttrium

Accepted for publication April 16, 1990.

Address reprint requests to Cornelius Borst, MD, Experimental Cardiology Laboratory, Heart Lung Institute, University Hospital Utrecht, Heidelberglaan 100, 3584 CX Utrecht, The Netherlands.

TABLE 1. Necropsy Timetable*

| Survival (days) | Animals | | Lesions | | | |
|--------------------|---------|------------|------------------|----------------|-------------------|---------------------|
| | Thermal | Mechanical | Spark erosion | Metal probe | Sapphire probe | Balloon catheter |
| 1 | 6 | 2 | 7 | 3 | 3 | 2 |
| 3 | 5 | 2 | 8 | 2 | 4 | 4 |
| 7 | 5 | 3 | 6 | 2 | 3 | 2 |
| 14 | 4 | 3 | 7 | 3 | 4 | 5 |
| 21 | 5 | 3 | 8 | 3 | 5 | 6 |
| 56 | 3 | 2 | 5 | 2 | 2 | 3 |
| Total | 28 | 15 | 41 | 15 | 21 | 22 |

*Postintervention intervals (survival days); number of animals with thermal or mechanical lesions, number of lesions.

aluminum garnet (Nd-YAG) laser [8, 9]; and c) the rounded sapphire contact probe in conjunction with a CW Nd-YAG laser [10, 11]. These thermal methods were compared with mechanical arterial wall damage induced by overstretching the artery with a balloon catheter [12].

MATERIALS AND METHODS

Animal Studies

Forty-nine normal rabbits (Flemish Giant, weight 5–7 kg) were used. Six additional rabbits were used to determine the energy dose for this near-perforation study. All animals were maintained on normal diet throughout the duration of the study.

Experimental Procedure

The animals were anesthetized with intravenous etomidate, 1 mg/kg, and sufentanyl citrate, 0.01 mg/kg, and placed on a pump ventilator (Amsterdam Infant Ventilator MK3) supplying a mixture of oxygen and nitrous oxide (1:2) with halothane (0.7%) added. Arterial pressure was monitored in the left central ear artery. The animals were not anticoagulated during the study. A 5F Swan-Ganz catheter was introduced through a carotid cutdown and positioned in the descending aorta. After a 6F sheath had been advanced, the Swan-Ganz catheter was exchanged for a 6F straight catheter. Angiography of the lower abdominal aorta and iliac arteries was performed before and after the interventions using Iohexol 647 mg/ml (Omnipaque) as contrast medium. Fluoroscopy was performed with a C-arm (Philips BV 22), and the images were stored on a videorecorder.

Four different angioplasty catheters described below were introduced and advanced un-

der fluoroscopy to either the aortic bifurcation (sapphire contact probe) or the left and right iliac arteries (spark erosion probe, metal laser probe, and balloon catheter). The lesion sites in the iliac artery were between 1 and 3 cm distal to the aortic bifurcation as measured with a radio-opaque ruler. The energy doses for the three thermal methods were chosen to be near the perforation level as determined in a prior dose finding study.

Animals were sacrificed by intracardial injection of potassium chloride, 20 mmol in 10 ml, at 1, 3, 7, 14, 21, and 56 days after the initial procedure (Table 1). Angiograms were made before the animals were killed. The iliac segments containing the lesions were marked with sutures. The aortic bifurcation was removed en bloc with the iliac arteries and fixed in 4% formalin.

Spark-Erosion Ablation

The spark-erosion catheter and the electrical-spark generator were modified for these in vivo experiments from the system described earlier [7]. The modified catheter consisted of a unipolar platinum-ring electrode placed 1 mm proximal to the catheter tip (Fig. 1). The radial surface of the spark electrode was 5 mm². The output impedance of the spark generator was 60 ohm, and its peak-to-peak square wave voltage was 1,400 V at a frequency of 500 kHz. The second indifferent electrode was fixed on a shaved part of the lower limb. An additional low-frequency cutoff filter was inserted between both electrodes and the generator to reduce neuromuscular stimulation. Spark erosion ablation of arterial tissue was effected with a single 5 millisecond pulse at 1 cm and at 3 cm distal to the aortic bifurcation. The ablation parameters had been determined in prior pilot experiments.

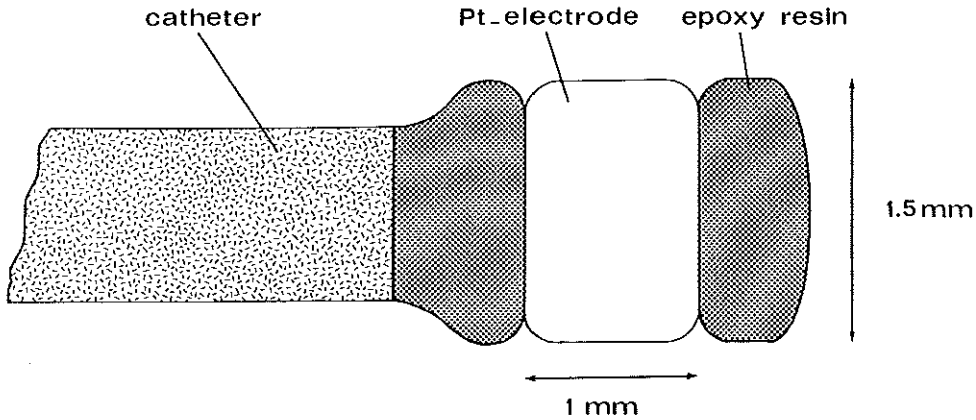


Fig. 1. The modified spark-erosion catheter. A cylindrical platinum electrode is isolated at two sides by epoxy resin.

Metal Laser-Probe Ablation

A 2.0 mm diameter metal-laser probe (SLR 2.0, Trimedynce, Santa Ana, CA, USA) mounted on a 0.3 mm core silica fiber was used. The temperature of the probe was monitored as described earlier [13]. In brief, a 0.3 mm type K thermocouple (response time 10 milliseconds) was wedged into the safety-wire channel of the probe to insure good contact. The thermocouple output was recorded on a pen recorder. The fiber and the thermocouple wires were incorporated into a straight guiding catheter.

The silica fiber was connected to a modified [14] CW Nd-YAG laser (Medilas-2, MBB, München, FRG) that delivered 8 W for 5 seconds to the probe. The delivered power was estimated by using an identical fiber not fitted with a metal probe and an external power meter (Laser Instrumentation, Basingstoke, Great Britain). The thermal lesions were produced during rapid, continuous back and forth movement of the probe to prevent unwanted sticking of the probe to the vessel wall.

Sapphire Contact Probe Ablation

A 1.8 mm-diameter rounded sapphire contact probe (SMRT 1.8, Surgical Laser Technologies, Malvern, PA) mounted on a 0.6 mm core silica fiber was used. The fiber was connected to the Nd-YAG laser described above. A saline flush (3 ml/min) prevented blood from entering the fiber-sapphire interface and cooled the sapphire crystal and the metal connector [11]. The output of the fiber was 15 W for 1 second. The spot size diam-

eter at the surface of the crystal was 1.0 mm, and the power density was 12 W/mm^2 . The laser was activated after the probe was wedged against the aortic bifurcation as determined by fluoroscopy using road-mapping techniques.

Balloon Dilation

In a separate series of 15 animals, both iliac arteries were overstretched with a balloon catheter (Schneider, 4 F coronary catheter, balloon diameter, 3.7 mm, length 20 mm) inflated to 5 bar for 1 minute to produce mechanical injury. The mean dilation ratio (balloon diameter/artery diameter) was 1.7 ± 0.6 (SD) ($n=26$).

Angiography

Hard-copy images (Mitsubishi video copy processor P60B) were obtained from the angiogram videotapes and evaluated by two independent observers using operating spectacles (magnification $\times 2$) and a caliper. The iliac segments containing lesions were scored as to angiographic appearance: normal, stenosed ($> 50\%$ diameter decrease), occluded, and aneurysm formation ($> 50\%$ diameter increase) relative to the adjacent noninjured parts of the artery.

Histology

The samples were dehydrated in graded alcohols and xylenes and embedded in paraffin. Transverse $5 \mu\text{m}$ -thick sections were made of each lesion at $150 \mu\text{m}$ intervals along the lesion. Depending on the length of the lesion, 15–100 sec-

TABLE 2. Complications for the Different Angioplasty Catheters

| | Spark erosion | Metal probe | Sapphire probe | Balloon catheter |
|--------------------------------------|---------------|-------------|----------------|------------------|
| Number of lesions | 41 | 15 | 21 | 22 |
| Macroscopic perforation | 2 | 3 | 0 | 0 |
| Microscopic perforation ^a | 8 | 6 | 1 | 0 |
| Occlusion ^b | 0 | 2 | 0 | 0 |
| Stenosis | 0 | 0 | 0 | 1 |

^aAngiographic perforations are included in microscopic perforation numbers.

^bBoth occlusions in cases of angiographic perforation.

tions per lesion were made in duplo. The aortic bifurcation lesions were sectioned sagittally without the 150 μ m steps. Control sections were taken from the iliac artery distal to the lesions.

Duplo sections were stained by routine staining procedures: a) hematoxylin and eosin to study the extent of cell necrosis and the progression of wall healing; and b) Weigert von Gieson's elastin stain to study the interruption (ablation) and reconstruction of the elastic tissue framework of the arterial wall [15].

The histologic sections were evaluated qualitatively. In animals, however, that had survived for at least 2 weeks, the maximum thickness of the neointima was measured using an ocular grid (Olympus WHK 10x).

RESULTS

Angiography

Extravasation of a limited amount of contrast was observed immediately after five thermal interventions, twice after spark erosion and three times after metal probe ablation (Table 2). No perforation was observed after balloon dilation. In two cases of metal probe perforation, occlusion was found at the time of sacrifice (at 7 and 21 days).

All thermal lesions that did not show angiographic perforation were patent without stenosis or aneurysm formation at 1–56 days following the intervention. All 21 thermally damaged aortic bifurcations showed patent origins of the iliac arteries. No aneurysms or occlusions were found 1–56 days after overstretching the iliac arteries and stenosis was found only once. No distinct contrast defect suggestive of a mural thrombus was found in any animal.

Microscopic Anatomy

Eight of 30 overdilated iliac artery segments in 15 animals showed no histological signs of medial necrosis nor myointimal proliferation.

These eight segments were not included in the description of the histological results.

Evidence of perforation was found microscopically in six spark-erosion lesions, three metal laser probe lesions, and one sapphire probe lesion, although no extravasation of contrast had been seen during the procedure (Table 2). All angiographic perforations were verified microscopically. The two occlusions after metal-probe injury consisted of organized thrombus (7 days) and organized thrombus with infiltration of connective tissue at 21 days.

Thermal angioplasty resulted generally in more conspicuous wall injury than balloon angioplasty. The major differences in injury between the three thermal angioplasty methods and the mechanical method were the absence of tissue ablation and adventitial necrosis in the latter (Fig. 2B). However, the progression of healing of the lesions produced by each method of thermal ablation and overstretching was remarkably similar.

Twenty-four hours (Fig. 2) and 3 days after the intervention, loss of nuclear staining of the smooth-muscle cells indicated necrosis of the media, often with a clearly demarcated transition between viable and necrotic tissue. Medial necrosis, frequently circumferential, occurred in both thermally and mechanically traumatized arteries. In these non-pressure-fixed specimens, the wavy internal elastic lamina was flattened locally after both thermal and mechanical injury.

In thermally damaged arteries, mural microthrombi were observed when luminal ablation and medial damage had been extensive. The external elastic lamina appeared compressed and less wavy, and the adventitia had a homogeneous and glassy appearance due to thermal coagulation of the collagen in the heated arteries. In over-stretched arteries, the external elastic lamina and adventitia appeared normal. Infiltrates with polymorphonuclear cells occurred in the subluminal layers of the media in all specimens.

At 7 days (Fig. 3), the neointima formation was found on the luminal surface of residual fibrin covering the ablation lesions and also on top of the intact internal elastic lamina in the less severely thermally and mechanically damaged arteries. The small foci of neointima were composed of five to six layers of myointimal cells, but little fibrosis or new elastin tissue was found in the lesions yet. The organization of the thermally coagulated adventitial collagen was associated with infiltrates of macrophages and a few lymphocytes.



Fig. 2. One day. Surviving (S) and necrotic (N) media in rabbit iliac artery after (A) spark erosion and (B) balloon angioplasty. Polymorphonuclear cells infiltrate the subluminal tissues of the necrotic media in both specimens. Arrow in A indicates thermal coagulation of adventitial collagen. Hematoxylin & Eosin, $\times 145$.

At 14 days (Fig. 4), in both thermal and mechanical lesions, myointimal proliferation had progressed to form a substantial neointimal layer as thick as the normal media (Table 3). Parts of the necrotic media were repopulated with myointimal cells. In other areas, the media was not repopulated with cells and remained thin. In those

areas, the total thickness of the wall was largely reconstituted by the thickened neointima (Fig. 4). Note in Figure 4A the myointimal proliferation with distinct deposition of elastin in response to extensive ablative injury by the metal probe.

At 21 days (Fig. 5), the thick neointima (Table 3) contained considerable amounts of thin



Fig. 3. Seven days. Ablation crater throughout the wall of a proximal iliac artery produced by the metal laser probe and resulting in perforation (perforation not shown in this section). Debris of thermally injured tissue is still present after 7 days. Note rim of carbonized tissue (C), fibrin (F), and neointima (N) extending over the fibrin layer. Weigert von Gieson, $\times 95$.

TABLE 3. Neointimal Proliferation*

| Survival (days) | Spark erosion | Metal probe | Balloon catheter |
|-----------------|---------------|----------------------------|------------------|
| 14 | 60–210 (n=7) | 30–200 (n=3) | 80–380 (n=5) |
| 21 | 140–370 (n=8) | 160–220 (n=2) ^a | 110–360 (n=6) |
| 56 | 70–370 (n=5) | 150–370 (n=2) | 180–310 (n=3) |

*Range of maximum neointimal thickness in a lesion, in microns (number of lesions in parentheses) measured from histological sections. Sapphire contact probe lesions were not included. Histology proved to be difficult to quantitate at the aortic bifurcation.

^aOne occluded vessel excluded from measurement.

elastin fibers and fibrotic tissue. Dystrophic calcifications were found focally in the necrotic media or around residual fragments of thermally damaged arterial wall trapped in the scar tissue. Richly vascularized granulomatous tissue was present in the adventitia of the arteries at points of thermal damage and perforation.

At 56 days, no necrotic areas were found in the media. The extent of neointima formation in all experimental types varied considerably, both along the axis and around the circumference of the vessels. After thermal injury, the maximal thickness of the neointima was up to 370 μm , after mechanical injury it was up to 380 μm (Table 3). The continuous membrane of the internal elas-

tic lamina, once ruptured, never reformed. However, the neointima covering the defects contained new thin, discontinuous elastin fibers.

Specific Results Related to Angioplasty Method

Electrical-spark erosion. In these in vivo experiments, electrical-spark erosion was associated with transmural coagulation necrosis of the iliac artery. Longitudinal, transmural coagulation necrosis extended about 200 μm from the ablation site.

Laser angioplasty. The peak temperature of the metal laser probe in the iliac artery averaged 130°C (70–295°C, n=15). In two cases, probe movement was hampered when the probe stuck to

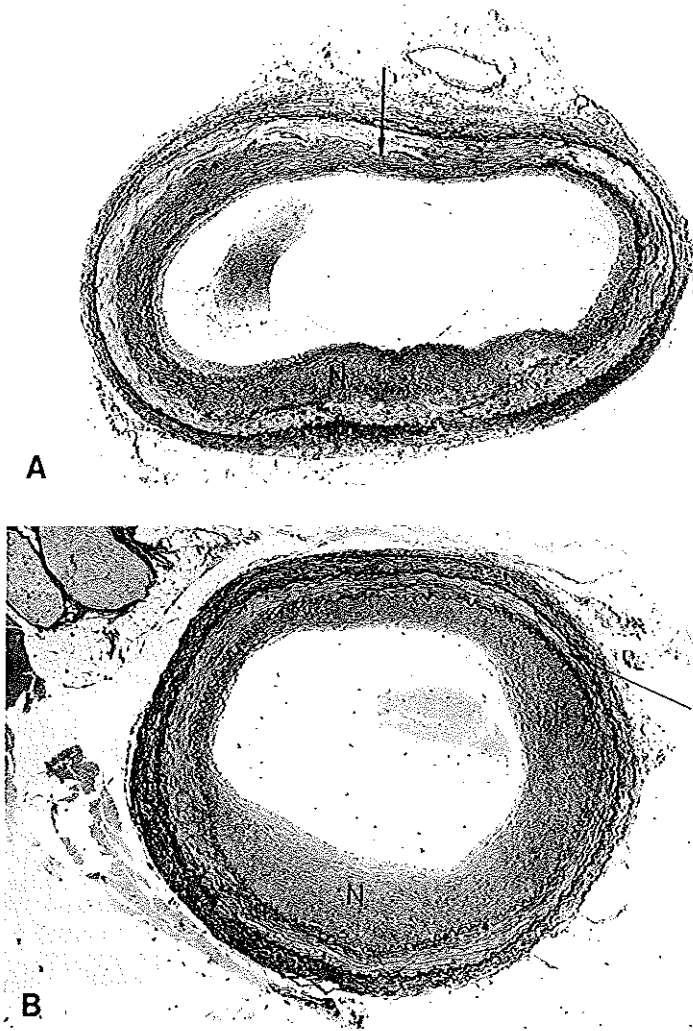


Fig. 4. Fourteen days. **A:** Thermal damage produced by a hot metal tip has led to extensive disruption of the internal elastic lamina and the media. Residual fragments of the internal elastic lamina are indicated by the arrow. Neointima (N) forms the substantial part of the reconstructed wall. **B:** The patent lumen of the overstretched artery is lined by thick neointima (N). Note the thin media in part of the wall with persistent necrosis (arrow). Weigert von Gieson, $\times 35$.

the vessel wall at temperatures exceeding 120°C. Perforation was never seen with probe temperatures below 140°C. Adhesion to the wall was never experienced with the sapphire contact probe or the spark-erosion catheter.

DISCUSSION

Provided the angioplasty catheters did not cause acute perforation (contrast extravasation), all arteries were found to be patent without aneurysm formation or late perforation 1–56 days after the intervention. Stenosis was found in one case of balloon dilation.

Histologically, the progression of the healing response was remarkably similar for the three thermal and the one mechanical angioplasty injuries. The pattern of wall healing depended on the extent of disruption of the various layers of the arterial wall. Wall healing resembled nonspecific wound healing responses [15]. However, the healing response of human arteries may be different and atherosclerosis and hypercholesterolemia may alter wall healing.

Laser Angioplasty and Temperature

Continuous wave laser irradiation produces thermal damage in the adjacent tissue [3–5, 10]. Tissue damage by the sapphire probe used with a CW Nd-YAG laser is attributed to direct laser light-tissue interactions [3, 4], direct and indirect heating of the sapphire crystal [11, 16], and heat conduction. The laser heated metal probes produce extensive radial wall damage by heat conduction [8, 9, 17].

In the present study, the peak temperature reached by the metal probe varied from 70° to 295°C. Complications of the metal probe, like sticking to the wall and perforation, were sometimes observed if peak temperature exceeded 120° and 140°C, respectively. Neither the sapphire probe nor the spark-erosion electrode adhered to the wall, but technically it was not yet feasible to record *in vivo* temperatures of the latter two probes. The circumferential heat distribution of the metal probe [8, 9, 13] may cause smooth muscle cell spasm and irreversible contracture of the wall [18]. This may enlarge the risk of the probe sticking to the wall. Tissue recovered from the metal surface of a stuck probe was identified histologically as fragments of thermally damaged arterial wall.

Spark-Erosion Angioplasty

Previous *in vitro* electrical spark erosion studies [7] had shown thermal tissue injury extending about 40 μm from the ablation lesion. The present *in vivo* investigation revealed that, generally, transmural coagulation of the wall occurred up to 200 μm from the ablation site. The augmented thermal damage zone in these experiments may be explained from physical factors as the difference in environmental temperature and electrode shape and material (Fig. 1). In addition, latent heat damage could not be observed in the *in vitro* experiments, because the full extent of heat-induced tissue necrosis will become apparent only after survival for 1 day. Despite the addition of a filter, the sparking pulse was still accompanied by neuromuscular stimulation, leading to excessive movement of the hind paw. Therefore, the design of the generator is being further modified.

Arterial Wall Damage and Complications

Four complications can arise from severe wall damage: a) acute perforation; b) weakening of the arterial wall with aneurysm formation and late perforation; c) mural and occlusive thrombosis; and d) (re)stenosis due to an excessive healing response (myointimal hyperplasia).

In this study macroscopic perforations were observed (Table 2), which in the case of the metal probe were associated with adherence of the probe to the vessel wall. The relatively high macroscopic perforation rates (metal probe 20%, spark erosion 5%) reflect the deliberate use of high energies in these thin-walled normal arteries and therefore should not be equated with an angioplasty risk. In our hands, angiography failed to reveal microperforations in 10 of 77 thermal lesions (14%). A similar finding was described in an experimental case study [19].

Thermally induced transmural necrosis and mechanically induced medial necrosis occurred without subsequent short-term complications. The thinned necrotic wall withstood transmural pressure. Even ablation of most of the media did not have adverse effects on the functional integrity of the arteries followed for 56 days. In contrast to Lee et al. [20], who reported aneurysm formation in

Fig. 5. Twenty-one days. A: Ablative sapphire contact probe lesion of aortic bifurcation. The internal elastic lamina has been interrupted (arrows). B: Nonablative metal laser probe lesion of iliac artery. C: Balloon angioplasty lesion. N, neointima, M, media. Weigert von Gieson, A $\times 90$, B $\times 145$, C $\times 145$.

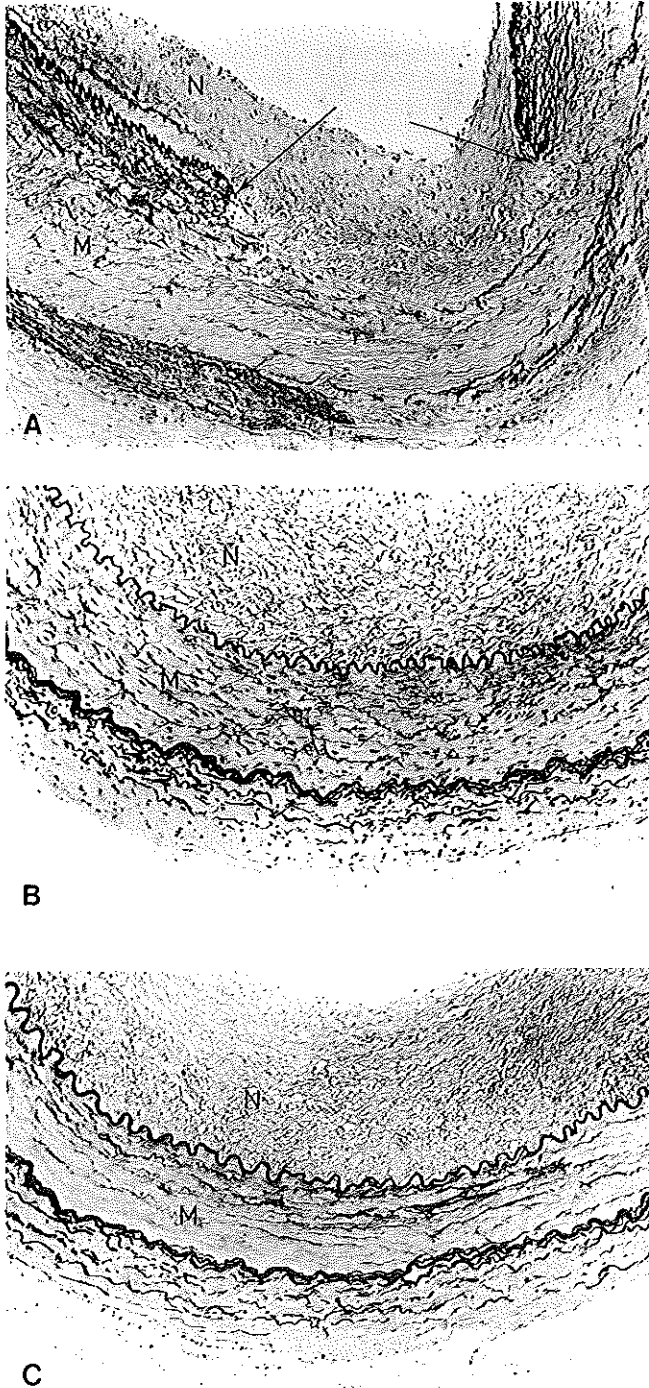


Fig. 5.

two of four atherosclerotic rabbits followed 1–14 days after surgical argon laser irradiation directed perpendicular to the aorta, we found no aneurysm formation in any of the 77 thermal lesion sites in 28 rabbits with normal arteries. Accordingly, transmural coagulation with the Spears' balloon at 95–140°C [21] seems to be well tolerated both experimentally [22,23] and clinically [24]. In a clinical trial of laser balloon angioplasty in 106 patients, only one aneurysm was found by angiography on long-term follow-up (38 at 3 months and 68 at ≥ 6 months) (JR Spears, personal communication, February 27, 1990).

No contrast defects suggestive of large mural thrombi were observed in any of the angiograms. In the thermal lesions, microscopic mural fibrin or platelet thrombi were a regular finding, whereas no such thrombi were found in non-heated arteries. Provided an acute angiographic perforation had not occurred, no thrombotic occlusions were found after the four angioplasty methods, and all arteries were patent on angiography at sacrifice. The two thrombotic occlusions that were found in metal probe lesions both were associated with macroscopic perforation. Sanborn et al. [25] recently reported a high incidence of perforation (3/10) and both occlusive (2/10) and mural thrombi (6/10) after metal laser probe (10 W, 3–5 seconds) manipulation in normal swine coronary arteries. Although in our study the complications of the metal probe should not be equated with an angioplasty risk, both studies may point to an inherent dosimetry problem of the metal probe. Although the healing response of the arterial wall consistently included myointimal proliferation, no angiographic stenosis was observed after the thermal interventions and only one after balloon dilation. To our surprise, in eight of 30 balloon distended arteries, no histological signs of overdistension were found. We are currently evaluating the influence of the predilation diameter of the artery on the outcome of balloon angioplasty.

Arterial Wall Healing

In a detailed histological analysis of wound healing of microvascular anastomoses made by laser welding and by conventional suture methods, Neblett et al. [15] concluded that wound healing in the two procedures followed similar paths chronologically and morphologically. We found that the healing pattern of the arterial lesions produced by the four different injury methods

progressed in a similar fashion. Therefore, we conclude that the early and late responses to mechanical and thermal injury consist of healing patterns that represent nonspecific reactions to injury.

Sanborn et al. [26] have observed a reduced fibrocellular proliferation after hot tip angioplasty compared to balloon angioplasty in the atherosclerotic rabbit iliac artery. The present experiments with normal rabbits do not suggest a reduced fibrocellular proliferation after thermal wall injury, but the large variation in neointima thickness in our study does not allow further conclusion.

Most of the earlier studies on arterial wall healing after CW laser injury involved small lesions created by irradiation perpendicular to the wall in the opened artery during surgery [27–30]. With the exception of the preliminary study by Lee et al. [20], these lesions healed without serious adverse effects. Pulsed lasers produce sharply delineated craters, which heal well [31, 32]. In the present study in which a CW laser was used, ablation with extensive thermal wall damage also healed well if no gross perforation had occurred. We infer from this impressive healing capacity that in the discussion on the relative merits of pulsed laser ablation vs. CW laser ablation for angioplasty [1, 2, 6], the absence of adjacent tissue injury might not be regarded as a decisive argument in favor of pulsed lasers.

In conclusion, provided no gross perforation of the arterial wall occurs, the normal rabbit artery wall recovered well after extensive thermal or mechanical injury. The healing pattern of the injured arterial wall resembled the pattern of nonspecific wound healing.

ACKNOWLEDGMENTS

The authors are indebted to Jan R. Tuntelder and Evelyn Velema for expert technical assistance; Etienne O. Robles de Medina, MD, for continuous support; Nienke Essed, MD, Mark J. Post, MD, and Pieter J. Slootweg, MD, for their critical review of this manuscript; the Department of Pathology for the use of their facilities; and Alinda I. Diepeveen for secretarial assistance.

This study was supported in part by the Netherlands Heart Foundation, The Hague (grants 34.001, R.M. Verdaasdonk, W.V.A. Vandenbroucke, and 37.007, S.L. Thomsen).

REFERENCES

- Grundfest WS, Litvack F, Forrester JS, Goldenberg TSVI, Swan HJC, Morgenstern L, Fishbein M, McDermid IS, Rider DM, Pacala TJ, Laudenslager JB: Laser ablation of human atherosclerotic plaque without adjacent tissue injury. *J Am Coll Cardiol* 1985; 5:929-933.
- Isner JM, Fortin Donaldson RF, Deckelbaum LI, Clarke RH, Laliberte SM, Ucci AA, Salem DN, Konstam MA: The excimer laser: Gross, light microscopic and ultrastructural analysis of potential advantages for use in laser therapy of cardiovascular disease. *J Am Coll Cardiol* 1985; 6:1102-1109.
- Abela GS, Normann S, Cohen D, Feldman RI, Geiser EA, Conti CR: Effects of carbon dioxide, Nd-YAG, and argon laser radiation on coronary atherosclerotic plaques. *Am J Cardiol* 1982; 50:1199-1205.
- Shelton ME, Hoxworth B, Shelton JA, Virmani R, Friesinger GC: A new model to study quantitative effects of laser angioplasty on human atherosclerotic plaque. *J Am Coll Cardiol* 1986; 7:909-915.
- Lawrence PF, Dries DJ, Moatamed F, Dixon J: Acute effects of argon laser on human atherosclerotic plaque. *J Vasc Surg* 1984; 1:852-859.
- Litvack F, Grundfest WS, Pappaioannou T, Mohr FW, Jakubowski AT, Forrester JS: Role of laser and thermal ablation devices in the treatment of vascular diseases. *Am J Cardiol* 1988; 61:81G-86G.
- Slager CJ, Essed CE, Schuurbijs JCH, Bom N, Serruys PW, Meester GT: Vaporization of atherosclerotic plaques by spark erosion. *J Am Coll Cardiol* 1985; 5:1382-1386.
- Sanborn TA, Faxon DP, Haudenschild CC, Ryan TJ: Experimental angioplasty: circumferential distribution of laser thermal energy with a laser probe. *J Am Coll Cardiol* 1985; 5:934-938.
- Welch AJ, Bradley AB, Torres JH, Motamedi M, Ghidoni JJ, Pearce JA, Hussein H, O'Rourke RA: Laser probe ablation of normal and atherosclerotic human aorta in vitro: a first thermographic and histologic analysis. *Circulation* 1987; 76:1353-1363.
- Geschwind HJ, Blair JD, Monksma D, Kern MJ, Stern J, Deligonul U, Kennedy JLL, Smith S: Development and experimental application of contact probe catheter for laser angioplasty. *J Am Coll Cardiol* 1987; 9:101-107.
- Verdaasdonk RM, Cross FW, Borst C: Physical properties of sapphire fibre tips for laser angioplasty. *Lasers Med Sci* 1987; 2:183-188.
- Rasmussen LH, Garbarsch C, Lorenzen I: Injury and repair of smaller muscular and elastic arteries. A light microscopic study on the different healing patterns of rabbit femoral and carotid arteries following dilation injuries by a balloon catheter. *Virchows Arch A* 1987; 411:87-92.
- Verdaasdonk RM, Borst C, Boulanger LHMA, Van Gemert MJC: Laser angioplasty with a metal laser probe ('hot tip'): probe temperature in blood. *Lasers Med Sci* 1987; 2:153-158.
- Verdaasdonk RM, Frank F, Borst C: Diaphragm in cavity for low output power application of 100 W Nd:YAG laser. In Wollenek G, Laufer G, Wolner E (eds): "Lasers in Cardiovascular Diseases." Munchen: Medizinischer Verlag EBM & MZV, 1986, pp 37-40.
- Neblett CR, Morris JR, Thomsen S: Laser-assisted microsurgical anastomosis. *Neurosurgery* 1986; 19:914-934.
- Geschwind H, Fabre M, Chaitman BR, Lefebvre-Villardeb M, Ladouch A, Boussignac G, Blair JD, Kennedy HL: Histopathology after Nd-YAG laser percutaneous transluminal angioplasty of peripheral arteries. *J Am Coll Cardiol* 1986; 8:1089-1095.
- Abela GS, Seeger JM, Barbieri E, Franzini D, Fenech A, Pepine CJ, Conti CR: Laser angioplasty with angioscopic guidance in humans. *J Am Coll Cardiol* 1986; 8:184-192.
- Gorisch W, Boergen KP: Heat-induced contraction of blood vessels. *Lasers Surg Med* 1982; 2:1-13.
- Gal D, Steg PG, Dejesus ST, Rongione AJ, Clarke RH, Isner JM: Failure of angiography to diagnose thermal perforation complicating laser angioplasty in a rabbit. *Am J Cardiol* 1987; 60:751-752.
- Lee G, Ikeda RM, Theis JH, Chan MC, Stobbe D, Ogata C, Kumagai A, Mason DT: Acute and chronic complications of laser angioplasty: vascular wall damage and formation of aneurysms in the atherosclerotic rabbit. *Am J Cardiol* 1984; 53:290-293.
- Jenkins RD, Sinclair IN, Anand R, Kafil AG, Schoen FJ, Spears JR: Laser balloon angioplasty: effect of tissue temperature on weld strength of human postmortem intima media separations. *Lasers Surg Med* 1988; 8:30-39.
- Sinclair IN, Jenkins RD, James LM, Sinofsky EL, Wagner MS, Sandor T, Schoen FJ, Spears JR: Effect of laser balloon angioplasty on normal dog coronary arteries in vivo (abstract). *J Am Coll Cardiol [Suppl A]* 1988; 11:108A.
- Jenkins RD, Sinclair IN, Leonard BM, Sandor T, Schoen FJ, Spears JR: Laser balloon angioplasty versus balloon angioplasty in normal rabbit iliac arteries. *Lasers Surg Med* 1989; 9:237-247.
- Spears JR, Reyes V, Sinclair IN, Hopkins B, Schwartz L, Aldridge H, Plokker HWT: Percutaneous coronary laser balloon angioplasty: preliminary results of a multicenter trial (abstract). *J Am Coll Cardiol [Suppl A]* 1989; 13:61A.
- Sanborn TS, Alexopoulos D, Marmur JD, Badimon JJ, Badimon L, Fuster V: Reduced coronary thrombosis with excimer vs thermal laser angioplasty (abstract). *Circulation* 1989; 80 [Suppl II]:477.
- Sanborn TS, Haudenschild CC, Garber GR, Ryan TJ, Faxon DP: Angiographic and histologic consequences of laser thermal angioplasty: comparison with balloon angioplasty. *Circulation* 1987; 75:1281-1286.
- Gerrity RG, Loop FD, Golding LAR, Ehrhart LA, Argenyi ZB: Arterial response to laser operation for removal of atherosclerotic plaques. *J Thorac Cardiovasc Surg* 1983; 85:409-421.
- Abela GS, Staples ED, Conti CR, Conti CR, Pepine CJ, Faro RS, Knauf DG, Alexander JA, Hay DA, Roberts AJ: Immediate and long-term effects of laser radiation on the arterial wall: light and electron microscopic observation. *Surg Forum* 1983; 34:464-466.
- Abela GS, Crea F, Seeger JM, Franzini D, Fenech A, Normann SJ, Feldman RL, Pepine CJ, Conti CR: The healing process in normal canine arteries and in atherosclerotic monkey arteries after transluminal laser irradiation. *Am J Cardiol* 1985; 56:983-988.
- Douville EC, Kempczinski RF, Doerger PT, Van der Bel-Kahn J, Sankar MY, Joffe SN: Effects of Nd:YAG laser energy on the arterial wall: evaluation of a new contact delivery system. *J Surg Res* 1987; 42:185-191.
- Cross FW, Bowker TJ, Brown SG: Arterial healing in the

dog after intraluminal delivery of pulsed Nd-YAG laser energy. *Br J Surg* 1987; 74:430-435.

32. Prevosti LG, Leon MB, Smith PD, Dodd JT, Bonner RF,

Robinowitz M, Clark RE, Virmani R: Early and late healing responses of normal canine artery to excimer laser irradiation. *J Thorac Cardiovasc Surg* 1988; 96:150-156.

CHAPTER 7

**ELECTRICAL NERVE AND MUSCLE STIMULATION
BY RADIO FREQUENCY SURGERY**

ROLE OF DIRECT CURRENT LOOPS AROUND THE ACTIVE ELECTRODE

Cornelis J. Slager, Johan C.H. Schuurbiers, Jan A.F. Oomen, Nicolaas Bom

Electrical Nerve and Muscle Stimulation by Radio Frequency Surgery: Role of Direct Current Loops Around the Active Electrode

Cornelis J. Slager, Johan Ch. H. Schuurbiens, Jan A. F. Oomen, and Nicolaas Bom

Abstract—Tissue cutting by electrosurgery is often accompanied with stimulation of nerves and muscles, despite the high frequency of the alternating current being applied. The main source of this stimulation is thought to be the generation of low frequency current by the nonlinear sparking process. However, measurement of this low-frequency current, in the generator electrode's circuit, showed relatively small values, barely sufficient to support this hypothesis. In this study more powerful low frequency current could be identified, indeed also originating from the nonlinear sparking process. Local direct and low frequency currents, at a level of tens of milliamperes, appeared to be generated between different sites of the active electrode-tissue interface. Probably these local currents have not been noticed before as they cannot be detected in the outer chain of generator, electrodes, and connecting wires. This finding may explain why most measures, intended to prevent stimulation by modifying this outer chain, had only limited success.

I. INTRODUCTION

IN surgical practice it has been noticed since long [1], [2] that tissue cutting with radio frequency current may produce stimulation of nerves and muscles. The observation obviously contradicted the, often too much generalized, statement of d'Arsonval [3] that alternating electrical current at frequencies above 10 kHz will not stimulate excitable neuromuscular tissue. To explain this controversy, several investigators formulated hypotheses and performed experiments to validate potential sources of the observed stimulation. It was concluded that sources, other than electrical current, such as heat, light, and mechanical impact do not explain the observed stimulation [4]. As a recurring view, most authors ascribed the generation of low frequency current to the varying and nonlinear impedance of the sparks [2], [5], [7]–[9] associated with cutting. In an attempt to reduce this current, generator frequency has been raised and low frequency blocking filters were added in series to the load. However, despite such measures, stimulation remained a problem for not well

understood reasons. The powerful high frequency current itself has also been suggested as source of stimulation [7]. This concerns especially monopolar underwater procedures, like trans urethral resections, which require a very high current to achieve tissue cutting.

We considered the idea of simultaneous conduction through sparking and nonsparking sites on a cutting electrode, such a process could introduce generation of local direct current, flowing between the differently behaving electrode sites, which is not detectable in the outer chain of generator, electrodes and connecting wires. Purpose of this study was to investigate in an *ex vivo* setup this potential local direct current generation by the sparking process, and to make an estimate of the intensity of such current.

II. MATERIAL AND METHODS

As a source, to deliver short pulses of high-frequency energy, an electrical generator, constructed in our own workshop, was applied. This generator has been designed for current delivery to very low-ohmic loads [10]. It is battery supplied and produces a 675 kHz symmetric square wave voltage with a peak value of 750 V. The transformerless output stage consists of a symmetric, full bridge configuration with a high frequency output resistance of 50 Ω . Each floating output terminal has a capacitor (10 nF) in series to the load, to prevent flow of direct current.

As a second, more commonly used source of high frequency energy, we applied a commercially available electrosurgical generator, the Valleylab SSE3B operating at a frequency of 750 kHz. The monopolar output was used in either the pure cutting mode or cutting with maximal coagulation effect (blend 3), both at a power dial setting of 80 W. In these modes peak output voltages are 500 V and 1500 V respectively. Nominal output impedance of this generator is 300 Ω .

Two types of active electrodes were constructed. A stainless steel foil, thickness 50 μm , was insulated at both sides with blades (thickness 1 mm) of machinable ceramics. A single edge of this composition was not insulated and wedge shaped to be used as active electrode area. The first type of electrode contains a foil of 10 \times 10 mm, and a 10 mm long edge was used as active area. The second type contains two foils of 5 \times 10 mm and exposes two 5 mm long edges as active areas in series, separated by a 0.1 mm gap, filled with insulating ceramics.

Manuscript received August 1, 1991; revised April 24, 1992. This work was supported in part by the Netherlands Heart Foundation under Grants 84.073, 37.007, the InterUniversity Cardiology Institute of the Netherlands and the Stichting voor Technische Wetenschappen under Grant RGN77-1257.

C. J. Slager, J. C. H. Schuurbiens, and J. A. F. Oomen are with the University of Hospital of Rotterdam-Dijkzigt, P. O. Box 1738, 3000 DR Rotterdam, The Netherlands.

N. Bom is with Thoraxcenter, Erasmus University of Rotterdam and the InterUniversity Cardiology Institute of the Netherlands, 3000 DR Rotterdam, The Netherlands.

IEEE Log Number 9205270.

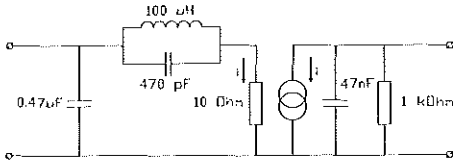


Fig. 1. Selective low frequency current amplifier (LF ampl.). The input of this amplifier may be thought to act as a short circuit for both low and high frequency currents.

A dual channel 175 MHz digital oscilloscope (LeCroy 9400A) was used for all measurements. Its incorporated wave form processor allowed on line signal processing. We applied averaging functions as well as the fast Fourier transform to calculate the power spectra and the averaged power spectra.

Sensitive measurement of low frequency current, separated from the intense high frequency current, was achieved by applying an active, battery supplied circuit (Fig. 1). This low frequency amplifier selectively transfers currents with frequencies up to 3.5 kHz (3 dB attenuation), by means of a transistor current mirror configuration, to its output. High frequency current is shunted at the input by a capacitor (0.47 μF). The input of this amplifier may be thought of as a short circuit for both low and high frequency currents. By selecting a 1 kΩ output resistor the circuit has a 1 V/mA sensitivity which provides a good signal to noise ratio for further processing. In addition proper wiring techniques had to be applied to avoid unwanted interference of the high frequency component by parasitic capacitive and inductive effects.

In a first series of experiments sparking was accomplished under saline. Salt concentration of the saline was 0.28% NaCl resulting in a resistivity of 200 Ω·cm at 21°C.

The single blade electrode was immersed in saline at 5 cm distance from a 4 cm diameter stainless steel return electrode. Ten single 0.8 ms pulses of high frequency energy (750 V, 675 kHz) were applied. Both the high frequency voltage over and the current through the electrode-electrolyte junction were measured, allowing study of the short term variation in the impedance of the single blade electrode. After each pulse the electrode was wiped by a tissue to remove sticking bubbles.

In a second, under saline experiment, a resistor of 1 kΩ (Fig. 2), in series with the low frequency current amplifier, was connected in parallel to the single blade electrode-saline pathway. A current shunt of 2.5 Ω was added to the input of the active circuit, to reduce the measured low frequency current by a factor of 5. This parallel configuration simulates the potential situation in which a cutting electrode is sparking from a limited part of its area, while other parts are still conducting through the metal-electrolyte interface without sparking. Energy was applied as 750 V, 675 kHz pulses during 0.8 ms. High frequency current through the electrode was measured as a voltage over a 10 Ω series resistor.

In a third under saline experiment the double blade electrode was studied. Both electrode parts were connected by a 2.5 Ω resistor which was shunted by the low frequency measuring circuit (Fig. 3). This configuration couples the high frequency energy with functionally equal intensity to both parts. Energy

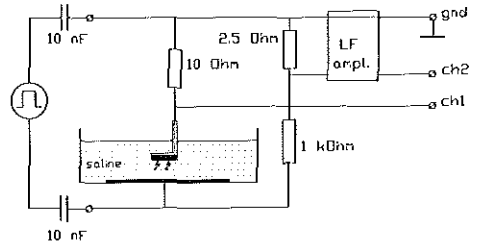


Fig. 2. Setup to measure radio frequency current (Ch1) through the electrode-electrolyte junction and low frequency current through the shunt resistance (Ch2).

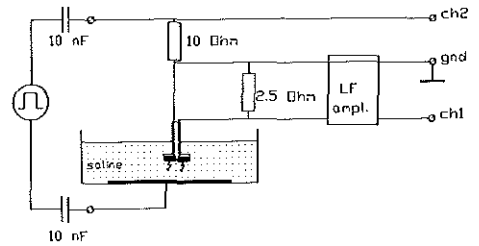


Fig. 3. Set up for measurement of total radio frequency current through both electrode blades (Ch2) and low frequency current between both electrode blades (Ch1).

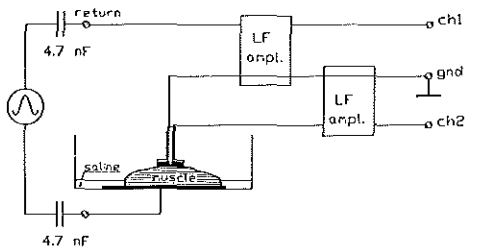


Fig. 4. Set up to measure low-frequency current in the 'generator-electrode's circuit (Ch1) as well as between the two electrode blades when cutting through tissue (Ch2). The input circuit of the LF amplifiers may be thought to act as being shorted (Fig. 1).

was applied as pulses of 750 V, 675 kHz during 0.8 ms. Total high frequency current through both electrode parts as well as low frequency current differences between the electrode parts were measured.

In another type of experiments, electrosurgical cutting was performed in porcine heart muscle which was positioned upon the saline wetted return electrode. For this purpose the double blade electrode was selected, and connected to the Valleylab generator (Fig. 4). The electrode was manually moved at a speed of approximately 5–10 cm/s during 1 s. For each setting of the generator ten cuts were made. Low frequency current was measured in the generator-electrode circuit as well as between both electrode blades. Consistent performance of the electrodes was maintained by regular cleaning and eventual polishing procedures.

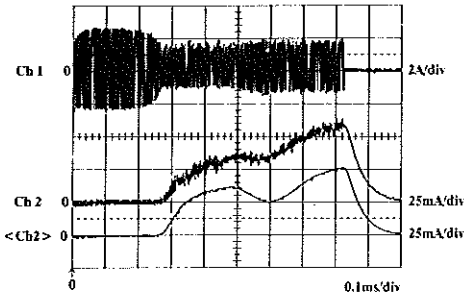


Fig. 5. Example of radio frequency current through the electrode-electrolyte junction (Ch1) and the simultaneous low frequency current (Ch2) for the set up of Fig. 2. <Ch2> depicts the average of Ch2 over ten successive pulses.

III. RESULTS

Radio frequency energy application on the single blade electrode, first resulted in a slightly decreasing electrode-saline resistance to a mean minimum value of $247 \pm 7 \Omega$ at 0.1 ms ($n = 10$). Then resistance gradually increased to a maximum of approximately twice the 0.1 ms value at 0.21 ± 0.02 ms. After this, current intensity became very irregular, even within the half-periods of the high frequency signal. As a result the impedance of the metal-electrolyte junction could no longer be described in simple linear terms like resistance.

An example of high frequency current through the electrode-electrolyte junction and the accompanied low frequency current through the parallel resistor is shown in Fig. 5. Low frequency current, averaged over ten pulses is shown as well. The high frequency current follows a similar pattern as during the first experiment. At 0.27 ms (0.26 ± 0.01 ms, $n = 10$) the current is at its minimum. Synchronous with the current dip, direct current starts to flow through the parallel resistor, it reaches a maximum value of 60 mA (mean 51 mA, $n = 10$) at the end of the pulse.

In Fig. 6 an example is given of the measurement results of the double blade electrode under saline. After passing the high frequency current dip at 0.28 ms (0.30 ± 0.02 ms, $n = 10$), low frequency current starts to flow between the two electrode parts, reaching a peak value of 67 mA at 0.49 ms. From pulse to pulse this low frequency current showed a quite varying behaviour. During a single pulse 2-4 relative minima and 1-3 relative maxima were observed. Maximum peak values of the low frequency current varied from 40 to 100 mA for the ten pulses studied.

Single stroke cuts in porcine heart muscle, made with the two-blade electrode, showed a maximum depth of 2-3 mm for the pure cut mode and 3-4 mm for cutting with maximal coagulation. A typical example of low frequency current registration during pure cutting is shown in Fig. 7. During the first 0.1 s no low frequency current is detected. After this warm-up period, sparking starts which is accompanied with cutting and low frequency current generation. During intense sparking, current in the generator electrode circuit reaches a peak value of 0.7 mA at 0.8-0.9 s. Duration of these peaks was only a few tenths of a ms. Low frequency current between

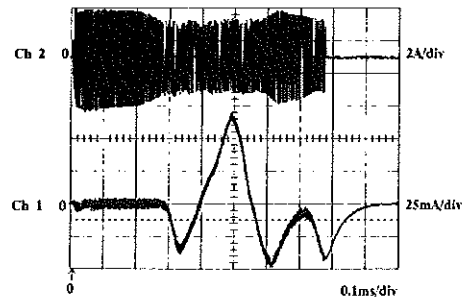


Fig. 6. Example of the total radio frequency current (Ch2) through the electrode-electrolyte junctions and the simultaneous differential low frequency current (Ch1) between both electrode blades for the set up of Fig. 3.

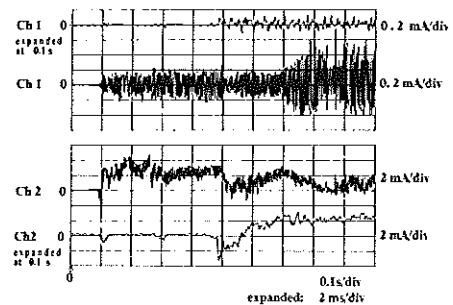


Fig. 7. Example of simultaneous registration of low frequency current in the generator-electrode's circuit (Ch1) and between both electrode blades (Ch2) during 1 s radio frequency cutting (pure mode) on muscle tissue for the set up of Fig. 4.

the two electrode parts reached a peak value of 4.4 mA at 0.26 s and showed a typical direct current character.

For both the pure cut and the blend mode, the averaged ($n = 10$) FFT power spectra of the low frequency current signals are shown in Fig. 8 for the range of 0-1 kHz, which is selected from a 0-6.25 kHz registration. In absolute terms a relative power of 0 dBm corresponds with a peak current value of 0.316 mA ($0.316 V_{\text{peak}}$ over 1 k Ω , see Fig. 1). For the pure cut mode (Fig. 8, the upper panel), current in the loop of the electrode blades, shows the highest magnitude for frequencies close to zero. In the range below 100 Hz, they appear to be 30-40 dB more powerful than in the generator-electrode circuit. For frequencies above 1 kHz the magnitude of the currents in the loop of the blades gradually decreased to a level of -38 dBm at the Nyquist frequency of 6.25 kHz. Intensity of the currents in the generator-electrode circuit was at a constant level of -50 dBm for frequencies above 100 Hz.

Blend cutting (Fig. 8, lower panel) is accompanied with a substantially increased generation of low frequency power. Above 100 Hz, current in the generator-electrode circuit has a power of -40 dBm. From 0 to 200 Hz the current in the loop between the electrodes is approximately 100 times (40 dB) as intense as the current in the generator-electrode circuit. Up to 1 kHz this difference remains above 30 dB, from 1 to 6.25 kHz it decreases to 20 dB.

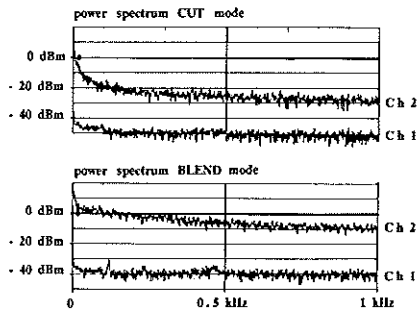


Fig. 8. Averaged ($n = 10$) power spectra of the low frequency currents in the generator electrode's circuit (Ch1) and between the electrode blades (Ch2) for both the pure and the blended cutting modes. Measuring setup as in Fig. 4.

The power spectrum data can be converted in terms of power density. For an equivalent noise bandwidth of 1.71 bins of the applied Blackman–Harris window and a frequency bin width of 1 Hz, 0 dBm in the power spectrum corresponds with a power density of $(0.316 \text{ mA}_{\text{peak}})^2 / (1.71 \text{ Hz})$. From this calculation it can be estimated that the low frequency energy available in, e.g., the frequency band of 0–200 Hz is equivalent to the energy of a single-frequency sinusoidal current with a peak value of 3–4 mA.

IV. DISCUSSION

Probably, stimulation of nerves and muscles, has been observed by most of the surgeons applying radio frequency electrosurgical cutting. Yet, literature is scarce on this subject. The authors of this paper were confronted with electrical stimulation as a side effect of a still experimental technique, designed to ablate atherosclerotic tissue in diseased arteries by high frequency electrical sparks [10]. When testing this technique in leg arteries of animals, contraction of leg muscles occurred. Apparently major nerves, located parallel and close to the arteries, thus could be easily stimulated. Applying direct current pulses in these arteries, using the same spark erosion electrodes, allowed estimation of the threshold for stimulation. When studying different application times of radio frequency energy, enabling comparison of a presparking warm up phase with the sparking phase, it appeared that stimulation was almost exclusively restricted to periods which included sparking; a finding also described by others [2]. This ruled out high frequency current passage [4] itself, as main source of stimulation. During warm up high frequency current is at a maximum. Many authors [2], [5], [7]–[9] concluded that rectification by the nonlinearly conducting ionization channels, i.e., by the sparks, generates the low frequency stimulating current. However, many of their attempts, as well as ours to reduce this current below the estimated stimulation threshold by, e.g., raising the generator frequency and minimizing the series output capacitors, did not eliminate stimulation.

We hypothesized that low frequency current, not detectable in the generator electrode's circuit, might flow between different sites of the active electrode, because of the not uniform distribution of sparking over its area. Experimental results, like

the observation of excessive electrolytic wear at non sparking areas of radio frequency cutting wire loops, directed our view to this potential source.

To study, in a reproducible way, the characteristics of under saline electrode warm-up and the transition from galvanic conduction to sparking, we first applied a generator able to deliver high peak power during short periods. This generator was originally designed to vaporize obstructions in atherosclerotic vessels [10]. For this purpose an unmodulated square wave voltage was selected as, under this condition, the expected amount of coagulation, expressed by the so called CREST factor, will be lowest. The CREST factor is the ratio between peak voltage and effective voltage. Furthermore, this generator, in contrast to most commonly used types, shows no transients in its characteristics at start up. Both the use of this generator and the stable saline environment for sparking, allowed the study of some basal electrical characteristics of sparking in a well controlled way without introducing unknown factors like varying generator output impedance, remaining wave form modulation effects, varying tissue impedance, electrode tissue contact pressure, electrode moving speed and so on. Salt concentration of the saline was chosen such that its resistivity was about equal to that of blood and not too far below the value for most body tissues [11].

To gather comparative data representative for normal clinical cutting conditions, we selected a more commonly used type of generator with settings typical for that application.

The specially constructed electrodes have mechanically strong, yet minimal active areas, which allowed the combined use for under saline operation and muscle cutting. The double blade construction enabled measurement of the assumed local current loop.

Measurement of the resistance of the single blade electrode to saline showed that initially resistance slightly decreased, probably because of warming up of the saline near the electrode. Next resistance increased because of gradually growing bubbles on the electrode surface. This could be confirmed in additional experiments applying radio frequency energy in pulses of 0.1–0.2 ms. Pulses longer than 0.2 ms produced visible sparking, accompanied with a less or more chaotic electric behavior. During the transition from warm up to sparking, mean voltage over the load showed a shift of approximately 100 V, which indicates passage of a direct current. This current loads the series capacitors until a new equilibrium settles for the apparently rectifying properties of the sparking process. To achieve current equilibrium, a higher voltage appears to be required for sparking from a positive electrode towards saline, than is needed reversely.

Addition of a shunt conductor to the electrode saline junction, slightly delayed the warm-up period to 0.27 ms. As a consequence of the rectification effects observed in the first experiment, direct current starts to flow through the shunt, synchronous with the onset of sparking. Probably, because of gradually further heating of the electrode, the direct current amplitude becomes very intense at the end of the pulse. This current also flows through the electrode–electrolyte junction in the direction from saline to active electrode. As a practical consequence of this observation it will be clear

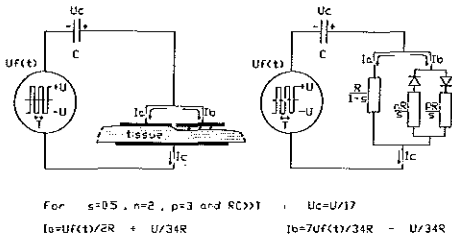


Fig. 9. First order model of a partially sparking electrode. Current I_a flows through the non sparking electrode part and I_b through the sparking part. R : galvanic electrode resistance; s : relative sparking part (range 0 to 1); n : relative change in resistance during negative sparking phase; p : relative change in resistance during positive sparking phase.

that previous attempts to reduce low frequency interference of electrosurgical procedures by adding a shunt inductor between the scalpel and dispersive electrode, thus short-circuiting low frequency currents, is indeed a life threatening modification [6]. Very intense direct current will flow through the scalpel-tissue-dispersive electrode-inductor loop.

Results of experiments with the double blade electrode under saline support the hypothesis that direct and low frequency currents may flow between different sites of a single electrode during sparking. Although the random nature of the observed low frequency current direction prohibited description of a standardized pattern, evidence existed that on the average, a net load transport occurred from one electrode blade to the other. Reversing the order of the electrode's connections showed that this preferential current direction remained the same. Probably small differences in e.g., the dimensions between the blades are a reason for this observation. Apparently the way of electrical coupling did not influence the sparking process.

To facilitate understanding of the measurements a first order model of a partially sparking electrode is provided in Fig. 9. The relative dimensions of the sparking electrode part are denoted by s , which varies from 0 to 1. The resistance of the electrode tissue interface in the early warm up phase is denoted by R . The relative change in resistance for the sparking part is respectively indicated by p for the phase with a positive active electrode and by n for the negative phase. For $RC \gg T$ the following expressions can be easily derived for the steady state condition when no direct current flows through capacitor C :

$$U_C = \frac{p-n}{p+n+2pn(1-2)/s} U \quad (1)$$

$$I_a = \frac{Uf(t)}{R/(1-s)} + \frac{U_C}{R/(1-s)} \quad (2)$$

$$I_b = \frac{Uf(t)}{R/(1-s)} \cdot \frac{p+n+2s/(1-s)}{p+n+2pn(1-s)/s} - \frac{U_C}{R/(1-s)} \quad (3)$$

In Fig. 9 a numerical example is presented, with parameters chosen to be typical for a practical situation. Principal result is the direct current component $U/34R$ in the loop between the electrode blades. For $U = 680$ V, and $R = 250 \Omega$ this current will be 80 mA.

As the parameters s , n , and p will vary during sparking, adaptation of U_C to the new conditions will continuously occur. This results in modulation of the direct current and introduces intense low-frequency current in the loop. As a consequence also low-frequency current flows in the generator electrode circuit to adapt U_C . Obviously the intensity of this current will be proportional to the value of series capacitor C .

With voltage settings as applied in surgical practice, cutting in muscle tissue confirmed the existence of local low frequency current generation around the active electrode. During the first 0.1 s after switching on the generator, no low-frequency current is detected by the measuring circuits. Apparently suppression of the high frequency current, which during this period will reach its maximum value, is amply sufficient. Only after this time, when sparking starts, low-frequency current is generated. Part of the detected low frequency currents appears to be direct current. A net direct current flowed from the frontal cutting blade to the rear blade, probably because the cooler frontal blade partially remains in the galvanically conducting warm up phase, while in its preheated track the rear blade may be sparking over the entire surface.

In surgical practice, differences in cutting speed and tissue resistivity will vary sparking conditions over the electrode. As the electrodes were moved with a speed as steady as possible, over a part of muscle with uniformly looking appearance, the measured direct current may be smaller than practical values. Nevertheless during pure cutting (Fig. 7), a direct current of 2 mA, with peak values over 4 mA, was observed in the loop between the electrodes. Such a level will probably be easily sufficient to stimulate excitable tissues [7] as the active electrode area is only 0.25 mm². In the generator electrode's circuit, peak values of 0.7 mA were reached occasionally, but duration was far less than 1 ms because of the generator's series output capacitors.

Comparison of different cutting modes was facilitated by applying Fourier analysis, which allowed averaging of the power spectrum of the current signals over ten successive cuts. Aliasing effects were avoided by the applied filtering techniques, this could be verified by performing additional Fourier transforms over a wider frequency range. From the spectral analysis it clearly appears that the low frequency energy available for stimulation is highest for the blended mode of cutting in the local blade-tissue-blade circuit. Apparently, the modulation of the radio frequency current to produce coagulative effects, magnifies the variations in spark distribution over the electrodes. In the pure cut mode, low frequency energy generated in the local blades circuit, is approximately 10 times smaller than in the blend mode. Close to zero frequency a strong direct current component exists, which is in agreement with the observations made in the normal time mode. For the analyzed frequency spectrum, current in the generator-electrode's circuit, is 10 to 100 times smaller than in the loop between the electrode blades and thus relatively unimportant to explain stimulation. Because of the local nature of the generated intense low frequency current, it should not be expected that different generators [2], [7] having similar cutting wave form characteristics and applying identical electrodes, will produce quite different stimulation effects.

Absolute comparison of current levels measured in this study, with data on stimulation thresholds is difficult. One of the main parameters determining stimulation threshold is current density. Therefore it is of crucial importance to know electrode geometry and positioning, in addition to usually provided data of current threshold. A study [7] suggesting stimulation of excitable tissues by the radio frequency current itself compared the spectral components of current in the generator electrode circuit, with previously determined thresholds for stimulation [4], but did not account for the different electrode sizes used.

Main implication of this study is the finding that locally around an active radio frequency cutting electrode, low-frequency current can be generated which is not detectable in the generator-electrode circuit. The level of this current may be much higher than the low-frequency current in the generator electrode circuit and probably plays a major role in explaining stimulation caused by radio frequency cutting.

ACKNOWLEDGMENT

We would like to thank G. H. Heuvelsland for constructing the special electrodes applied in this study.

REFERENCES

- [1] J. H. Hobika and B. G. Clarke, "Use of neuromuscular blocking drugs to counteract thigh-adductor spasm induced by electrical shocks of obturator nerve during trans urethral resection of bladder tumors," *J. Urol.*, vol. 85, pp. 295-296, 1961.
- [2] R. J. Prentiss, G. W. Harvey, W. F. Bethard, D. E. Boatwright, and R. D. Pennington, "Massive adductor muscle contraction in trans urethral surgery: Cause and prevention; development of new electrical circuitry," *J. Urol.*, vol. 93, pp. 263-271, 1965.
- [3] A. d'Arsonval, "Action physiologique des courants alternatifs," *Comp. Rend. Soc. Biol.*, vol. 43, pp. 283-286, 1891.
- [4] J. R. Lacourse, W. T. Miller III, M. Vogt, and S. M. Selikowitz, "Effect of high-frequency current on nerve and muscle tissue," *IEEE Trans. Biomed. Eng.*, vol. 32, pp. 82-86, 1985.
- [5] J. A. Pearce, *Electrosurgery*. London: Chapman and Hall, 1986, pp. 121-126.
- [6] J. A. Pearce, *Electrosurgery*. London: Chapman and Hall, 1986, p. 117.
- [7] J. R. Lacourse, M. C. Vogt, W. T. Miller III, and S. M. Selikowitz, "Spectral analysis interpretation of electrosurgical generator nerve and muscle stimulation," *IEEE Trans. Biomed. Eng.*, vol. 35, pp. 505-509, 1988.
- [8] L. A. Geddes, W. A. Tacker, and P. Cabler, "A new electrical hazard associated with the electrocautery," *Med. Instr.*, vol. 9, pp. 112-113, 1975.
- [9] R. D. Tucker, O. H. Schmitt, C. E. Sievert, and S. E. Silvis, "Demodulated low frequency currents from electrosurgical procedures," *Surg. Gyn. Obst.*, vol. 159, pp. 39-43, 1984.
- [10] C. J. Slager, C. E. Essed, J. C. H. Schuurbiens, N. Bom, P. W. Serruys, and G. T. Meester, "Vaporization of atherosclerotic plaques by spark erosion," *J. Amer. Coll. Card.*, vol. 5, pp. 1382-1386, 1985.
- [11] L. A. Geddes and L. E. Baker, "The specific resistance of biological material: A compendium of data for the biomedical engineer and physiologist," *Med. Biol. Eng.*, vol. 5, pp. 271-293, 1967.



in diagnostic and therapeutic instruments for interventional cardiology.



aspects of interventional cardiology.



systems for biophysical data processing and representation in the cardiac catheterization laboratory and patient care unit. His current interest pertains to the processing and representation of biophysical data collected during open heart surgery.



of the Netherlands (ICIN) and at the Erasmus University Rotterdam in 1979. In 1987 he received a honorary doctorate from the Technological faculty of the University of Lund, Sweden, for his work and inventions in the field of echocardiography.

Dr. Bom is a member of the Scientific Board and the Board of Directors of ICIN since 1983.

Cornelis J. Slager was born in Scherpenisse, Zeeland, The Netherlands, in 1945. He received the M.Sc. degree in electrical engineering from Delft University of Technology in 1971.

During his graduate work he invented an automated border recognition system for ventriculograms. After teaching electronics at the Delft University, he joined the Biomedical Technology Group of the Thoraxcenter, University Hospital Dijkzigt-Rotterdam in 1973. His research interests are in quantitative processing of cardiological images and

Johan Ch. H. Schuurbiens was born in Vlaardingen, the Netherlands in 1950. He received a degree in electrical engineering from the College of Aeronautics and Electronics, Den Haag in 1972.

Until 1976, while studying electronic engineering, he was involved in industrial engineering. In 1976 he joined the Cardiology Department of the Dijkzigt Hospital as a research technician. His interests are in real-time image processing and analysis techniques, digital/analog hardware, software for biomedical signal processing and data acquisition and technical

Johannes A. F. Oomen was born in Oosterhout, The Netherlands in 1937. He received a M.Sc. degree in electronics from the University of Cincinnati in 1971, while working for AVCO Electronics, where he designed automatic tuning systems for radio transmitters.

He joined the Biomedical Technology group of the Thorax Center, University Hospital Dijkzigt, Rotterdam in 1971. In 1973 he acquired a M.Sc. degree from the Delft University of Technology.

He has contributed to the design of automated data processing and representation in the cardiac catheterization laboratory and patient care unit. His current interest pertains to the processing and representation of biophysical data collected during open heart surgery.

Nicolaas Bom was born at Velsen, The Netherlands, in 1937. He received the M.Sc. degree from the University of Technology, Delft, in 1961 and the Ph.D. from the Erasmus University Rotterdam in 1972.

In 1969 he joined the Thoraxcenter of the Erasmus University to set up a diagnostic ultrasound research and development program. Since 1974, he is head of the Biomedical Engineering Group of the Thoraxcenter. He became Professor of Medical Ultrasound at the Interuniversity Cardiology Institute

CHAPTER 8

**DIRECTIONAL PLAQUE ABLATION BY SPARK EROSION
UNDER ULTRASOUND GUIDANCE**

FIRST EVALUATION OF A CATHETER
INCORPORATING BOTH TECHNIQUES

Cornelis J. Slager, Johan C.H. Schuurbiers, Jan Heim van Blankenstein,
Patrick W. Serruys, Nicolaas Bom.

DIRECTIONAL PLAQUE ABLATION BY SPARK EROSION UNDER ULTRASOUND GUIDANCE: FIRST EVALUATION OF A CATHETER INCORPORATING BOTH TECHNIQUES

Cornelis J. Slager, Johan C.H. Schuurbijs, Jan Heim van Blankenstein, Patrick W. Serruys, N. Bom

Abstract-The goal of removing atherosclerotic plaques from narrowed coronary arteries, to restore the lumen to normal dimensions by a single pass catheter based method, stimulated many new technical developments. At present only mechanical debulking systems have become clinically applicable. We describe the design and first tests of a prototype catheter which incorporates spark erosion and intravascular ultrasound imaging to debulk a narrowed vessel lumen up to a diameter of 2.7 mm. With this catheter selective application of spark erosion, under ultrasound guidance, is techni-

cally feasible. Preliminary *in vitro* tests on 2 obstructed coronary artery specimens demonstrated the potential use of the method but also resulted in a vessel perforation. Previously observed problems associated with spark erosion, i.e. gas production and electrical stimulation, are greatly reduced. Speed of tissue ablation is approximately 0.1 - 0.2 mm/s. Histology did not show further side effects. Technical problems, related to the drive shaft of the rotating tip configuration, must be solved to develop this combined approach into a clinical operating device.

INTRODUCTION

Since the advent of dilatation of coronary arterial stenoses by balloon inflation this procedure was associated with a high restenosis rate. The mechanism of tearing the vessel wall is rather crude and damage imparted to the adventitia is a major factor causing restenosis by vessel shrinkage. Currently, to withstand this negative vessel remodeling, stents are successfully applied in routine clinical practice. However, also stents are confronted with restenosis by intimal hyperplasia and progression of atherosclerosis. Therefore repeated interventions are required which are restricted by the foreign body left in the vessel.

To improve on this type of transluminal, catheter based, treatment, it has since long been felt that application of a plaque debulking method could provide a better solution. At present mechanically driven atherectomy devices have achieved some position in clinical practice. However, compared to the balloon, their advantage is still under debate^{1,2}. The problems to be solved in order to achieve a successful catheter based plaque removal technique are at least four:

Firstly, the technique must be effective in removing atherosclerotic plaque leaving an unobstructed lumen, without causing dissections, releasing obstructive material in the blood stream or provoking other major side-effects.

Secondly, as no removal mechanisms have been found which discriminate effectively between plaque and normal wall, the technique needs to be directionally applicable, i.e. in case of eccentric plaque deposition only the plaque should be removed and the normal wall be left undamaged.

Thirdly, some sensing or imaging technique must be incorporated, having its reference system unambiguously coupled to the removal technique, in order to determine the plaque location to be removed.

Fourthly, after having succeeded in removing the plaque, both the acute complications and restenosis rate should compare favorably or at least rival the balloon and stent combination.

Technical developments aiming at a single pass plaque removal device, which requires means for selective application and guidance, have been only few. Recently, directional atherectomy has been combined in a single catheter with intravascular ultrasound imaging³. Inherent limitations of this design are the rigidity of the rather long tube containing the cutting mechanics and the small angle of view for the ultrasound beam passing through the sleeve which is open for cutting.

Previously we introduced spark erosion for plaque removal⁴. This technique provides attractive opportunities for directed application⁵. Purpose of this study is to learn from the fabrication and feasibility testing of a prototype catheter, incorporating spark erosion and ultrasound imaging, in order to answer questions like:

1. Can a catheter tip, combining ultrasound imaging and spark erosion, be constructed with dimensions suitable for intravascular application?
2. Can such a device be made operational for a minimum period being relevant for clinical application?
3. How can the information shown in the intravascular ultrasound images be used to select the section to be ablated?
4. Can the spark erosion be selectively applied to the section selected?
5. What are the side effects of such a combined device?

DESIGN CONSIDERATIONS AND PRELIMINARY TESTS

Spark erosion electrode

Previously, experience had been obtained with a catheter which also incorporated spark erosion and intravascular imaging⁶. On the tip of this catheter multiple spark erosion electrodes were arranged in a circumferential pattern and a rotating mirror was applied for deflection of the ultrasound. By activating a single electrode, the direction of plaque ablation could be selected. To be useful as a single pass plaque removal technique such a catheter tip needs to restore the lumen up to a diameter of 2.5 to 3 mm. In this respect the multiple electrode design had some practical limitations. A rather wide gap between neighboring electrodes must be maintained to prevent arcing between the electrodes. Such gaps limit the effective area of plaque to be attacked. For this reason other configurations are more attractive. For example a single electrode, covering part of a catheter tip's circumference, can be eccentrically positioned by manual rotation of the catheter⁵. By incorporating ultrasound imaging, the electrode position relative to a detected plaque can be optimized. A major disadvantage of this solution is the rather large area required for such a single electrode. This requires relatively high voltages to achieve spark erosion, which makes the ablation process less controllable in terms of gas production and electrical stimulation. For these reasons, in the present study a single, very small electrode is selected, which needs to be moved during spark erosion to cover the area of the lesion selected for ablation. This can be achieved by applying a continuously rotating catheter tip, which contains a single electrode. Platinum was selected as material for the electrode because of its high resistance against corrosion.

Profile of the catheter tip

Testing of spark erosion with stationary electrodes had shown a linear relationship between application time and ablated volume of tissue⁴. Subsequent testing with electrodes, being moved along a surface, showed this principle to be maintained, i.e. as a first approximation it holds that total tissue volume ablated along the path traveled is directly related to application time. This implies that at a certain location the thickness of the layer ablated will be inversely related to the locally applied electrode speed.

Extrapolation of this finding to the application of a rotating electrode, with constant width as shown in Figure 1a, offers some rules for the design of an optimal tip profile. The most frontal part of the tip will be excluded from these considerations, i.e. at that part where the constant electrode width cannot be maintained because of the tip's decreasing circumference.

From the moving electrode analogy it is assumed that for equal parts (Δl) of the electrode (Figure 1b) the tissue volume removed during one tip revolution will be a constant called ΔV . Otherwise stated, the removed volume per unit length i.e. $\Delta V/\Delta l$ is constant for a fixed period of time. This constant $\Delta V/\Delta l$ has the dimension of an area and will be expressed by A . The ablation distance D (Figure 1c), measured normal to the surface can with good approximation (Δl and D small with respect to r) be derived from the local tip radius r and A by:

$$D \ 2\pi r \ \Delta l = \Delta V \text{ which results in: } D = A/2\pi r \quad (1)$$

The tissue layer removed, provides a free space S (Figure 1d) allowing the tip to move forward over a distance that preferably must be a constant for the whole area of the tip being in contact with tissue. As can be derived from Figure 1d space S is related to D and to the local slope α of the tip profile. This local slope is determined by the first derivative function of radius r to its axial coordinate x :

$$\text{tg } \alpha = dr/dx \quad (2)$$

From Figure 1d it can be derived that:

$$S = D/\sin \alpha \quad (3)$$

From (1) and (3) it follows:

$$S = A/2\pi r \sin \alpha \quad (4)$$

So, the condition to obtain a constant space S is:

$$r \sin \alpha = A/2\pi S = \text{constant} \quad (5)$$

Dividing by $\cos \alpha$ delivers ($\cos \alpha \neq 0$):

$$r \operatorname{tg} \alpha = r \operatorname{dr}/dx = A/2\pi S \cos \alpha \quad (6)$$

Because α is a function of x , an analytical solution of this differential equation is not easy to obtain. Substituting $\cos \alpha = 1$, which by good approximation holds for the widest part of the electrode, results in:

$$r = \sqrt{(A/\pi S)} \cdot \sqrt{x} \quad (7)$$

Rewriting this expression gives for S :

$$S = A x / \pi r^2 \quad (8)$$

Expression (8) illustrates that, as would be expected, forward ablation speed S is proportional to the general ablation settings characterized by A , and by the profile of the tip. Increasing the length x for a certain selected tip radius will increase S .

Numerically solving expression (6) shows a slight deviation from the above calculated quadratic profile, and results in a more blunted nose of the tip. In Figure 2 this difference is depicted. Both profiles are 2.6 mm wide and have a 1 to 4 slope at the widest location. Below a radius of 0.315 mm the numerical expression cannot give a real number solution because the primary condition, i.e. maintain a constant tip advancement distance S , cannot longer be fulfilled. As a practical consequence this implies that even a flat nose of the tip will be slightly more aggressive than the conical part, a feature which does not seem to be undesirable.

Electrical settings and ablation results

In contrast with earlier electrical settings⁴ for spark erosion, in this study the use of lower voltages was investigated. To achieve sparking in the vapor layer between the electrode and the tissue, electrical breakdown must occur. When applying high voltages like the 600V to 720V effective values used previously, breakdown will occur at relatively large distances between electrode and tissue. However, long ionized sparking channels probably promote a greater percentage of small tissue fragments to be converted into gas. Another disadvantage of the use of higher voltages is the increase in power of provoked stimulation currents. Lower voltages will help to reduce the reported gas production and electrical stimulation⁴. Because of the selected small electrode size, rather low voltages can be applied to pass the warming up phase and reach the state of sparking sufficiently fast, i.e. within milliseconds, thus reducing the accumulation of thermal energy in the tissue which remains after a spark ablation period.

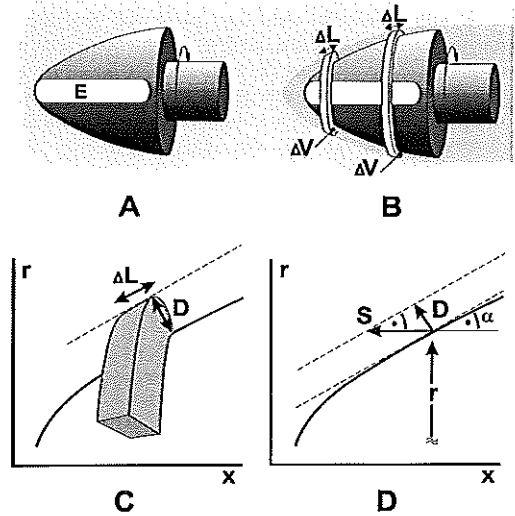


Figure 1. For a rotating tip (fig. 1a) containing a constant width active electrode E, rules can be derived to optimize its profile. Considering equal parts of the electrode ΔL (fig. 1b), the tissue volume ΔV being ablated during one tip revolution is constant (details see text). This allows to derive a relation, described in the text, between ablation distance D (fig. 1c), tip radius r , forward ablation speed S (fig. 1d) and the slope α of the profile. All variables are a function of the location x .

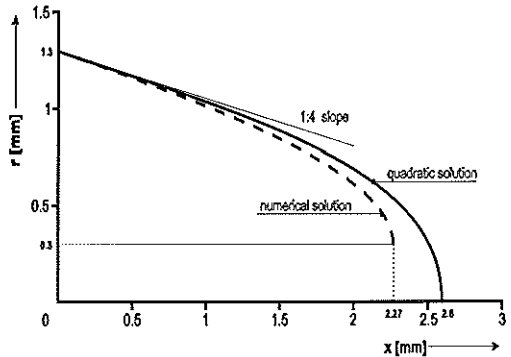


Figure 2. The relation between r and α describing an optimal tip profile can be analytically solved (solid line) by good approximation assuming $\cos \alpha = 1$. This results in a quadratic relationship between x and r . Dimensions selected represent the tip profile to be fabricated. A numeric solution (dotted line), starting with equal slope at $r = 1.3$ mm, results in a slightly more blunted nose of the tip (details see text).

In vitro feasibility tests were performed applying a rotating electrode with the quadratic profile described by equation (7). The tip was positioned perpendicular to the wall of fresh *porcine aorta*, immersed in a 0.45% NaCl saline solution. Tip length and diameter were 2 mm and electrode width 0.5 mm. Tip rotating frequency was 25 Hz, and a 1.8 MHz alternating voltage of 360 V effective value was applied. Pulses lasted 40 ms and were applied at 1 s intervals. These settings imply that for each pulse the electrode was active over a complete tip revolution. In these experiments a forward ablation rate of 0.1 mm/pulse was achieved.

Subsequent testing was performed on *human atherosclerotic aorta* specimens. In these experiments the force applied by the tip on the tissue was controlled by applying weights of respectively 7, 17 and 27 gram. The pressure equivalent, exerted by the tip on the tissue, can be calculated by taking the frontal area projection of the tip into account. The resulting pressures equal respectively 164, 398 and 632 mmHg. At control sites, where no spark erosion was applied, the tip was allowed to rotate for 20 s with an added weight of 17 gram.

In Figure 3 an example of a histologic section stained by hematoxylin-eosin is shown of the human atherosclerotic tissue at the site of spark erosion application. The cavities shown, from left to right, were respectively produced by 13 and 18 pulses under a 27 gram weight.

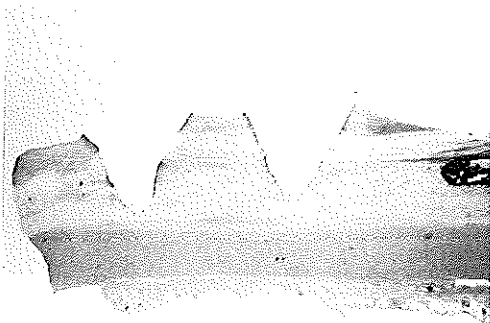


Figure 3. Example of a histologic section stained by hematoxylin-eosin of experiments on human atherosclerotic tissue applying a 2.6 mm diameter rotating tip electrode. The cavities shown, were produced by 13 (left) and 18 (right) spark erosion pulses under a 27 gram weight. Generator settings see text. Discoloration near the edges of the cavity was minimal and no sign of disrupted tissue layers by gas intrusion can be observed.

With application of a 7 gr weight a progression of 0.06 ± 0.02 mm/pulse (mean \pm SD, $n=5$) was obtained. This distance became 0.16 ± 0.02 mm ($n=5$), when the weight was increased to 17 gr. No further increase was observed for the two experiments using a 27 gr weight; in

that case ablation speed was 0.13 mm/pulse. Locations ($n=3$) where calcium prohibited ablation were excluded from these data. At the control sites a layer with a thickness of approximately 0.1 mm had been removed because of the applied friction on the surface.

Qualitative inspection of the eosin hematoxylin stained histologic sections by light microscopy revealed a zone showing some discoloration being generally less than 50 μ m wide. The edges of the cavities were very smooth and, in contrast with the earlier results after spark erosion applying higher voltages, no zone of disruption between cellular layers by intruding gas bubbles could be detected.

Also in contrast with the high voltage experiments, qualitative inspection showed that with the present low voltage settings the amount and the size of produced gas bubbles was much smaller. Bubble size was estimated to be less than 200 μ m diameter rather than 1 mm as has been observed before. This implies a volume reduction per bubble by more than a factor of 100. Based on these observations and our previous studies on gas embolism we do not expect that with these settings major embolizing problems⁷ will occur.

Sparking occurs in a very small zone, i.e. less than a few tenths of a mm. For this reason the diameter of the cavities was not expected to exceed the tip diameter significantly. From those histologic sections being free from folding artifacts, the widest diameter of the cavities exceeding a depth of 2 mm was measured. This diameter was approximately 2.1 mm, which barely exceeds the 2 mm diameter of the tip.

The increase in ablation efficacy by changing weight from 7 to 17 gr, may be explained from the fact that at a certain voltage setting, the vapor layer generated between the electrode and the tissue should not grow too wide as this will limit the amount of sparks being generated. Especially when the electrode is enclosed by tissue while vapor cannot escape, some pressure is needed to overcome the pressure exerted by the vapor layer and to keep the electrode in close contact with the tissue. As has been learned from other experimental tip designs ablation rate can be increased by application of holes or slits in the tip allowing the vapor to escape.

Return electrode and electrical stimulation

The active electrode is mounted in the tip between two thin layers of insulating ceramics. The ceramics are mounted in a slot in the tip. Because the active electrode covers only a very small part of the tip area, the remaining area, if constituting of a metal, could be used as a local indifferent return electrode. An advantage of such a configuration is its potential to reduce electrical stimulation of nerves and muscle. As has been shown previously, sparking can generate direct currents⁸ between different

parts of tissue being attacked by the active electrode. The resulting potential differences can be equalized by the short circuiting function of a local return electrode. For this reason the body of the tip was made of stainless steel.

In 3 *anesthetized pigs*, it was investigated whether stimulation would indeed be reduced by applying such a local return electrode. For this purpose a tip configuration as shown in figure 4 was mounted on a catheter and inserted in the pig's femoral artery into the distal direction. Short lasting direct current pulses (25 - 50 μ s) were applied between either the active Pt electrode and a large indifferent electrode fixed to the animal's back (unipolar stimulation) or between the active electrode and the tip stainless steel body acting as the return electrode (bipolar stimulation). The minimum current threshold for stimulation was determined for each pulse duration by observing whether any motion of a part of the animal's body, generally a part of the skin or a toe, occurred. The location of maximal sensitivity for stimulation was searched by moving the catheter in 0.5 cm steps through the vessel over a distance up to 18 cm. Anodal (active electrode positive) as well as cathodal stimulation was applied.

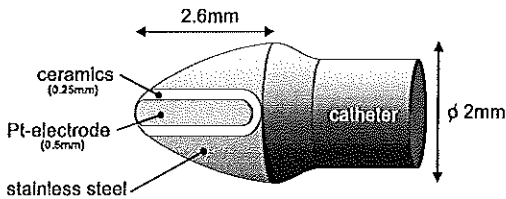


Figure 4. Tip configuration as applied for electrical stimulation experiments in pig femoral arteries.

In the animals investigated, anodal stimulation always showed a higher threshold than cathodal stimulation.

The determined threshold for stimulation, expressed in charge units, varied from 65 nC for unipolar cathodal stimulation to 940 nC for bipolar anodal stimulation. Bipolar stimulation always showed a higher threshold than unipolar stimulation (ratio 1.88 ± 0.6 , $n = 8$). This observation confirms the short circuiting function of the return electrode. Current is forced in an area more close to the tip which reduces current density at distant locations being sensitive for stimulation. One should further realize that in comparison to a non metal tip, the threshold determined for unipolar stimulation is increased already by the very presence of the metal tip body. Part of the current from the active electrode reaching the tissue flows via the tip body to the actually applied indifferent electrode. Therefore this equalizing function of the differences in the electrical tissue potentials by the metal tip will reduce spark erosion stimulation by more than the observed ratio of 1.88.

In the latter experiments, after determination of the stimulation threshold at the most sensitive location, a 10 ms spark erosion pulse (360V effective voltage, 1.8 MHz), was applied. Stimulation by spark erosion occurred in only one animal, the one which had shown the lowest thresholds for stimulation. From the thresholds observed it was concluded that for the applied settings, the level of stimulation charge, which is produced by spark erosion is in the range of a few hundreds nC.

To get an estimate of stimulation by spark erosion, when using a rotating electrode, testing was performed in another group of 3 *anesthetized pigs* in the distal femoral artery at multiple 1 cm distant locations. The following settings were applied: tip rotation frequency 12.5 Hz, effective voltage 360 V, generator frequency 1.8 MHz and pulse duration 40 - 70 ms.

Stimulation, being manifested by weak superficial muscle contractions, was observed in only one animal at 3 out of 14 locations investigated. These preliminary findings show that spark erosion does not necessarily lead to electrical stimulation. This observation is quite different from our previous experience using higher voltages and larger active electrode configurations in pig's or rabbit's⁹ femoral and iliac arteries. In those experiments stimulation occurred at every sparking pulse and generally showed a rather heavy muscle contraction.

When extrapolating these findings to the application of plaque ablation in atherosclerotic arteries it is likely that stimulation will be further reduced. In that application area wall thickness will be much greater than the estimated 0.2-0.3 mm of the pig's femoral artery. Furthermore the area being sensitive for stimulation will be at a much greater distance of the ablation location. Indeed these improvements in reducing stimulation may not be necessary for spark erosion application in the coronary arteries where an ECG triggered way of pulsing can be applied⁴ which makes use of the refractive period of the heart for stimulation. Nevertheless, technical improvements which eliminate stimulation, will widen the potential of the spark erosion technique in cardiac as well as in non cardiac applications.

ULTRASOUND

Previously, expertise had been obtained in the development of a multiple element ultrasound catheter¹⁰ for intra cardiac application. As a more practical solution for the combination with spark erosion it was decided^{5,6} to use a single mechanically driven element, either an ultrasound transducer or an acoustic mirror, to create a rotating sweep of ultrasound. Furthermore, other design features had to be taken into account as for example the ultrasound system must facilitate selection and synchronization of the activation period of the spark erosion electrode to cover a certain segment of a vessel cross section.

This can be accomplished by mounting a single ultrasound transducer in a rotating tip which also contains the electrode. In this way the moment to start sparking can be derived directly from the time coding signals being applied for the ultrasound image formation.

The transducer consisted of a 1 mm diameter, ceramic piezoelectric element. This was mounted over an epoxy backing using conventional technology. Ultrasound frequency obtained by this transducer was 20 MHz.

For ease of prototype fabrication the location of the ultrasound imaging plane was chosen proximal of the active electrode. Otherwise, because of limited space, several additional problems would need to be solved.

To maintain a smooth and circular symmetric tip circumference, the cavity in the tip containing the ultrasound transducer, was covered by an ultrasound transparent sleeve made of polymethylpenten (TPX[®], Mitsui Petrochem. Ind., Tokyo, JP). This sleeve had a conical shape to avoid direct ultrasound reverberations in the cavity and could be easily removed to allow fluid filling of the cavity.

Selection of the segment of tissue ablation must be obtained on base of the wall thickness observed in the ultrasound cross sectional image. In Figure 5 a situation is depicted as may occur in a curved vessel when applying the current prototype. We expect that by aiming for a centered position of the catheter with respect to the *outer* vessel wall, a reliable selection of the ablation direction can be obtained, despite the small radius (20 mm) of the selected vessel curve. Probably, in practice, stiffness of the catheter axis would be more of a problem in passing such a curve. The question may arise to what extent guidance might improve when positioning the transducer opposite of the electrode. Imaging problems due to air bubbles will then increase. Imaging at the widest lumen part may be more sensitive to prevent perforation. More comprehensive simulations as shown here may be necessary to better understand and optimize the mechanisms of the designed way of guidance. For this purpose useful data can be obtained in three dimensional space from ANGUS vessel reconstructions^{11,12}.

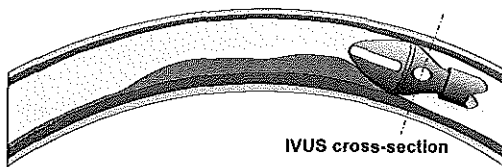


Figure 5. Proper spark erosion steering is required to prevent perforation. In this example the catheter tip (2.6 mm diameter) is positioned in a vessel with a very small curve of 20 mm radius. The ultrasound cross sectional image located just behind the tip's widest diameter will show whether the catheter is centered with respect to the outer vessel wall. It is expected that by aiming to maintain a centered position of the catheter, proper selection of the ablation direction can be obtained.

DRIVE SHAFT AND MOTOR UNIT

For the drive shaft of the tip a 0.7 mm outer diameter stainless steel tube was selected. Both, the coaxial wiring required for the ultrasound signals and a high voltage wire connecting the active electrode were fed through the 0.4 mm inner diameter of this tube. To prevent the revolving tube from contacting tissue it was enclosed in a regular 5.2 F catheter. Near the proximal end the drive shaft was provided with a slip ring construction to allow electrical connection between the electrode wire and the spark erosion generator. At the actual end of the tube a standard connector was applied which fitted to the motor drive unit of a regular ultrasound imaging system (Dumed, Rotterdam, the Netherlands).

The selected drive shaft is torsionally very stiff and guarantees true synchrony between the tip's angular orientation and its distant read out at the motor drive unit. For in vivo application such a drive axis will have too less flexibility and other driving systems will need to be developed.

TESTING THE PROTOTYPE CATHETER

In Figure 6, both the design of the catheter tip, incorporating spark erosion and ultrasound imaging, and the fabricated prototype are shown. The active electrode, surrounded by the ceramics, and the circular ultrasound transducer can be clearly observed. The sleeve covering the ultrasound transducer cavity is withdrawn to allow fluid filling. Tissue contacting surfaces were highly polished to minimize endoluminal surface abrasion.

Tests of this catheter were performed in a saline solution (0.45% NaCl), applying a 400V, 1.8 MHz square wave alternating voltage. Tip rotation frequency was 12.5 Hz implying an 80 ms revolution period. First technical tests showed sparking and ultrasound imaging to function properly. One of our concerns, i.e. a potential deterioration of ultrasound image quality after sparking either by changes in the piezoelectric transducer or by the generation of cavitation bubbles in the transducer cavity, appeared to be irrelevant.

For in vitro vessel recanalization testing, an obstructed *coronary artery specimen* was used. Cautious testing of the vessel by differently sized probes had shown the resting lumen diameter to be less than 1.5 mm. Unfortunately additional testing with a 1 mm probe caused a vessel perforation. To prevent further damage no attempts were performed in trying to document the apparently very small remaining lumen by an intravascular imaging catheter. The vessel was fixed proximally unto an 8F sheath and side branches were tight up. Both the sheath and the distal vessel end were fixed to a mechanical support and immersed in a saline solution. The so called combi-tip catheter was inserted through the sheath and manually



Figure 6. View on the design of the catheter tip combining spark erosion and ultrasound imaging and the fabricated tip of the catheter prototype as applied in the experiments. Both the active electrode, surrounded by ceramics, and the circular ultrasound transducer can be observed. In the photograph the sleeve covering the ultrasound transducer is withdrawn to allow fluid filling of the cavity.

advanced until some resistance was detected. During testing a pump driven 2 ml/min flow of 0.45% saline solution was maintained through the catheter and the vessel. Being in contact with the obstruction, the segment on which spark erosion should be applied was selected on base of the ultrasound image. Timing of the start of the spark erosion pulse was related to the timing signals obtained from the ultrasound imaging equipment. By superimposing a fraction of the generator radiofrequency signal to the ultrasound signal the position of sparking could be easily observed in the ultrasound image. Before applying high voltage to the sparking electrode this procedure allowed to adjust start and duration of the sparking pulse such that this would cover the segment selected for ablation.

In Figure 7 a series of ultrasound images show the events (left to right, top to bottom) occurring after application of a single spark erosion pulse. The first image shows the cross section in the situation where the tip cannot be further advanced. At the top of the image a calcified lesion can be observed and some wall thickening on the left. It was decided to apply spark erosion to the left half and upper vessel segment. Because of electrical interference, induced by the sparking pulse into the ultrasound signal, the segment covered by the spark erosion period can be observed in the next two images. The time difference between these images is 40 ms which can be derived from the numbers superimposed in the upper left corner. These numbers indicate the time in seconds i.e. 7 followed by the number of video fields passed. Video field repetition rate was 50 Hz and therefore 20 ms passes be-

tween successive fields. The third image, which captured the complete sparking period, shows an interesting increase of echogenicity in the area which was not covered by the pulse (2 to 6 o'clock position). When interpreting this observation one should realize that sparking can only occur at a distance of approximately 1 mm to 3.5 mm distal of the transducer location. In the fourth image it is shown how the increased echogenicity became present in the complete cross section up to a depth of 6 mm. Also in the saline, outside of the vessel, some individual ultrasound reflecting elements can be observed. In the fifth image the echogenicity has almost disappeared. In the sixth picture an image comparable to the first one can be observed again.

The most likely explanation of the observed temporal increase in echogenicity is the generation of micro bubbles by cavitation. From the observed decay time of 240 - 400 ms and using the Plesset formula¹³ it was derived that the size of these bubbles is 5 to 6 microns which corresponds with the size of the capillaries.

No regional ablation effect can be observed in the sixth image after application of this single pulse. This is to be expected because the catheter advancement after a single pulse is in the order of 0.1 to 0.2 mm which is too small to move the ultrasound imaging plane into the ablation area.

As a next step, a series of 30 successive pulses at 1 s intervals was applied. During this pulse sequence the ultrasound image gradually faded away. Probably the area in which bubbles are generated by the vaporization of tissue, then entered the plane of imaging. After the pulse sequence the catheter was slightly pulled back. Next it took approximately 10 s before the image gradually became normal again. Apparently clearance from gas bubbles, originating from vaporized tissue, takes more time than clearance from the generated cavitation bubbles.

After the recanalization procedure, ultrasound imaging during pull back of the catheter did not reveal further details upon the procedural success. Throughout the experiment color video recordings had been made of the test set up which allowed to study some events in more detail from the video replay. At the moment of starting the pull back a faint suspension and some small bubbles left the distal vessel end. Furthermore the replay showed the isolated vessel to rotate over an angle of approximately 30 degrees when applying tip rotation.

Histologic examination of sections of the formalin fixed vessel showed that the wall had been perforated by spark erosion and also a dissection of the eccentric plaque from the media was observed. Signs of spark erosion i.e. interruption of the normal cellular lining and a small zone (0.05 - 0.2 mm) of discoloration (hematoxylin eosin stain), were observed over an axial vessel distance of approximately 5 mm. No intrusion of gas bubbles at the edges of ablated cellular layers was observed.

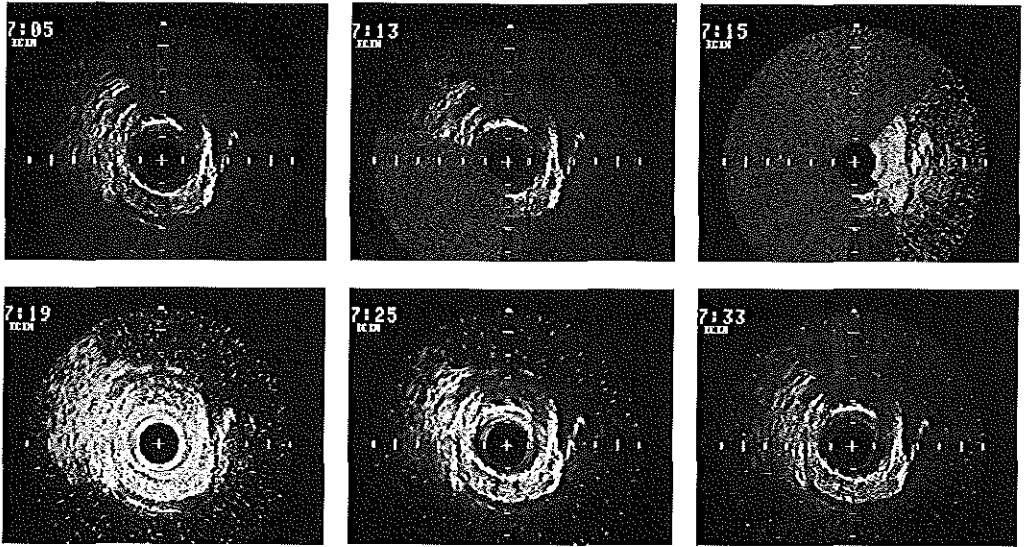


Figure 7. Sequence of ultrasound images showing, from left to right and from top to bottom, in the first image a vessel cross section before spark erosion application. In the second and third image the start and end of the spark erosion period is shown which covers the left half and the top of the cross section. A segment showing increased echogenicity becomes apparent in the non ablated part of the cross section (2 to 6 o'clock position). This echogenicity can be observed in the complete cross section 120 ms after the pulse (fourth image) and has almost disappeared during the next period until 240 ms after the sparking pulse (fifth image). After 400 ms the sixth image looks normal again. Obviously, as explained in the text, at this location proximal of the electrode no ablation effect can be observed after a single sparking pulse.

In another test set up, a stenosed segment of a *coronary artery specimen* with 15 mm length, was used. The specimen was glued between two electrically conductive plastic plates, which were mounted in a frame. The plates were positioned in parallel at such a distance that the vessel lumen was not deformed. The frame was immersed in a saline solution such that the catheter could enter the proximal lumen entrance in a vertical top down approach. The catheter was free to move in the lateral direction over a distance of 3 mm. Force of the catheter tip upon the stenosis was controlled and forward motion was measured.

First testing was applied with a 5 gr force. A half vessel circumference, partly showing calcified plaque deposition, was selected for sparking. After application of 40 pulses no significant progress had been obtained. Increasing the weight to 10 gr induced progress. A total of 160 pulses were needed to pass the approximately 6.5 mm long stenosis.

In Figure 8 a histologic section (elastin von Gieson stain) of the recanalized vessel is shown. On base of the applied selection, the effect of sparking should be expected from the 6 to 12 o'clock position. The lesion contained a lot of calcified areas near the 12 o'clock position and no ablation can be observed at this location, a feature

which explains the slow speed of progression. In Figure 8 at site A, spark erosion ablation can be recognized from interruption of cellular layers. There are no signs of bubble intrusion into the cellular layers at this location. Some discoloration was observed in the area contacted by the electrode immediately following the sparking zone (Figure 8, location B). Probably this has to do with the heat stored in the electrode. Such an effect may be reduced by downsizing the electrode's volume, thereby reducing its heat capacity.

DISCUSSION:

From the very start of investigating spark erosion as an intra arterial plaque removal technique⁴ it was realized that one of the major problems to be solved would be the appropriate steering and guidance of this method. Ideally such a removal technique should be selective, i.e., the mechanism of ablation should attack only the diseased parts of the wall. For spark erosion this was not a realistic option. Although for some lasers selectivity has been claimed, this principle has never been demonstrated to be clinically applicable. Neither was the idea to use a steerable fiberoptics laser catheter under guidance of spectral fluoroscopy¹⁴. As a first step to solve the

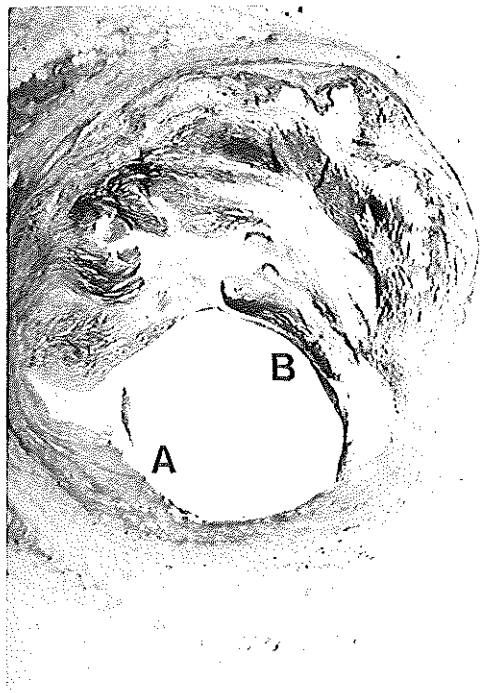


Figure 8. Histologic cross section (hemotoxylin-eosin stain) of an atherosclerotic human coronary artery at a site of spark erosion as applied with a clockwise rotating tip under ultrasound guidance. Spark erosion was applied at a segment from the 6 to 12 o'clock position. At location A interruption of cellular layers can be recognized but no bubble intrusion in between the cellular layers. At location B some discoloration was observed.

guidance problem for spark erosion, fiber optic angiography has been tested at some limited scale but was found to be not useful. Another more attractive option which has been studied more extensively was the intraluminal measurement of electrical tissue impedance¹⁵. As might be expected, fatty and calcific deposits will raise electrical tissue impedance. However, both the angioscopic and impedance measurement technique have in common that they are mainly sensitive in the detection of endoluminal surface abnormalities. Plaques to be removed may pass undetected because of a covering cap of relatively normal endoluminal tissue¹⁵. Furthermore, during the process of plaque removal, information is needed of remaining wall thickness to prevent perforation. For these reasons intravascular ultrasound imaging^{5,6} was selected for guidance of spark erosion. Only this technique provides information on wall thickness and to some extent also on the composition of the vessel wall.

In this study it has been shown that combining spark erosion and ultrasound imaging in a single catheter is feasible by using a rotating tip. The part of the circumference where spark erosion will be applied is visualized in the ultrasound image allowing easy directional adjustment. By the use of a small electrode, important progress could be made in reducing previously reported problems of gas production and electrical stimulation. Further studies will be required to fully explore these new important findings. In the current study the primary focus was concentrated on finding solutions which would allow feasibility testing of the combi-tip catheter.

Generally a new development, which deviates significantly from currently applied techniques, will raise new problems to be solved. For example, during application of spark erosion by the rotating electrode in the pigs, perforation of the femoral artery occurred in two of four animals. By visual inspection the adventitial layer appeared to have been wrapped around the tip which had worsened the damage induced to the vessel. This wrapping did not seem to be related to surface roughness of the tip or to its profile as was concluded from testing seven differently shaped, highly polished tips of various materials being slowly rotated against an adventitial layer of a vessel *in vitro*. All types showed a tight wrapping of the adventitia around the tip. Probably the adventitia initially behaves as a fluid which adheres to the rotating surface until the multiple collagen fibers become stretched and next become firmly wrapped around the tip. For this reason prevention of perforation when applying a rotating tip will be of crucial importance.

Other questions arising are: How can the optimal axial force be applied? What clinical strategy is needed when progressing at a speed of 0.1 mm per ablation pulse? How can a flexible high torque tip driving system be realized?

Obviously, further testing and learning will be needed to determine the usefulness of ultrasonic guidance of spark erosion recanalization through complex lesions like investigated in these preliminary experiments. More information is needed on the aspect of vessel rotation and its influence on the selection of the segment to be ablated. Also the potential role of torsional forces on plaque dissection should be studied.

In conclusion: spark erosion, using a small rotating electrode, can be selectively applied under ultrasound guidance in stenosed vessels. Luminal dimensions can be restored to almost normal dimensions. When applying relatively low voltages, speed of progression is rather low, but gas bubble formation and electrical stimulation are no longer major problems. Technical solutions for a number of mechanical problems need to be found for the development of a clinically operational device.

ACKNOWLEDGMENTS

The valuable contributions of Gerard Heuvelsland and Wim van Alphen to this project are greatly acknowledged. They skillfully fabricated prototypes of the combi-tip catheter and provided very helpful tips for its design.

This project has been partially funded by grants from the Foundation of Technological Sciences (STW grant RGN79-1257), the Dutch Heart Foundation (NHS grant 37.007) and from the Inter University Cardiology Institute of the Netherlands (ICIN project 12).

REFERENCES

1. Topol EJ, Leya F, Pinkerton CA, et al. "A comparison of directional atherectomy with coronary angioplasty in patients with coronary artery disease" *N Engl J Med* 1993, 329: 221-227
2. Adelman AG, Cohen EA, Kimball BP, et al. "A comparison of directional atherectomy with balloon angioplasty for lesions of the left anterior descending coronary artery" *N Engl J Med* 1993, 329: 228-233
3. Fitzgerald PJ, Belef M, Connolly AJ, Sudhir K, Yock PG. "Design and initial testing of an ultrasound-guided directional atherectomy device" *Am Heart J* 1995, 129: 593-598
4. Slager CJ, Essed CE, Schuurbijs JCH, Bom N, Serruys PW, Meester GT. "Vaporization of atherosclerotic plaques by spark erosion" *JACC* 1985, 5, 6: 1382-1386
5. Slager CJ. "Echo-vonkerosie rekanalisatie inrichting" *Ned octrooi aanvraag* 1987: 87.00632
6. Bom N, Slager CJ, Egmond FC van, Lancée CT, Serruys PW. "Intra-arterial ultrasonic imaging for recanalization by spark erosion" *Ultrasound Med Biol* 1988, 14: 257-261
7. Blankenstein JH van, Slager CJ, Schuurbijs JCH, Strikwerda S, Verdouw PD. "Heart function after injection of small air bubbles in a coronary artery of pigs" *J Appl Physiol* 1993, 75, 3: 1201-1207
8. Slager CJ, Schuurbijs JCH, Oomen JAF, Bom N. "Electrical nerve and muscle stimulation by radio frequency surgery: role of direct current loops around the active electrode" *IEEBE Trans on Biomed Engng* 1993, 40, 2: 182-187
9. Oomen A, Erven L van, Vandenbroucke WVA, Verdaasdonk RM, Slager CJ, Thomson SL, Borst C. "Early and late arterial healing response to catheter-induced laser, thermal, and mechanical wall damage in the rabbit" *Lasers in Surg and Med*, 1990, 10: 363-374
10. Bom N, Lancée CT, Van Egmond FC. "An ultrasonic intracardiac scanner" *Ultrasonics* 1972, 10: 72-76
11. Slager CJ, Laban M, von Birgelen C, Krams R, Oomen JAF, den Boer A, Li W, de Feijter PJ, Serruys PW, Roelandt JRTC. "ANGUS: A new approach to three-dimensional reconstruction of geometry and orientation of coronary lumen and plaque by combined use of coronary angiography and IVUS" *J Am Coll Cardiol*, 1995, 25: 1444
12. Laban M, Oomen JAF, Slager CJ, Wentzel JJ, Krams R, Schuurbijs JCH, den Boer A, von Birgelen C, Serruys PW, de Feijter PJ. "ANGUS: A new approach to three-dimensional reconstruction of coronary vessels by combined use of angiography and intravascular ultrasound" *IEEBE Comp. Card.* 1995, *IEEBE Comp Soc. Piscataway*, 95CH35874: 325-328.
13. Epstein PS, Plesset MS. "On the stability of gas bubbles in liquid gas solutions" *J Chem Phys*, 1950, 18: 1505-1509
14. Cothren RM, Hayes GB, Kramer JR, Sacks B, Kittrell C, Feld MS. "A multifiber catheter with an optical shield for laser angioplasty". *Laser Life Sci* 1986, 1: 1-12
15. Slager CJ, Phaff AC, Essed CM, Bom N, Schuurbijs JCH, Serruys PW. "Electrical impedance of layered atherosclerotic plaques on human aortas" *IEEE Trans Biomed Engng* 1992, 39, 4: 411-419

CHAPTER 9

**SPARK EROSION MYECTOMY IN
HYPERTROPHIC OBSTRUCTIVE CARDIOMYOPATHY**

Lex P.W.M. Maat, Cornelis J. Slager,
Lex A. van Herwerden, Johan C.H. Schuurbiers, Robert Jan van Suylen,
Marcel J.M. Kofflard, Folkert J. ten Cate, Egbert Bos

Spark Erosion Myectomy in Hypertrophic Obstructive Cardiomyopathy

Lex P. W. M. Maat, MD, Cornelis J. Slager, MSc, Lex A. van Herwerden, MD, Johan C. H. Schuurbijs, BSc, Robert J. van Suylen, MD, Marcel J. M. Kofflard, MD, Folkert J. ten Cate, MD, and Egbert Bos, MD

Departments of Thoracic Surgery, Cardiovascular Research, and Cardiology, Thoraxcenter, and the Department of Pathology, Erasmus University Rotterdam and University Hospital Dijkzigt, Rotterdam, The Netherlands

The design features of the cutting electrode and the electrical characteristics of a monopolar electro-surgical device were specially adapted for performing a septal myectomy in patients with hypertrophic obstructive cardiomyopathy. Both the cutting behavior and electrode design were found to facilitate myectomy.

(*Ann Thorac Surg* 1994;58:536-40)

Septal myectomy is effective in relieving the symptoms of hypertrophic obstructive cardiomyopathy refractory to medical treatment. Although many procedures have been advocated for the surgical treatment of hypertrophic obstructive cardiomyopathy, most surgeons approach the septum through an aortotomy, but some surgeons add a ventriculotomy to improve exposure [1-16]. A conventional myectomy can be technically demanding because of the midventricular location of the obstruction and the risk of disrupting septal integrity. The monopolar electro-surgical device called *spark erosion* was originally

See also page 575.

designed for intravascular applications [17]. Impressed by its cutting characteristics, we constructed a modified device for use in septal myectomy.

Material and Methods

The cutting electrode is a quadrangular monopolar electrode composed of a metal foil (Fig 1). The electrode is covered with an electrically insulating synthetic resin, except for the cutting front side, which is 50 μ m wide. The insulation is able to withstand temperatures up to 400°C. The cutting electrode is connected to a pencil with a malleable connection to allow the electrode to be adjusted with respect to the orientation of the handle. The width and depth of the myectomy depend on the dimensions of the electrode. Currently available (but not commercially) electrode sizes are 10 \times 6.5 mm, 11 \times 9 mm, and 14 \times 9 mm (width \times depth) (Fig 2). After an initial resection, the width and depth of the myectomy can be adjusted further.

Accepted for publication June 8, 1994.

Address reprint requests to Dr Maat, Department of Thoracic Surgery, Thoraxcenter BD 156, University Hospital Dijkzigt, Dr. Molewaterplein 40, 3015 GD Rotterdam, The Netherlands.

Because of the cutting characteristics, additional resections then can be done easily without fragmentation of the muscle tissue.

The generator is battery operated, with an output impedance of 60 ohm delivering an alternating square-wave voltage at a frequency of 500 kHz, with an effective value of 700 V [18]. Direct current is blocked at both output terminals by capacitors to minimize stimulating side effects [19]. Energy is applied during short pulses of 1.5 ms at a repetition rate of 12 Hz. These characteristics make possible a cutting speed through heart muscle of approximately 2 mm/s. Transparent Perspex (methacrylic acid) retractors were constructed in several sizes to optimize visibility and probe orientation during the procedure and to protect the aortic valve cusps, the mitral valve, and the anterior papillary muscle (Fig 3).

Between February 1987 and March 1993, spark erosion septal myectomy was performed in 18 patients with hypertrophic obstructive cardiomyopathy. All these patients were symptomatic despite optimal medical treatment. The demographic data, preoperative and postoperative pressure gradients, and preoperative and postoperative New York Heart Association functional class are summarized in Table 1. The peak systolic left ventricular outflow tract gradient was measured with continuous-wave Doppler echocardiography and expressed in millimeters of mercury. In 17 patients, the pattern of hypertrophy was graded as type III according to the classification scheme of Maron and colleagues [20]. Patient 9 was classified as having type II hypertrophy.

Patients were operated on with cardiopulmonary bypass and moderate hypothermia. Cardiac arrest was induced by topical cooling and aortic root cardioplegia (St. Thomas' Hospital solution). The ventricular septum was approached via the ascending aorta through a hockey-stick incision.

Septal exposure and visualization were improved by passing the appropriate-sized transparent retractor through the aortic valve toward the left ventricular apex. Further improvement of exposure was obtained by exerting counterpressure on the external left ventricular wall. In 3 patients, there was an important mitral insufficiency that was not caused by systolic anterior motion of the anterior mitral valve leaflet.

Patient 3 had been treated for bacterial endocarditis 5 years preoperatively. After the myectomy, the valve was

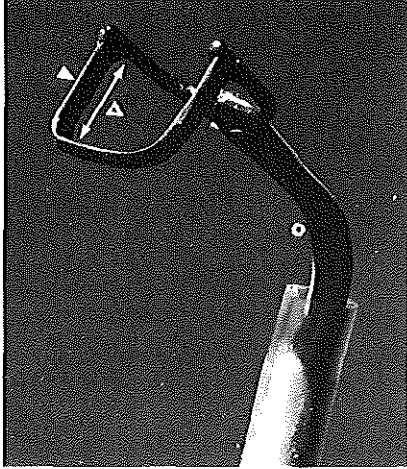


Fig 1. The electrode, showing some of the special features. The cutting front side (solid arrowhead) can be distinguished easily from the insulated part of the electrode. The electrode support (open arrowhead) limits the depth of the myectomy. The malleable connection (open circle) is shown here in a heavily bent position, but can be positioned to any angle from +90 degrees to -90 degrees.

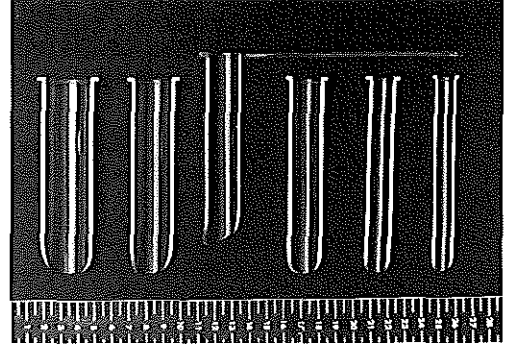


Fig 3. The set of transparent Perspex (methacrylic acid) retractors.

successfully repaired (closure of a tear in the anterior leaflet and commissuroplasty). Patient 9 had a destroyed anterior mitral valve leaflet as the result of recent bacterial endocarditis. At the time of operation, reconstruction of the valve seemed impossible and, in addition to the myectomy, the valve was replaced with a mechanical



A



B

Fig 2. The myectomy procedure in a pig heart. (A) The electrode has been advanced a few centimeters. (B) The electrode is withdrawn. The surface of the trough is very smooth and no coagulation effects can be observed on visual inspection.

Table 1. Preoperative and Postoperative Characteristics

| Patient No. | Sex | Age (y) | Peak Gradient* (mm Hg) | | NYHA Class | | Additional Procedures |
|-------------|-----|---------|------------------------|--------|------------|--------|-------------------------|
| | | | Preop | Postop | Preop | Postop | |
| 1 | F | 51 | 36 | 8 | III | II | ... |
| 2 | F | 61 | 80 | 6 | III | II | ... |
| 3 | F | 19 | 62 | ? | III | I | Mitral valve repair |
| 4 | M | 38 | 36 | 10 | III | II | ... |
| 5 | M | 32 | 125 | 25 | II | I | ... |
| 6 | F | 30 | 10 | 5 | III | III | ... |
| 7 | M | 58 | 81 | 5 | III | I | ... |
| 8 | M | 44 | 38 | 8 | III | II | ... |
| 9 | M | 40 | 36 | 8 | IV | I | Mitral valve prosthesis |
| 10 | F | 36 | 100 | 50 | II | I | ... |
| 11 | F | 36 | 108 | 36 | III | I | ... |
| 12 | F | 61 | 100 | 8 | III | I | Mitral valve prosthesis |
| 13 | F | 24 | 80 | 10 | III | I | Mitral valve patch |
| 14 | M | 29 | 74 | 8 | III | I | Mitral valve patch |
| 15 | M | 67 | 92 | 6 | III | I | Mitral valve patch |
| 16 | M | 55 | 200 | 4 | III | I | Mitral valve patch |
| 17 | M | 43 | 148 | 7 | III | I | ... |
| 18 | M | 31 | 140 | 16 | III | I | Mitral valve patch |

* Peak systolic left ventricular outflow tract gradient measured by continuous-wave Doppler echocardiography.

F = female; M = male; NYHA = New York Heart Association.

prosthesis (St. Jude Medical, St. Paul, MN). Patient 11 had severe mitral insufficiency stemming from a heavily calcified posterior mitral valve leaflet and annulus. After myectomy, the systolic anterior motion of the mitral valve decreased considerably but the mitral insufficiency persisted. An attempt to repair the valve failed, so this valve was also replaced with a mechanical valve (St. Jude Medical).

More recently, a patch technique has been used in selected patients in addition to the myectomy. Figure 4 shows the epicardial echocardiograms from a patient obtained before and after spark erosion myectomy and mitral valve patch placement.

The removed tissue was cut into 5- μ m sections after formalin fixation, paraffin embedding, and staining with hematoxylin-eosin and elastic van Gieson. All specimens were evaluated by one pathologist and one surgeon. The depth of thermal injury was measured by multiplying the number of injured cells by the diameter of the hypertrophied myocytes.

Results

Our clinical experience, spanning February 1987 to March 1993, consists of septal myectomy performed in 18 patients. There were no perioperative deaths. Two patients received a permanent pacemaker: in 1 patient, because of a newly formed atrioventricular conduction block; in the other, because of conduction abnormalities preoperatively, which was followed by periods of normal atrioventricular conduction postoperatively. Damage to the aortic or mitral valve was not encountered during or after the procedure, and no ventricular septal defects were created.

Light microscopic evaluation of the surgical specimens from the 18 patients revealed a uniform pattern (Fig 5). The depth of complete cell destruction by thermal energy was two to three cell layers; complete destruction of four or more cell layers was never seen. Between this zone and the "normal" myocardium was a zone of five to eight cell layers that showed hypereosinophilia, increased vacuolization, and, in some cells, contraction bands. The cross-sectional diameter of myocytes in the setting of hypertrophic obstructive cardiomyopathy is between 25 and 35 μ m (normal, 10 to 15 μ m). The maximum depth of the thermal injury is thus between 175 and 385 μ m if the damage to the hypereosinophilic zone is irreversible. Otherwise, the depth of the thermal injury is between 50 and 105 μ m.

Patient 5 died suddenly 8 months after the operation, and autopsy revealed a recent myocardial infarction. The surface of this patient's myectomy was covered with a thin and smooth connective tissue layer. His initial postoperative course had been uneventful.

Comment

Treatment of hypertrophic obstructive cardiomyopathy with an electrosurgical device is not new. A wire-loop electrode, connected to a standard electrosurgical device, was used by Dobell and Scott in 1960 [4]. Cooley and colleagues [9] also used a loop cautery device in 1 patient. To our knowledge, none of these devices stood the test of time and most surgeons use a surgical scalpel or a scalpel-like device for myectomy or myotomy. However, the depth of the myectomy is not precisely controlled with this instrument, and the fear of septal perforation may cause the depth of the septal resection to be inadequate. In

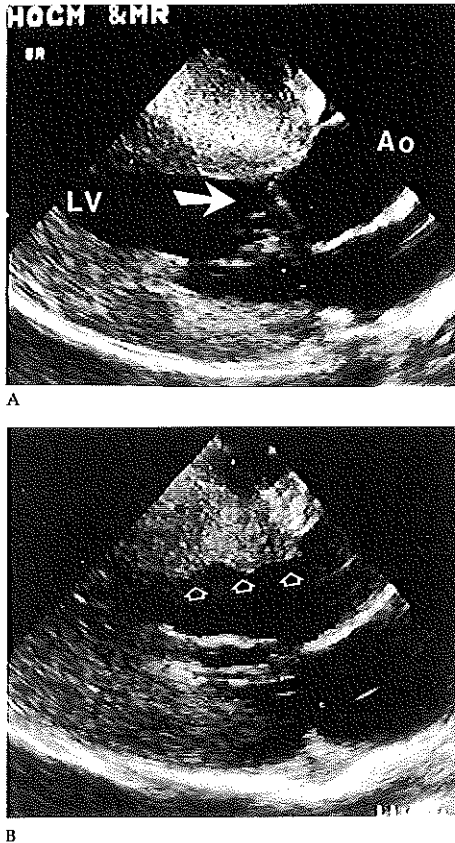


Fig 4. Epicardial echocardiograms in the left ventricular long axis, before (A) and after (B) spark erosion myectomy and patch plasty of the mitral valve. Systolic frames with an open aortic valve. (A) The closed arrow points to the area of systolic anterior motion of the anterior mitral valve leaflet. (B) The open arrows point to the site of myectomy. Systolic anterior motion has completely disappeared. (Ao = aorta; LV = left ventricle; HOCM = hypertrophic obstructive cardiomyopathy; MR = mitral valve regurgitation.)

performing a resection with a scalpel, small myocardial fragments and a rough myocardial surface may be a source of concern. Therefore, a more controlled way of performing septal myectomy is desirable.

In our opinion, the uncontrolled depth of thermal injury accomplished with traditional electro-surgical devices makes them unsuitable for use in septal myectomy. The coagulating properties of electro-surgical devices depend on the so-called crest factor (voltage peak divided by the voltage root mean squared).

We developed a dedicated electro-surgical unit and electrodes for septal myectomy possessing minimal coagulation effects. Compared with the properties of readily available electro-surgical units, our device has a much

lower output impedance in combination with a high effective voltage. This minimizes the warm-up time needed to form a steam envelope around the electrode, which is required before sparking and cuttings can commence.

With our device, the crest factor reaches its theoretical minimal value of 1, rather than the usual 1.4 to 2 seen in conventional electro-surgical devices, by applying an unmodulated square-wave alternating voltage. These specifications allow application of a brief cutting pulse, and this plus the low repetition rate maintain highly effective cutting with a minimal accumulation of thermal energy. In addition, the electrical insulation of the electrodes improves the cutting behavior by minimizing the cutting area and preventing the backward arcing of sparks to areas already passed. Smoke and vapor production during cutting are negligible. The low cutting speed of 2 mm/s allows the electrode to be accurately guided during the procedure. Compared with a wire-loop electrode, the quadrangular electrode is much stronger.

The height of the electrode supports limits the depth of the myectomy to the electrode size selected, thereby reducing the risk of creating a ventricular septal defect. The malleable connection of the electrode to the pencil allows for the electrode to be precisely adjusted with respect to the orientation of the handle.

No patient in the present series died and no ventricular septal defect was caused by the procedure. In the study group, 1 patient (5.5%) suffered a new atrioventricular conduction block. This does not seem excessive in light of the experience described in the literature [21-23]. Light microscopic reevaluation revealed there was no difference between this patient and the other patients with respect to the depth of thermal injury. Most likely this complication was related to a surgical technical imperfection, rather than to the electrical device.

In conclusion, both the design features and the cutting characteristics of the spark erosion device facilitate the performance of myectomy in patients with hypertrophic obstructive cardiomyopathy.

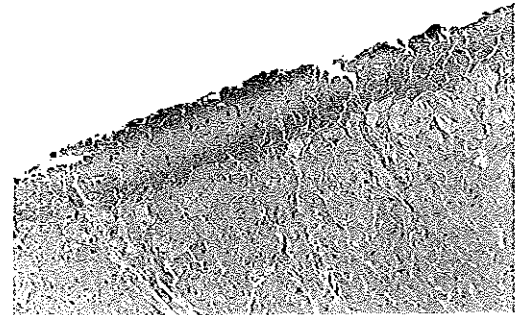


Fig 5. Representative photomicrograph of a resection specimen. The surface layer contains destroyed cells; the hypereosinophilic zone and the "normal" myocytes can be recognized easily. (Elastic van Gieson stain; $\times 180$ before 54% reduction.)

This research was supported in part by a grant (84.073) from the Netherlands Heart Foundation.

References

- Goodwin JF, Hollman A, Cleland WP, Teare D. Obstructive cardiomyopathy simulating aortic stenosis. *Br Heart J* 1960;22:403-14.
- Morrow AG, Brockenbrough EC. Surgical treatment of idiopathic hypertrophic subaortic stenosis. Technic and hemodynamic results of subaortic ventriculotomy. *Ann Surg* 1961;154:181-9.
- Lillehei CW, Levy MJ. Transatrial exposure for correction of subaortic stenosis. *JAMA* 1963;186:114-9.
- Dobell ARC, Scott HJ. Hypertrophic subaortic stenosis: evolution of a surgical technique. *J Thorac Cardiovasc Surg* 1964;47:26-39.
- Swan H. Subaortic muscular stenosis: a new surgical technique for repair. *J Thorac Cardiovasc Surg* 1964;47:681-4.
- Harken DE. Discussion of [4]. *J Thorac Cardiovasc Surg* 1964;47:33-4.
- Julian OC, Dye WS, Javid H, Hunter JA, Meunster JJ, Najafi H. Apical left ventriculotomy in subaortic stenosis due to a fibromuscular hypertrophy. *Circulation* 1965;31, 32(Suppl 1):44-56.
- Bigelow WG, Trimble AS, Auger P, Marquis Y, Wigle ED. The ventriculomyotomy operation for muscular subaortic stenosis. A reappraisal. *J Thorac Cardiovasc Surg* 1966;52:514-24.
- Cooley DA, Bloodwell RD, Hallman GL, LaSorte AF, Leachman RD, Chapman DW. Surgical treatment of muscular subaortic stenosis. Results from septectomy in twenty-six patients. *Circulation* 1967;35, 36(Suppl 1):124-32.
- Binet JP, Langlois J, Leiva-Semper A, David P, Bigelow WG. Ventriculomyotomy in hypertrophy of the left ventricle. *J Thorac Cardiovasc Surg* 1968;56:469-76.
- Cooley DA, Leachman RD, Wukash DC. Diffuse muscular subaortic stenosis: surgical treatment. *Am J Cardiol* 1973;31:1-6.
- Alferi O, Subramanian S. A new instrument for surgical exposure of subaortic and subpulmonary stenosis. *Ann Thorac Surg* 1975;19:589-91.
- Morrow AG, Reitz BA, Epstein SE, et al. Operative treatment in hypertrophic subaortic stenosis. Techniques, and the results of pre- and post-operative assessments in 83 patients. *Circulation* 1975;52:88-102.
- Dembitsky WP, Weldon CS. Clinical experience with the use of a valve-bearing conduit to construct a second left ventricular outflow tract in case of unresectable intra-ventricular obstruction. *Ann Surg* 1976;184:317-23.
- Robicsek F, Daugherty HK. A new instrument to facilitate myectomy in subaortic stenosis. *J Thorac Cardiovasc Surg* 1988;95:533-4.
- Dowling RD, Landreneau RJ, Gasior TA, Zjady GM, Armitage JM. Septal myectomy with a carbon dioxide laser for hypertrophic cardiomyopathy. *Ann Thorac Surg* 1993;55:1558-60.
- Slager CJ, Essed CE, Schuurbijs JCH, Bom N, Serruys PW, Meester GT. Vaporization of atherosclerotic plaques by spark erosion. *J Am Coll Cardiol* 1985;5:1382-6.
- Slager CJ, Bom N, Serruys PW, Schuurbijs JCH, Vandembroucke WVA, Lancee CT. Spark erosion and its combination with sensing devices for ablation of vascular lesions. In: Vogel JK, King SB III, eds. *Interventional cardiology: future directions*. St. Louis: Mosby, 1989:157-69.
- Slager CJ, Schuurbijs JCH, Oomen JAF, Bom N. Electrical nerve and muscle stimulation by radio frequency surgery: role of direct current loops around the active electrode. *IEEE Trans Biomed Eng* 1993;40:182-7.
- Maron BJ, Gottdreiner JS, Epstein SE. Patterns and significance of distribution of left ventricular hypertrophy in hypertrophic cardiomyopathy. A wide angle, two-dimensional echocardiographic study in 125 patients. *Am J Cardiol* 1981;48:418-28.
- Williams WG, Wigle ED, Rakowski H, Smallhorn J, Leblanc J, Trusler GA. Results of surgery for hypertrophic obstructive cardiomyopathy. *Circulation* 1987;76(Suppl 5):104-8.
- Krajcer Z, Leachman RD, Cooley DA, Coronado R. Septal myotomy-myectomy versus mitral valve replacement in hypertrophic cardiomyopathy. Ten-year follow-up in 185 patients. *Circulation* 1989;80(Suppl 1):57-64.
- Mohr R, Schaff HV, Puga FJ, Danielson GK. Results of operation for hypertrophic obstructive cardiomyopathy in children and adults less than 40 years of age. *Circulation* 1989;80(Suppl 1):191-6.

APPENDIX

**INTRA ARTERIAL DEVICE FOR THE REMOVAL
OF ARTERIAL OBSTRUCTIONS BY SPARK EROSION**

INTRA ARTERIËLE INRICHTING VOOR HET DOOR MIDDEL VAN
VONKEROSIE VERWIJDEREN VAN OBSTRUCTIES IN BLOEDVATEN

Cornelis J. Slager

Octrooiraad



⑫A **Terinzagelegging** ⑪ **8700632**

Nederland

⑲ NL

- ⑤4 **Intra-arteriële inrichting voor het door middel van vonkerosie-
verwijderen van obstructies in bloedvaten.**
- ⑤1 Int.Cl⁴: A61B 17/36.
- ⑦1 Aanvrager: Stichting Biomedical Engineering te Rotterdam.
- ⑦4 Gem.: Ir. Th.A.H.J. Smulders c.s.
Vereenigde Octroobureaux
Nieuwe Parklaan 107
2587 BP 's-Gravenhage.

-
- ②1 Aanvraag Nr. 8700632.
- ②2 Ingediend 17 maart 1987.
- ③2 Uitvinder: Cornelis J. Slager te Dordrecht
- ③3 --
- ③1 --
- ③2 --

-
- ④3 Ter inzage gelegd 17 oktober 1988.

De aan dit blad gehechte stukken zijn een afdruk van de oorspronkelijk ingediende beschrijving met conclusie(s) en eventuele tekening(en).

Intra-arteriële inrichting voor het door middel van vonkerosie verwijderen van obstructies in bloedvaten.

De uitvinding heeft betrekking op een intra-arteriële inrichting voor het door middel van vonkerosie verwijderen van obstructies in bloedvaten, omvattende een katheter die aan of nabij het uiteinde is voorzien van ten minste
 5 een elektrode, welke ten minste ene elektrode via een door de katheter verlopende elektrische geleider koppelbaar is met een elektrische vonkgenerator.

Een dergelijke inrichting is bekend uit het artikel in J. American Coll. of Cardiology, Vol. 5, nr. 6 (1985),
 10 blz. 1382-1386. Met de bekende inrichting werden blijkens het artikel proefnemingen in vitro uitgevoerd op een aantal segmenten van bloedvaten, waarin obstructies voorkwamen. Alvorens in vivo toepassing mogelijk is, zullen, aldus het artikel, nog wijzigingen nodig zijn. Met name wordt
 15 gewezen op de noodzaak de vonkerosie te beheersen om asymmetrische of excentrische obstructies te kunnen behandelen. Daarvoor zullen, aldus het artikel, nog uitvindingen moeten worden gedaan. Afgezien daarvan leert het artikel evenmin hoe obstructies kunnen worden gedetecteerd en hoe de bekende
 20 inrichting zou moeten worden ingericht om de vonkerosie ter plaatse van een gedetecteerde obstructie te laten geschieden.

De uitvinding heeft tot doel de bekende inrichting te verbeteren en een inrichting van het in de aanhef omschreven type te verschaffen, waarmede in vivo kan worden gewerkt.
 25 Het gestelde doel wordt volgens de uitvinding bereikt met een inrichting die is voorzien van middelen om de vonkerosie te besturen en desgewenst excentrisch ten opzichte van de katheteras te doen plaatsvinden, alsmede van met het
 30 uiteinde van de katheter gekoppelde detectiemiddelen voor het vaststellen van de plaats en eventueel aard van een te behandelen obstructie.

Tot dusverre toegepaste methoden voor het opheffen van obstructies vereisen veelal een gecompliceerde operatieve ingreep. Een voorbeeld is de zgn. by-pass operatie. In de medische wereld bestond en bestaat daarom een sterke
5 behoefte aan een techniek, die minder risico's meebrengt, minder invasief is en minder kostbaar is. Een inmiddels reeds veel toegepaste nieuwe werkwijze wordt beschreven in het artikel in N. Engl. J. Med. 301, blz. 61-68. Bij deze katheter-ballon dilatatiemethode wordt de obstructie
10 als het ware weggedrukt door het opblazen van een aan een katheter bevestigd ballonnetje. In een relatief groot aantal gevallen komt de obstructie echter terug.

Recentelijk zijn een aantal zowel mechanische als niet-mechanische katheter-methoden ontwikkeld om binnen
15 arteriën en venen een obstructie te verwijderen. Een met grote snelheid roterende draad, voorzien van abrasief materiaal is voorgesteld in het artikel in Circulation 74: II-362. Een atherectomie kathetertipmethode wordt beschreven in het artikel in Circulation 74: II-202. Als voorbeeld
20 van een niet-mechanisch systeem kan worden genoemd de zgn. "hot-tip" methode, beschreven in het artikel in J. Am. Coll. Cardiol 3:490. Hierbij wordt via een glasvezel-laser of langs elektrische weg het metalen uiteinde van een katheter verhit en als het ware door de obstructie gebrand. Ook
25 de via een glasvezel overgebrachte laserenergie op zich is in recente publicaties beschreven als mogelijkheid om perfusie door een vernauwd of verstopt vat te verbeteren. Het lasereinde kan daarbij al dan niet van b.v. een saffiertip worden voorzien, zie b.v. Am. J. Cardiol 50: 1209-1211.

30 Bij desobstructiemethoden is het kunnen lokaliseren van de obstructie binnen b.v. de kransslagader in relatie tot het verloop van het vat belangrijk. De obstructie is immers vaak excentrisch. Men wil slechts de obstructie verwijderen zonder de vaatwand te beschadigen. Het uiteinde-
35 lijke succes van de te realiseren therapie hangt af van het vermogen tot lokalisatie en mogelijk ook identificatie

van de samenstelling van de obstructie. Met röntgencontrast-angiografie is het, zeker in bochtige vaten, niet mogelijk om voldoende morfologische gegevens te verkrijgen en de oriëntatie van de gewoonlijk excentrische obstructie ten opzichte van de oorspronkelijke vaatwand vast te stellen. Voorts zijn de hiervoor genoemde mechanische en niet-mechanische methoden ter verwijdering van een obstructie niet gemakkelijk stuurbaar in de zin van excentrisch toepasbaar binnen een vat als daarbij ook nog opname van noodzakelijke detectiemiddelen is vereist.

De vonkerosiemethode kan excentrisch bestuurbaar worden gemaakt. Dit is echter pas waardevol indien door een detectiemethode direct en ter plaatse kan worden vastgesteld hoe het vonkerosieproces excentrisch moet worden uitgevoerd. Met de inrichting volgens de uitvinding wordt een en ander mogelijk gemaakt doordat deze is voorzien van middelen voor het besturen van de vonkerosie en van detectiemiddelen voor het vaststellen van plaats en aard van een te behandelen obstructie. Bij voorkeur omvatten daarbij de laatstgenoemde middelen een transducent voor het uitzenden van en opvangen van echo's van hoogfrequente ultrasone trillingen.

Een voor de hand liggende detectiemethode zou zijn een methode gebaseerd op elektrische impedantiemeting. Gebleken is echter dat de meeste obstructies aan de binnenzijde van een vat zijn bedekt met een, elektrisch gezien, niet sterk van normaal afwijkende weefsellaag. Impedantiemeting levert daardoor te weinig informatie. Detectie door lokale observatie van de obstructie via een vezeloptische katheter zou ook mogelijk zijn. Dit evenwel vergt een continu spelen met een transparante vloeistof, hetgeen bezwarend is. In de praktijk zal slechts een detectiemethode met diepe penetratie voldoen. De volgens de uitvinding bij voorkeur toegepaste echodetectiemethode is een zodanige. Aldus is de combinatie in de inrichting volgens de uitvinding van detectiemiddelen waarmee een geheel doorsnedebeeld en daarmee

de juiste morfologie van de obstructie kan worden verkregen en van middelen om de vonkerosie te besturen een waardevolle verbetering ten opzichte van het bekende.

5 De inrichting volgens de uitvinding kan zeer geschikt worden toegepast in coronairvaten. Andere toepassingen, zoals in beenvaten of andere lichaamsholten zijn evenwel ook mogelijk.

Het toepassen van de echo-detectiemethoden in holten in het menselijk of dierlijk lichaam is reeds geruime
10 tijd bekend. In een artikel in *Polak Przegląd Chirurg* 33:1071 (1961) wordt beschreven hoe echo's werden verkregen van de binnenkant van het hart met behulp van een enkel-element bevattende katheter, die via een vene in een hond was ingebracht. In een artikel in *Ultrasonics* 2: 82-86
15 (1964) wordt de toepassing van een intraveneuze echosonde beschreven. Daarmede kon men de maat van een atrium septum defect in patiënten met een congenitaal vitium vastleggen. Tomogrammen werden verkregen door rotatie en terugtrekken van de sonde, die in het rechter atrium was geïntroduceerd
20 via een vene. In het artikel in *Ultrasonics* (1967) 80-83 werd de intraveneuze methode voor het verkrijgen van een doorsnede zelfs superieur geacht vergeleken bij een aftastmethode vanuit de slokdarm. De drager van de sonde bestond uit een roestvrij stalen buisje met een buitendiameter
25 van 1,2 mm en een wanddikte van 0,2 mm. Aangezien de beweging van de transducent zeer langzaam geschiedde, werden de tomogrammen verkregen via triggering op basis van het electrocardiogram van het hart.

De ontwikkelingen van systemen voor gebruik binnen
30 het hart en gebaseerd op het op het kathetereinde monteren van kleinere transducenten gingen door. In het artikel in *Circ. Res.* 22: 545-548 (1968) wordt een omnidirectionale enkel-element katheter beschreven waarmee de maten van de hartkamers via het meten van de echo-aankomsttijden
35 kunnen worden gereconstrueerd. In *Ultrasonics* 17: 143-153 (1970) is een katheter beschreven met 4 elementen die onder-

ling 90° zijn verschoven. Langzame rotatie van deze katheter (8 seconden voor het opnemen van een beeldje) in combinatie met computerreconstructie leverde intracardiale tomogrammen. Opnieuw noodzaakten de lange beeld-acquisitietijden tot triggering op basis van het electrocardiogram. De beschreven katheter werd geïntroduceerd via de carotide en bewoog enige millimeters gedurende de hartcyclus. Er was daarom een tracking mechanisme noodzakelijk, anders kon later het doorsnedebeeld niet worden gereconstrueerd.

De eerste zeer snelle real-time intracardiale scanner werd beschreven in *Ultrasonics* 10: 72-76 (1972). Deze katheter bestond uit een cirkelvormig stelsel met 32 elementen met een buitendiameter van 3,2 mm, welk stelsel was gemonteerd op het uiteinde van een No. 9 French katheter. Door de elektronische schakeling was de beeldsnelheid geen limitatie meer. Problemen bij dit systeem bleken echter de excessieve beweging van de katheter in de hartkamer gedurende de hartcyclus en de beperkte karakteristieken van de ultrageluidsbundel. De beschreven katheter werkte bij 5,7 MHz en bezat weliswaar een nauwe hoofdbundel, maar zeer geprononceerde gevoeligheid in de zijrichting. Hierdoor ontstonden onacceptabele fouten in het beeld.

In *Proc. Conf. Engn. Med. Biol.* 9:27 (1967) is een op een kathetertip gemonteerde echotransducent beschreven voor Doppler snelheidsmeting in de arterie. In *Excerpta Medica* 150-161 (1974) wordt een kathetersysteem met twee transducenten beschreven. Wanneer de katheter in een curve werd gebogen binnen de hartkamer, kon daarmee de maat worden vastgesteld.

De partieel invasieve echoaftastmethoden, zoals rectaal onderzoek en onderzoek via de slokdarm werden verder uitgebouwd. In *Nature* 232:335 (1971) worden resultaten beschreven van Doppler methoden vanuit de slokdarm. In *J. Appl. Physiology* 38:6 (1975) wordt een transoesofagale of slokdarm Doppler techniek beschreven. In *Circulation* 54:102 (1976) wordt de diagnostische methode via de slokdarm

voorgesteld. De eerste real time slokdarmtransducent wordt in Proc. Japan Soc. of Ultrasonics in Med. 32: 43-44 (1977) vermeld in de vorm van een roterend element in een met olie gevuld compartiment, waarmee sectoraftastbeelden verkregen werden. In J. Nucl. Med. All Sci 28: 115-121 (1984) wordt een soortgelijk systeem beschreven. Men ontwikkelde ook een mechanische aftaster met lineair stelsel, die werd beschreven in Proc. Japan Soc. of Ultrasonics in Med. 35: 115-116 (1978). Een enkel element bewoog daarbij parallel aan de lange as van een buis waardoor 8-20 beelden per seconde konden worden verkregen. In Lancet I: 629 (1980) wordt een real time 10 MHz lineair stelsel gemonteerd op een endoscoop beschreven. Voorts noemt het artikel in IEEE Trans. Biomed. Eng. 29: 707 (1982) de eerste elektronische sector scanner, gemonteerd voor onderzoek vanuit de slokdarm.

Gezien het voorgaande kan worden gesteld dat echosystemen bestaande uit een enkele of een aantal elementen en gemonteerd op een kathetereinde zijn beschreven. Ditzelfde geldt voor een aantal roterende enkel-elements systemen met of zonder spiegel voor toepassingen zoals binnen de slokdarm.

Zoals opgemerkt verdient het volgens de uitvinding de voorkeur voor het detecteren een hoogfrequent echosysteem toe te passen. Gevonden werd dat een optimale beeldvorming kan worden bereikt bij frequenties van meer dan 15 MHz. Volgens een verdere voorkeur is de transducent in de inrichting volgens de uitvinding dan ook ingericht voor het uitzenden van ultrasone trillingen met een frequentie van meer dan 15 MHz.

De inrichting volgens de uitvinding kan zodanig zijn uitgevoerd dat voor het vonkerosieprocédé een getriggerde pulsering wordt toegepast. Dit kan nuttig zijn om de natuurlijke elektrische stimulatie van het hart niet te verstoren. In beginsel zijn voor het toepassen van vonkerosie een groot aantal vormen van elektroden mogelijk. De elektrode kan b.v. een holle pijp zijn, of een konisch of bolvormig

geleidend uiteinde omvatten.

De elektrode kan b.v. ook een stelsel van afzonderlijke metalen "eilandjes", ingebed in een isolerend materiaal bevatten. Deze afzonderlijke metalen gebieden dienen dan
 5 door evenzovele afzonderlijke elektrodedraden gevoed te kunnen worden. Het oppervlak van het elektrodelichaam behoeft niet vlak te zijn, doch kan voorzien zijn van groeven, of kan poreus zijn.

Indien bij de inrichting volgens de uitvinding
 10 preciese positionering van het uiteinde, van de katheter in een bloedvat noodzakelijk of gewenst is kan daarin worden voorzien door nabij het uiteinde van de katheter één of meerdere ballonnetjes te monteren, dat of die in geheel of tendele opgeblazen toestand het kathetereinde op de
 15 gewenste positie in het desbetreffende bloedvat houdt of houden.

Bij een uitvoeringsvorm van de inrichting volgens de uitvinding kan op geschikte wijze de katheter nabij het uiteinde zijn voorzien van een aantal vast opgestelde
 20 transducenten, die ieder een andere positie ten opzichte van de as innemen, terwijl de inrichting voorts is voorzien van elektronische schakelmiddelen om de transducenten hetzij afzonderlijk of in subgroepen beurtelings en afwisselend te bekrachtigen. Bij deze uitvoeringsvorm worden de echo-ele-
 25 menten door geschikt elektronisch schakelen derhalve zodanig gebruikt dat de geluidsbundel een doorsnedebeeld van het betrokken bloedvat oplevert. Afhankelijk van de opstelling van de transducenten kan dit doorsnedebeeld loodrecht op de lengteas van het bloedvat staan, dan wel een konische
 30 doorsnede weergeven. Ook is het mogelijk bij deze uitvoeringsvorm een beperkt aantal transducenten toe te passen, zodat niet de volledige doorsnede wordt weergegeven, maar slechts in een beperkt aantal richtingen wordt gemeten, b.v. vier. Het is mogelijk daarmee reeds de buitenwand van een arterie
 35 en derhalve ook een eventuele obstructie te lokaliseren.

Bij een andere, geschikte uitvoeringsvorm van de

inrichting volgens de uitvinding is in het vast uitgevoerde uiteinde van de katheter een holte voorzien waarin een mechanisch roteerbaar of transleerbaar spiegeltje of echo-kristal (transducent) is opgesteld, terwijl de inrichting
5 is voorzien van middelen om het spiegeltje of echo-kristal in die holte te doen roteren of transleren.

Bij nog een andere geschikte uitvoeringsvorm van de inrichting volgens de uitvinding is de katheter voorzien van een roteerbaar uiteinde, welk uiteinde aan één zijde
10 is voorzien van een elektrode en aan een andere zijde van hetzij een spiegellend oppervlak, hetzij de transducent, terwijl de inrichting voorts is voorzien van middelen om het kathetereinde te doen roteren. Een voordeel van deze uitvoeringsvorm is dat de ultrasone bundel vrijwel dezelfde
15 doorsnede aftast die door vonkerosie vanaf de elektrode in een volgende fase therapeutisch kan worden behandeld. Doordat slechts één elektrode wordt toegepast is deze uitvoeringsvorm betrekkelijk eenvoudig. Het aandrijven van het roteerbare uiteinde van de katheter kan geschieden door
20 middel van een flexibele aandrijfdraad, die door de katheter is gevoerd en buiten de katheter op geschikte wijze wordt geroteerd. Het is evenwel ook mogelijk in een lokale aandrijving van het kathetereinde te voorzien, b.v. door middel van een in te spuiten vloeistof en schoepen of sleuven
25 aan of in het te roteren onderdeel.

Bij toepassing van spiegels of spiegelende oppervlakken in de inrichting volgens de uitvinding kunnen deze zodanig zijn gevormd dat daardoor gereflecteerde, van een transducent afkomstige straling, wordt gefocusseerd. Een
30 enigszins hol oppervlak kan daarvoor b.v. dienstig zijn. Het voordeel van de toepassing van spiegels is overigens dat daardoor de aanvangstbaan van de stralingsbundel wordt verlengd. Hierdoor worden zgn. transienteffecten onderdrukt zodat men in feite dichterbij het katheteroppervlak kan
35 meten.

Op geschikte wijze kan in de inrichting volgens

de uitvinding de katheter zijn voorzien van een lumen voor het daardoorheen leiden van een voerdraad voor het geleiden van de katheter naar een obstructie. Daarbij kan een dergelijke voerdraad reeds in de arterie zijn opgesteld en de
 5 katheter als het ware over de opgestelde voerdraad worden geschoven. Voorts kan de katheter van de inrichting volgens de uitvinding nabij het uiteinde zijn voorzien van één of meer ballonnetjes, terwijl de inrichting is voorzien van middelen om het of de ballonnetje(s) geheel of gedeelte-
 10 lijk op te blazen na aanbrengen van de katheter in een bloedvat, teneinde het kathetereinde daarin te positioneren.

In het kathetereinde kan desgewenst een asymmetrie zijn ingebouwd, zodat het bij het "kijken" met behulp van de hoogfrequente ultrasonore straling duidelijk is, waar
 15 men zich ten opzichte van de katheter bevindt. De katheter kan voorts nog zijn voorzien van op zichzelf bekende middelen om een vloeistof door de katheter te leiden voor het desgewenst schoon spoelen van een te onderzoeken bloedvat. Veelal is het ook gewenst de ruimte waarin de transducenten zich
 20 bevinden te spoelen, aangezien anders de doorgang van de hoogfrequente straling niet goed mogelijk is.

De uitvinding wordt toegelicht aan de hand van de tekening, waarin:

fig. 1 een weergave in doorsnede is door het uiteinde
 25 van de katheter van een uitvoeringsvorm van de inrichting volgens de uitvinding;

fig. 2 een doorsnede weergeeft langs de lijn II-II in fig. 1; en

fig. 3 een weergave in doorsnede is door het uiteinde
 30 van de katheter van een andere uitvoeringsvorm van de inrichting volgens de uitvinding.

In fig. 1 is in doorsnede het uiteinde weergegeven van de katheter van een uitvoeringsvorm van de inrichting volgens de uitvinding. De katheter omvat in wezen een dunne
 35 flexibele buis 1, b.v. van kunststofmateriaal. De diameter van de buis 1 bedraagt b.v. 0,8-2 mm in het geval de inrich-

ting bedoeld is voor het behandelen van coronairvaten. Voor beenvaten kan de diameter groter zijn. Hetzelfde geldt voor urologische toepassing.

Het uiteinde van de katheter wordt gevormd door
5 een afgerond cilindrisch lichaam 2 van b.v. een keramisch isolerend materiaal. In het lichaam 2 zijn aan het oppervlak een viertal elektroden 3, 4, 5 en 6 ingebed. Het oppervlak van het lichaam 2 met de daarin opgestelde elektroden kan van groeven zijn voorzien. De elektroden 3 t/m 6 zijn van
10 elkaar gescheiden en zijn symmetrisch langs de omtrek van het lichaam 2 opgesteld. Ieder van de elektroden 3 t/m 6 is verbonden met een van een isolerende mantel voorziene geleidende draad. Weergegeven is de draad 7, die door middel van b.v. de soldeermassa 8 is verbonden met de elektrode
15 3. Evenzo is de elektrode 5 door middel van de soldeermassa 9 verbonden met de draad 10. De draden 7 en 10 bestaan b.v. uit koper of een ander geschikt geleidend materiaal.

Het uiteinde van de flexibele buis 1 van de katheter is afgedicht door middel van een kunststofschiif 11. De
20 draden, die van de elektroden 3 t/m 6 door de katheter zijn gevoerd om buiten de katheter met een niet weergegeven vonkgenerator te worden verbonden, zijn ter plaatse van het lichaam 2 en de schiif 11 daarin ingebed. Door die draden, o.m. 7 en 10, die schiif 11 en dat lichaam 2 wordt
25 als het ware een kooi 12 gevormd. In de kooi 12 is een afgeschuind cilindrisch lichaam 13 roteerbaar om zijn as opgesteld. Het afgeschuinde vlak 14 van de cilinder 13 is een spiegelvlak. Het lichaam 13 kan b.v. van roestvrij staal zijn en het vlak 14 kan tot spiegelvlak zijn gepolijst.
30 Het is uiteraard mogelijk dat een afzonderlijke vlakke spiegel op het afgeschuinde vlak 14 van de cilinder 13 is bevestigd. Desgewenst kan het spiegelvlak 14 een van de vlakke vorm afwijkende vorm hebben, b.v. enigszins hol zijn, zodat de spiegel 14 focusserend werkt. De cilinder
35 13 is bevestigd op een flexibele aandrijfdraad 15. De draad 15 is door de schiif 11 gevoerd en leidt door de katheter

naar buiten, alwaar hij op een geschikt aandrijforgaan kan zijn aangesloten om de draad 15 en derhalve de cilinder 13 te roteren. In de schijf 11 zijn één of meer kanalen 33 voorzien voor het in bedrijf door de katheter naar de kooi 12 leiden van een spoelvroestof. In plaats van kanalen kunnen ook langsgroeven in het oppervlak van de schijf 11 zijn voorzien.

In het afgeronde lichaam 2 is aan de naar de kooi 12 toegewende zijde een holte 16 voorzien. De holte 16 wordt afgesloten door een vlak echokristal 17 dat wordt ondersteund op geschikt gevormde schouders 18 aan de voorzijde van de holte 16. Het echokristal 17 is b.v. een plaatje van piezo-elektrisch keramisch materiaal. Het kan ook bestaan uit een folie van piezo-elektrisch materiaal, aangebracht op een geschikte drager. Het echokristal 17 is verbonden met een tweetal elektrische leidingen 19 en 20, die langs de draden 7, resp. 10 zijn geleid en eveneens door de katheter naar buiten voeren voor aansluiting op daarvoor geschikte, bekende middelen om het echokristal te bekrachtigen en door het kristal opgevangen echo's te signaleren en in beelden om te zetten.

In bedrijf wordt door het kristal 17 uitgezonden hoogfrequente ultrasonore straling gericht op de spiegel 14 en vandaar gereflecteerd naar buiten de kooi 12. Uit de opgevangen echo's wordt een beeld gecreëerd van de omgeving en van vlak voor het kathetereinde, mede doordat de spiegel 14 tijdens het uitzenden en ontvangen wordt geroteerd. Aldus kunnen obstructies in een bloedvat, waarin het kathetereinde is opgesteld worden gelokaliseerd. Door selectief bekrachtigen van één van de elektroden 3 t/m 6, in afhankelijkheid van de waargenomen plaats van de obstructie, kan op aldus asymmetrisch stuurbare wijze vonkerosie worden toegepast.

In fig. 3 is een doorsnede weergegeven door het uiteinde van een katheter van een andere uitvoeringsvorm van de inrichting volgens de uitvinding. Bij deze uitvoerings-

vorm is de katheterbuis 21 aan de voorzijde afgedicht door een schijfvormig of propvormig lichaam 22. Op het van de buis 21 afgewende voorvlak van de schijf of prop 22 is een echokristal 23 bevestigd. Aan het kristal 23 zijn elek-
5 trisch geleidende draden 24 en 25 bevestigd, die door de schijf of prop 22 zijn gevoerd en via de katheterbuis 21 naar buiten leiden. Op de schijf of prop 22 is een afgerond cilindrisch lichaam 26 roteerbaar opgesteld. Het lichaam 26 bestaat b.v. uit een geschikt keramisch isolerend materiaal.
10 Aan de van de schijf 22 afgewende zijde is een excentrisch ten opzichte van de as gelegen deel van het lichaam 26 uitgevoerd als een in het keramisch isolerende materiaal ingebedde elektrode 27. De elektrode 27 is verbonden met de langs de as van het lichaam 26 en door het keramische
15 materiaal gevoerde geleiderdraad 28. De geleiderdraad 28 is, van een isolerende mantel voorzien, voorts gevoerd door het kristal 23, de schijf 22 en de katheterbuis 21 en dient behalve voor voeding van de vonkerosie-elektrode 27 ook als aandrijfdraad voor het roteren van het lichaam
20 26.

Aan de naar de prop of schijf 22 toegewende zijde is het lichaam 26 voorzien van een inkeping 29. Het de inkeping 29 begrenzende schuine vlak 30 van het lichaam 26 is uitgevoerd als spiegelvlak. Dit kan b.v. zijn geschied
25 doordat een spiegelende bekleding op het vlak 30 is aangebracht. In de prop of schijf 22 is ten minste een kanaal 34 voorzien voor het in bedrijf door de katheter naar de ruimte van de inkeping 29 leiden van een spoelvloeistof.

In bedrijf wordt door het echokristal 23 uitgezonden
30 ultrasonore straling tegen het spiegelvlak 30 gereflecteerd en tegen de bloedvatwand buiten de kathetertip gericht. Opgevangen echo's worden op bekende wijze verwerkt. Door roteren van het lichaam 26 kan een doorsnedebeeld van het bloedvat worden verkregen. Aanwezige obstructies kunnen
35 door via de elektrode 27 toegepaste vonkerosie worden verwijderd.

Bij de in fig. 3 weergegeven uitvoeringsvorm van de inrichting volgens de uitvinding is nog voorzien in middelen om de positie van de inkeping 29 en derhalve de richting van de tegen het spiegelvlak 30 gerichte en daardoor afgebogen straling van de transducent 23 vast te stellen. Deze middelen omvatten een gecodeerd schijfje 31, dat op de aandrijfdraad 28 is bevestigd en met de draad 28 mee roteert. In de katheterbuis 21 is voorts een glasvezel 32 vast opgesteld, via welke het codeschijfje 31 kan worden waargenomen. Door waar te nemen welk deel van het schijf 31 zich voor het uiteinde van de vezel 32 bevindt is de met dit deel corresponderende stand van de inkeping 29 voor de waarnemer bekend. Andere wijzen van plaatsdetectie zijn uiteraard ook mogelijk.

15 Aan de hand van de figuren zijn slechts twee uitvoeringsvormen van de inrichting volgens de uitvinding toegelicht. Het zal duidelijk zijn dat vele varianten mogelijk zijn.

CONCLUSIES

1. Intra-arteriële inrichting voor het door middel van vonkerosie verwijderen van obstructies in bloedvaten, omvattende een katheter die aan of nabij het uiteinde is voorzien van ten minste een elektrode, welke ten minste
5 ene elektrode via een door de katheter verlopende elektrische geleider koppelbaar is met een elektrische vonkgenerator, met het kenmerk, dat de inrichting is voorzien van middelen om de vonkerosie te besturen en desgewenst excentrisch
10 ten opzichte van de katheteras te doen plaatsvinden, alsmede van met het uiteinde van de katheter gekoppelde detectiemid-
delen voor het vaststellen van de plaats en eventueel aard van een te behandelen obstructie.
2. Inrichting volgens conclusie 1, met het kenmerk, dat de detectiemiddelen een transducent voor het uitzenden
15 van en opvangen van echo's van hoogfrequente ultrasone trillingen omvatten.
3. Inrichting volgens conclusie 2, met het kenmerk, dat de transducent is ingericht voor het uitzenden van
ultrasone trillingen met een frequentie van meer dan 15 MHz.
- 20 4. Inrichting volgens conclusies 2-3, met het kenmerk, dat de katheter nabij het uiteinde is voorzien van een aantal vast opgestelde transducenten, die ieder een andere positie ten opzichte van de as innemen, terwijl de inrichting
voorts is voorzien van elektronische schakelmiddelen om
25 de transducenten hetzij afzonderlijk of in sub-groepen beurtelings en afwisselend te bekrachtigen.
5. Inrichting volgens conclusies 2-3, met het kenmerk, dat in het vast uitgevoerde uiteinde van de katheter een
holte is voorzien waarin een mechanisch roteerbaar of trans-
30 leerbaar spiegeltje of echokristal (transducent) is opgesteld, terwijl de inrichting is voorzien van middelen om het spiegeltje of echokristal in die holte te doen roteren of transleren.
6. Inrichting volgens conclusies 2-3, met het kenmerk, dat de katheter is voorzien van een roteerbaar uiteinde,

welk uiteinde aan een zijde is voorzien van een elektrode en aan een andere zijde van hetzij een spiegelen oppervlak, hetzij de transducent, terwijl de inrichting voorts is voorzien van middelen om het kathetereinde te doen roteren.

- 5 7. Inrichting volgens conclusies 5-6, uitgevoerd met een spiegel of spiegelen oppervlak, met het kenmerk, dat de spiegel of het spiegelen oppervlak zodanig is gevormd dat daardoor gereflecteerde, van een transducent afkomstige straling wordt gefocusseerd.
- 10 8. Inrichting volgens conclusies 1-7, met het kenmerk, dat de katheter van een lumen is voorzien voor het daar doorheen leiden van een voerdraad voor het geleiden van de katheter naar een obstructie.
9. Inrichting volgens conclusies 1-8, met het kenmerk,
- 15 dat de katheter nabij het uiteinde is voorzien van één of meer ballonnetjes en de inrichting is voorzien van middelen om het of de ballonnetje(s) geheel of gedeeltelijk op te blazen na aanbrenge van de katheter in een bloedvat, teneinde het kathetereinde daarin te positioneren.

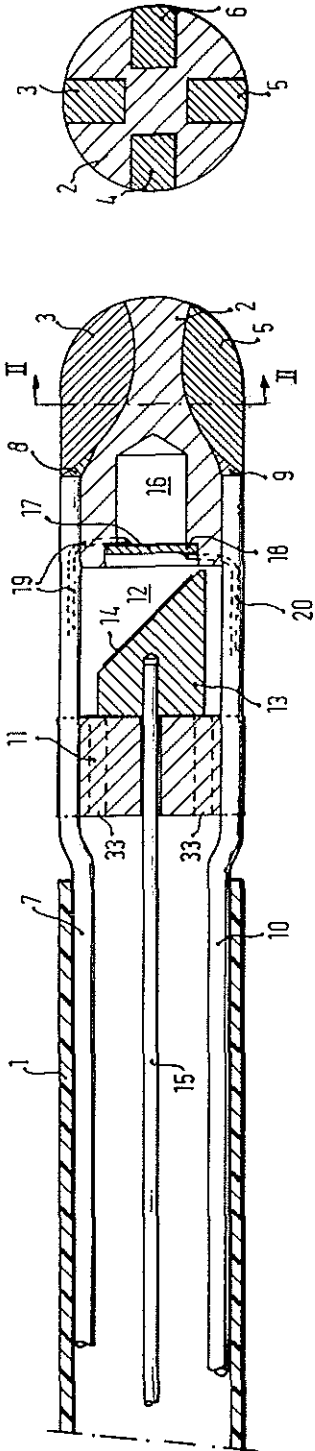


FIG. 1

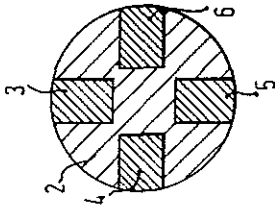


FIG. 2

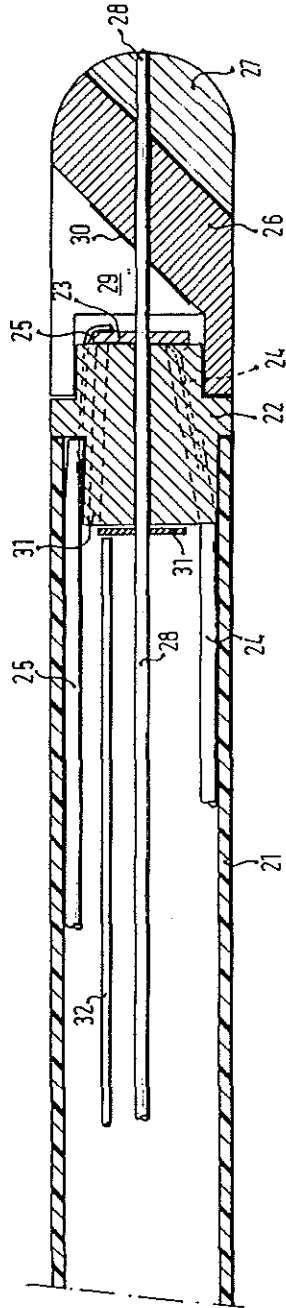


FIG. 3

**SUMMARY
DISCUSSION AND
CONCLUSIONS**

SUMMARY, DISCUSSION AND CONCLUSIONS

Since early times the application of heat in medicine has been widely practiced. Particularly, to achieve hemostasis, cauterization by a heated instrument was already applied in the ancient Egyptian culture as described approximately 1900 BC. This application remained much the same until the (re)discovery of electricity in the 18th century. One believed this to be another form of ordinary fire and electric shocks and sparks were applied for many medical treatments. However, whether the described methods have been effective may be really doubted. At the end of the 19th century electricity became of real importance in medicine after the invention of current generators which allowed electrical heating of cauterization instruments. Progress in this area really accelerated when high frequency alternating current could be generated. Passage of such current through body tissues appeared to be non stimulating. This discovery opened the wide field of radiofrequency electrosurgery at the beginning of the 20th century. At present the technique of electrosurgical cutting and coagulation has become a major working tool for all kinds of surgery including the modern minimal invasive procedures.

Since a few decades, powerful tissue heating and cutting can also be achieved by applying focused laser light. Laser energy can be easily transported to the application area through thin and flexible fiber optic systems. This raised the idea to vaporize arterial atherosclerotic obstructions by means of a laser catheter. The way of

approaching a lesion with a catheter in a minimal invasive, percutaneous, transluminal way had been paved by the previously introduced, and meanwhile widely practiced, method of balloon angioplasty. The vaporization approach, which was suggested to be easily performed by a laser catheter, triggered a variety of other technical developments all aimed to remove arterial obstructions in a transluminal way.

In chapter 2 is described that electrical spark erosion is also able to vaporize atherosclerotic plaques in an efficient way being competitive with earlier proposed laser techniques. Spark erosion is a modified radiofrequency electrosurgical cutting technique. New features are the low output impedance of the current generator and the application of a square wave radiofrequency signal at high voltage (peak to peak value 1200 V) during relatively short periods of several ms. This enables the use of the flat side of an active electrode for tissue cutting, while maintaining a minimal coagulation effect. This is quite different from the commonly used electrosurgical technique which purposely applies a flat electrode to avoid cutting and to achieve tissue coagulation. This new way of applying tissue removal by electrical sparks generated from flat electrodes resembles the direct current electric discharge machining (EDM) technique. EDM is widely applied in the machining industry for the production of intricate holes in metals. In Dutch this technique is referred to as "vonkerosie" which literally can be translated by "spark erosion".

When dissipating electric current of sufficiently high intensity at the electrode-tissue interface, this area becomes rapidly heated and, particularly at the electrode edge, water boiling temperature is reached within a few milliseconds. The rapidly expanding vapor bubbles clean up the interface between electrode and tissue from water, after which the sparking process starts manifested by a local electrical breakdown of the vapor layer. Sparks should be considered as very tiny current conductors contacting the tissue at continuously varying microscopically small spots. On basis of calculations it is assumed that, at the spark target locations, dissipated energy density reaches such high values that within fractions of a microsecond the tissue water content is heated above boiling temperature. The deposited heat subsequently induces micro-explosions which blast cellular contents and supporting connective tissue structures out of the target zone. The accompanying rapid vapor expansion also takes away the heat from the target area and contributes to maintaining the vapor layer between electrode and tissue required for the sparking condition.

The first tests of radiofrequency spark erosion for tissue removal were performed *in vitro*. Six human atherosclerotic aortic specimens were obtained and immersed in a saline solution. Spark erosion was applied at 30 atherosclerotic lesions using a flat 1.5 mm diameter electrode. In general, the sparking electrode easily produced cavities by tissue vaporization and pulverization while gas bubbles were observed escaping from the target area. From light microscopic studies, we concluded that vaporization of fibromuscular, collagenous and lipid constituents of plaques could be achieved with minimal thermal side effects. Width of the thermally damaged zone varied from 40 up to 200 μm and was maximal in fatty plaques. Only in the thermally affected areas some raggedness of the edge was observed. Vaporization of calcified plaques was not possible. Width of the cavities slightly exceeded the diameter of the applied electrode by 0.1-0.2 mm.

On the average, tissue removal in the non calcified spots was 0.18 mm per 10 ms period, and was not different at various spots. This speed was similar to that which we had measured previously on normal porcine aorta.

The electrical safety of spark erosion application was tested in coronary arteries of anesthetized pigs. In seven pigs it was demonstrated that triggered delivery of the spark erosion pulse within a period of 300 ms after the R wave, did not produce any effect on heart rhythm or blood pressure. When triggering outside this time window ectopic beats were generally induced, indicating an electrical stimulation effect of the technique.

On the basis of these results, problems were defined which required further study before *in vivo* application of spark erosion in patients could be considered. These studies included areas of catheter guidance and steering techniques to prevent arterial perforation, the effect of gas bubbles on coronary embolization and tissue healing response.

An attractive idea to discriminate between normal and atherosclerotic tissue was to sense the electrical impedance with the contacting spark erosion electrodes and to use this parameter for the guidance of spark erosion (**chapter 3**). It was anticipated that both lipid and calcified plaque constituents would have a lower electrical conductance than normal wall tissue because of their lower ion contents.

Electrical impedance measurements were performed at 67 spots on 13 atherosclerotic human aortic specimens. Impedance was measured by a specially adapted single point-like electrode. Values were compared with a detailed description of histologic sections taken at the measurement spots.

The results indicated that at 17 atherosclerotic spots, which showed fatty and calcified components at the luminal surface, resistivity ranged from 200 ($n=2$) up to 1450 ohm-cm with a mean value of 550 ohm-cm. This deviates from the values measured at normal spots ($n=11$) which

ranged from 150 to 200 ohm-cm. However, at the majority of atherosclerotic spots ($n=39$), a fibrous cap covered the atherosclerotic lesion. At these locations the resistivity ranged from 100 to 450 ohm-cm. These values clearly overlap the range found at normal spots.

Physical modeling of the layered structure of the atherosclerotic plaques explained the measurement results and allowed a better understanding of the measurement set-up. It was concluded that, despite the confirmation of the high ohmic properties of the calcified or lipid plaque deposits, the detection of atherosclerotic lesions by impedance measurement would raise too many technical difficulties. Indeed there is an inherent risk of detecting high resistivity spots at normal endoluminal locations because of fat tissue covering the adventitia. Only if the fibrous cap, which normally covers the lesion, is very thin or absent, lesion detection with relatively simple means might be possible.

Rather than extending our investigations towards more complex remote impedance measuring techniques, we decided to focus on the development of intravascular ultrasound as a guidance technique. This approach is described in **chapter 4**. The idea to apply a single, small rotating ultrasound transducer or an ultrasound beam reflecting mirror in front of such a transducer, enabled the design of catheters with dimensions allowing intravascular application to visualize the arterial wall and atherosclerotic plaque (see also the **Appendix**).

The quality of the first cross-sectional images obtained from coronary arteries by rotation of a single 1 mm diameter transducer was highly encouraging. Good quality images could also be obtained with a 2 mm diameter prototype catheter which combined ultrasound imaging with directional spark erosion. Selectively directed application of spark erosion could be achieved by activating at choice one of three tip electrodes. From our initial results we concluded that intravascular ultrasound (IVUS) imaging, being a spin off from our search for guiding techniques, could become an important method in itself. Therefore the re-

search on IVUS was pursued separately to develop this imaging modality into a stand alone technique. During this development period, problems of the spark erosion plaque ablation technique were further studied.

In **chapter 5** a first study is described on heart function of pigs after selective injection of small bubbles of air in a coronary artery. One of the primary concerns of plaque ablation by spark erosion in the arteries was the potential embolization of the distal vascular bed by persistent gas bubbles. Previously obtained chemical measurements had shown that the gas, resulting from spark erosion application, partly consisted of a variety of hydrocarbons which may easily go into solution. Another major constituent, however, was nitrogen which does not dissolve that fast.

Air bubbles with diameters of respectively 75, 150 or 300 μm were selectively injected during subsequent experimental tests in the left anterior descending coronary artery of anesthetized pigs (28 ± 3 kg, $n = 7$). Total amount of air injected for each test was 2 μl per kg body weight.

After injection, left ventricular blood pressure and the peak positive derivative did not change. The peak negative derivative showed a minor transient depression. In particular, measurement of regional myocardial shortening showed a statistically significant peak depression two minutes after air bubble injection. For the different bubble sizes, the depression of myocardial function was respectively 27, 45 and 58 %. These differences were statistically significant. Bubble size appeared to be an important factor. Recovery of function was completed after 10 minutes.

Considering the recovery time and the results of dose determining pilot experiments, we concluded that the dose being injected for the largest bubbles was close to a critical level to be tolerated by the myocardium. From this study we also learned that regional myocardial functional depression after injection of air bubbles could easily pass unnoticed on the basis of global hemodynamic measurements alone.

In **chapter 6** the healing response to spark erosion application is described in a series of forty nine normal rabbits. From our point of view one of the primary questions to be answered was whether, besides the application of local heat by spark erosion, the additional passage of intense currents would lead to a healing response different from that observed with other techniques.

In this study lesions were produced in the iliac arteries by spark erosion and by a metal laser probe. At the distal aorta bifurcation a Nd-YAG laser sapphire contact probe was applied. High energy doses were applied to induce substantial damage to the vessel wall, but not exceeding a level that would lead to perforation. Thermal lesions ($n = 77$) were also compared with mechanical lesions ($n = 22$) induced in the iliac arteries by oversized balloon dilation.

With a spark erosion electrode, especially designed to minimize the risk of perforation, 41 lesions were produced. Only two lesions showed a perforation on the contrast angiogram made after the procedure. The metal laser probe appeared less easy to apply and by this method 15 lesions were produced of which 3 showed macroscopic perforation on the contrast angiogram.

At follow up after healing, only two of the three vessels perforated by the metal laser probe, appeared to be occluded. All other vessels were patent. Histologic examination of healing as judged from intimal proliferation did not show differences between the different injuries, whether thermal or mechanical.

Compared to the initial *in vitro* findings, the zone of thermal coagulation produced by spark erosion generally extended up to 200 μm from the ablation site. This may be explained by a number of different physical factors. Electrode shape was rounded to prevent perforation, but this delayed the start of sparking and extended the period of heat accumulation. Environmental temperature of the spark erosion process was different. Furthermore, latent heat damage may be observed only when subsequent tissue necro-

sis has become fully expressed. Another finding, although not unexpected, was the neuromuscular stimulation associated with each spark erosion pulse. Insertion of additional direct current and low frequency blocking filters in the generator - electrodes chain could reduce but not completely eliminate this side effect.

Neuromuscular stimulation limits the application of spark erosion in peripheral vessels, not only from the point of view of discomfort, but also because the provoked motion may cause recurrent catheter dislocation or even mechanical perforation. Although cardiac application may take advantage from R-wave triggering, this method puts some restriction on the achievable speed of ablation and there always remains some risk from false triggering.

In **chapter 7** is described how we detected, much sought after but not yet observed, rather intense very low frequency and direct currents around the active electrode, which were generated during spark erosion radiofrequency cutting. Several investigators had been studying this problem before and suspected the non linear behavior of the sparking process to be the source of generating low frequency currents. These investigators had focused their studies on the chain of generator, electrodes and tissue, in which indeed some low frequency current can be detected during tissue cutting. However, the measurable intensity of these currents, especially after adding appropriate filters and raising the generator frequency, is insufficient to explain the intensity of the still remaining stimulation.

In our study we used an active electrode consisting of two equally sized and closely joined parts. The parts were electrically connected and as a couple they behaved as a single cutting electrode. However, low frequency current measurement could be performed between the different parts. This set-up enabled to detect low frequency and direct currents around the cutting electrode at a much higher level than observed before, reaching tens of milli amperes.

From the experiments we learned that the direct currents indeed originate from the non linear behavior of the ionization channels created during sparking. These channels partly behave as current rectifiers. Theoretically, for a single ionization channel, back and forward current might be easily kept in balance by a direct current blocking series capacitor. However, considering the whole area of an electrode, it should be realized that active sparking sites may be paralleled by galvanic conducting sites elsewhere. Therefore a single series blocking capacitor will not neutralize local current imbalances. Because of this very local process, minimization of these stimulation currents can be achieved by new electrode designs rather than by changing generator specifications.

The new insights in the process of spark erosion and related fields were translated into the design of a new prototype catheter which also incorporated the meanwhile developed technique of intravascular ultrasound imaging. In **chapter 8** calculations show why the rotating tip of this catheter, which contains a single active electrode, must be parabolically shaped. Directional plaque ablation was to be achieved by segmental electrode activation (see **Appendix**). Rotational spark erosion is an attractive method, which, with the current prototype catheter, enables to restore luminal dimension up to a value of 2.6 mm diameter, while using a small electrode with an area of less than 1 mm².

The reduction of the electrode size allowed application of lower voltages, i.e. 800 V peak to peak value, while tissue vaporization by sparking could be maintained without an increase of thermal damage. Lowering the voltage for larger types of electrodes extends the warming-up phase which precedes the sparking phase and leads to an increase in thermal damage.

In vitro tests on human atherosclerotic aorta specimens showed an average ablation speed of 0.16 mm per 80 ms active sparking time of the electrode, a period which corresponded to one

tip revolution. Light microscopic inspection of histologic sections showed a 50 µm wide zone of discoloration as a result of thermal damage.

The applied settings greatly reduced the size of produced gas bubbles from diameters in the range of 1 mm to diameters of less than 200 µm.

Another important improvement allowed by the rotating design, was that the largest part of the tip area could be used to function as a return electrode. This was expected to reduce neuromuscular stimulation. In sparking experiments in the femoral arteries of anesthetized pigs it was demonstrated that indeed neuromuscular stimulation by this new catheter design was almost absent.

In vitro, two obstructed specimens of human coronary arteries, were used to test restoration to normal luminal dimensions by the prototype catheter. The incorporated intravascular ultrasound imaging technique was used to guide the selection of the segment to be ablated by spark erosion.

Histologic examination of the recanalized areas showed plaque dissection and perforation in one of the arteries. The other procedure was successful. Similar to previous studies, ablation of calcified regions could not be demonstrated.

These first experiments of applying rotating spark erosion under ultrasound guidance showed that the method is technically feasible and significantly reduced neuromuscular stimulation and gas production. However, some problems require further study, among them the role of torsional forces on plaque dissection and the technical difficulty how to realize an appropriate flexible drive shaft for the rotating tip.

Another interesting spin-off of studying spark erosion plaque ablation is described in **chapter 9**. The technically demanding operation of removing muscular and fibrous tissue from the narrowed left ventricular outflow tract in patients, suffering from hypertrophic obstructive cardiomyopathy, could be greatly facilitated by applying spark erosion.

A special, partly insulated, cutting electrode was designed, which, combined with a pulsed mode of high voltage radiofrequency energy application, allowed to perform the myectomy safely and effectively. Cutting speed was limited to approximately 2 mm/s, while thermal coagulation could be kept at a minimal level. Depth of the cut was precisely controlled by the electrode design.

Histologic study of the excised tissue specimens by light microscopy showed depth of complete cell destruction to be limited to two or three cell layers.

Application of the new method in a series of 18 patients generally showed no peri-operative complications. Only one patient suffered an atrioventricular conduction block requiring a permanent pacemaker implantation. No septal defects were caused by the procedure. Post operatively no complications related to the procedure have been noticed.

In the **Appendix** the original Dutch patent application for an arterial recanalization device is given which describes several ways for combining intra-arterial directional plaque ablation by spark erosion under guidance of intravascular ultrasound.

CONCLUSIONS

Electrical spark erosion is able to vaporize electrically conductive atherosclerotic lesions without causing significant thermal damage to bordering tissue. Similar to other methods, the technique does not discriminate between normal and diseased tissue.

The *in vivo* intravascular application of spark erosion should be restricted to targets to be selected. In principle this selection can be achieved by the use of existing catheter technology, but further study in this area is warranted.

Guidance for selection of plaques can be obtained by integration of spark erosion with intravascular ultrasound imaging.

Further requirements for *in vivo* intravascular application include careful electrode design and appropriate choice of electrical parameters to avoid problems caused by gas bubble formation and neuromuscular stimulation.

Healing after spark erosion in rabbit iliac arteries was uneventful and was not different from that observed with other thermal or mechanical techniques.

Application of spark erosion myectomy during open heart surgery has shown to greatly facilitate the surgical treatment of patients with hypertrophic obstructive cardiomyopathy.

**SAMENVATTING
DISCUSSIE EN
CONCLUSIES**

SAMENVATTING, DISCUSSIE EN CONCLUSIES

Het gebruik van warmte in de praktijk van de geneeskunde dateert al van zeer lang geleden. Het stelpen van bloedingen door het dichtschroeien van wonden met een verhit instrument werd al toegepast in de oude Egyptische cultuur zoals werd beschreven ca. 1900 voor Christus. Aan deze toepassing veranderde weinig totdat in de 18^e eeuw na Christus elektriciteit (opnieuw) werd ontdekt. Men dacht dat dit een speciale vorm van gewoon vuur was en paste het toe in de vorm van elektrische schokken en vonken voor allerlei medische behandelingen. Maar of de beschreven methoden ook effectief waren mag met recht worden betwijfeld. Op het einde van de 19^e eeuw werd elektriciteit echt van belang in de geneeskunde toen er stroomgeneratoren waren uitgevonden die het elektrisch verhitten van instrumenten, bedoeld voor het dichtschroeien van wonden mogelijk maakten. De vooruitgang op dit gebied ging nog veel sneller toen er wisselstromen van hoge frequentie konden worden opgewekt. Het bleek dat dergelijke stromen door de lichaamsweefsels konden worden gevoerd zonder dat dit gepaard ging met elektrische stimulatie. Deze ontdekking opende het brede gebied van de radiofrequente elektrochirurgie in het begin van de 20^e eeuw. Op dit moment is de techniek van elektrochirurgisch snijden en coaguleren het belangrijkste gereedschap geworden voor alle soorten van chirurgie inclusief de moderne minimaal invasieve procedures.

Sinds enkele tientallen jaren is het ook mogelijk om op een effectieve manier weefsel te snijden en te verhitten met gefocuseerd laserlicht. Laserenergie kan gemakkelijk worden ge-

transporteerd naar het toepassingsgebied via dunne en flexibele glasvezels. Deze mogelijkheid deed het idee ontstaan om atherosclerotische obstructies in bloedvaten met een lasercatheter te gaan verdampen. De eenvoudige, weinig invasieve weg om met een catheter een bloedvatobstructie te benaderen door de huid en via de bloedbaan was al geëffend door de eerder geïntroduceerde en intussen alom toegepaste methode van het oprekken van de obstructie door het opblazen van een ballon. Het idee om obstructies te verdampen, waarvan werd gesuggereerd dat dit met een lasercatheter gemakkelijk gedaan zou kunnen worden, bracht een grote verscheidenheid aan andere technische ontwikkelingen op gang die allen waren gericht op het verwijderen van obstructies via de bloedbaan.

In hoofdstuk 2 wordt beschreven dat ook met elektrische vonkersie atherosclerotische plaques op een efficiënte manier, vergelijkbaar met de laser, verdampt kunnen worden. Vonkersie is een aangepaste vorm van de radiofrequente elektrochirurgische snijtechniek. Nieuw toegevoegde eigenschappen zijn de lage uitgangsimpedantie van de elektrische wisselstroomgenerator en het toepassen van een blokvormige wisselspanning met hoge amplitude (top top waarde 1200 V) gedurende relatief korte periodes van enkele milliseconden. Hierdoor is het mogelijk de vlakke zijde van een actieve elektrode te gebruiken voor snijden, terwijl toch het eiwitstollende (coagulatie) effect minimaal blijft. Dit is sterk afwijkend van de gebruikelijke elektrochirurgische praktijk waar juist met opzet de vlak-

ke zijde van een elektrode wordt gebruikt om snijden te vermijden en coagulatie van weefsel te verkrijgen. Deze nieuwe manier om weefsel te verwijderen met elektrische vonkjes, die opgewekt worden vanaf vlakke elektrodes, lijkt op de gelijkstroom vonkerosie metaalbewerkingstechniek die ook elektrische ontladingen gebruikt. Met deze techniek kunnen allerlei ingewikkeld gevormde gaatjes in metalen worden gemaakt. Spark erosion is de letterlijke vertaling van vonkerosie naar het Engels terwijl in deze taal de techniek EDM (electric discharge machining) wordt genoemd.

Wanneer een elektrische stroom van voldoende sterkte door het grensgebied van elektrode en weefsel loopt, wordt dit snel verhit en zal, vooral op de rand van de elektrode, de kooktemperatuur van water binnen enkele *milliseconden* bereikt worden. De daarbij snel expanderende dampbellen verwijderen het resterende water tussen elektrode en weefsel, waarna het vonkproces start dat gekenmerkt wordt door lokale elektrische doorslag van de damplaaag. Vonken moeten beschouwd worden als zeer fijne stroomgeleidende kanaaltjes die contact maken met het weefsel op steeds van positie wisselende, microscopisch kleine, vlakjes. Op basis van berekeningen wordt aangenomen dat op de trefvlakjes van de vonken, de dichtheid van de gedissipeerde energie zulke hoge waarden bereikt dat binnen een fractie van een *microseconde* de temperatuur van het door weefsel bevatte water ver boven het kookpunt kan komen. De warmte die daarbij wordt achtergelaten zal dan micro-explosies opwekken die de inhoud van de cellen en de verbindende weefselstructuren uit het getroffen gebied verwijderen. De daarmee gepaard gaande snelle uitzetting van de dampbellen voert ook de warmte uit het doelgebied weg en draagt bij aan het handhaven van een damplaaag tussen elektrode en weefsel die vereist is voor het handhaven van de conditie die nodig is voor vonkopwekking.

De eerste testen van radiofrequente vonkerosie voor het verwijderen van weefsel werden *in vitro* uitgevoerd. Er werden zes humane atherosclerotische aorta specimens verkregen die in een fysiologische zoutoplossing werden ondergedompeld. Vonkerosie werd toegepast met een vlakke elektrode (diameter 1.5 mm) op 30 atherosclerotische laesies. In het algemeen maakte de vonkelektrode gemakkelijk gaatjes door weefselverdamming en -verpulvering waarbij gasbellen werden waargenomen die uit het doelgebied van de atherosclerotische plaque ontsnapten. Uit studies met lichtmicroscopie concludeerden we dat het verdampen van fibromusculaire, collagene en vette bestanddelen van plaques mogelijk was terwijl thermische neveneffecten in het achterblijvende randgebied minimaal waren. De breedte van de thermisch beschadigde randzone varieerde van 40 tot 200 μm en was het breedst in de vette plaques. Alleen in de thermisch beschadigde zones werd wat rafeligheid van de rand waargenomen. Het verdampen van verkalkte plaques was niet mogelijk. De diameter van de gaatjes was iets meer dan die van de toegepaste elektrode nl. 0.1 - 0.2 mm extra. Op de niet verkalkte plaatsen werd gemiddeld 0.18 mm weefsel verwijderd per periode van 10 milliseconde. Deze snelheid van verwijderen van weefsel was gelijk voor de verschillende gebieden en kwam overeen met de al eerder bepaalde waarden op gezonde aorta van varkens.

De elektrische veiligheid van het toepassen van vonkerosie werd getest in de kransslagaderen van 7 varkens onder narcose. Er werd aangehouden dat het selectief toedienen van de vonkerosie puls binnen een periode van 300 milliseconde na de R-top van het electrocardiogram geen effect had op het hartritme of op de bloeddruk. Wanneer buiten dit tijdvenster werd gevinkt werden er in het algemeen abnormale hartslagen opgewekt, waarmee duidelijk tot uiting kwam dat de techniek een elektrisch stimulerend effect heeft.

Naar aanleiding van deze resultaten werden er problemen geformuleerd die verdergaande studie vereisten voordat er aan toepassing van vonkerosie in patiënten kon worden gedacht. Deze studies betroffen gebieden als het kunnen lokaliseren van de te bewerken laesie en het richten van de catheter om vaatwand perforatie te voorkomen, het effect van gasbellen op het blokkeren van de bloedstroom en wondgenezing.

Een aantrekkelijk idee om onderscheid te kunnen maken tussen normaal en atherosclerotisch weefsel was het meten van de elektrische impedantie met de aanliggende elektrode en deze grootte te gebruiken voor het besturen van de vonkerosie (hoofdstuk 3). Er werd verwacht dat zowel vette als verkalkte plaques een minder goede elektrische geleiding zouden hebben dan normale vaatwand vanwege hun lagere ionen concentratie.

Elektrische impedantiemetingen werden uitgevoerd op 67 lokaties van 13 atherosclerotische specimens van menselijke aorta. De impedantie werd gemeten met een enkele, speciaal aangepaste puntvormige elektrode. De waarden werden vergeleken met een gedetailleerde beschrijving van weefselsecties die genomen werden uit het gebied van de meetlokatie.

De resultaten gaven aan dat op 17 atherosclerotische lokaties, waarbij vette en verkalkte componenten op het lumen oppervlak aanwezig waren, de weerstand varieerde van 200 ($n = 2$) tot 1450 ohm-cm met een gemiddelde waarde van 550 ohm-cm. Dit is een belangrijke afwijking van de waarden die gemeten werden op normale vaatwandlokaties ($n = 11$) die varieerden van 150 tot 200 ohm-cm. Echter bij de meeste atherosclerotische lokaties ($n = 39$) bedekte een fibreuse kap de atherosclerotische laesie. Op deze lokaties varieerde de weerstand van 100 tot 450 ohm-cm. Deze waarden overlappen duidelijk het gebied van waarden die op de normale lokaties gevonden werden.

Door de gelaagde structuur van de atherosclerotische laesies fysisch te modelleren werd

een verklaring gevonden voor de meetresultaten en werd de manier van meten beter doorzien. Ook al was de hoge weerstand van de verkalkte en vette plaque bestanddelen duidelijk aangetoond, toch werd de conclusie getrokken dat de detectie van atherosclerotische laesies met een elektrische impedantie meetmethode te veel technische problemen zou opleveren. Zo ligt het voor de hand dat er een kans bestaat op het detecteren van gebieden met hoge weerstand op een normale vaatwand omdat het buiten het vat liggende adventitia weefsel door vet omgeven kan zijn. Alleen in het geval dat de fibreuse kap, die normaal gesproken een laesie bedekt, erg dun is, of niet aanwezig, zouden laesies met een relatief eenvoudige techniek gedetecteerd kunnen worden.

In plaats van ons onderzoek uit te breiden in de richting van meer complexe op afstand gevoelige impedantie meettechnieken, werd besloten het onderzoek te concentreren op het ontwikkelen van een intravasculaire ultrageluidskijktechniek om laesies te lokaliseren. Deze benadering is beschreven in hoofdstuk 4. Het idee om bijvoorbeeld een enkele kleine roterende ultrageluidstransducer te gebruiken, maakte het mogelijk catheters te maken die klein genoeg waren voor toepassing binnen de aderen om van daaruit de vaatwand en de atherosclerotische plaque te kunnen visualiseren. (zie ook Appendix)

De kwaliteit van de eerste beelden van kransslagaderen in dwarsdoorsnede, die gemaakt werden met een enkele transducer (diameter 1 mm), was zeer bemoedigend. Beelden met een goede opname kwaliteit konden ook verkregen worden met een prototype catheter met een diameter van 2 mm waarin de ultrageluidskijktechniek was gecombineerd met een vonkersietechiek die naar richting instelbaar was. Richtingsselectie werd verkregen door naar keuze een van de drie op een cathetertip in het rond aangebrachte elektrodes te activeren. Op grond van onze eerste resultaten concludeerden wij dat het intravasculair kijken met ultrageluid

(Engels: IVUS - intravascular ultrasound), wat een nevenresultaat was van ons zoeken naar een plaque lokalisatie techniek, een belangrijke methode op zichzelf zou kunnen worden. Om deze reden werd het verdere onderzoek naar het ontwikkelen van een op zichzelf staande intravasculaire ultrageluidskijktechniek apart voortgezet. Gedurende deze ontwikkelingen konden dan de problemen van het verwijderen van plaques met vonkerosie verder bestudeerd worden.

In hoofdstuk 5 wordt een eerste studie beschreven in biggen naar de functie van het hart nadat er kleine luchtbelletjes selectief in een kransslagader waren gespoten. Een van de eerst vermoede problemen van het toepassen van plaque verwijdering met vonkerosie of laser in de kransslagaderen was de mogelijke blokkade van de bloedstroom in het stroomafwaarts gelegen vaatbed door niet snel oplosbare gasbellen. Chemische bepalingen van het gas dat vrijkomt bij vonkerosie op plaques hadden al eerder uitgewezen dat een gedeelte hiervan uit een grote verscheidenheid van waarschijnlijk gemakkelijk oplosbare koolwaterstoffen bestaat. Echter een andere belangrijke component was stikstof uit de omgeving dat niet gemakkelijk in oplossing gaat.

Luchtballen met diameters van respectievelijk 75, 150 of 300 μm werden gedurende een aantal opvolgende testen selectief geïnjecteerd in de linker voorwandarterie van het hart van 7 onder narcose verkerende biggen (28 ± 3 kg). De totale hoeveelheid geïnjecteerde lucht voor iedere bellensoort was 2 μl per kg lichaamsgewicht.

Na de injectie was er geen verandering in de linkerhartkamerdruk en in de positieve eerste afgeleide hiervan. Alleen de piek van de negatieve eerste afgeleide liet een kleine snel voorbijgaande daling zien. Het waren vooral de metingen van de regionale hartspierverkorting die een statistisch significante afname lieten zien, twee minuten na de injectie. Voor de oplopende groottes van de ballen bedroeg de afname in regionale spierfunctie respectievelijk 27, 45 en 58 %. Deze ver-

schillen waren statistisch significant. Belgrootte bleek dus een belangrijke factor te zijn. Na 10 minuten was de functie volledig hersteld.

Kijkend naar de gevonden hersteltijd en ook naar de resultaten van eerdere dosis bepalende proefnemingen, concludeerden wij dat de geïnjecteerde hoeveelheid lucht dicht bij een kritisch niveau lag dat nog door het hartspierweefsel getolereerd kon worden. Uit deze studie leerden we ook dat de daling van de regionale hartspierfunctie gemakkelijk ongemerkt voorbij zou kunnen gaan wanneer alleen naar globale hemodynamische gegevens gekeken zou worden.

In hoofdstuk 6 wordt de genezingsresponsie beschreven na het toepassen van vonkerosie in een serie van 49 gezonde konijnen. Vanuit ons oogpunt bezien was de centrale vraag die beantwoord moest worden of de bij vonkerosie extra aangebrachte passage van intense elektrische stromen een ander genezingsverloop zou hebben dan dat wat gezien werd na het uitsluitend toepassen van hitte.

In deze studie werden beschadigingen aangebracht in de iliacale arterie met vonkerosie en met een door een laser verhitte metalen tip. Bij de aorta bifurcatie werd een Nd-Yag laserlicht geleidende saffiertip toegepast. Er werd gekozen voor het aanbrengen van een hoge dosis energie om een flinke vaatwandbeschadiging te verkrijgen maar niet zoveel dat er perforatie zou optreden. De thermisch aangebrachte beschadigingen ($n = 77$) werden ook vergeleken met mechanische beschadigingen ($n = 22$) van de iliacale arteriën die door het oplazen van een relatief grote ballon werden verkregen.

Met een vonkerosie elektrode, die speciaal was ontworpen om het risico op perforatie te minimaliseren, werden 41 laesies gemaakt. Slechts twee laesies toonden een geringe perforatie op het contrastangiogram dat direct na de ingreep werd gemaakt. De metalen, door de laser verhitte, tip bleek minder gemakkelijk te hanteren. Met deze methode werden 15 laesies gemaakt waarvan er 3 een perforatie lieten zien op de contrastangiografische opname.

Bij controle na genezing van de ingreep bleken alleen van de 3 door de hete metaaltip geperforeerde vaten er 2 voor de bloedstroom afgesloten te zijn. Voor de andere technieken trad geen vaatafsluiting op. Onderzoek van het soort en hoeveelheid nieuw aangegroeid weefsel op de binnenwand van de bloedvaten liet geen verschillen zien voor de thermisch of de mechanisch aangebrachte beschadigingen.

In vergelijking met onze eerdere in vitro bevindingen na toepassing van vonkerosie, reikte het gebied dat thermische coagulatie liet zien in het algemeen tot een afstand van 200 μm vanaf de rand van het verwijderde weefsel. Dit kan verklaard worden door enkele verschillen in fysische factoren. De elektrodevorm was wat ronder gekozen om perforatie te voorkomen, hierdoor wordt het starten van het vonkproces vertraagd en de periode van warmteaccumulatie verlengd. Verder is de omgevingstemperatuur van het vonkproces verschillend. Ook kan er een latente schade door hitte zijn aangebracht die pas gezien wordt als het daaropvolgende weefselversteringsproces volledig tot expressie is gekomen. Een andere, weliswaar niet onverwachte, waarneming bij de experimenten was de stimulatie van zenuwen en spieren die gepaard ging met iedere vonkerosiepuls. Het in de stroomkring opnemen van blokkerende filters voor gelijkstroom en lage frequenties verminderde dit effect maar kon het niet wegnemen.

Deze stimulatie van spieren en zenuwen beperkt de toepassingsmogelijkheid van vonkerosie in perifere vaten. Dit niet alleen vanwege de nare gewaarwording maar ook omdat de opgewekte beweging steeds de catheter uit positie kan sturen en additionele vaatwandschade kan aanbrengen. Zoals genoemd kan de toepassing in het hart met voordeel gebruik maken van de ongevoelige periode voor stimulatie vlak na de R-top uit het electrocardiogram, maar dit houdt wel een beperking in voor de maximaal te behalen snelheid van weefselverwijdering; ook is het niet denkbeeldig dat er enig risico bestaat dat toch een verkeerd moment gekozen wordt.

In hoofdstuk 7 wordt beschreven hoe wij niet eerder door anderen waargenomen, maar wel gezochte, intense stromen van zeer laagfrequent en gelijkstroom karakter konden detecteren rondom de actieve elektrode gedurende het snijden met radiofrequente elektrochirurgie. Verschillende onderzoekers hadden deze problematiek al eerder bestudeerd en daarbij het vermoeden uitgesproken dat het niet lineaire karakter van het vonkproces de bron was van het genereren van laagfrequente stromen. Deze onderzoekers hadden zich daarbij vooral gericht op de kring van generator, elektrodes en weefsel waarin inderdaad wat laagfrequente stromen gedetecteerd kunnen worden gedurende het snijden van weefsel. Echter de te meten sterkte van deze stromen, zeker nadat geschikte filters zijn aangebracht en de generator frequentie is verhoogd, is onvoldoende om de intensiteit van de dan nog steeds waar te nemen stimulatie te verklaren.

In onze studie gebruikten wij een actieve elektrode die uit twee nauw aaneensluitende gelijke delen bestond. Deze delen werden elektrisch doorverbonden en samen werkten ze als een enkele snijdende elektrode. Het was echter mogelijk om laagfrequente stroommetingen te verrichten tussen de afzonderlijke delen. Deze opzet maakte het mogelijk om stromen van laagfrequent en gelijkstroom karakter te detecteren rondom de actieve elektrode die op een aanzienlijk hoger niveau lagen dan ooit eerder was waargenomen. Er werden door ons waarden tot enkele tientallen milliampères gemeten.

Uit deze experimenten leerden wij dat de fysische oorzaak van de gelijkstromen inderdaad gelegen is in het niet lineaire karakter van de ionisatie kanalen die worden opgewekt gedurende het vonken. Deze kanalen gedragen zich gedeeltelijk als stroomgelijkrichters. In theorie kan, om stimulatie te voorkomen, voor een enkel ionisatiekanaal de balans van de heen en weer gaande stroom gemakkelijk in evenwicht worden gehouden door een gelijkstroomblokkerende seriecondensator in de kring op te nemen.

Maar hierbij moet bedacht worden dat verdeeld over het gehele oppervlak van de elektrode, galvanisch geleidende delen parallel kunnen staan aan vonkende delen. Daarom zal één enkele, gelijkstroom blokkerende, condensator het lokaal uit balans zijn van de stroom niet kunnen voorkomen. Vanwege dit zeer lokaal optredende proces, zal het verminderen van de stimulatiestromen eerder bereikt kunnen worden door nieuwe ontwerpen van elektrodes dan door het veranderen van de generator specificaties.

De nieuwe inzichten in het proces van vonkerosie en de aangrenzende gebieden werden vertaald in een nieuw ontwerp van een prototype catheter die ook de intussen verder ontwikkelde intravasculaire ultrageluidskijktechniek moest bevatten. In hoofdstuk 8 geven berekeningen aan waarom de roterende tip van deze catheter, die een enkele actieve elektrode bevat, parabolisch gevormd moet zijn. Het kiezen van de richting voor weefsel verwijdering zou verkregen moeten worden door de elektrode alleen over een bepaald segment te activeren (zie ook Appendix). Roterende vonkerosie is een aantrekkelijke methode die, met het voorgestelde prototype, herstel van het lumen mogelijk maakt tot een diameter van minimaal 2.6 mm (oppervlak 5.3 mm^2) terwijl toch een kleine elektrode kan worden gebruikt met een oppervlak van minder dan 1 mm^2 .

De reductie in de afmeting van de elektrode geeft de mogelijkheid om lagere spanningen te gebruiken nl. 800 V top-top, terwijl toch weefselverdamping door vonken kan worden gehandhaafd zonder dat de thermische schade toeneemt. Bij een grotere elektrode zou toepassing van lagere spanningen nl. leiden tot een te lang verkeren in de opwarmfase die aan de vonkfase vooraf gaat. Dit leidt dan tot een toename van de thermische schade in de randzone.

In vitro tests op specimens van menselijke aorta lieten een gemiddelde weghaalsnelheid van weefsel zien van 0.16 mm per 80 ms actieve vonktijd, een periode die overeenkwam met één omwenteling van de tip. Inspectie van het weef-

sel met lichtmicroscopie liet een randzone zien van 50 μm breed waarin verkleuring was opgetreden als gevolg van thermische schade.

Het gebruik van lagere spanningen leidde tot vorming van veel kleinere gasbellen dan voorheen. In plaats van ca. 1 mm werden nu gemiddeld diameters van ca. 200 μm waargenomen.

Een andere belangrijke verbetering die mogelijk was geworden, dankzij het roterende ontwerp, was dat nu het grootste deel van de tip gebruikt kon worden als retour elektrode voor de elektrische stroom. Hiervan werd verwacht dat dit de stimulatie door vonkerosie zou verminderen. In experimenten met vonkerosie in de femoraal arterie van varkens onder narcose werd aangetoond dat inderdaad de stimulatie van spieren en zenuwen met de nieuw ontworpen catheter vrijwel afwezig was.

Om het herstellen van normale lumen afmetingen met de prototype catheter te testen werden als eerste proef twee afgesloten coronair vaten, verkregen bij autopsie, gebruikt. De intravasculaire ultrageluidskijktechniek werd gebruikt om het segment te selecteren dat door vonkerosie werd weggehaald.

Onderzoek van het weefsel rond de nieuw gemaakte kanalen liet zien dat er dissectie van de plaque en perforatie van de wand was opgetreden in een van de vaten. Het andere vat toonde een goed resultaat. Zoals ook in vorige studies was gevonden was er geen effect op verkalkte laesies te zien.

Deze eerste experimenten met het toepassen van roterende vonkerosie, op geleide van ultrageluid en gecombineerd in één catheter, lieten zien dat dit technisch kan worden uitgevoerd en dat hiermee een belangrijke vermindering van neuromusculaire stimulatie en gasbel productie wordt bereikt. Sommige gebieden echter vragen om verdere bestudering, waaronder een mogelijk verband tussen de torderende krachten van de tip op de vaatwand en het optreden van plaque dissectie en het technische probleem om een oplossing te vinden voor het aandrijven van de tip met een torsiestijve maar toch buigslappe aandrijfjas.

Een ander interessant nevenproduct van het ontwikkelen van de vonkersietechniek is beschreven in **hoofdstuk 9**. De technisch lastig uit te voeren chirurgische ingreep van het weghalen van spier- en bindweefsel uit het vernauwde uitstroomgebied van de linkerhartkamer bij patiënten die lijden aan een abnormale spierverdikking van het hart, kon belangrijk verbeterd worden door vonkerosie toe te passen.

Er werd een speciale, gedeeltelijk geïsoleerde, vonkerosie elektrode ontworpen die met een gepulseerde toediening van de radiofrequente energie het wegsnijden van de spier op eenvoudige en effectieve wijze mogelijk maakte. De snij snelheid werd beperkt tot ca. 2 mm/s terwijl de coagulatie minimaal kon worden gehouden. De diepte van de snede kon precies gestuurd worden dankzij het elektrode ontwerp.

Bestudering van weefselsecties van de weggesneden stukjes spier met de lichtmicroscopie liet zien dat de diepte van celvernietiging beperkt bleef tot twee of drie cellagen.

Toepassing van vonkerosie in een eerste serie van 18 patiënten liet geen belangrijke acute complicaties zien. Een patiënt vertoonde een geleidingsstoornis van het atrium naar de ventrikels waarvoor een pacemaker werd geïmplanterd. Ook later na de operatie zijn geen complicaties waargenomen die in betrekking zouden kunnen staan tot de procedure.

In de **Appendix** is de originele Nederlandse octrooiaanvraag opgenomen waarin diverse oplossingen worden beschreven voor een catheter die vonkerosie combineert met een intravasculaire ultrageluids kijktechniek.

CONCLUSIES

Met elektrische vonkerosie kunnen elektrisch geleidende atherosclerotische laesies verdampt worden zonder dat noemenswaardige thermische schade optreedt aan het omliggende weefsel. Zoals ook geldt voor andere methoden maakt de techniek daarbij geen onderscheid tussen normaal en ziek weefsel.

Om deze reden moet de intravasculaire in vivo toepassing van vonkerosie beperkt worden tot aan te geven doelgebieden. Deze beperking kan in principe met bestaande catheter technologie verkregen worden, maar verdere studie op dit gebied is zeker gerechtvaardigd.

Het aangeven van de richting voor het selecteren van weg te halen plaques kan verkregen worden door vonkerosie te integreren met de intravasculaire ultrageluidskijktechniek.

Aan andere vereisten voor in vivo intravasculaire toepassing kan worden tegemoet gekomen met een afgewogen elektrodeontwerp en een goede keus voor de elektrische parameters om problemen door gasbellen en neuromusculaire stimulatie te voorkomen.

De genezing van de iliacale arteriën in konijnen, na toepassing van vonkerosie, verliep zonder complicaties en was niet verschillend van die welke werd waargenomen na toepassing van ander thermische of mechanische technieken.

Door speciale vormgeving van elektrodes is een nieuwe techniek voor het snijden van weefsel verkregen. Toepassing hiervan in patiënten heeft de operatieve behandeling van de hypertrofische obstructieve cardiomyopathie in belangrijke mate vergemakkelijkt.

DANKWOORD

DANKWOORD

Na mijn jarenlange betrokkenheid bij de cardiale quantitative beelddiagnostiek en haar vele wetenschappelijke facetten was ik zelf wel de laatste om te bedenken dat mijn excursie naar het therapeutische terrein alsnog zou leiden tot het schrijven van een proefschrift. Het waren dan ook de niet aflatende stimuli van anderen die mij tot het samenstellen van dit boekje hebben gebracht. Hiervoor komt lof toe aan Prof. dr. ir. N. Bom en Prof. dr. J.R.T.C. Roelandt, mijn promotoren, en de hoogleraren Prof. dr. P.D. Verdouw en Prof. dr. P.W. Serruys.

Klaas, jij was vanaf het begin bij dit project betrokken en altijd weer enthousiasmerend voor het aanpakken van de nieuwe mogelijkheden die zich voordeden. Bij het uitdragen van onze ideeën wist je steeds die boeiende en inspirerende toon te vinden die nodig is voor het behalen van succes. Jos, je pittige memo's om het promotievuurtje gaande te houden, prikkelden tot verzet maar ook tot inzet. Je deskundige en kritische inbreng bij het goed beschrijven en in het juiste kader plaatsen van zoveel bevindingen heb ik zeer gewaardeerd. Piet, jij hebt me als een van de eersten over de streep getrokken om eens wat artikelen te bundelen. Je gastvrijheid is te roemen, waar nodig zijn je dierexperimentele faciliteiten steeds beschikbaar. Ook was je altijd bereid om even mee te denken over het goed opzetten van de zo sterk wisselende experimenten. Patrick, ik waardeer je voor je vriendschappelijke en collegiale opstelling bij zoveel projecten waar onze wegen samenliepen. Vanaf het eerste moment was jij een belangrijke stimulator van de gedachte om de plaque echt uit het vat te verwijderen. Het spijt me heel erg, dat we dit doel nog niet bereikt hebben.

Bij het opzetten van dit project was de steun van Prof. dr. G.T. Meester zeer waardevol. Geert, ik ben je dankbaar voor je vriendschappelijke begeleiding bij het opdoen van mijn eerste werkervaringen in het Thoraxcentrum. Ook dank ik Prof. dr. ir. J. Davidse die mij voor deze praktijk zo goed had geschoold. Prof. P.G. Hugenholtz legde voor het kunnen samenwerken van zoveel disciplines de grondslag. Paul, je charismatisch leiderschap zal ik nooit vergeten.

Bij het met vertrouwen inslaan van een zo geheel nieuwe richting was het een belangrijke factor mij van de inbreng van Hans Schuurbijs verzekerd te weten. Hans, je kritische benadering om nieuwe ideeën goed aan de tand te voelen is zeer waardevol. Je eigen creatieve inbreng en nauwgezette wijze van uitvoering waren belangrijk om de vele ideeën ook gerealiseerd te krijgen. Ik hoop dat we nog lang kunnen samenwerken.

Dr. A.C. Phaff, Anton, ik wil je graag bedanken voor je inzet bij het solide funderen van het impedantieverhaal. Je hulp bij het opzetten van de gasmetingen was belangrijk. Je fysisch inzicht hielp om meer van het vonkproces te gaan begrijpen. Jammer dat je bijdrage maar van zo korte duur kon zijn.

Voor het verrichten van de gasmetingen aan de Technische Universiteit te Eindhoven wil ik dr. ir. J.A. Rijks en Andrew van Es bedanken.

Voor het onderzoeken van het effect van gasbellen in de coronaire vaten van proefdieren was drs. J.H. van Blankenstein bereid een aantal jaren zijn aandeel te leveren. Jan Heim ik denk met waardering terug aan het werk dat je bij mij hebt verricht. De mooie publikaties die er uit voort zijn gekomen vragen om meer.

Velen waren betrokken bij het maken van allerlei prototype catheters en elektrodes. Na eerst een jaar met veel genoegen met Jan Starrenburg van de CRW te hebben samengewerkt nam Gerard Heuvelsland dat over. Gerard jij hebt met grote inzet en veel enthousiasme er voor gezorgd dat we zoveel ideeën en vragenstellingen steeds weer op korte termijn konden testen en beantwoorden. Je humeur was onverwoestbaar, zelfs als bij een "vrijdag-middag" experiment je werk van vele weken binnen enkele seconden in rook opging. Ook Wim van Alphen wil ik bedanken voor het met grote precisie vervaardigen van wat de mooiste combi-tip catheter is geworden. Ook voor al die andere CID specialisten die steeds weer bereid waren even mee te denken of iets uit te zoeken wil ik graag mijn waardering uitspreken. Ik denk aan Leo Bekkering, Jan Ekas, Bernard Mulder, Ruud Niesing en Arie den Ouden en aan hen die nog steeds werk leveren voor de klinische toepassing van vonkerosie zoals Joop Bos en Ton Vlasveld.

Dr. C.E. Essed bracht mij geduldig de fineses bij van de opbouw van de atherosclerotische laesie en samen leerden wij hoe vonkerosie-ablatie te herkennen is. Nienke het was een genoegen en een voorrecht om met je samen te werken en diverse artikelen getuigen van de bijdrage die je leverde. Ook drs. Robert Jan van Suylen wil ik bedanken voor zijn aandeel in het bestuderen van de myectomie coupes. Coby Peekstok wil ik bedanken voor haar goede verzorging van alle weefselpreparaten die steeds weer anders dan gewend gesneden moesten worden.

Voor het opzetten en uitvoeren van in vitro testen van rekanalisatie met vonkerosie in beenvaten leverde drs. W.V.A. Vandenbroucke een belangrijke bijdrage. De medewerking van Prof. dr. H. van Urk was hierbij onontbeerlijk. Walda vooral ook voor je inzet om van het project in Utrecht een succes te maken ben ik je veel dank verschuldigd.

Met genoegen denk ik terug aan het opzetten van deze dierexperimenten in Utrecht. Toon

Oomen, Ruud Verdaasdonk en Lieselotte van Erven, het was een plezier om samen te werken. Prof. dr. C. Borst was hiervan de belangrijke stimulator. Kees met genoegen denk ik terug aan de boeiende discussies over de mogelijkheden van gestuurde rekanalisatie op geleide van echo.

Voor de experimenten in eigen huis wil ik ook de medewerkers van het dierexperimentele laboratorium bedanken. Rob van Bremen die altijd bereid was assistentie te leveren, Jan van Meegen die soms lange dagen moest maken bij de bellenexperimenten en al die anderen die als stagiaire of tijdelijk onderzoeker behulpzaam waren bij het leveren van materiaal of meehielpen met een kleine pilot studie als uitloop van hun eigen experiment. Ook aan de hulp van dr. E. Gussenhoven voor het beschikbaar stellen van vaatmateriaal en experimentele faciliteiten denk ik dankbaar terug.

De stap om metterdaad met ultrageluid intravasculair te gaan werken werd medio '86 genomen nadat de toevallig passerende ir. C. Ligtfoot desgevraagd enkele eigenschappen van de enkele ultrageluidstransducer nader had uitgelegd. Dr. ir. C.T. Lancée was als steeds bereid om met zijn grote expertise de ideeënstroom te vermenigvuldigen en zich mede in te zetten om een en ander te realiseren. De gedurende lange avonden met de "Le Croy" verkregen eerste plots van vaten bewaar ik nog altijd als een kostbaar document. Charles, je collegialiteit is een voorbeeld voor velen, bedankt dat je altijd bereid bent om mee te denken en te helpen. Ook de andere collega's van de Experimentele Echocardiografie groep met wie in dit project nauw werd samengewerkt dr. ir. H ten Hoff, dr. ir. N. de Jong, Frans van Egmond en Jan Honkoop wil ik graag in mijn dank betrekken.

Voor het opzetten van de myectomie procedure met vonkerosie in patiënten was de hulp van Ton van Dalen onmisbaar. Prof. dr. E. Bos kwam hiervoor op een goed moment met een concrete vraag. Egbert ik vond het erg spannend het O.K. terrein te betreden. Van je nuchtere professionele instelling heb ik veel geleerd.

Dank gaat ook uit naar dr. L.A. van Herwerden met wie de goede samenwerking is voortgezet en die met drs. A.P.W.M. Maat een belangrijke hand had in het opschrijven van onze eerst behaalde resultaten in patiënten.

Rondom het voorbereiden van dit proefschrift ontving ik steun van Marianne Eichholtz die hielp om de vaart erin te houden, van Corrie Eefting die waar mogelijk praktische assistentie verleende en van Frits Mastik die in de kleine uurtjes de printer op gang hield. Ook wil ik Jan Tuin bedanken, die door alle jaren heen altijd klaar stond voor het professioneel verzorgen van het nodige beeldmateriaal.

Ad den Boer wil ik graag noemen voor zijn visionaire aandeel in diverse discussies waarin we probeerden uit te vinden waar het met de behandeling van patiënten naar toe zou moeten. Zijn praktische tips en daadwerkelijke hulp bij het uitvoeren van diverse testen worden zeer gewaardeerd.

De vrienden en collega's van het eigen laboratorium Rob Krams, Jan Oomen, Hans Schuurbiers en Jolanda Wentzel, wil ik bedanken voor de ruimte die ze me gaven om me achter de computer te kunnen zetten voor dit nodige schrijfwerk. Aan de kritische discussies over de stellingen denk ik met plezier terug. Vooral de bijdrage van Jan was goed voor het aanscherpen van die op theologisch gebied. Graag zal ik me straks weer meer in jullie projecten verdiepen.

Bij een project met zoveel raakvlakken kan het haast niet anders of ik heb nog deze of gene in mijn dankwoord vergeten te betrekken. Ik bied daarvoor mijn welgemeende verontschuldigingen aan en vind het niet erg mijn geheugen door u wie het aangaat op te laten frissen.

Ten slotte, waar de uitkomsten van mijn werk tot nut waren of nog zullen zijn wil ik alle eer daarvoor geven aan Hem die mij de gaven en de lust heeft gegeven om me daartoe te bekwamen en in te zetten.

PUBLICATIONS

ARTICLES and BOOK CHAPTERS

QUANTITATIVE IMAGE ANALYSIS

Left Ventricular Geometry

1. Slager CJ, Jong LP de. "Anordnung für die Wiedergabe eines Bildes auf einem Fernsehmonitor und die Gröszenbestimmung von eingrenzbaeren Bildbereichen" Patentschrift 2414806, Deutsches Patentamt, 1975.
2. Jong LP de, Slager CJ. "Automated detection of the left ventricular outline in angiographs using television signal processing techniques" IEEE Trans BME, 1975, 22, 230-237.
3. Slager CJ, Reiber JHC, Schuurbiens JCH, Meester GT. "Automated detection of the left ventricular outline" In: Proc. of the ACEMB 1977, 19, 288.
4. Slager CJ, Reiber JHC, Schuurbiens JCH, Meester GT. "Contouromat- A hardwired left ventricular angio-processing system. I. Design and applications. Comp Biomed Res 1978, 11, 491-502.
5. Reiber JHC, Slager CJ, Schuurbiens JCH, Meester GT. "Contouromat- a hardwired left ventricular angio processing system. II. Performance evaluation. Comp Biomed Res 1978, 11, 503-523.
6. Slager CJ, Reiber JHC, Schuurbiens JCH, Meester GT. "Automated detection of left ventricular contour, concept and application" In: Roentgen-video-techniques. Heintzen PH, Bürsch JH (eds.). Georg Thieme, Stuttgart 1978, 158-167.
7. Slager CJ, Reiber JHC, Meester GT, Schuurbiens JCH. "Contouromat: An automated border recognition system for left ventricular angiograms" In: Proc. Bio Sigma, Paris, 1978, 42-46.
8. Slager CJ, Reiber JHC, Meester GT, Schuurbiens JCH. "Automated feature extraction from cineangiograms" Micr Acta Suppl 1979, 3, 231-233.
9. Hooghoudt TEH, Slager CJ, Reiber JHC, Brower RW, Castellanos S, Zorn ICJ, Hugenholtz PG. "Observer variability in the visual assessment of regional wall motion and in computer assisted analysis of regional left ventricular function" In: Computer analysis of left ventricular cineangiograms. TEH Hooghoudt, Thesis 1982, Erasmus University Rotterdam, 98-110.
10. Slager CJ, Hooghoudt TEH, Serruys PW, Reiber JHC, Schuurbiens JCH. "Automated quantification of left ventricular angiograms" In: Physical Techniques in Cardiological Imaging. Short MD et al (eds.), Adam Hilger, Bristol 1983, 163-172.
11. Meester GT, Slager CJ, Hugenholtz PG. "Angiographie quantitative dans les cardiopathies valvulaires acquises" In: Acar J, ed, Cardiopathies valvulaires acquises. Paris: Flammarion Medecine Sciences, 1985, 160-165.
12. Assmann PE, Slager CJ, Dreyse ST, Borden SG van der, Oomen JAF, Roelandt JRTC. "Two dimensional echocardiographic analysis of the dynamic geometry of the left ventricle: The basis for an improved model of wall motion". J Am Soc Echocard 1988, 1, 393-405.
13. Borden SG van der, Oomen JAF, Slager CJ, Assmann P. "Computer assisted echocardiographic analysis. A semi-automated approach" In: Comp Card Los Angeles, IEEE Soc, 1988, 425-428.
14. Zeelenberg C, Bom N, Bos E, Oomen JAF, Rijsterborg H, Slager CJ. "Proposal for a standard for storage, coding and manipulation of cardiac contour data" Computers in Cardiology, Los Angeles, IEEE Comp Soc, 1988, 635-637.

QUANTITATIVE IMAGE ANALYSIS

Vessel Geometry

15. Reiber JHC, Booman F, Hong Sie Tan, Slager CJ, Schuurbiens JCH, Gerbrands JJ, Meester GT. "A cardiac image analysis system. Objective quantitative processing of angiocardiograms" In *IEEE Comp. in Cardiology 1978*, 239-242.
16. Booman F, Reiber JHC, Gerbrands JJ, Slager CJ, Schuurbiens JCH, Meester GT. "Quantitative analysis of coronary cineangiograms" In: *Computers in Cardiology 1979*, CH1462-1, IEEE Comp Soc, Los Angeles, 177-180.
17. Reiber JHC, Tan HS, Booman F, Gerbrands JJ, Slager CJ, Schuurbiens JCH, Meester GT. "Quantification of coronary occlusions from cine-coronary angiograms" *Biomed Techn*, 1979, 24 suppl, 199-200.
18. Reiber JHC, Booman F, Tan HS, Slager CJ, Schuurbiens JCH, Gerbrands JJ, Meester GT. "A cardiac image analysis system, objective quantitative processing of angiocardiograms" *Computers in Cardiology, IEEE Comp Soc, Los Angeles*, 1980, 239-242.
19. Kooijman CJ, Reiber JHC, Gerbrands JJ, Schuurbiens JCH, Slager CJ, Boer A den, Serruys PW. "Computer aided quantitation of the severity of coronary obstructions from single view cineangiograms" *IEEE Comp Soc Int Symp on Med Images and Image Interpr*, 1982, IEEE 82 CH1804-4, 59-64.
20. Reiber JHC, Booman F, Gerbrands JJ, Slager CJ, Schuurbiens JCH, Serruys PW, Boer A den, Boxma Y, Meester GT, Hugenholtz PG. "Methode voor objectieve kwantitatieve analyse van coronaire cineangiogrammen" *Hart Bulletin*, 1981, 12, 19-24.
21. Reiber JHC, Booman F, Tan HS, Slager CJ, Schuurbiens JCH, Gerbrands JJ, Meester GT. "A cardiac image analysis system, objective quantitative processing of angiocardiograms" *Computers in Cardiology, IEEE Comp Soc, Los Angeles*, 1980, 239-242.
22. Reiber JHC, Slager CJ, Schuurbiens JCH, Boer A den, Gerbrands JJ, Troost GJ, Scholts B, Kooijman CJ, Serruys PW. "Transfer functions of the x-ray-cine-video chain applied to digital processing of coronary cineangiograms". In: *Digital imaging in cardiovascular radiology*. Heintzen PH and Brenneke R eds, Georg Thieme, Stuttgart, New York, 1983, 89-103.
23. Reiber JHC, Kooijman CJ, Slager CJ, Gerbrands JJ, Schuurbiens JCH, Boer A den, Wijns W, Serruys PW. "Computer assisted analysis of the severity of obstructions from coronary cineangiograms: a methodological review" *Automedica* 1984, 5, 219-238.
24. Reiber JHC, Kooijman CJ, Slager CJ, Gerbrands JJ, Schuurbiens JCH, Boer A den, Wijns W, Serruys PW, Hugenholtz PG. "Coronary artery dimensions from cineangiograms - methodology and validation of a computer-assisted analysis procedure" *IEEE Trans Med Imaging* 1984, MI-3.3, 131-141.
25. Reiber JHC, Serruys PW, Kooijman CJ, Wijns W, Slager CJ, Gerbrands JJ, Schuurbiens JCH, Boer A den, Hugenholtz PG. "Assessment of short-, medium- and long-term variations in arterial dimensions from computer-assisted quantitation of coronary cineangiograms" *Circ* 1985, 71/2, 280-288.
26. Reiber JHC, Kooijman CJ, Slager CJ, Ree EJB van, Kalberg RJN, Tijdens FO, Plas J van der, Frankenhuyzen J van, Claessen WCH. "Taking a quantitative approach to cine-angiogram analysis" *Diagnostic Imaging Int* 1985, 87-89.
27. Kooijman CJ, Kalberg RJN, Slager CJ, Tijdens FO, Plas J van der, Reiber JHC. "Densitometric analysis of coronary arteries" In: Young IT et al eds. *Signal Processing III*. Amsterdam: Elsevier Science Publishers, 1986, 1405-1408.
28. Reiber JHC, Kooijman CJ, Slager CJ, Tijdens FO, Serruys PW. "A novel approach to the accurate assessment of coronary arterial

- dimensions from cine angiograms by means of digital imaging techniques" Pinerola: Tipolitografia Giuseppini. 1986, 89-98.
29. Reiber JHC, Serruys PW, Kooijman CJ, Slager CJ, Schuurbijs JCH, Boer A den. "Approaches towards standardization in acquisition and quantitation of arterial dimensions from cineangiograms" Boston, Dordrecht, Lancaster, Martinus Nijhoff Publ. 1986, 145-172.
 30. Reiber JHC, Kooijman CJ, Slager CJ, Tijdens FO. "Quantitative analysis of arterial diameters from cineangiograms" In: Maurer PC et al, eds., What is new in angiology? Trends and controversies. München, Bern, Wien: Zuckschwerdt Verlag, 1986, 66-68.
 31. Reiber JHC, Gerbrands JJ, Kooijman CJ, Schuurbijs JCH, Slager CJ, Boer A den, Serruys PW. "Quantitative coronary angiography with automated contour detection and densitometry: technical aspects" In: Just H, Heintzen PH, eds. Angiocardiology: current status and future developments. Berlin, Heidelberg, New York, London, Paris, Tokyo: Springer Verlag, 1986, 311-331.
 32. Reiber JHC, Kooijman CJ, Slager CJ, Gerbrands JJ, Boer A den, Ommeren J van, Zijlstra F, Serruys PW. "Quantitative digital angiographic techniques" In: Spaan JAE, et al, eds. Coronary circulation, from basic mechanisms to clinical implications. Boston, Dordrecht, Lancaster: Martinus Nijhoff Publ., 1987, 109-133.
 33. Reiber JHC, Kooijman CJ, Slager CJ. "Improved densitometric assessment of percent area-stenosis from coronary cineangiogram" In: Proceedings Advances in Image Processing 1987, 804, 152-158.
 34. Haase J, Mario C di, Slager CJ, Giessen WJ van der, Boer A den, Feyter PJ de, Reiber JHC, Verdouw PD, Serruys PW. "In vivo validation of on-line and off-line geometric coronary measurements using insertion of stenosis phantoms in porcine coronary arteries" Cath Card Diagn 1992, 27, 16-27.
 35. Haase J, Mario C di, Slager CJ, Giessen WJ van der, Feyter PJ de, Verdouw PD, Reiber JHC, Serruys PW. "Accuracy and relevance of angiocardigraphic coronary measurements" In: Onnasch D, Simon R, Reiber JHC eds. ASH COMETT Training Course: Quality Assurance in Digital Angiocardiology. 1992, 20, 1-3.
 36. Haase J, Nugteren SK, Montauban van Swijndregt E, Slager CJ, Di Mario C, Feyter PJ de, Serruys PW. "Digital geometric measurements in comparison to cinefilm analysis of coronary artery dimensions" Cath Card Diagn 1993, 28, 283-290.
 37. Haase J, Escaned J, Montauban van Swijndregt E, Ozaki Y, Gronenschild E, Slager CJ, Serruys PW. "Experimental validation of geometric and densitometric coronary measurements on the new generation cardiovascular angiography analysis system (CAASII)" Cath Card Diagn 1993, 30, 104-114.
 38. Haase J, Keane D, Mario C di, Escaned J, Slager CJ, Serruys PW. "How reliable are geometric coronary measurements? In vitro and in vivo validation of digital and cinefilm based quantitative coronary analysis systems" In: Quantitative coronary angiography in clinical practice. eds. PW Serruys, DP Foley, PJ de Feyter. Kluwer Ac Publ, Dordrecht, London, New York, 1994, 27-50.
 39. Slager CJ, Haase J, Schuurbijs JCH. "On the use of the parameters accuracy and precision for validation of QCA systems" In: Quantitative coronary angiography in clinical practice. eds. PW Serruys, DP Foley, PJ de Feyter. Kluwer Academic Publ., Dordrecht, London, New York, 1994, 45-48.
 40. Haase J, Keane D, Di Mario C, Escaned J, Ozaki Y, Slager CJ, Bremen R van, Giessen WJ van der, Serruys PW: "Percutaneous implantation of coronary stenosis phantoms in an anesthetized swine model to validate current quantitative angiography analysis systems. In: Reiber JHC, Serruys PW (eds): "Progress in Quantitative Coronary Arteriography" Kluwer Academic Publ, Dordrecht, London, New York, 1994, 49-66.

41. Keane D, Gronenschild E, Slager CJ, Ozaki Y, Haase J, Serruys PW. "In vivo validation of an experimental adaptive quantitative coronary angiography algorithm to circumvent overestimation of small luminal diameters" *Cath Card Diagn* 1995, 36, 17-24.
42. Keane D, Haase J, Slager CJ, Montauban van Swijndregt E, Lehmann KG, Ozaki Y, di Mario C, Kirkeeide R, Serruys PW. "Comparative Validation of quantitative coronary angiography systems: results and implications from a multicenter study using a standardized approach" *Circulation* 1995, 91, 2174-83
43. Birgelen C von, Di Mario C, Li W, Schuurbijs JCH, Slager CJ, de Feyter PJ, Roelandt JRTC, Serruys PW. "Morphometric analysis in three-dimensional intracoronary ultrasound: an in vitro and in vivo study performed with a novel system for the contour detection of lumen and plaque" *Am Heart J* 1996, 132(3), 516-527.

QUANTITATIVE IMAGE ANALYSIS

3-D Vessel reconstruction

44. Reiber JHC, Gerbrands JJ, Booman F, Troost GJ, Boer A den, Slager CJ, Schuurbijs JCH. "Objective characterization of coronary obstructions from monoplane cineangiograms and three-dimensional reconstruction of an arterial segment from two orthogonal views" In: *Appl Comp in Med. MD Schwartz* (ed.) 1982, IEEE cat. TH0095-0, 93-100.
45. Reiber JHC, Gerbrands JJ, Kooijman CJ, Troost GJ, Schuurbijs JCH, Slager CJ, Boer A den, Serruys PW. "Computer aided analysis of coronary obstructions from monoplane cineangiograms and three-dimensional reconstruction of an arterial segment from two orthogonal views" In: *Physical Techniques in Cardiological Imaging. Short MD et Bristol* 1983, 173-188.
46. Schuurbijs JCH, Slager CJ, Serruys PW "Luminal Volume Reconstruction from Angioscopic Video Images of Casts from Human Coronary Arteries" *Am J Cardiol* 1994, 74, 764-768
47. Roelandt JRTC, DiMario C, Pandian NG, Wenguan Li, Keane D, Slager CJ, Feyter de PJ, Serruys PW. "Three-dimensional reconstruction of intracoronary ultrasound images - Rationale, approaches, problems, and directions" *Circ* 1994, 90, 2, 1044-1055.
48. Feyter PJ de, Mario C Di, Slager CJ, Serruys PW, Roelandt JRTC. "Towards complete assessment of progression/regression of coronary atherosclerosis: Implications for intervention trials" In: Reiber JHC, Serruys PW (eds): "Progress in Quantitative Coronary Arteriography" Kluwer Academic Publ, Dordrecht, New York, 1994, 295-306.
49. Haase J, Slager CJ, Keane D, Foley DP, Boer den A, Doriot PA, Serruys PW. "Quantification of intracoronary volume by videodensitometry: Validation study using fluid filling of human coronary casts" *Cath Card Diagn* 1994, 33, 1, 89-94.
50. Schuurbijs JCH, Slager CJ, Serruys PW. "Quantification of angioscopic images from casts of human coronary arteries using a lightwire" In: de Feyter PJ, DiMario C and Serruys PW eds. *Quantitative Coronary Imaging. Barjesteh, Meeuwes & Co*, 227-237, 1995.
51. Birgelen C von, Erbel R, DiMario C, Li W, Prati F, Ge J, Bruining N, G6rge G, Slager CJ, Serruys PW, Roelandt JRTC. "Three-Dimensional Reconstruction of Coronary Arteries with Intravascular Ultrasound" *Herz* 1995, 20, 277-289 (Nr. 4).
52. Slager CJ, Laban M, Oomen JAF, von Birgelen C, Li W, Krams R, Schuurbijs JCH, den Boer A, Serruys PW, Roelandt JRTC, de Feyter PJ. "Three-dimensional geometry and orientation of coronary lumen and plaque. Reconstruction from angiogra-

- phy and ICUS (ANGUS)" Thoraxcenter J, 1995, 7/3, 36-37.
53. Laban M, Oomen JA, Slager CJ, Wentzel JJ, Krams R, Schuurbijs JCH, den Boer A, von Birgelen C, Serruys PW, de Feyter PJ. "ANGUS: A new approach to three dimensional reconstruction of coronary vessels by combined use of angiography and intravascular ultrasound" Computers in Cardiology 1995, 95CH35874, IEEE Comp. Soc, Piscataway, NJ, 325-328.
 54. Von Birgelen C, Di Mario C, Wenguang L, Slager CJ, de Feyter PJ, Roelandt JRTC. "Volumetric Quantification by Intracoronary Ultrasound" In: de Feyter et al, eds. Quantitative Coronary Imaging, Barjesteh Meeuwes & Co and Thoraxcenter Rotterdam 1995, 211-26.
 55. von Birgelen C, Slager CJ, DiMario C, de Feyter PJ, Serruys PW. "Volumetric Intracoronary Ultrasound: A new maximum confidence approach for the quantitative assessment of progression-regression of atherosclerosis?" Atherosclerosis 118 (Suppl.) 103-113, 1995
 56. Slager CJ, Wentzel JJ, Oomen JAF, Schuurbijs JCH, Krams R, von Birgelen C, Tjon A, Serruys PW, de Feyter PJ. "True reconstruction of vessel geometry from combined X-ray angiographic and intracoronary ultrasound data" Semin Intervent Card , 1997, 2, 43-47
 57. von Birgelen C, deVrey E, Mintz GS, Nicotia A, Bruining N, Li W, Slager CJ, Roelandt JRTC, Serruys PW, de Feyter PJ. "ECG-gated three-dimensional intravascular ultrasound: feasibility and reproducibility of the automated analysis of coronary lumen and atherosclerotic plaque dimensions in humans", Circulation 1998, in press.
 58. Slager CJ. "Catheter for obtaining three-dimensional reconstruction of a vascular lumen and wall, and method of use" U.S patent application 09/637,318. 1997/9, allowed for issuance as a patent

QUANTITATIVE IMAGE ANALYSIS

Colorimetry

59. Oomen JAF, Slager CJ, Schuurbijs JCH, Roelandt JRTC. "Objective analysis of fiberoptic angioscopy" Thoraxcenter J 1994, 6, 5, 16-20
60. Oomen JAF, Slager CJ, Lehmann KG, Schuurbijs JCH, Serruys PW. "Color quantification in angioscopic video images" Med Progr Techn 1995, 21, 39-46.
61. Oomen JAF, Schuurbijs JCH, Lehmann KG, Slager CJ, Serruys PW. "Color quantization in angioscopic images" In: Cardiovascular Imaging, 1996, 367 - 377. Editors JHC Reiber and EE van der Wall. 1996 Kluwer Ac Publ.
62. Lehmann KG, Suylen RJ van, Stibbe J, Slager CJ, Oomen JAF, Maas A, di Mario C, Feyter P de, Serruys PW. "The composition of human thrombus assessed by quantitative colorimetric angioscopic analysis" in press Circulation 1997.

BIOMECHANICS of the Left Ventricle

LV motion and pump function

63. Slager CJ, Hooghoudt TEH, Reiber JHC, Schuurbijs JCH, Booman F, Meester GT. "Left ventricular contour segmentation from anatomical landmark trajectories and its application to wall motion analysis" Computers in Cardiology, IEEE Comp Soc, Los Angeles, 1979, CH1462-1, 347-350.
64. Hooghoudt TEH, Slager CJ, Reiber JHC, Serruys PW, Schuurbijs JCH, Meester GT. " Regional contribution to global ejection

- fraction -used to assess the applicability of a new wall motion model to the detection of regional wall motion in patients with asynergy" *Computers in Cardiology 1980, IEEE Comp Soc, Los Angeles, 253-256.*
65. Hooghoudt TEH, Serruys PW, Reiber JHC, Slager CJ, Brand M van de, Hugenholtz PG. "The effect of recanalization of the occluded coronary artery in acute myocardial infarction on left ventricular function". *Eur Heart J*, 1982, 3, 416-421.
 66. Hooghoudt TEH, Slager CJ, Reiber JHC, Schuurbiens JCH, Meester GT, Hugenholtz PG. "Quantitative assessment of regional pump- and contractile function. Part I: The normal human heart. In: Computer analysis of left ventricular cine angiograms". TEH Hooghoudt, Thesis 1982, Erasmus University Rotterdam, 59-81.
 67. Hooghoudt TEH, Serruys PW, Slager CJ, Reiber JHC, Schuurbiens JCH, Meester GT, Hugenholtz PG. "Quantitative assessment of regional pump- and contractile function. Part II: Changes in regional wall motion and pump function induced by pacing in patients with coronary artery disease". In: Computer analysis of left ventricular cine angiograms. TEH Hooghoudt, Thesis 1982, Erasmus University Rotterdam, 82-89.
 68. Serruys PW, Hooghoudt TEH, Reiber JHC, Slager CJ, Brower RW, Hugenholtz PG. "Influence of intracoronary nifedipine on left ventricular function, coronary vasomotility, and myocardial oxygen consumption" *Br Heart J* 1983, 49, 427-441.
 69. Hooghoudt TEH, Slager CJ, Reiber JHC, Serruys PW. "A new method to quantify regional left ventricular wall motion, as well as pump- and contractile function" In: Sigwart U, Heintzen PH, eds. *Ventricular wall motion*. Stuttgart, New York, Georg Thieme Verlag, 1984, 229-244.
 70. Serruys PW, Wijns W, Brand MJBM van de, Meij SH, Slager CJ, Schuurbiens JCH, Hugenholtz PG, Brower RW. "Left ventricular performance, regional blood flow, wall motion, and lactate metabolism during transluminal angioplasty" *Circulation* 1984, 70, 25-36.
 71. Serruys PW, Wijns W, Brand MJBM van de, Meij SH, Slager CJ, Schuurbiens JCH, Hugenholtz PG, Brower RW. "Left ventricular function during transluminal angioplasty: A haemodynamic and angiographic study" *Acta Med Scand*, 1984, 694, 197-206.
 72. Slager CJ, Hooghoudt TEH, Reiber JHC, Schuurbiens JCH, Verdouw PD, Hugenholtz PG. "Left ventricular wall motion as derived from endocardially implanted radiopaque markers and from contrast angiocardiograms" In: Sigwart U, Heintzen PH, eds. *Ventricular wall motion*. Stuttgart, New York, Georg Thieme Verlag, 1984, 150-159.
 73. Verdouw PD, Slager CJ, Bremen RH van, Verkeste CM. "Is nisoldipine capable of reducing left ventricular preload?" *Eur J Pharm* 1984, 137-140.
 74. Serruys PW, Wijns W, Brand MJBM van den, Slager CJ, Grimm J, Jaski BE, Brower RW, Hess OM, Hugenholtz PG. "Effect of coronary occlusion during percutaneous transluminal angioplasty on systolic and diastolic left ventricular function" In: Meyer J, Erbel R, Rupprecht HJ, eds. *Improvement of myocardial perfusion*. Boston, Dordrecht, Lancaster: Martinus Nijhoff Publ., 1985, 236-254.
 75. Hooghoudt TEH, Slager CJ, Reiber JHC, Serruys PW. "Quantitation of regional ventricular function using the endocardial landmark model - clinical results" In: Just H, Heintzen PH, eds. *Angiocardiography: Current status and future developments*. Berlin, Heidelberg, New York, Springer Verlag, 1986, 227-251.
 76. Serruys PW, Piscione F, Wijns W, Slager CJ, Feyter PJ de, Brand MJBM van den, Hugenholtz PG, Meester GT. "Ejection filling and diastasis during transluminal occlusion in man. Consideration on global and regional left ventricular function" In: *Coronary*

- Angioplasty. Boston, Dordrecht, Lancaster: Martinus Nijhoff Publ. 1986, 151-188.
77. Slager CJ, Hooghoudt TEH, Serruys PW, Schuurbijs JCH, Reiber JHC, Meester GT, Verdouw PD, Hugenholtz PG. "Quantitative assessment of regional left ventricular motion using endocardial landmarks" *JACC* 1986, 7, 317-326.
 78. Slager CJ, Hooghoudt TEH, Reiber JHC, Schuurbijs JCH, Verdouw PD. "Use of endocardial landmarks in the evaluation of left ventricular function: advantages and limitations of automated analysis of the ventriculogram" In: Just H, Heintzen PH, eds. *Angiocardiography: current status and future developments*. Berlin, Heidelberg, New York, London, Paris: Springer Verlag, 1986, 213-226.
 79. Assmann PE, Slager CJ, Borden SG van der, Dreyse ST, Tijssen JGP, Sutherland GR, Roelandt JR. "Quantitative echocardiographic analysis of global and regional left ventricular function: a problem revisited" *J Am Soc Echocardiogr*, 1990, 3, 478-487.
 80. Serruys PW, Piscione F, Wijns W, Slager CJ, Feyter PJ de, Brand MJB van den, Hugenholtz PG, Meester GT. "Ejection filling and diastasis during transluminal occlusion in man" In: Serruys PW, Simons R, Beatt K, eds. *PTCA. An investigational tool and a non-operative treatment of acute ischemia*. Kluwer Academic Publ 1990, 233-266.
 81. Assmann PE, Slager CJ, Borden SG van der, Sutherland GR, Roelandt JR. "Reference systems in echocardiographic quantitative wall motion analysis with registration of respiration" *J Am Soc Echocardiogr* 1991, 4, 224-234.
 82. Assmann PE, Slager CJ, Roelandt JR. "Systolic excursion of the mitral annulus as an index of left ventricular systolic function" *Am J Cardiol* 1991, 68, 829-830.
 83. Assmann PE, Slager CJ, Borden SG van der, Tijssen JGP, Oomen JAF, Roelandt JR. "Comparison of models for quantitative left ventricular wall motion analysis from two-dimensional echocardiograms during acute myocardial infarction" *Am J Cardiol* 1993, 71, 1262-1269.

BIOMECHANICS of the Left Ventricle

LV wall stress

84. Wijns W, Serruys PW, Slager CJ, Grimm J, Krayenbuhl HP, Hugenholtz PG, Hess OM. "Effect of coronary occlusion during percutaneous transluminal angioplasty in humans on left ventricular chamber stiffness and regional diastolic pressure-radius relations" *JACC* 1986, 7, 455-463.
85. Krams R, Janssen M, Lee C van der, van Meegen J, de Jong JW, Slager CJ, Verdouw PD. "Loss of elastic recoil in post ischemic myocardium induces rightward shift of the systolic pressure-volume relationship" *Am J Physiol* 267, (Heart Circ Phys 36) 1994, H1557-H1564.
86. Assmann PE, Aengevaeren WR, Tijssen JGP, Slager CJ, Vlieter W, Roelandt JR. "Early identification of patients at risk for significant left ventricular dilation one year after myocardial infarction". *J Am Soc Echocardiography* 1995, 8(2), 175-84, 1995.

BIOMECHANICS of Arteries

Shear stress and flow

87. Kroon MGM de, Slager CJ, Gussenhoven WJ, Serruys PW, Roelandt JR, Bom N. "Cyclic changes of blood echogenicity in high-frequency ultrasound" *Ultrasound Med Biol* 1991, 17, 7, 723-728.
88. Krams R, Wentzel JJ, Oomen JAF, Schuur-

- biers JCH, de Feyter PJ, Serruys PW, Slager CJ. "Evaluation of endothelial shear stress and 3D geometry as factors determining the development of atherosclerosis and remodeling in human coronary arteries in vivo. Combining 3D reconstruction from arteriography and IVUS (ANGUS) with computational fluid dynamics. *Arterioscl Tromb. Vasc Biol*, 1997, 17, in press.
89. Di Mario C, Slager CJ, Linker DT, Serruys PW. "Quantitative assessment of coronary artery stenosis by intravascular Doppler catheter technique" Letter to the editor. *Circ*. 1992, 2016.
90. Blankenstein JH van, Slager CJ, Schuurbiens JCH, Strikwerda S, Verdouw PD. "Heart function after injection of small air bubbles in a coronary artery of pigs" *J Appl Physiol* 1993, 75, 3, 1201-1207
91. Di Mario C, Feyter PJ de, Slager CJ, Jaegere de P, Roelandt JRTC, Serruys PW. "Intracoronary blood flow velocity and transstenotic pressure gradient using sensor-tip pressure and Doppler guide wires: A new technology for the assessment of stenosis severity in the catheterization laboratory" *Cath Card Diagn* 1993, 28, 311-319
92. Di Mario C, Feyter PJ de, Schuurbiens JCH, Jaegere P de, Gil R, Emanuelsson J, Slager CJ, Serruys PW. "Assessment of coronary severity from simultaneous measurement of transstenotic pressure gradient and flow. A comparison with quantitative coronary angiography." In : *Quantitative coronary angiography in clinical practice*. eds. PW Serruys, DP Foley, PJ de Feyter. Kluwer Academic Publ., Dordrecht, London, New York, 1993, 283-306.
93. Di Mario C, Meneveau N, Gil R, de Jaegere P, de Feyter PJ, Slager CJ, Roelandt JRTC, Serruys PW. "Maximal Blood Flow Velocity in Severe Coronary Stenoses Measured with a Doppler Guidewire. Limitations for the application of the continuity equation in the assessment of stenosis severity" *Am J Card*, 1993, 71, 54D-61D
94. Mannaerts HFJ, Menevea N, Gil R, Jaegere PPT, Feyter PJ de, Slager CJ, Roelandt JRTC, Serruys PW. Maximal blood flow velocity in severe coronary stenoses measured with a Doppler guidewire. Limitations for the application of the continuity equation in the assessment of stenosis severity. *Am J of Card*. 1993, 71, 54D-61D.
95. Blankenstein JH van, Slager CJ, Soei LK, Boersma H, Verdouw PD. "Effect of arterial blood pressure and ventilation gasses on cardiac depression induced by air embolism" *J Appl Physiol* 1994, 77, 4, 1896-1902
96. Blankenstein JH van, Slager CJ, Soei LK, Boersma H, Stijnen Th, Schuurbiens JCH, Krams R, Lachmann B, Verdouw P. "Cardiac depression after experimental air embolism in pigs. Role of addition of a surface active agent" *Card. Vasc. Res*. 1997, 34, 473-482
97. Wentzel JJ, Krams R, van der Steen AFW, Li W, Cespedes EI, Bom N, Slager CJ. "Disturbance of 3-D velocity profiles induced by an IVUS catheter. Evaluation with computational fluid dynamics" *IEEE Comp in Cardiol*, 1997, in press.

INTERVENTIONAL TECHNIQUES

Transluminal Arterial Imaging

98. Bom N, Lancée CT, Slager CJ, Jong N de. "Ein Weg zur intraluminaren Echoarteriographie" *Ultraschall in der Medizin*. Stuttgart, New York: Georg Thieme Verlag, 1987, 5, 233-236.
99. Bom N, Slager CJ, Egmond FC van, Lancée CT, Serruys PW. "Intra-arterial ultrasonic imaging for recanalization by spark erosion" *Ultrasound Med Biol* 1988, 14, 257-261.
100. Bom N, Lancée CT, Jong N de, Slager CJ, "Special transducers" *Chin. J Ultrasound Med* 1988, 4, suppl, 12-15.

101. Bom N, Hoff H ten, Lancée CT, Gussenhoven WJ, Serruys PW, Slager CJ, Roelandt JRTC. "Early and present examples of intraluminal ultrasonic echography" SPIE Microsensors and Catheter-Based Imaging Technology 1989, 1068, 146-150.
102. Gussenhoven WJ, Essed CE, Frietman P, Mastik F, Lancée CT, Slager CJ, Serruys PW, Gerritsen P, Pieterman H, Bom N. "Intravascular echographic assessment of vessel wall characteristics: A correlation with histology" International J of Cardiac Imaging 1989, 4, 105-116.
103. Bom N, Gussenhoven WJ, Slager CJ. "Percutane intravasculaire tweedimensionale echocardiografie" Techniek in de Gezondheidszorg Noordervliet B.V. 1990, 4, 35
104. Bom N, Gussenhoven WJ, Lancée CT, Slager CJ, Serruys PW, Hoff H ten, Roelandt JRTC. "Intra-arterial ultrasonic imaging" In: S. Iliceto, P Rizzon, JRTC Roelandt eds. Ultrasound in Coronary Artery Disease. Kluwer Academic Publ. 1991, 277-284.
105. Bom N, Bosch JG, Reiber JHC, Gussenhoven WJ, Slager CJ, Brower RW. "Current intra-arterial ultrasound imaging systems and automatic contour detection" In: Reiber JHC, Serruys PW eds. Quantitative Coronary Arteriography. Kluwer Academic Publ. 1991, 199-210.

INTERVENTIONAL TECHNIQUES

Transluminal Arterial Modification

106. Slager CJ, Essed CE, Schuurbijs JCH, Bom N, Serruys PW, Meester GT. "Vaporization of atherosclerotic plaques by spark erosion" JACC 1985, 5, 6, 1382-1386.
107. Bom N, Slager CJ, Phaff AC. "Sensing methods for selective recanalization by spark erosion" In: Proc. Ninth Annual Conf of the IEEE Engineering in Medicine and Biology Soc. 1987, 205-206.
108. Slager CJ. "Echo-vonkerosie rekanalisatie inrichting" Ned octrooi aanvraag 1987, 87.00632.
109. Slager CJ, Vandenbroucke WVA, Phaff AC, Schuurbijs JCH, Bom N, Serruys PW. "Thermal ablation of atherosclerotic plaques by spark erosion" In: Proc. Ninth Annual Conf of the IEEE Engineering in Medicine and Biology Soc., 1987, 198-199.
110. Slager CJ, Phaff AC, Essed CM, Schuurbijs JCH, Bom N, Vandenbroucke WVA, Serruys PW. "Spark erosion of arteriosclerotic plaques" Zeitschrift für Kardiologie 1987, 76 (suppl.), 67-71.
111. Bom N, Slager CJ, Egmond FC van, Lancée CT, Serruys PW. "Intra-arterial ultrasonic imaging for recanalization by spark erosion" SPIE microsensors and catheter based imaging technology 1988, 904, 107-109.
112. Slager CJ, Meester GT, Phaff AC, Schuurbijs JCH, Essed CM. "Plaque reduction in arteries by spark erosion" Eur Heart J 1988, 9, suppl. C, 21-24.
113. Slager CJ, Hugenholtz PG, Bom N, Lancée CT, Schuurbijs JCH, Serruys PW. "Spark erosion: an alternative to laser recanalization" In: Biamino G, Muller GJ, eds, Advances in Laser Medicine I. Ecomed GmbH, 1988, 244-250.
114. Slager CJ, Bom N, Serruys PW, Schuurbijs JCH, Vandenbroucke WVA, Lancée CT. "Spark erosion and its combination with sensing devices for ablation of vascular lesions" In: JHK Vogel, SB King, eds. Interventional Cardiology: future directions. The C.V. Mosby Comp. 1989, 157-169.
115. Oomen A, Erven L van, Vandenbroucke WVA, Verdaasdonk RM, Slager CJ, Thomson SL, Borst C. "Early and late arterial healing response to catheter-induced laser, thermal, and mechanical wall damage in the rabbit" Lasers in Surg and Med, 1990, 10, 363-374.

116. Giessen WJ van der, Slager CJ, Beusekom HMM van, Ingen Schenau DS van, Huyts RA, Schuurbijs JCH, Klein WJ de, Serruys PW, Verdouw PD. "Development of a polymer endovascular prosthesis and its implantation in porcine arteries" *J Interv Card* 1992, 5, 175-185
117. Slager CJ, Phaff AC, Essed CM, Bom N, Schuurbijs JCH, Serruys PW. "Electrical impedance of layered atherosclerotic plaques on human aortas" *IEEE Trans Biomed Engng* 1992, 39, 4, 411-419.
118. Giessen WJ van der, Beusekom HMM van, Slager CJ, Schuurbijs JCH, Verdouw PD. "An experimental cardiologist's view on coronary stents" In: *Advances in quantitative coronary angiography*, eds. JHC Reiber, PW Serruys. Kluwer Academic Publishers, 1993, 537-552.
119. Giessen WJ van der, Slager CJ, Gussenhoven EJ, Beusekom HMM van, Huijts RA, Schuurbijs JCH, Wilson RA, Serruys PW, Verdouw PD. "Mechanical features and in vivo imaging of a polymer stent". *Int J Cardiac Imaging* 1993, 9, 219-226.
120. Keane D, Schuurbijs JCH, Slager CJ, Ozaki Y, den Boer A, Bruining N, Serruys PW. "Comparative quantitative mechanical, radiographic, and angiographic analysis of eight coronary stent designs" In "Coronary Stenting: a quantitative angiographic and clinical evaluation" Thesis D. Keane, Erasmus University, pp 243- 271, 1995.

INTERVENTIONAL TECHNIQUES

Transluminal Pacing

121. Meester GT, Slager CJ, Spaa W, Schuurbijs JCH, Verdouw PD, Hugenholtz PG. "A fluid column pacemaker (FCP) for use in the intensive care unit (ICU)" *Proc World Congr Med Physics and Biomed Engng. Hamburg* 1982, 12,
122. Meester GT, Simoons ML, Slager CJ, Kint PP, Spaa W, Hugenholtz PG. "Use of the fluid column in a cardiac catheter for emergency pacing" *Cath Card Diagn* 1983, 9, 507-513.
123. Meester GT, Simoons ML, Slager CJ, Kint PP, Spaa W, Hugenholtz PG. "Emergency pacing using the fluid column of a cardiac catheter" In: Steinbach K, Glogar D, Laszkovics eds. Darmstadt: Steinkopf Verlag, 1983, 943-946.
124. Meester GT, Slager CJ, Simoons ML, Spaa W, Hugenholtz PG. "Stimulatie van het hart via de vloeistofkolom van een catheter" *Hart Bulletin* 1984, 15, 75-77.

INTERVENTIONAL TECHNIQUES

Thrombolysis

125. Giessen WJ van der, Mooi W, Rutteman AM, Vliet HHDM van, Slager CJ, Verdouw PD. "A new model for coronary thrombosis in the pig: preliminary results with thrombolysis" *Eur H J* 1983, 4, Suppl C, 69-76.
126. Serruys PW, Suryapranata H, Slager CJ, Vermeer F, Brand MJB van den, Verheugt FW, Res J, Domburg RT van, Simoons ML, Hugenholtz PG. "Quantitative assessment of regional left ventricular motion after early thrombolysis using endocardial landmarks" In; Effert S, et al, eds. *Facts and hopes in Thrombolysis in Acute Myocardial Infarction*. Steinkopf Verlag, 1986, 101-124.

INTERVENTIONAL TECHNIQUES*Left Ventricular Myectomy*

127. Slager CJ, Schuurbiens JCH, Oomen JAF, Bom N. "Electrical nerve and muscle stimulation by radio frequency surgery: role of direct current loops around the active electrode" *IEEE Trans on Biomed Engng* 1993, 40, 2, 182-187.
128. Maat LPWM, Slager CJ, Herwerden LA van, Schuurbiens JCH, Suylen RJ van, Kofflard MJM, Cate FJ ten, Bos E. "Spark erosion myectomy in hypertrophic obstructive cardiomyopathy" *Ann Th Surg* 1994, 58, 2, 536-540.

BOOKS:**QUANTITATIVE IMAGE ANALYSIS**

1. Reiber JHC, Serruys PW, Slager CJ. "Quantitative coronary and left ventricular cineangiography: Methodology and clinical applications" Boston, Dordrecht, Lancaster: Martinus Nijhoff Publ., 1986, 454 pages.

INTERVENTIONAL TECHNIQUES

2. Slager CJ. "Removal of cardiovascular obstructions by spark erosion". Thesis, 1997, 160 pages.

CURRICULUM VITAE

CURRICULUM VITAE

Kees Slager werd geboren op 31 augustus 1945 te Scherpenisse.

Hij is getrouwd met Jany Scholten en samen hebben zij 5 kinderen: Janneke, getrouwd met Marco; Jos, getrouwd met Janine; Lenette, getrouwd met Harm Jan; Koos en David.

Hij behaalde aan de Rijks Hogere Burger School te Bergen op Zoom het HBS-B diploma in 1963 en aan de Technische Universiteit Delft het doctoraal examen elektrotechniek in 1971.

De anatomie van het grotere proefdier werd grondig verkend, als slager in deeltijd, in het ouderlijk bedrijf van 1966 tot 1970.

Hij was student assistent aan de Technische Universiteit Delft, afdeling Elektronica, van 1969 tot 1971.

Tijdens een onderzoeksstage, verricht aan de Katholieke Universiteit Nijmegen, afdeling Medische Fysica, werd een methode voor

ademhalingsregistratie met impedantiemetingen opgezet in 1969.

Het afstudeerwerk, verricht ten behoeve van het Thoraxcentrum Academisch Ziekenhuis Rotterdam-Dijkzigt, in de periode 1969-1970 leverde de grondslag voor het detecteren van cardiovasculaire contouren in angiografische beelden.

Na het behalen van het doctoraal diploma was hij als wetenschappelijk medewerker verbonden aan de Technische Universiteit Delft, afdeling Elektronica, van 1971 tot 1975.

Als erkend gewetensbezwaarde werd de vervangende dienstplicht verricht aan het Thoraxcentrum, Erasmus Universiteit Rotterdam van 1972 tot 1974.

Sinds 1975 is hij verbonden aan het Thoraxcentrum, Academisch Ziekenhuis Rotterdam-Dijkzigt en geeft daar leiding aan de groep Haemodynamiek.

